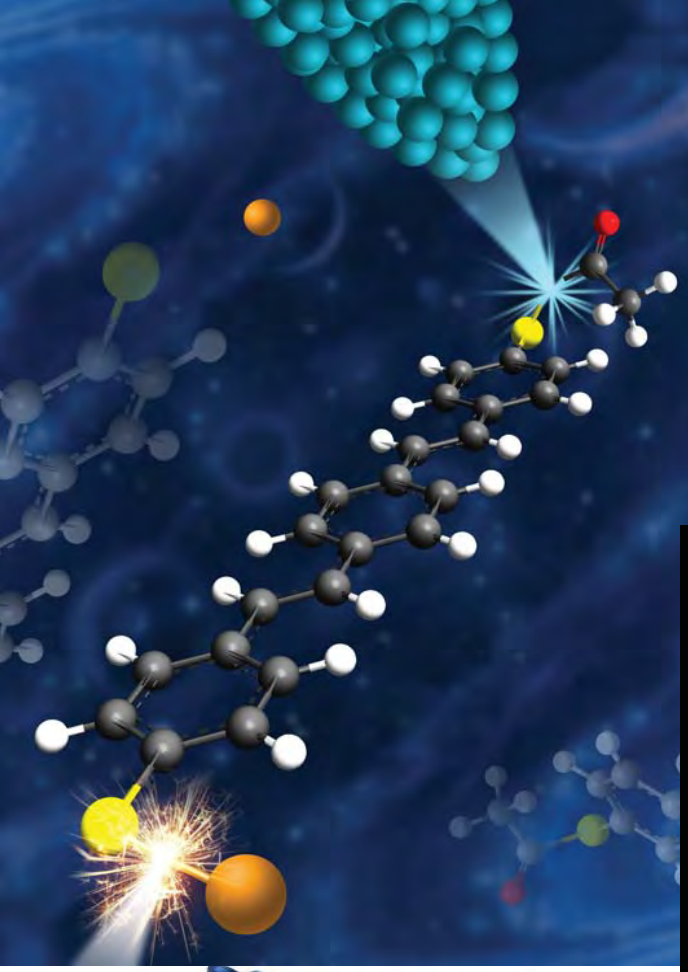

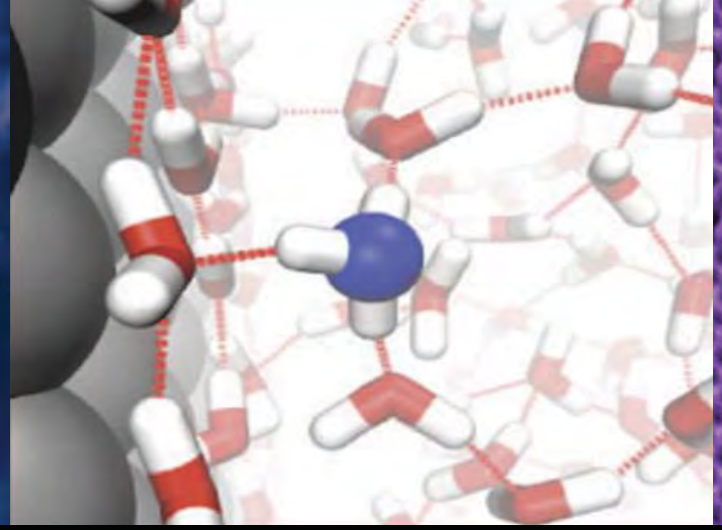

CPIMS 9

Ninth Condensed Phase and Interfacial Molecular Science (CPIMS) Research Meeting

Bolger Conference Center
Potomac, MD
October 20 - 23, 2013

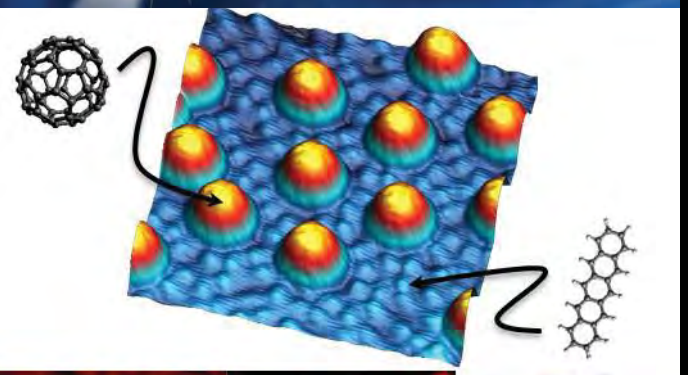

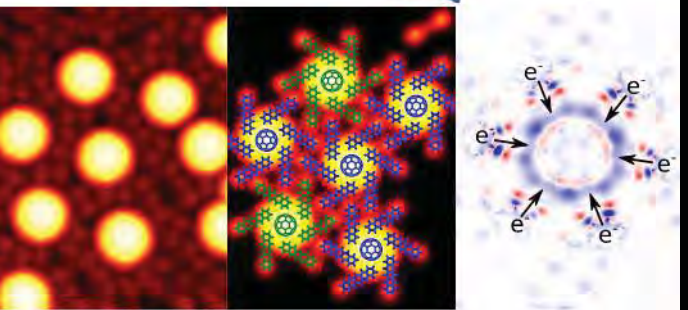

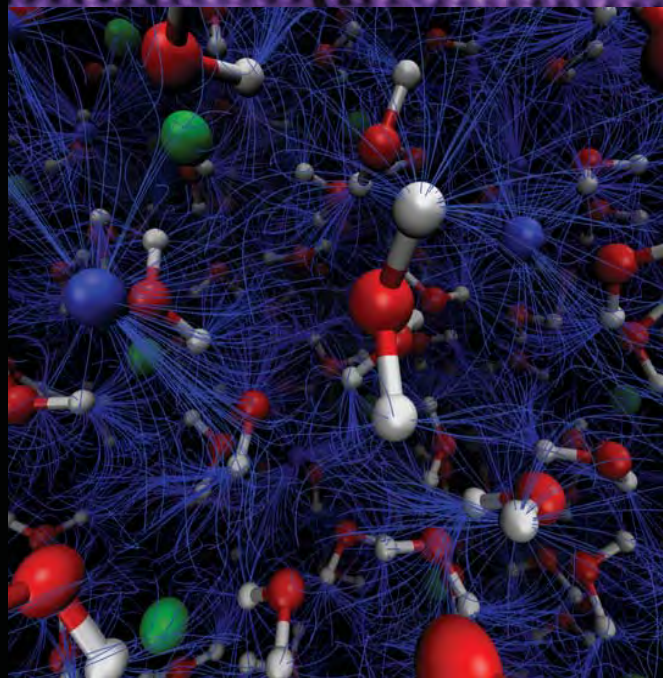

U.S. DEPARTMENT OF ENERGY | Office of Science

Office of Basic Energy Sciences
Chemical Sciences, Geosciences & Biosciences Division

The beam of electrons emitted from the tip of a scanning tunneling microscope (STM) selectively cleaves the sulfur-acetyl bond and welds the sulfur-gold bond in a 1,4-bis[4'-(acetylthio)styryl]benzene molecule adsorbed on a NiAl(110) surface. Bond selective chemistry is one of the ultimate goals of chemistry. Achieving bond-selectivity in a complex molecule with different functional groups is particularly important for demonstrating control of chemistry. By locally injecting energy-tunable tunneling electrons in a scanning tunneling microscope (STM) into a single thiol-based π-conjugated molecule, it is possible to abstract selectively different functional groups. Furthermore, it is possible to form a Au-S bond by manipulating and attaching a single gold atom to the sulfur atom exposed at each end of the molecule. Ultimately, these results lead to the understanding and control of chemistry at the single bond level.

Y. Jiang, Q. Huan, L. Fabris, G. C. Bazan and W. Ho, *Nature Chemistry* 5, 36 (2013).

Submitted by Wilson Ho (University of California, Irvine)

For further information, see abstract on pages 74-76.

Novel computational methods have allowed the Chandler group to simulate water in a nano-scale electrochemical cell. The emergent dynamics is remarkably rich: soft water-vapor-like interfaces fluctuate on time scales of 10 ps or longer, and adlayer reorganizations on scales of 10 ns or longer, all of which is modulated by dynamics in the liquid where hydrogen-bond and dipole reorganization occurs on time scales of 1 ps or shorter. The results of the simulations reveal a dynamic fluctuating system that is far from the static or averaged picture generally invoked in electrochemistry. Implications likely extend far beyond the Pt surfaces considered in this work because the underlying physics is common to many systems. It will appear whenever strong metal-water hydrogen bonds impose geometry of a metal surface incommensurate with that of favorable hydrogen bonding patterns of water.

Limmer, D. T., A. P. Willard, P. A. Madden and D. Chandler, *Proceedings of the National Academy of Science,* 110, 4200 (2013); Willard, A. P., D. T. Limmer, P. A. Madden and D. Chandler, *Journal of Chemical Physics* 138, 184702 (2013).

Submitted by David Chandler (Lawrence Berkeley National Laboratory)

For further information, see abstract on pages 18-21.

CPIMS 9

About the Cover Graphics

Dissociation and subsequent spillover of reactants from one site to another is important in heterogeneous catalysis and has recently been shown to enhance hydrogen storage in a variety of materials. We discovered that the hydrogen spillover pathway on single atom alloys can be controlled by reversible adsorption of a spectator molecule such as CO. Individual Pd atoms in a Cu surface serve as hydrogen dissociation sites from which H atoms can spill over onto surrounding Cu regions. During desorption of hydrogen, Pd atoms act as recombination and exit pathways. Selective adsorption of CO at these atomic Pd sites is shown to either prevent the uptake of hydrogen on, or inhibit its desorption from, the surface. In this way, the hydrogen coverage on the whole surface can be controlled by molecular adsorption at minority sites, which we term the "molecular cork" effect. We illustrate how the molecular cork effect can control uptake and release of hydrogen in a model storage system and show that it is present in a surface catalyzed hydrogen reaction.

M. Marcinkowski, A. Jewell, M. Stamatakis, M. Boucher, E. Lewis, C. Murphy, G. Kyriakou and C. Sykes *Nature Materials*, 12, 523 (2013).

Submitted by E. Charles H. Sykes (Tufts University)

For further information, see abstract on pages 158-161.

Achiral and highly symmetric acceptor (C60) and donor (pentacene) molecules were demonstrated to self-assemble into in-plane chiral donor-acceptor heterojunctions on Cu(111) using ultrahigh vacuum (UHV) scanning tunneling microscopy (STM), showing that a structural 'handedness' can emerge in the self-assembly of even highly symmetric molecules on surfaces. Density functional theory (DFT) calculations show that these superstructures are indeed energetically favorable and are characterized by charge transfer between the donor and acceptor molecules, suggesting that they are actually chiral heterojunctions. Both a mixed chirality structure and a single chirality superstructure with long-range order were observed.

Unlike the other images on the CPIMS 9 cover, this image consists of four separate figures. Here, the top and bottom left figure show an UHV STM image of the mixed-chirality, C60-Pn in-plane chiral heterojunctions. In the bottom middle figure, the STM image is overlaid with a molecular model showing the chiral morphology indicated by the color (green is right-handed, blue is left-handed). On the bottom right, the difference in charge density of the pinwheel heterojunction and 'isolated' Pn and C60 molecules is shown to reveal the charge transfer between the Pn and the C60 due to the action of the heterojunction (blue (red) is greater (lower) electron density).

Reprinted with permission from J. A. Smerdon, R. B. Rankin, J. P. Greeley, N. P. Guisinger, J. R. Guest, *ACS Nano* 7, 3086 (2013). Copyright 2013 American Chemical Society.

Submitted by Jeffrey R. Guest and Nathan Guisinger (Argonne National Laboratory)

For further information, see abstract on pages 66-69.

Electric fields (in blue) in 6.7M aqueous NaCl (O-red, H-white, Na-blue, Cl-green). Observation of crystalloluminescence suggests that strong electric field fluctuations in the condensed phase can drive changes in electronic structure (e.g., as in Marcus theory). Emission of UV/vis light during these processes is characteristic of the mechanism producing this emission. We find extremely strong E-fields ranging from 5 to 20 GV/m in these electrolytes. By calculating the charge and field fluctuations in aqueous electrolytes we can begin to understand the nature of the driving forces underlying crystallization and associated luminescence.

B. Sellner, M. Valiev, and S.M. Kathmann, *Journal of Physical Chemistry B*, Cover Article, 117, 10869 (2013).

Submitted by Shawn M. Kathmann (Pacific Northwest National Laboratory)

For further information, see abstract on pages 89-92.

Agenda and Abstracts for

CPIMS 9

Ninth Research Meeting of the Condensed Phase and Interfacial Molecular Science (CPIMS) Program

Bolger Conference Center
Potomac, MD
October 20-23, 2013

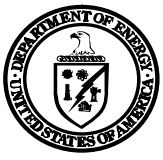

U.S. DEPARTMENT OF ENERGY | Office of Science

Office of Basic Energy Sciences
Chemical Sciences, Geosciences & Biosciences Division

The research grants and contracts described in this document are supported by the U.S. DOE Office of Science, Office of Basic Energy Sciences, Chemical Sciences, Geosciences and Biosciences Division.

FOREWORD

This volume summarizes the scientific content of the Ninth Research Meeting on Condensed Phase and Interfacial Molecular Science (CPIMS) sponsored by the U. S. Department of Energy (DOE), Office of Basic Energy Sciences (BES). The research meeting is held for the DOE laboratory and university principal investigators within the BES CPIMS Program to facilitate scientific interchange among the PIs and to promote a sense of program awareness and identity.

This year's speakers are gratefully acknowledged for their investment of time and for their willingness to share their ideas with the meeting participants. During past CPIMS research meetings, investigators from other research programs have been invited to present their work. The hope is that the cross-fertilization of ideas is promoted, and the invited presentations have been well received. This year, we are pleased to note that Dr. Libai Huang (Notre Dame Radiation Laboratory) has agreed to present her work, which is supported by the Solar Photochemistry program, and complements several of the CPIMS research topics scheduled for presentation on Monday, October 21. We are indebted to Dr. Huang for agreeing to prepare a presentation for CPIMS 9.

This year, to save money and conserve resources, we are disseminating the abstract the book electronically in pdf format with the extensive use of file compression. It is hoped that the resulting visual quality is acceptable to readers.

A recent tradition is the use of the cover of this book to display research highlights from CPIMS-supported research. This year, we have included five research highlights on the cover. These images were selected from highlights submitted by CPIMS investigators during the past year. We thank the investigators for allowing us to place their images on the cover of this book, and we thank all CPIMS investigators who submitted research highlights. CPIMS Investigators are encouraged to submit highlight of their results; we will continue to receive these stories of success with great pride.

We are deeply indebted to the members of the scientific community who have contributed valuable time toward the review of proposals and programs. These thorough and thoughtful reviews are central to the continued vitality of the CPIMS Program. We appreciate the privilege of serving in the management of this research program. In carrying out these tasks, we learn from the achievements and share the excitement of the research of the many sponsored scientists and students whose work is summarized in the abstracts published on the following pages.

Special thanks are reserved for the staff of the Oak Ridge Institute for Science and Education, in particular, Connie Lansdon and Tim Ledford. We also thank Diane Marceau, Robin Felder, and Michaelene Kyler-King in the Chemical Sciences, Biosciences, and Geosciences Division for their indispensable behind-the-scenes efforts in support of the CPIMS program.

Gregory J. Fiechtner, Mark R. Pederson, and Michael P. Casassa
Chemical Sciences, Geosciences and Biosciences Division
Office of Basic Energy Sciences

Agenda

CPIMS 9

U.S. DEPARTMENT OF ENERGY | Office of Science

Office of Basic Energy Sciences
Chemical Sciences, Geosciences & Biosciences Division

Ninth Condensed Phase and Interfacial Molecular Science (CPIMS) Research Meeting

Sunday, October 20

3:00-6:00 pm **** Registration ****
6:00 pm **** Reception (No host, Pony Express Bar & Grill) ****
7:00 pm **** Dinner (Osgood's Restaurant) ****

Monday, October 21

7:30 am **** Breakfast (Osgood's Restaurant) ****

All Presentations Held in Stained Glass Hall

8:30 am *Introductory Remarks*
Gregory J. Fiechtner, DOE Basic Energy Sciences

Session I Chair: **Cynthia J. Jenks**, Ames Laboratory

9:00 am *Controlling Hydrogen Dissociation, Spillover, Storage and Reactivity with Single Atom Alloys*
E. Charles H. Sykes, Tufts University

9:30 am *Many Body and Extrapolation Methods to Obtain Highly Accurate Correlation Energies*
Theresa L. Windus, Ames Laboratory

10:00 am *The Dynamics of the Dissociative Chemisorption of Methane on Ni and Pt Surfaces*
Bret Jackson, University of Massachusetts, Amherst

10:30 am **** Break ****

Session II Chair: **William A. Tisdale**, Massachusetts Institute of Technology

11:00 am *The Role of Fast Charge Dynamics in Heterogeneous Catalysis*
Tanja Cuk, Lawrence Berkeley National Laboratory

11:30 am *Single-Molecule Interfacial Electron Transfer Dynamics*
H. Peter Lu, Bowling Green State University

12:00 noon *Elucidating Energy Relaxation in Single Nanostructures with Ultrafast Microscopy*
Libai Huang, Notre Dame Radiation Laboratory

12:30 pm **** Lunch (Osgood's Restaurant) ****

1:30 pm–4:30 pm Free/Discussion Time

Session III Chair: **Eric O. Potma**, University of California, Irvine

4:30 pm *More New Properties of the Solid and Hollow Surface Plasmonic Nanoparticles*
Mostafa A. El-Sayed, Georgia Institute of Technology

5:00 pm *Recent Advances in Molecular Scale Chemical Imaging*
Mark C. Hersam, Northwestern University

5:30 pm *Spectroscopic Imaging of Molecular Functions at Surfaces*
Wilson Ho, University of California, Irvine

6:00 pm **** Reception (no host, Pony Express Bar & Grill) ****

7:00 pm **** Dinner (Osgood's Restaurant) ****

Tuesday, October 22

7:30 am **** Breakfast (Osgood's Restaurant) ****

Session IV Chair: **Michael A. Duncan**, University of Georgia

8:30 am *Free Radical Reactions at Hydrocarbon Interfaces of Nanoparticles and Droplets*
Kevin R. Wilson, Lawrence Berkeley National Laboratory

9:00 am *Elementary Structural Motifs in Isolated and Carbon Dioxide Doped Ionic Liquids Through Cryogenic Ion Vibrational Predissociation (CIVP) Spectroscopy*
Mark Johnson, Yale University

9:30 am *Experimentally Motivated Simulations of Cluster Anions*
Kenneth D. Jordan, University of Pittsburgh

10:00 am **** Break ****

10:30 am *Laser Spectroscopy of Small Organometallic Radicals and Actinide Molecules*
Michael D. Morse, University of Utah

11:00 am *Experimental and Theoretical Properties of Late Transition Metal Containing Molecules*
Timothy C. Steimle, Arizona State University

11:30 am **** Lunch (Osgood's Restaurant) ****

12:30 pm–4:30 pm Free/Discussion Time

Session V Chair: **Andrei Tokmakoff**, University of Chicago

4:30 pm *Structure and Energetics of Hydrogen Bonded Systems*
Sotiris S. Xantheas, Pacific Northwest National Laboratory

5:00 pm *Water and Room Temperature Ionic Liquids*
Michael D. Fayer, Stanford University

5:30 pm *Solvent-Driven Ionic Processes: Surface Adsorption and Cation-Cation Pairing Studied by X-ray Absorption and UV-SHG Spectroscopy*
Richard J. Saykally, Lawrence Berkeley National Laboratory

6:00 pm **** Reception (No Host, Pony Express Bar & Grill) ****

7:00 pm **** Dinner (Osgood's Restaurant) ****

Wednesday, October 23

7:30 am **** Breakfast (Osgood's Restaurant) ****

Session VI Chair: **James F. Wishart**, Brookhaven National Laboratory

8:30 am *Radiolysis of Aromatic Compounds*
Jay A. LaVerne, Notre Dame Radiation Laboratory

9:00 am *Geminate Recombination in Tetrahydrofuran*
John R. Miller, Brookhaven National Laboratory

9:30 am *Modification of Semiconductor Surfaces Monitored by X-ray Photoelectron Spectroscopy*
Sylwia Ptasinska, University of Notre Dame

10:00 am **** Break ****

10:30 am *Reduction of Nitric Oxide and Reactivity of the Nitroxyl Products*
Sergei Lymar, Brookhaven National Laboratory

11:00 am *Chemistry of Solvated Anion and Radical Species: Ab Initio Simulations in Clusters and Bulk Environments.*
Marat Valiev, Pacific Northwest National Laboratory

11:30 am *Closing Remarks*
Gregory J. Fiechtner, DOE Basic Energy Sciences

12:00 noon **** Meeting Adjourns ****

Table of Contents

TABLE OF CONTENTS

Solar Photochemistry Principal Investigator Abstract

Elucidating Energy Relaxation in Single Nanostructures with Ultrafast Microscopy

Libai Huang
Radiation Laboratory
University of Notre Dame, Notre Dame, IN, 46556

The frontier in renewable energy research now lies in designing mesoscale functionalities from nanostructured and molecular components. One key research challenge is to integrate functional entities across multiple length scales in order to achieve optimal energy flow. To attack the above-mentioned frontier, we aim to understand multiscale energy flow across both multiple length and time scales, coupling simultaneous high spatial, structural, and temporal resolution. In my talk, I will focus on our recent progress on unraveling energy relaxation and propagation pathways in single nanostructures employing ultrafast optical microscopy. The research presented here is supported by the Solar Photochemistry Program at the Chemical Sciences, Geosciences, and Biosciences Division, Office of Basic Energy Sciences.

We have probed environmental-dependent energy relaxation pathways in single nanostructures by single-particle transient absorption microscopy (TAM).[1-3] Figure 1 shows an example of TAM experiments performed on suspended and substrate-supported graphene on SiO_2.[1] We observed that the hot phonon effect occurs at much lower excitation intensity for suspended graphene compared to substrate-supported graphene. These results show the importance of the environment in controlling the properties of graphene.

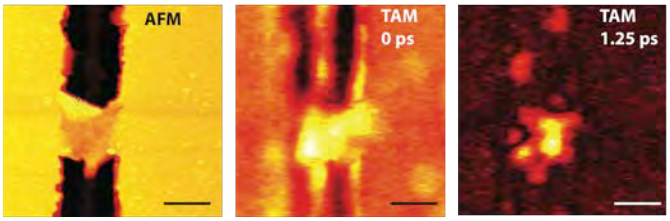

Figure 1 *Correlated AFM and TAM images for suspended graphene at two different delay times. Scale bars: 2 μm*

We have also initiated an investigation into exciton dynamics in graphene-like 2D atomically thin crystals.[2] Femtosecond transient absorption spectroscopy and microscopy were employed to study exciton dynamics in suspended and Si_3N_4 substrate-supported monolayer and few-layer MoS_2 2D crystals. Exciton dynamics for the monolayer and few-layer structures were found to be remarkably different from those of the bulk. Fast trapping of excitons by surface trap states was observed in both monolayer and few-layer structures, pointing to the importance of controlling surface properties in atomically thin crystals such as MoS_2 in addition to controlling their dimensions.[2]

Another challenge in nanotechnology research is inhomogenous distributions of size, shape, and surface properties of nanoparticles in *as synthesized* samples. We have successfully demonstrated structure-specific transient absorption imaging of single-walled carbon nanotubes as a way to investigate intrinsic relaxation pathways.[3] The dielectric screening effects by the substrate induced a ~ 40 meV red-shift of the lowest exciton transition in metallic nanotubes. Energy relaxation in individual metallic nanotubes was observed with decay constants of a few hundred fs and about 10 ps. We attributed the fast and slow decay components to carrier scattering by optical and acoustic phonons, respectively.

(1) Gao, B.; Hartland, G.; Fang, T.; Kelly, M.; Jena, D.; Xing, H. G.; Huang, L. *Nano Lett* **2011**, *11*, 3184.
(2) Shi, H.; Huang, L.; *et.al.*; *ACS Nano* **2013**, *7*, 1072.
(3) Gao, B.; Hartland, G. V.; Huang, L. *J Phys Chem Lett* **2013**, *4*, 3050.

CPIMS
Principal Investigator
Abstracts

Mass Spectrometry Based Approaches to Probe Electronic Structure, Chemical Transformations and Dynamics of Surfaces, Interfaces and Clusters.

Musahid Ahmed
MS 6R-2100, 1 Cyclotron road, Chemical Sciences Division
Lawrence Berkeley National Laboratory, Berkeley, CA 94720
mahmed@lbl.gov

Program scope - Mass spectrometry coupled with synchrotron radiation and ambient ionization methods is being applied to probe chemistry on surfaces, interfaces and clusters in this program. The systems being investigated range from fundamental studies of proton and charge transfer in model systems which are theoretically tractable and extend to imaging mass spectrometry of complex biological and chemical processes.

Recent progress -A core part of the experimental portfolio is to investigate proton and charge transfer in hydrogen bonded, π-stacked and solvated systems using synchrotron based molecular beams mass spectrometry coupled with electronic structure calculations. Proton transfer is ubiquitous in chemistry and biology, but has always been described in the context of hydrogen-bonding networks ("proton wires") acting as proton conduits. We report efficient intramolecular ionization-induced proton transfer across a 1,3-dimethyluracil dimer (DMU), a model π-stacked system with no hydrogen bonds. Upon photoionization by tunable VUV synchrotron radiation, the dimethyluracil dimer undergoes proton transfer and dissociates to produce a protonated monomer. Deuterated DMU experiments confirm that proton transfer occurs from the methyl groups and not from the aromatic C–H sites. Calculations reveal qualitative differences between the proton transfer reaction coordinate in the π-stacked and hydrogen-bonded base pairs, and that proton transfer in methylated dimers involves significant rearrangements of the two fragments, facilitating a relatively low potential energy barrier of only 0.6 eV in the ionized dimer.[1]

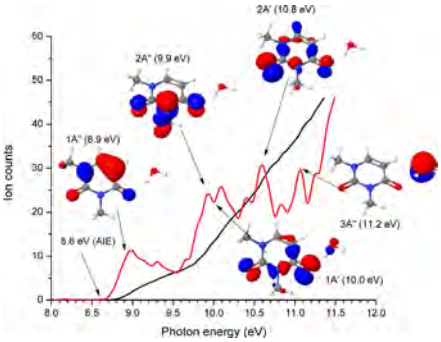

Figure 1: Experimental photoionization efficiency spectra and calculated molecular orbitals and ionization energies for DMU.H_2O (ref. 2, 11)

Water plays a central role in chemistry and biology by mediating the interactions between molecules, altering energy levels of solvated species, modifying potential energy profiles along reaction coordinates, and facilitating efficient proton transport through ion channels and interfaces. We showed that water shuts down ionization-induced proton transfer between DMU dimers, which is very efficient in unsolvated clusters. Instead, a new pathway opens up in which protonated DMU are generated by proton transfer from the ionized water molecule and elimination of a hydroxyl radical. Electronic structure calculations reveal that the shape of the potential energy profile along the proton transfer coordinate depends strongly on the character of the molecular orbital from which the electron is removed; i.e., the proton transfer from water to DMU is barrier less when an ionized state localized on water is accessed. The computed energies of proton transfer is in excellent agreement with the experimental appearance energies. Possible adiabatic passage on the ground electronic state of the ionized system, though energetically accessible at lower energies, is not efficient. Thus, proton transfer is controlled electronically, by the character of the ionized state, rather than statistically, by simple energy considerations.[2] This we believe, provides a novel platform (water wires) to study proton and charge transfer in model well defined systems which are computationally tractable, and will have ramifications in probing aqueous interfaces, membranes, and water in confined spaces.

The ionization of water clusters is of paramount interest in a number of fields spanning biology, chemistry, and physics. Understanding the changes in electronic structure that occur in these ionic clusters is critical to unveil their structure and function and is important in fields as diverse as cloud nucleation in the earth's atmosphere, radiation biology, and catalysis and most important, can act as model systems for understanding solvation. In this program, we used mixed water-Ar clusters to follow charge and exciton transfer. It is revealed that the exciton energy deposited in an argon cluster (Ar_n, $\langle n = 20 \rangle$) using VUV radiation, is transferred to softly ionize doped water clusters ($(H2O)_n$, n = 1−9), leading to the formation of unfragmented clusters. Following the initial excitation, electronic energy is channeled to ionize the doped water cluster while evaporating the Ar shell, allowing identification of fragmented and complete water cluster ions. Examination of the photoionization efficiency curve shows that cluster evaporation from excitons located above 12.6 eV is not enough to cool the energized water cluster ion and leads to their dissociation to $(H2O)_{n-2}H^+$ (protonated) clusters.[3]

Fundamental studies on the photoionization dynamics of both inter and intra hydrogen bonded systems are being performed using alcohols and sugars as a template. It is revealed that the glycerol monomer and dimer has a very high tendency to fragment upon photoionization, which is due to the extremely weakened carbon framework in the glycerol radical cation. A novel six-membered hydrogen-transfer transition state, leading to a common intermediate, comprised of water, formaldehyde and vinyl alcohol radical, which exhibits a very short and strong hydrogen bond was discovered.[4] In the case of deoxyribose, the experimental threshold for neutral water elimination upon ionization is captured well theoretically, and qualitative insights are provided by molecular orbital analysis and molecular dynamics snapshots along the reaction coordinate.[5] These studies are being extended to larger sugars and alcohols.

Synchrotron Laser Desorption Post Ionization (LDPI) mass spectrometry is introduced as a novel analytical tool to characterize the molecular properties of organic compounds in mineral-organic samples, and it is demonstrated that when combined with Secondary Ion Mass Spectrometry (SIMS), can provide complementary information on mineral composition. The combination of synchrotron-LDPI and SIMS shows that the energetic conditions involved in desorption and ionization of organic matter may be a greater determinant of mass spectral signatures than the inherent molecular structure of the organic compounds investigated. The latter has implications for molecular models of natural organic matter that are based on mass spectrometric information.[6]

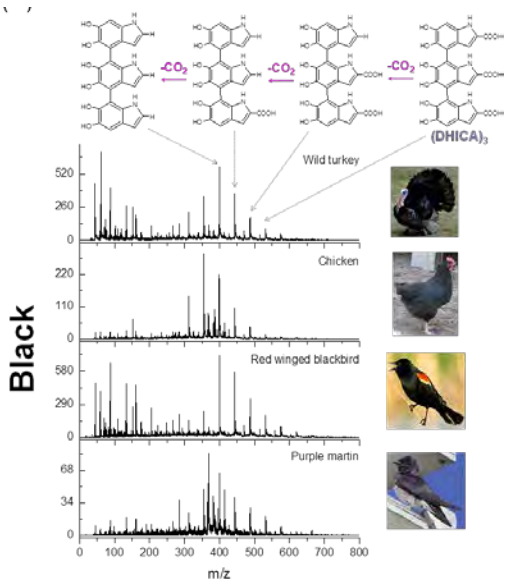

Figure 2: Mass spectra of melanin extracted from bird feathers.

Melanin is the most pervasive and widespread pigment in living organisms and creates a broad range of black, brown and grey colors. Melanin possesses an intriguing set of physical-chemical properties including: broadband monotonic absorbance; extremely low radiative quantum yield; and condensed phase electrical and photoconductivity. This has led to the suggestion that melanin could be useful as a bio-inspired material in applications such as bioelectronics, chemical sensing, and photon detection. Recent work has suggested that melanin does not behave as an amorphous semiconductor and upon hydration allows charge to travel through it via proton transfer. However, although extensive experimental studies have been conducted on both natural and synthetic melanin, the structure, composition, and how these units are put together to form the oligomers of melanin are not well understood, let alone the electronic structure. In this program, synchrotron based laser desorption mass spectrometry has been applied to study the chemical composition of melanin extracts from bird feathers. The mass spectra of melanin exhibits clear and discrete peaks that are expected for macromolecules of various redox forms of 5,6-dihydroxyindole and 5,6-

dihydroxyindole-2-carboxylic acid, which are the two main melanin precursors (see figure 2). So far, 27 melanin samples from black, brown, and grey feathers have been tested, and statistical analysis has been applied to clarify the correlation between the color of the feather and the chemical structure of melanin. Future work will concentrate on elucidating the electronic properties of this intriguing system.

The knowledge gained from studies of fundamental photoionization mechanisms of model biomass compounds (lignin & carbohydrates) are being applied to imaging mass spectrometry. The decomposition of biomass (plant cell wall components) are being imaged with high spatial resolution and molecular specificity. Using synchrotron-LDPI, we have demonstrated imaging using a 30 μm laser spot size from organic surfaces and this lends itself well for extracting mass spectra from individual plant cells which typically are between 20-100 μm in diameter. By decoupling the desorption step from photoionization, it was also demonstrated that imaging resolution of 5 μm could be obtained from a 30 μm laser spot size[7] and has been applied to plant cells. Future work will seek to use these mass spectrometry techniques to understand how surfaces impact the thermal and laser decomposition of biomass.

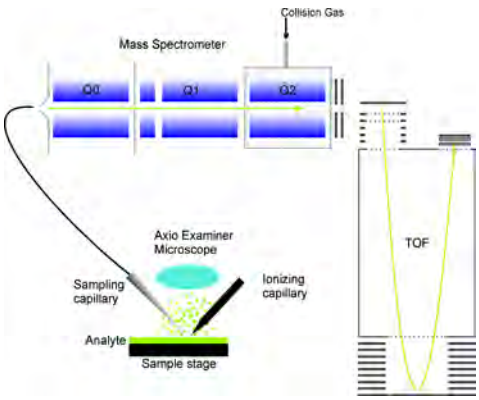

Figure 3: Correlated ambient pressure mass spectrometry and fluorescence microscopy experimental platform.

Future plans- A novel experimental platform to perform chemical imaging under ambient conditions is being developed. Nanospray Desorption Electrospray Ionization (nanoDESI) is a liquid-extraction surface sampling method in mass spectrometry performed under ambient conditions. This approach facilitates the work with nanogram-sized samples, enabling direct analysis of small molecules as well as large molecules off surfaces, e.g. living plants, without any sample preparation. This technique will be applied to probe reactive surfaces and interfaces. In addition, nanoDESI-MS is being combined with fluorescence microscopy to acquire multi-dimensional data, to provide insights into sample components, distribution and reaction mechanisms under ambient and aqueous conditions. Initial experiments will focus on probing interfacial chemical transformations of biomass (sugars, lignin, etc.) with ionic liquids and mesoporous catalysts.

The dynamics of proton and charge transfer in solvated systems that arise upon electronic excitation will be investigated with a recently commissioned molecular beams velocity map imaging (VELMI) apparatus coupled with a delay line anode detector. The first experiments being performed are to visualize the excited states of water clusters using a unique combination of a high rep. rate laser system synchronized to the ALS (Figure 4). In the last year, two laser systems have been commissioned to this end. One is a 150 kHz tunable IR-OPO 10 ns pulse-width laser, and the other, an fixed wavelength 8 MHz UV/Vis Nd:YAG 10 ps pulse-width laser. While the use of these lasers has so far been limited to testing, calibration, and integration with the molecular beams apparatus, their application is to investigate the dynamics of a plethora of chemical systems. This becomes especially interesting when multiple laser systems are used in tandem with synchrotron radiation to perform a range of three-color experiments. In these three-color experiments, a third photon may be used to selectively depopulate vibrational/electronic states in an excited or ground-state manifold thus depleting ion/electron signal generated from two-color excitation processes. Such action spectroscopies are especially useful in gleaning information from states that are too short-lived or dissociative.

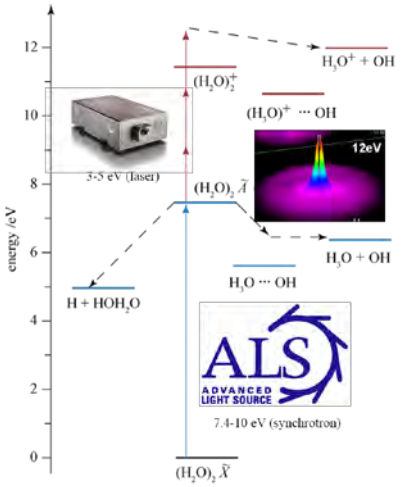

Figure 4: Schematic illustrating two color synchrotron/laser excitation for imaging the excited states of the water dimer.

The future plan involving the VELMI spectrometer includes extensive photoemission studies of a wide variety of chemical and biological species using VUV and/or laser radiation. First focus will be to study the photoionization dynamics of ionic liquids. The rich hydrogen bonded polymeric network of cations and anions in ionic liquids, also known as "zwitterionic supramolecules", makes them attractive candidates to understand inter and intra hydrogen bonded interactions at the fundamental level. Subsequently their interactions with biomass (sugars & lignin) will be probed via these techniques, as ionic liquids have the potential of breaking down cellulosic biomass for enzymatic hydrolysis into fermentable sugars. While these systems have been studied from a chemical engineering point of view, a molecular level understanding is severely lacking. Our previous experiences with VELMI of nanomaterials showed that the imaging experiments provide useful insights on the electronic structures, EM fields and photoionization dynamics.[8] In order for studying various species in the gas phase, we will incorporate aerosol, electrospray ionization (ESI) and atmospheric pressure chemical ionization (APCI) sources to the present molecular beams-VELMI set up. The tunable light from the synchrotron will be used to photoionize a molecular beam of interest in order to obtain photoelectron spectra and angular distributions. These advances in experimental techniques will afford novel insight into the electronic structure and charge transfer in molecules, clusters and interfaces.

Papers citing CPIMS-DOE support. (2011 to present)

1. A. Golan, K. B. Bravaya, R. Kudirka, O. Kostko, S. R. Leone, A. I. Krylov, and M. Ahmed. *"Ionization of stacked dimethyluracil dimers leads to facile proton transfer in the absence of H-bonds,"* Nature Chem. (2012) 4, 323

2. K. Khistyaev, A. Golan, K. B. Bravaya, N. Orms, A. I. Krylov, and M. Ahmed, *"Proton transfer in nucleobases is mediated by water,"* J. Phys. Chem. A, In press

3. A. Golan and M. Ahmed, *"Ionization of water clusters mediated by exciton energy transfer from argon clusters,"* J. Phys. Chem. Lett. (2012) 3, 458

4. F. Bell, Q. N. Ruan, A. Golan, P. R. Horn, M. Ahmed, S. R. Leone, and M. Head-Gordon, *"Dissociative Photoionization of Glycerol and its Dimer Occurs Predominantly via a Ternary Hydrogen-Bridged Ion-Molecule Complex"* J. Am. Chem. Soc. In press

5. D. Ghosh, A. Golan, L. Takahashi, A.I. Krylov and M. Ahmed *"A VUV photoionization and Ab initio determination of the ionization energy of a gas-phase sugar (deoxyribose),"* J. Phys. Chem. Lett. (2012) 3, 97

6. S-Y. Liu, M. Kleber, L. K. Takahashi, P. Nico, M. Keiluweit, and M. Ahmed, *"Synchrotron based mass spectrometry to investigate the molecular properties of mineral-organic associations,"* Anal. Chem. (2013) 85, 6100

7. O. Kostko, L. K. Takahashi, and M. Ahmed. *"Desorption Dynamics, Internal Energies and Imaging of Molecules from Surfaces with Laser Desorption and Vacuum Ultraviolet (VUV) Photoionization,"* Chem. Asian. J. (2011) 6, 3066

8. M. J. Berg, K. R. Wilson, C. Sorensen, A. Chakrabarti, and M. Ahmed, *"Discrete Dipole Approximation Model for Low-Energy Photoelectron Emission from NaCl Nanoparticles,"* J. Quant. Spectrosc. Radiat. Transfer (2012) 113, 259

9. A. Golan and M. Ahmed, *"Molecular beam mass spectrometry with tunable vacuum ultraviolet (VUV) synchrotron radiation,"* J. Vis. Exp. (2012) 68, e50164

10. L.K. Takahashi, J. Zhou, O. Kostko, A. Golan, S. R. Leone and M. Ahmed, *"VUV Photoionization and Mass Spectrometric Characterization of the Lignin Monomers Coniferyl and Sinapyl Alcohol,"* J. Phys. Chem. A (2011) 115, 3279

11. K. Khistyev, K. B. Bravaya, E. Kamarchik, O. Kostko, M. Ahmed, and A. I. Krylov, *"The effect of microhydration on ionization energies of thymine,"* Faraday Disc. (2011) 150, 313

12. M. T. Blaze, L.K. Takahashi, J. Zhou, M. Ahmed, F. D. Pleticha, and L. Hanley, *"Brominated Tyrosine and Polyelectrolyte Multilayer Analysis by Laser Desorption VUV Postionization and Secondary Ion Mass Spectrometry,"* Anal. Chem. (2011) 83, 4962

Model Catalysis by Size-Selected Cluster Deposition

PI: Scott L. Anderson
Chemistry Department, University of Utah
315 S. 1400 E. Rm 2020
Salt Lake City, UT 84112
anderson@chem.utah.edu

Program Scope

The goal of our research is to explore correlations between supported cluster size, electronic and morphological structure, the distributions of reactant binding sites, and catalytic activity, for model catalysts prepared using size-selected metal cluster deposition. The work to date has focused on catalysts with catalytically active metal clusters deposited on metal oxide supports, and on electrocatalysis by metal clusters on glassy carbon electrodes.

The experimental setup is quite flexible. The instrument has a mass-selecting ion deposition beamline fed by a laser vaporization source that produces high fluxes at low deposition energies (~10^9 Pd_{10}/sec in a 2 mm diameter spot at 1 eV/atom, for example). Typical samples with 0.1 ML-equivalent of metal, deposited in the form of M_n^+ can be prepared in 2 to 5 minutes, and our analysis methods are also quite fast. Speed is important, because even in UHV these samples are highly efficient at collecting adventitious contaminants, due to substrate-mediated adsorption. Sample morphology is probed by low energy He^+ ion scattering (ISS), electronic structure is probed by x-ray and UV photoelectron spectroscopy and ion neutralization spectroscopy (XPS, UPS, INS), and reactivity is studied using a differentially pumped mass spectrometer surrounded by a cluster of pulsed and cw gas inlets that can be used to dose the sample while various temperature programs are executed.

The main UHV analysis chamber has a port in the bottom, equipped with a gate valve and a triple differential seal. One of several interchangeable small chambers with their own pumping systems can be connected here, and when the sample is positioned in the lower chamber is it isolated from the main UHV system. This lower chamber is used for high pressure procedures such as alumina film growth or *in situ* electrochemical studies, and also as a load-lock.

Recent Progress

Electronic Structure - Activity Correlations

We previously demonstrated[1] a one-to-one correlation between the binding energy of the Pd 3d core level, and the activity for CO oxidation of $Pd_n/TiO_2(110)$. Correlations between core level energies and activity have also been found for electrooxidation of carbon by water over Pt_n,[2] and CO oxidation over Pd_n deposited on several types of alumina films.[3-4] Recently we have been measuring valence level binding energies using UPS, for comparison to the core level energetics, since one would expect the chemistry to be controlled by valence electronic structure. One of the measures of interest is the position of the top of the metal filled states, relative to the Fermi level (E_F) of the sample. For these studies, we take advantage of the fact that the onset of the bands associated with the metal clusters is in the band gap of the TiO_2 or alumina, so that it can be studied without interference from the O 2p band of the oxide support. In addition to providing another way of looking at electronic structure-activity correlations, in cases where XPS is difficult due to high background from the support (e.g., Pt/alumina/Re(0001)), UPS produces a measure of electronic properties.

Pd_n/TiO_2: Figure 1 shows the correlation between the Pd 3d binding energy measured by XPS, and the top of the Pd filled levels measured by UPS, for samples with 0.1 ML-equivalent of Pd deposited on rutile $TiO_2(110)$ in the form of different size Pd_n. The valence information is given as the shift with respect to E_F, and the XPS results are given as shifts relative to the Pd 3d binding energy in bulk Pd. In both cases there is a systematic decrease in binding energy with increasing cluster size, expected from consideration of final state charging/screening in small clusters on an insulating support. Superimposed, are oscillations in the binding energies that give insight into the initial state electronic structure. Clearly, the two measures of electronic properties are generally well correlated, which presumably explains why XPS is

correlated with activity.

In addition to the onset energy trends, we also see qualitative changes in the shapes of the Pd band with increasing cluster size. For Pd_n, $n \leq 10$, the growth of Pd density of states (DOS) with energy below E_F is slow, while for all larger clusters, there is higher DOS near E_F, then the DOS levels off deeper in the band. This distinctly different behavior for clusters with more or less than 10 atoms is interesting in light of evidence from an earlier ISS study[1] which suggested that Pd morphology changes from single layer islands to multilayer structures for sizes above 10 atoms. We also have used UPS to examine how the Pd_n band onsets and shapes change as the clusters are exposed to O_2 and CO reactants, and after completion of temperature-programmed reaction experiments. It is found that O_2 exposure (10 L at 400 K) has relatively little effect on the Pd band, while CO exposure significant depletes the DOS in the near-E_F region of the spectra, shown for Pd_7 in Figure 2. This effect of CO binding is in good agreement with DFT results from Ping Liu[5] shown in the inset to the figure. In agreement with our TD-ISS results,[6] it was found that the first few CO molecules on Pd_7 adsorb strongly on top of the cluster, and that when these sites are saturated, additional CO binds more weakly around the periphery of the cluster. Interestingly, the DFT results show that it is these last few COs that have the largest effect on the Pd 4d band.

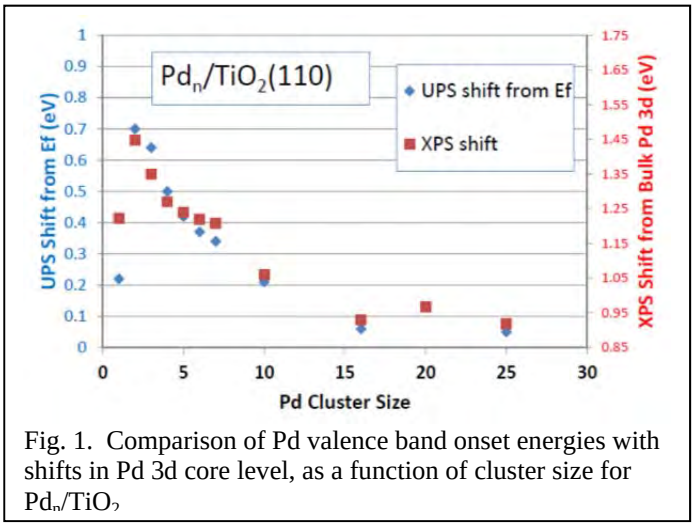

Fig. 1. Comparison of Pd valence band onset energies with shifts in Pd 3d core level, as a function of cluster size for Pd_n/TiO_2

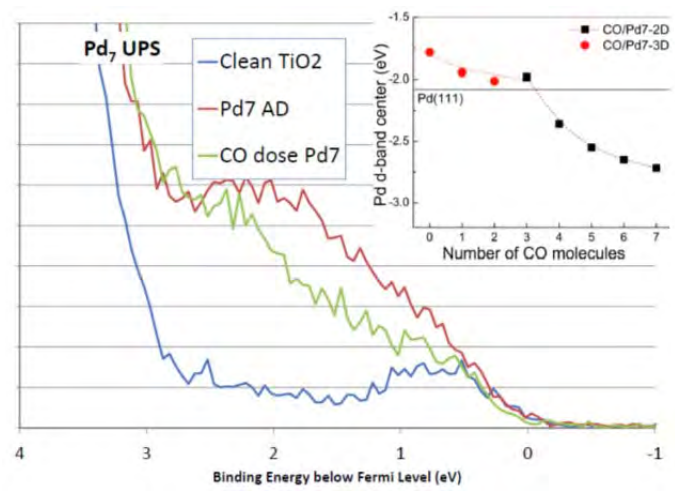

Fig. 2. Main: Near-E_F spectrum of TiO_2, Pd_7/TiO_2, and Pd_7/TiO_2 after saturation CO exposure. Inset: Results of Liu, showing that the Pd 4d band center drops upon adsorption of the last few CO molecules.

Pd_n/alumina: Similar CO oxidation studies were carried out on Pd clusters deposited on alumina films of controlled thicknesses, grown on both Ta(110) and Re(0001). On both substrates, the thickness of the alumina film was found to tune the CO oxidation chemistry for films thinner than ~4 nm, but thicker films were found to give thickness-independent chemistry. We, therefore, have used films with ~5 nm thickness for the size-dependent studies. CO oxidation on these samples is substantially more efficient than on Pd/TiO_2, and as might be expected for an efficient reaction, the activity is only weakly dependent on cluster size, oxidation temperature, and other variables we have tested. The activity varies by only ~25% for different cluster sizes, as opposed to the factor of eight variation seen for Pd/TiO_2. Nonetheless, there does still seem to be a correlation between the Pd 3d binding energy and the activity. We have also completed a detailed UPS study of Pd_n/alumina/Re(0001), and are collaborating with Shiv Khanna on a joint experimental/computational analysis of the electronic structure as a function of size and adsorbate binding.

Pt_n/alumina/Re(0001): We are just completing a detailed study of CO oxidation with UPS analysis of electronic structure, and ISS probing of sample morphology, for Pt_n deposited on 5 nm alumina grown on

Re(0001). Activity in this system is strongly size dependent, varying by a factor of ~9 from Pt_2 (the least reactive) to Pt_{14} (the most reactive). There is some evidence for a change to 3D morphology for clusters larger than Pt_7, but there is no one-to-one correlation with activity. The UPS measurements (which are done separately to avoid contamination of the as-deposited clusters) are still underway, but it is clear that there are size effects on the metal band onset energy, and strong effects of adsorbate binding. One other point about this system is that the clusters sinter rapidly at temperature above 300 K, and for deposited Pt atoms, sintering is rapid even at temperatures below 180 K.

Electrochemistry studies: At last year's meeting, initial results were presented showing strong size dependence for electrochemical activity of Pt_n deposited on glassy carbon substrates, and studied in N_2- and O_2-saturated $HClO_4$ electrolyte without air exposure. This experiment was completed and published this year.[2] Air exposure was found to passivate the samples, and for such small clusters, it was not possible to remove adventitious adsorbates by electrochemical cleaning, as is typically done in electrochemistry work. Some clusters (7, 10, 11 atoms) showed normal looking oxygen reduction reaction (ORR) activity, but most of the small clusters showed, instead, very high activity for carbon oxidation by water. The switch between ORR and carbon oxidation was correlated with the Pt 4f binding energy, measured by XPS after cluster deposition. Oxidation of carbon electrodes (also known as carbon corrosion) is a serious problem in fuel cells, however, for conventional Pt nanoparticle electrodes, it is a slow process in the potential range of interest for oxygen reduction. Our results raise the question of whether small clusters that form during fuel cell operation may be responsible for this degradation mechanism.

To further this effort in *in situ* size-dependent electrochemistry, we have improved our cluster source to generate clusters containing up to 18 Pt atoms, compared to 11 in the previous work. This will allow us to work in a size range similar to that studied by the Arenz group (although they are not able to avoid air exposure).[7] In addition, we have developed a new *in situ* electrochemical cell. The original cell had the working (cluster) electrode and counter electrode in a single 15 μL compartment, with the Ag/AgCl reference electrode in a separate compartment, communicating via a small fritted glass plug, to minimize interdiffusion of the electrolytes in the two compartments. To reduce the possibility of contamination of the cluster electrode by species generated at the counter electrode, the new cell has all three electrodes in their own compartments, communicating via small frits, as shown in figure 3. For scale, the diameter of the working compartment is 3 mm. The working and reference electrode compartments both have ports where gases generated in the cell can vent, and I plan to develop capability to monitor these by online mass spectrometry. We are just completing bench-top testing of this new cell, and expect to begin a new set of experiments with deposited clusters in early September. In addition to the new cell, we have also prepared and bench-top tested the use of indium tin oxide (ITO) substrates for the working electrode in methanol oxidation and ORR. ITO will allow us to more easily observe the electrochemistry for those clusters that are active for oxidation of glassy carbon electrodes.

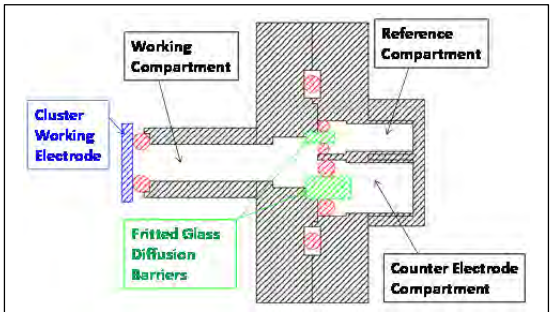

Fig. 3. Three compartment cell constructed of PEEK

Future Plans

In September, we will start a new set of electrochemistry experiments. I plan to test several reactions to see what has interesting cluster size effects, and then we will concentrate on those. Candidate reactions include ORR over Pt/ITO and Pt/glassy carbon, CO_2 reduction over Cu/carbon, Cu/ITO, Au/carbon, and Au/ITO, water splitting over Pt/ITO and Pt/carbon, and methanol oxidation over Pt/carbon and Pt/ITO. In parallel, we will continue gas-surface UHV experiments looking at correlations between activity and adsorbate binding energies, with morphology and electronic structure. We will focus on systems that are as closely analogous as possible to the electrochemical systems chosen for study.

References Cited:

(1) Kaden, W. E.; Wu, T.; Kunkel, W. A.; Anderson, S. L., *Science* **2009,** *326*, 826-9.
(2) Proch, S.; Wirth, M.; White, H. S.; Anderson, S. L., *J. Am. Chem. Soc.* **2013,** *135*, 3073−3086.
(3) Wu, T.; Kaden, W. E.; Kunkel, W. A.; Anderson, S. L., *Surface Science* **2009,** *603*, 2764-2770.
(4) Kane, M. D.; Roberts, R. S.; Anderson, S. L., *Faraday Disc.* **2013,** *162*, 323 - 340.
(5) Liu, P., *J. Phys. Chem. C* **2012,** *116*, 25337−25343.
(6) Kaden, W. E.; Kunkel, W. A.; Roberts, F. S.; Kane, M.; Anderson, S. L., *J. Chem. Phys.* **2012,** *136*, 204705/1-204705/12.
(7) Nesselberger, M.; Ashton, S.; Meier, J. C.; Katsounaros, I.; Mayrhofer, K. J. J.; Arenz, M., *Journal of the American Chemical Society* **2011,** *133*, 17428-17433.

Recent Publications acknowledging DOE support

"Size-dependent oxidation of Pd_n ($n \leq 13$) on alumina/NiAl(110): Correlation with Pd core level binding energies." Tianpin Wu, William E. Kaden, William A. Kunkel, and Scott L. Anderson, Surf. Sci. 603 (2009) 2764-77.

"Electronic Structure Controls Reactivity of Size-Selected Pd Clusters Adsorbed on TiO_2 Surfaces", William E. Kaden, Tianpin Wu, William A. Kunkel, Scott L. Anderson, Science. 326 (2009) 826 - 9.

"CO Adsorption and Desorption on Size-Selected Pd_n/TiO_2 Model Catalysts: Size Dependence of Binding Sites and Energies, and Support-Mediated Adsorption" William E. Kaden, William A. Kunkel, F. Sloan Roberts, Matthew Kane and Scott L. Anderson, J. Chem. Phys. 136 (2012) 204705 12 pages, doi: 10.1063/1.4721625

"Strong effects of cluster size and air exposure on oxygen reduction and carbon oxidation electrocatalysis by size-selected Pt_n ($n \leq 11$) on glassy carbon electrodes", Sebastian Proch, Mark Wirth, Henry S. White, and Scott L. Anderson, J. Am. Chem. Soc. **135** (2013) 3073−3086, DOI: 10.1021/ja309868z

"Alumina support and Pd_n cluster size effects on activity of Pd_n for catalytic oxidation of CO", Matthew D. Kane, R. Sloan Roberts, and Scott L. Anderson, Faraday Disc., 162 (2013) 323 - 340, DOI: 10.1039/c3fd20151a

FUNDAMENTAL ADVANCES IN RADIATION CHEMISTRY

Principal Investigators:

DM Bartels (bartels.5@nd.edu), I Carmichael, DM Chipman, I Janik, JA LaVerne, S Ptasińska
Notre Dame Radiation Laboratory, University of Notre Dame, Notre Dame, IN 46556

SCOPE

Research in fundamental advances in radiation chemistry is organized around two themes. First, energy deposition and transport seeks to describe how energetic charged particles and photons interact with matter to produce tracks of highly reactive transients, whose recombination and escape ultimately determine the chemical effect of the impinging radiation. The work described in this part is focused on fundamental problems specific to the action of ionizing radiation. Particular projects include measurement of radiolytic product yields in low temperature aqueous ices, experimental study and theoretical treatment of the VUV spectrum of water up to supercritical conditions, investigation of spur and track recombination and radiolytic yields in aromatic hydrocarbon liquids and the determination of recombination and yields in various supercritical fluids. The second thrust deals with structure, properties and reactions of radicals in condensed phases. Challenges being addressed include the experimental and theoretical investigation of solvated electron reaction rates, measurement of radical reaction rates as a function of density in supercritical fluids, theoretical characterization of free radical structure and solvation, and time-resolved resonance Raman investigation of free radical transients.

PROGRESS AND PLANS

With a view toward a better understanding of changes in the peak position and shape of the first absorption band of water with condensation or temperature, results from electronic structure calculations using high level wavefunction based and time-dependent density functional methods have been obtained for water pentamers. Excitation energies, oscillator strengths, and redistributions of electron density have been determined for the quasitetrahedral water pentamer in its C_{2v} equilibrium geometry and for many pentamer configurations sampled from a molecular simulation of liquid water. Excitations associated with surface molecules have been removed in order to focus on those states associated with the central molecule, which are the most representative of the liquid environment. The effect of hydrogen bonding on the lowest excited state associated with the central molecule was studied by adding acceptor or donor hydrogen bonds to tetramer and trimer substructures of the C_{2v} pentamer, and by sampling liquid-like configurations having an increasing number of acceptor or donor hydrogen bonds of the central molecule. The results provide clear evidence that the blueshift of excitation energies upon condensation is essentially determined by acceptor hydrogen bonds, and the magnitudes of these shifts are determined by the number of such, whereas donor hydrogen bonds do not induce significant shifts in excitation energies. Based on these results, it is concluded that the peak position of the first absorption band is mainly determined by the relative distribution of single and double acceptor hydrogen bonding environments, whereas the shape of the first absorption band is mainly determined by the relative distribution of acceptor and broken acceptor hydrogen bonding environments.

Vacuum ultraviolet (VUV) absorption measurements of hydrogen bonding and non-hydrogen bonding fluids in sub- and supercritical conditions were carried out at the Synchrotron Radiation Center, University of Wisconsin. The VUV absorption apparatus that was successfully used in studies of the first absorption band of supercritical water was applied to measurements of charge

transfer to solvent (CTTS) absorptions in a series of aqueous solutions of simple inorganic anions. The peak of CTTS absorption spectrum of hydroxide ions in light water shifts red by about ~0.6 eV as a function of temperature between room temperature and 350 ºC. At the same time its half width increases from 0.76 to 1.2 eV Analogous results were obtained in studies of aqueous solutions of halide anions: iodide (I^-), bromide (Br^-) and chloride (Cl^-). In supercritical aqueous solutions of I^- at 392 ºC a slight blue shift (~0.05 eV) was observed upon decrease of the density of supercritical fluid in the pressure range 270-210 bar. The red shift observed in subcritical solutions of simple anions as a function of increasing temperature (decreasing density) can be related to the weakening of the hydrogen bonding network, likely destabilizing the ground state. The nature of the blue shift in supercritical conditions remains unclear at the moment and requires further studies.

The hydrated electron solvation structure has been debated for decades and the debate continues with competing MD simulations in the past several years. In principle the EPR spectrum should play a role in this debate, but because there is only a single exchange-narrowed line it has been difficult to make qualitative use of this measurement. In the past year we have measured significant change in the hydrated electron g-factor as a function of temperature. The experiment shows that the e^-_{aq} *g*-factor increasingly deviates from the free electron *g*-factor (2.00232) with temperature up to 190°C. To explain any reduction in g-factor from the vacuum value, the electron orbital must have some non-zero angular momentum character, presumably from interaction with water oxygen atoms. The decreasing *g*-factor near ambient condition is usually interpreted as the electron being delocalized over a larger number of water molecules. Above 190°C one can see an opposite behavior, which we assume will continue as at the limit of zero density the electron *g*-factor must reach that of free electron. Without application of a model it is not immediately obvious how this data relates to the ongoing debate regarding the solvation structure of the hydrated electron. It is certain that any "final" model of the hydrated electron structure will need to reproduce these results.

A program to investigate radiolysis reactions of transition metal cations $(M^{2+})_{aq}$ was continued during this year to support studies of nuclear reactor corrosion. Metal ions chosen for study are the aqueous (mostly hexa-aquo) complexes of Mn^{2+}, Fe^{2+}, Co^{2+}, Ni^{2+}, Cu^{2+} and Zn^{2+}. Rate constants for reaction of the metal ions with hydrated electron up to 300 °C, were reported last year. Even though some of the reactions approach diffusion control at room temperature, it could be clearly determined on the basis of the temperature dependence that e^-_{aq} reactions with all of the metal complexes are activation controlled. The most astonishing aspect of this series of reactions is their very large pre-exponential factors, as high as 8×10^{15} M^{-1} s^{-1} for reduction of Zn^{2+}. To understand these reactions, it is first essential to know the energetics of the reduction process. The reduction potential of the hydrated electron is well established as -2.9 V relative to SHE, but we were surprised to find that except for Cu(I), reduction potentials for the M^{+1}/M^{+2} redox couples are not known. Experiments are underway to narrow the range of uncertainty. If we apply Marcus theory to these reactions and their activation energies, we require extraordinarily large reorganization energies. However, it is difficult to rationalize the very large pre-exponential factors in terms of Marcus theory. Generally a very large pre-exponential factor must be explained in terms of a large positive activation entropy. Marcus electron transfer theory essentially discounts entropy as a major effect.

A new radiation source, an atmospheric pressure plasma jet (APPJ), was used to induce chemistry on silicon (Si) wafers. Hydrofluoric acid pre-treated Si wafers, from which hydrocarbons and silica were totally removed, were irradiated with a helium APPJ at ambient air conditions. Reactive species in the helium APPJ produced amorphous silicon oxynitride (SiN_xO_y) films on the silicon wafer. The growth of SiN_xO_y was monitored by X-ray photoelectron spectroscopy (XPS). The XPS spectra showed the presence of nitride species with binding energy at 398 eV formed upon the APPJ treatment. The spectra taken from different areas of the Si wafers indicated that the formation of nitrides is highly localized due to direct interactions with the plasma jet. Along with an increase of N1s XPS signal, a considerable decrease of C1s signal was observed. It has been estimated that using common chemical methods of contamination removal can remove up to 80% of carbon-containing impurities while 5 min of APPJ treatment removes up to 95%. Several nitrogen containing gases such as N_2, N_2O, NO and NH_3 were doped into the helium stream in order to increase the concentration of reactive nitrogen species in the APPJ. Nitrogen or ammonia gas mixed with helium produced the highest intensity of the nitride signal. In future work the optical emission spectra of the APPJ will be measured to characterize the chemistry in the plasma jet for these different mixtures to understand the nitride formation mechanism by the plasma reactive species. Besides APPJ treatment of solid materials the chemistry in plasma-irradiated liquids will be also investigated.

A low energy electron beam has been used to irradiate different ratios of nitrogen and methane mixtures embedded in ultracold helium droplets, producing a variety of species detected with a high resolution time-of-flight mass spectrometer. The geometrical structures and binding energies of the homogeneous and heterogeneous species formed have been studied with high level electronic structure calculations. Notably, the calculations show that synthesis of a CN chemical bond occurs to form $CH_3N_2^+$. The formation of CN bonds in organic molecules can be important for understanding atmospheric chemistry, particularly in Titan's atmosphere. A number of other structures with hydrocarbon fragments bound to one or two nitrogen molecules have also been fully characterized.

Radiation chemistry studies of simple alcohol ices condensed on aluminum have been performed in order to understand the role of interfaces. A high vacuum ice chamber was used to condense various simple alcohols onto the surface of alumina. Typical thicknesses of the ice samples were on the order of 50 nm. Radiolytic degradation by 1 keV electrons was followed *in situ* by infrared spectroscopy. Methanol, ethanol and isopropanol all show formation of CO and CO_2 at 77K due to the complete dissociation of the parent compounds. Each alcohol also produces traces of a carbonyl due to the conversion of the alcohol group. This process should at least begin with the formation of an H atom, which could then lead to molecular hydrogen formation. Quantification of gas formation was not yet available with the ice chamber so molecular hydrogen formation was examined conventionally from frozen methanol, ethanol, and isopropanol. Molecular hydrogen yields were found to be slightly lower at 77 K than at room temperature presumably because of geminate recombination. Gas formation in combination with IR spectroscopy will be very useful for the mechanistic evaluation of the medium decomposition so the ice chamber will soon be equipped with a mass spectrometer for temperature programmed desorption studies.

PUBLICATIONS WITH BES SUPPORT SINCE 2011

Baidak A.; Badali M.; LaVerne J.A. *J. Phys. Chem. A.* **2011**, **115**, 7418-27 Role of the low-energy excited states in the radiolysis of aromatic liquids.

Balcerzyk A.; LaVerne J.A.; Mostafavi M. *J. Phys. Chem. A.* **2011**, **115**, 4326-33 Direct and indirect radiolytic effects in highly concentrated aqueous solutions of bromide.

Chipman D.M. *J. Phys. Chem. A* **2011**, **115**, 1161-71 Hemibonding between hydroxyl radical and water.

Ferreira da Silva F.; Ptasinska S.; Denifl S.; Gschliesser D.; Postler J.; Matias C.; Mark T.D.; Limao-Vieira P.; Scheier P. *J. Chem. Phys.* **2011**, **135**, 174504-1--7 Electron interaction with nitromethane embedded in helium droplets: attachment and ionization measurements.

Hug G.L.; Mozumder A. Electron localization and trapping in liquid hydrocarbons: The Anderson model. In *Charged Particle and Photon Interactions with Matter: Recent Advances, Applications, and Interfaces*; Hatano, Y., Katsumura, Y., Mozumder, A., Eds.; CRC Press, Taylor & Francis Group: Boca Raton, FL, 2011; pp 209-35.

Ptasinska S.; Gschliesser D.; Bartl P.; Janik I.; Scheier P.; Denifl S. *J. Chem. Phys.* **2011**, **135**, 214309-1--6 Dissociative electron attachment to triflates.

Roth O.; LaVerne J.A. *J. Phys. Chem. A* **2011**, **115**, 700-8 Effect of pH on H_2O_2 production in the radiolysis of water.

Schmitt C.; LaVerne J.A.; Robertson D.; Bowers M.; Lu W.T.; Collon P. *Nucl. Instr. Meth. Phys. Res., Sect. B* **2011**, **269**, 721-8 Target dependence for low-Z ion charge state fractions.

do Couto P.C.; Chipman D.M. *J. Chem. Phys.* **2012**, **137**, 184301 Insights into the ultraviolet spectrum of liquid water from model calculations: the different roles of donor and acceptor hydrogen bonds in water pentamers.

El Omar A.K.; Schmidhammer U.; Rousseau B.; Laverne J.A.; Mostafavi M. *J. Phys. Chem. A* **2012**, **116**, 11509-18 Competition reactions of $H_2O^{\bullet+}$ radical in concentrated Cl^- aqueous solutions: picosecond pulse radiolysis study.

Jheeta S.; Ptasinska S.; Sivaraman B.; Mason N.J. *Chem. Phys. Lett.* **2012**, **543**, 208-12 The irradiation of 1:1 mixture of ammonia:carbon dioxide ice at 30 K using 1 keV electrons.

LaVerne J.; Baidak A. *Radiat. Phys. Chem.* **2012**, **81**, 1287-90 Track effects in the radiolysis of aromatic liquids.

Patterson L.K.; Mazière J.-C.; Bartels D.M.; Hug G.L.; Santus R.; Morlière P. *Amino Acids* **2012**, **42**, 1269-75 Evidence for a slow and oxygen-insensitive intra-molecular long range electron transfer from tyrosine residues to the semi-oxidized tryptophan 214 in human serum albumin: Its inhibition by bound copper(II).

Chipman D.M. *J. Phys. Chem. B* **2013**, **117**, 5148-55 Water from ambient to supercritical conditions with the AMOEBA model.

El Omar A.K.; Schmidhammer U.; Balcerzyk A.; LaVerne J.; Mostafavi M. *J. Phys Chem. A.* **2013**, **117**, 2287-93 Spur reactions observed by picosecond pulse radiolysis in highly concentrated bromide aqueous solutions.

Janik I.; Marin T.W. *Nucl. Instr. Meth. Phys. Res. A* **2013**, **698**, 44-8 A vacuum ultraviolet filtering monochromator for synchrotron-based spectroscopy.

Janik I.; Tripathi G.N.R. *J. Chem. Phys* **2013**, **139**, 014302 The nature of the superoxide radical anion in water.

Janik I.; Tripathi G.N.R. *J. Chem. Phys* **2013**, **138**, 44506-1-4 The early events in the OH radical oxidation of dimethyl sulfide in water.

Jheeta S.; Domaracka A.; Ptasinska S.; Sivaraman B.; Mason N.J. *Chem. Phys. Lett.* **2013**, **556**, 359-64 The irradiation of pure CH_3OH and 1:1 mixture of NH_3:CH_3OH ices at 30 K using low energy electrons.

Klas M.; Ptasinska S. *Plasma Sources Sci. Technol.* **2013**, **22**, 025013 Characteristics of N_2 and N_2/O_2 atmospheric pressure glow discharges.

Mozumder A.; Wojcik M. *Radiat. Phys. Chem.* **2013**, **85**, 167-72 Initial electron-ion distance distribution in irradiated high-mobility liquids: Application of the metropolis method.

Nuzhdin K.; Bartels D.M. *J. Chem. Phys* **2013**, **138**, 124503-1-8 Hyperfine coupling of the hydrogen atom in high temperature water.

Surface Chemical Dynamics

N. Camillone III and M. G. White
Brookhaven National Laboratory, Chemistry Department, Building 555, Upton, NY 11973
(nicholas@bnl.gov, mgwhite@bnl.gov)

1. Program Scope

This program focuses on fundamental investigations of the dynamics, energetics and morphology-dependence of thermal and photoinduced reactions on planar and nanostructured surfaces that play key roles in energy-related catalysis and photocatalysis. Laser pump-probe methods are used to investigate the dynamics of interfacial charge and energy transfer that lead to adsorbate reaction on metal and metal oxide surfaces. State- and energy-resolved measurements of the gas-phase products are used to infer the dynamics of product formation and desorption. Time-resolved correlation techniques follow surface reactions in real time and are used to infer the dynamics of adsorbate–substrate energy transfer. Measurement of the interfacial electronic structure is used to investigate the impact of adsorbate–surface and interadsorbate interactions on molecular orbital energies. Capabilities to synthesize and investigate the surface chemical dynamics of arrays of supported metal nanoparticles (NPs) on oxide surfaces include the deposition of size-selected gas-phase clusters as well as solution-phase synthesis and deposition of narrow-size-distribution nanometer-scale particles.

2. Recent Progress

Ultrafast Surface Chemical Dynamics. The ultimate goal of this work is to follow surface chemical processes in real time. We investigate the dynamics of substrate–adsorbate energy transfer by injecting energy with ~100-fs near-IR laser pulses to initiate surface reactions by substrate-mediated processes such as DIMET (desorption induced by multiple electronic transitions) and heating via electronic friction. Time-resolved monitoring of the complex is achieved by a two-pulse correlation (2PC) method wherein the surface is excited by a “pump” pulse and a time-delayed “probe,” and the delay-dependence of the product yield reports on the energy transfer rate.

We are currently focused on using the 2PC method to follow desorption and reaction dynamics on small (nanometer-diameter) metal NPs supported on oxide surfaces. NPs on wide band gap oxides are photoexcited much more efficiently than the support. Thus time-resolved measurements should probe the rate of energy transfer from the NP to the support and to adsorbates on the NP surfaces. Such systems serve as more realistic model catalysts for surface dynamics studies and also provide the opportunity to explore the size-dependence of the dynamics in the metal-to-nonmetal transition size regime.

We are using inverse micelle synthesis to prepare palladium NP assemblies supported on TiO_2(110). This involves segregation of a metal salt [$Pd(OAc)_2$] in the hydrophilic core of inverse micelles of an amphiphilic diblock copolymer suspended in solution. The micelles are spin coated onto UHV-cleaned TiO_2(110) supports. The challenge is to establish protocols for removing the polymer and reducing the metal that result in highly monodisperse arrays of metallic NPs that are suitable for ultrafast photoinduced surface chemistry studies. Recently we have succeeded in preparing NP array consisting of a mixture of 4- and 11-nm diameter particles that expose clean Pd surfaces.

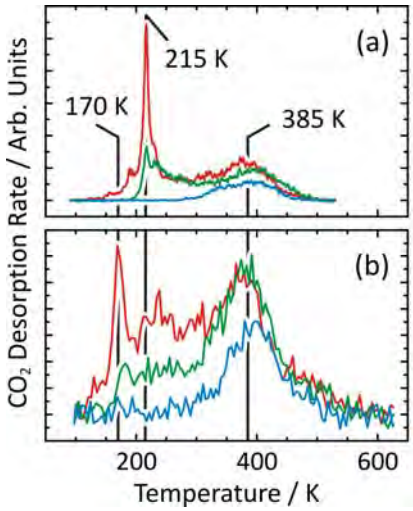

FIG. 1. CO_2 desorption from (a) single crystal Pd(111) and (b) Pd_{NP}/TiO_2(110) following coadsorption of O (to saturation at room temperature) and CO (various coverages up to saturation at ~ 100 K).

We have completed an initial survey of thermal and photoinduced chemistry at the surfaces of these NP arrays. Our measurements indicate that some aspects of the thermal chemistry and photoinduced dynamics are similar to those of the bulk single crystal surface, while others are clearly distinct.

The thermal chemistry of O_2 and CO indicate that the NPs expose largely clean surfaces with strong (111) texturing. Thermal oxidation of CO (Fig. 1) shows high-temperature behavior similar to that observed on the single crystal, but the strong attenuation of low-temperature oxidation suggest that the CO–O phase segregation observed on the single crystal is largely suppressed on the NPs. We hypothesize that this phase segregation requires (111) terraces of a scale larger than that available on the NP surfaces (*i.e.*, $> \sim 10$ nm), pointing to a fundamental change in the phase diagram of this mixed adlayer system at the nanoscale.

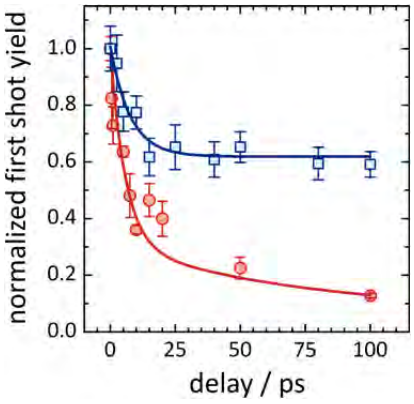

FIG. 2. Dynamics of CO_2 desorption from single crystal Pd(111) (circles) and $Pd_{NP}/TiO_2(110)$ (squares) following adsorption of mixed monolayers of O (to saturation at room temperature) and CO (to saturation at ~ 100 K).

The CO photooxidation dynamics on the NPs show a weaker degree of nonlinearity with respect to photon fluence than on the single crystal. The timescale for energy flow that drives the $CO + O \rightarrow CO_2$ reaction is similar at short times; both show decays on the order of a few ps in 2PC measurements (Fig. 2). However, the ratio of the zero-delay peak to long time baseline is significantly smaller for the NPs than for the single crystal, consistent with the weaker degree of nonlinearity. We are investigating whether this indicates confinement of electronic excitation leading to extended lifetimes or perhaps a more dominant role for phonon-mediated chemistry in the NPs.

Pump-Probe Studies of Photodesorption and Photooxidation on TiO_2(110) Surfaces. Measurements of the final state properties of gas-phase products are being used as a probe of the mechanism and dynamics of photodesorption and photooxidation on well-characterized TiO_2(110) surfaces. Recent studies have focused on the photooxidation of $R(CO)CH_3$ molecules (R = H, CH_3, C_2H_5, C_6H_5) co-adsorbed with oxygen on a reduced TiO_2(110) surface. Laser pump-probe measurements show that the kinetic distributions for the methyl radical fragments ($CH_3^{\bullet}$) from all four molecules are very similar, with "slow" and "fast" components. The "fast" methyl dissociation channel is attributed to a prompt fragmentation process involving an excited intermediate $[R(COO)(CH_3)_{(ad)}]^*$ which is formed by charge transfer at the TiO_2(110) surface following UV photoexcitation.

In the case of 2-butanone photooxidation, α-carbon bond breaking leads to both methyl and ethyl radical fragments, with ethyl loss being the dominant pathway. Similar to that seen previously by Henderson, our product mass spectrum also showed the presence of other $C_2H_x^+$ (x = 2-4) fragments which could originate from ethyl radical secondary surface chemistry or dissociative ionization. Using two different VUV probe energies, it was possible to show that the fragment ions at mass 27 ($C_2H_3^+$) and mass 28 ($C_2H_4^+$) are not due to secondary reactions of ethyl radicals on the surface, but rather from dissociative ionization of the ethyl radical parent ion (mass 29). More recently, we have used velocity map imaging and a new time-resolved imaging camera (obtained through a collaboration with Andrei Nomerotski, Mark Brouard, Claire Vallance at Oxford) to obtain ion images of the mass 27-29 fragments following butanone photooxidation. The ion images (see Figure 3) clearly show that masses 27 and 29 have gained transverse momentum as a

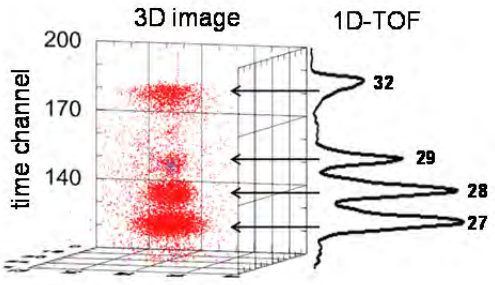

FIG 3: Time-resolved ion images for the species observed in the product mass spectrum from photooxidation of 2-butanone on TiO_2(110).

result of dissociative ionization of the parent ethyl radical following VUV ionization.

Other recent studies include an investigation of the rovibrational state distribution of methyl radicals resulting from UV photooxidation from acetone. Specifically, we used (2+1) REMPI via the $^2A_2''$ ($3p_z$) state to probe the population of the ν_2 "umbrella mode" which is expected to be excited due to the change in the methyl geometry in the fragmentation process (tetrahedral to planar). For "fast" methyl radical products, the vibrational distribution in the ν_2 mode can be characterized by T_{vib} = 151 ± 15 K assuming a Boltzmann distribution. This value, which is significantly colder than gas-phase measurements, implies that methyl radical ejection from the acetone-diolate complex proceeds via a late transition state such that significant vibrational relaxation occurs prior to fragmentation. Translational energy distributions also show that less kinetic energy is available for vibrationally excited methyl radicals and that this energy difference is close to the ν_2 vibrational spacing.

Interfacial Electronic Structure of Supported Clusters. The unique catalytic activity of supported nanoparticles versus their bulk counterparts is often attributed to electronic interactions with the support that result in "activating" the particle through charge transfer, structural changes or creation of new active sites at the particle-support interface. One measure of particle-support interactions is the amount and direction of charge transfer, which strongly affects the electronic structure and reactivity of the supported particle. Recently, we have shown that two-photon photoemission (2PPE) can be used to probe interfacial charge transfer at the cluster-support interface via local work function measurements. In these experiments, model supported catalysts are prepared by depositing mass-selected clusters onto a metal oxide film or metallic support, with a surface coverage that varies smoothly from the center to the edges of the substrate. The small laser focus (~200 μm) allows us to obtain 2PPE spectra as a function of cluster coverage by rastering the laser across the surface. Hence, we can map out the change in work function (relative to the bare surface) as a function of cluster coverage over the range 0.05-1 ML for a *single* deposition experiment. The coverage dependent work function data can be used to quantitatively extract interfacial dipoles for individual clusters as a function of cluster size, composition and support material.

In our initial studies of Mo_xS_y clusters deposited on an ultrathin alumina film (supported on a NiAl(110) surface), we discovered that the interfacial dipoles were reversed relative to what was expected for Mo→O charge transfer. By analogy with electron "charging" observed for Au adatoms and clusters on similar ultrathin oxide films, our observations were attributed to electron tunneling from the NiAl(110) substrate through the ultrathin alumina film to the Mo_xS_y clusters. Electron "charging" is consistent with the high electron affinities of the clusters (>2.5 eV) and the lowered work function of the NiAl substrate due to the presence of the alumina film. More recently, we have been exploring the electronic properties of metal oxide clusters on other metallic and metal oxide surfaces, as model catalyst systems for reactions such as the water-gas-shift (WGS) or methanol synthesis. Preliminary work function measurements versus coverage for the stoichiometric clusters Ti_3O_6, Mo_3O_9, W_3O_9 on Cu(111) are shown in Figure 4. The overall work function shifts are consistent with Bader charge analysis obtained from DFT calculations which show that the charge transfer is significantly greater for Mo_3O_9 (1.37 e) and W_3O_9 (1.37 e) compared to Ti_3O_6 (0.33 e). The trends observed for charge transfer can also be correlated with their ability to dissociate adsorbed water molecules, which is an important step in the WGS reaction. For the these oxide clusters deposited on Cu_2O films grown on Cu(111) surface we find similar trends among the clusters, but the work function changes are even larger (>1 eV). In the near future we are planning to

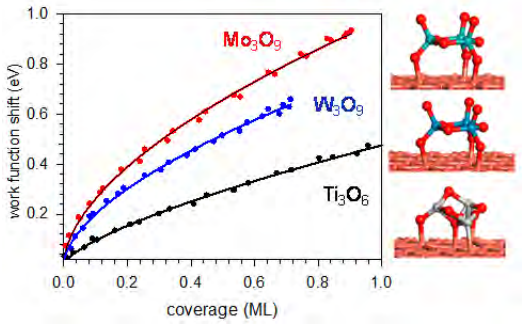

FIG. 4: Coverage dependent work function measurements for three oxide clusters deposited on a Cu(111) surface, along with their adsorption structures from DFT calculations.

investigate the catalytically important Ce_xO_y and Zr_xO_y clusters using a new RF power supply which can be used to sputter resistive oxide targets.

3. Future Plans

Our planned work develops three interlinked themes: (i) the chemistry of supported NPs and nanoclusters (NCs), (ii) the exploration of chemical dynamics on ultrafast timescales, and (iii) the photoinduced chemistry of molecular adsorbates. The investigations are motivated by the fundamental need to connect chemical reactivity to chemical dynamics in systems of relevance to catalytic processes—in particular metal and metal-compound NPs and NCs supported on oxide substrates. They are also motivated by fundamental questions of physical changes in the electronic and phonon structure of NPs and their coupling to adsorbates and to the nonmetallic support that may alter dynamics associated with energy flow and reactive processes.

Future work on ultrafast photoinduced reactions will involve modeling of the energy transfer rates to elucidate the novel dynamics we have observed. In addition, further experiments on progressively smaller nanoparticles (towards sub-nm) will be pursued to further explore fundamental changes in surface reaction kinetics and dynamics as the size of the metal substrate material is reduced from macroscopic (planar bulk surfaces) to the nanoscale. Future work in surface photochemistry using pump-probe techniques will continue to explore mechanistic aspects of semiconductor photoreactions, including the development of new instrumentation for time-resolved studies using ultrafast lasers. New studies in size-selected clusters will focus on metal oxide nanoclusters (Ti, Ce, Mo, W) supported on single crystal metal and metal oxide supports (e.g., Cu(111), TiO_2(110)) to explore cluster-support electronic interactions that can provide a basis for understanding their reactivity.

DOE-Sponsored Research Publications (2011–2013)

Photooxidation of Ethanol and 2-Propanol on TiO_2(110): Evidence for Methyl Radical Ejection, M. D. Kershis and M. G. White, *Phys. Chem. Chem. Phys*., accepted for publication.

Exploring Gas-Surface Photoreaction Dynamics using Pixel Imaging Mass Spectrometry (PImMS), M. D. Kershis, D. P. Wilson, M. G. White, J.J. John, A. Nomerotski, M. Brouard, J. Lee, C. Vallance, R. Turchetta, *J. Chem. Phys*., in press.

Final State Distributions of Methyl Radical Desorption from Ketone Photooxidation on TiO_2(110), D. P. Wilson, D. Sporleder, and M. G. White, *Phys. Chem. Chem. Phys*., **14**, 13630-13637 (2012).

Dynamics of Acetone Photooxidation on TiO_2(110): State-resolved Measurements of Methyl Photoproducts, M. D. Kershis, D. P. Wilson, M. G. White, *J. Chem. Phys*., **138**, 204703 (2013).

Final State Distributions of the Radical Photoproducts from the UV Photooxidation of 2-Butanone on TiO_2(110), D. P. Wilson, D. P. Sporleder, M. G. White, *J. Phys. Chem. C, **117***, 9290–9300 (2013).

Photocatalytic Activity of Hydrogen Evolution Over Rh doped $SrTiO_3$ Prepared by Polymerized Complex Method, P. Shen, J. C. Lofaro, Jr., W. Worner, M. G. White and A. Orlov, *Chem. Eng. J.*, **223**, 200–208 (2013).

Final State Distributions of Radical Photoproducts from the Photooxidation of Acetone on TiO_2(110), D. Sporleder, D. P. Wilson and M. G. White, *J. Phys. Chem. C*, **116**, 16541–16552 (2012).

Local Work Function of Size-Selected Mo_xS_y Clusters on Al_2O_3/NiAl(110), J. Zhou, J. Zhou, N. Camillone III and M. G. White, *Phys. Chem. Chem. Phys*.**, 14,** 8105-8110 (2012).

Adsorption structures and electronic properties of 1,4-phenylene diisocyanide on Au(111) surface, J. Zhou, D. Acharya, N. Camillone III, P. Sutter and M.G. White, *J. Phys. Chem. C*, **115**, 21151–21160 (2011).

Theory of Dynamics of Complex Systems

David Chandler

Chemical Sciences Division, Lawrence Berkeley National Laboratory
and
Department of Chemistry, University of California, Berkeley CA 94720

chandler@berkeley.edu

DOE funded research in our group concerns the theory of dynamics in systems involving large numbers of correlated particles. Glassy dynamics is a quintessential example. Here, dense molecular packing severely constrains the allowed pathways by which a system can rearrange and relax. The majority of molecular motions that exist in a structural glass former are trivial small amplitude vibrations that couple only weakly to surrounding degrees of freedom. In contrast, motions that produce significant structural relaxation take place in concerted steps involving many particles, and as such, dynamics is characterized by significant heterogeneity in space and time. Our recent contributions to this topic have established that these heterogeneities are precursors to a non-equilibrium phase transition, and that this transition underlies the glass transition observed in laboratory experiments [7,10,14,18].[1] We have also shown that relaxation leading up to this transition exhibits a surprising degree of universality [6], even applying to supercooled water [11,17,18].

Liquid interfacial dynamics is another important example, and here too our Group has made several new contributions. Much of this latest work is based upon two advances: i. our general and efficient procedure for identifying instantaneous interfaces from molecular coordinates (see, for example, Ref. [13]), and ii. our generalization of umbrella sampling methods for collecting statistics on rare but important density fluctuations [3]. We have used these methods to examine pathways of water evaporation [13] (an example of which is illustrated in the top panel of the Figure 1), the structure and dynamics of water at a Pt surface [12,15] (lower-right panel), and the structure and dynamics of water at oily surfaces [2,4,8,9] (lower-left panel). Related work examining charge fluctuations in non-aqueous nano-scale capacitors [19] promises an understanding of super capacitance relevant for new classes of energy storage devices.

An insightful perspective on the nature of hydrophobic effects, created in our Group's work over the last decade, focuses on the role of interfacial fluctuations in dynamics and forces of assembly [1]. Quantitative detail on this perspective is found in our recent advances [2, 4,8,9]. The principal effects of interfacial fluctuations can be captured with coarse-grained modeling, as illustrated in Publication [2]. The fact that this understanding can be used to formulate a quantitatively accurate and computationally

[1] Numbers in square brackets refer to papers in the list of Recent DOE Supported Research Publications.

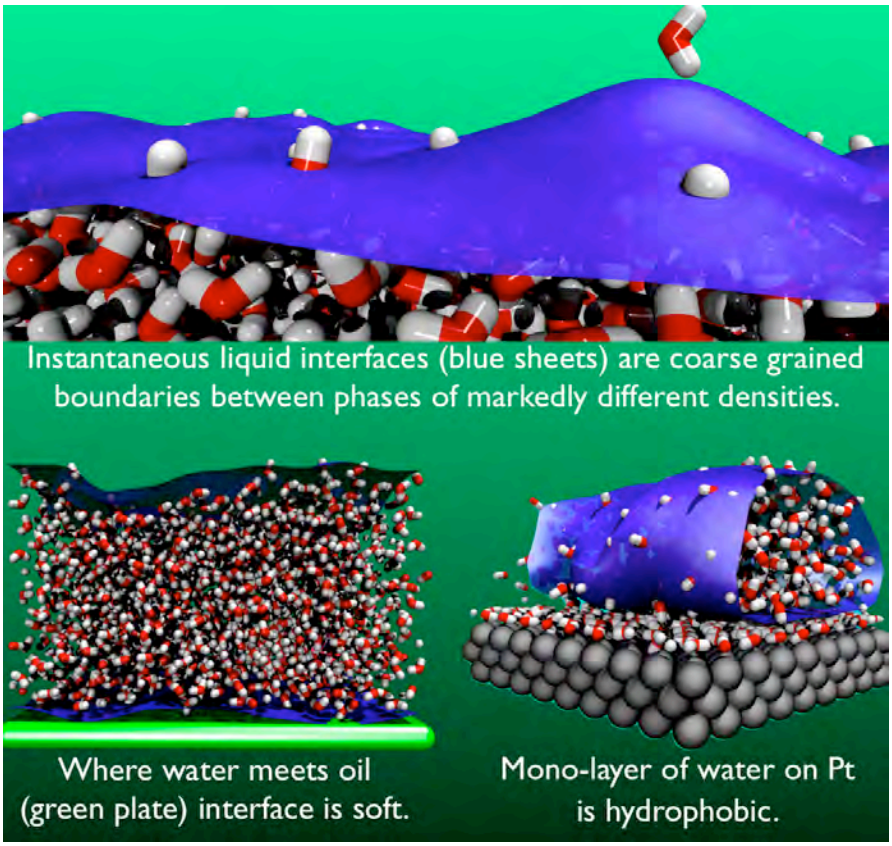

Figure 1: Snap shots from molecular dynamics trajectories showing some of the systems examined by the Chandler research group in their DOE funded studies of liquid interfaces.

convenient theory of solvation and hydrophobic effects is established for the first time in Publication [1].

Finally, we have embarked upon a program of understanding the properties of liquid and solid water at conditions far from bulk equilibrium. Just as hydrophobicity is controlled by interfaces because of the proximity of liquid-vapor coexistence, the behaviors of cold water in bulk, in confinement and in non-equilibrium, depend upon interfaces because of the proximity of crystal-liquid coexistence. Figure 2 illustrates some of our recent results on this topic [11,18]. H. E. Stanley and his many coworkers and followers have widely written on how properties of cold and supercooled liquid water might reflect a metaphysical liquid-liquid transition and critical point. The need for such an unseemly explanation is no longer, as all these properties are now shown to reflect nothing more than easily observed water-ice coexistence and associated pre-melting phenomena [5,11,16,17]. This newly developed understanding of confined cold water sets the stage for interpreting crystal, liquid and amorphous-solid phase behaviors of aerosols, a topic of significant importance to climate science, and a topic we plan to examine in the near future.

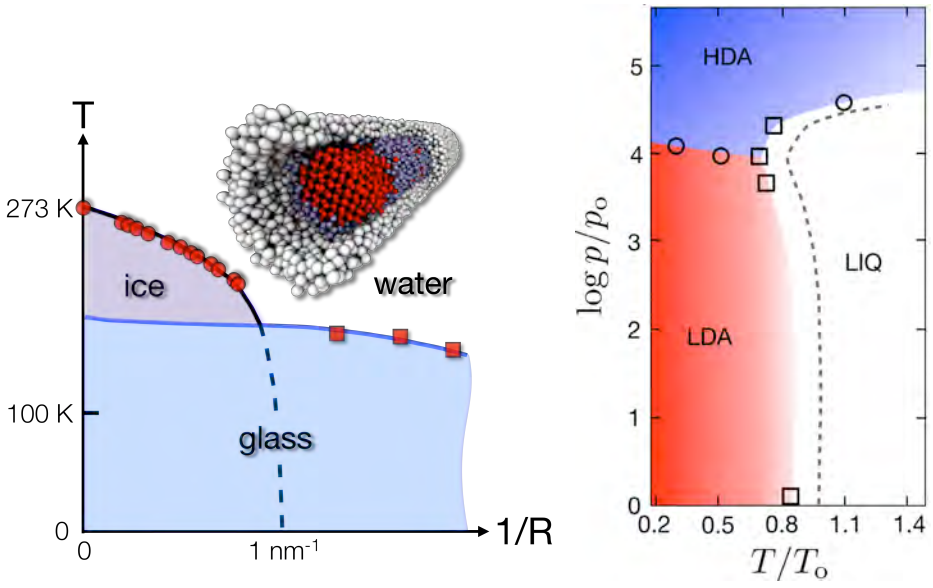

Figure 2: **Left**. Low pressure phase diagram for water confined to a disordered hydrophilic nano-pore of radius R. [Adapted from Ref. 11.] Lines are theoretical curves derived from effects of the interfaces present as the result of confinement (there are no adjustable parameters, only measured bulk transport properties, thermodynamics and liquid-ice interfacial tension enter the theoretical analysis). Experimental data points are from calorimetric observations of the water-ice and water-glass transitions. **Right.** Non-equilibrium phase diagram in corresponding states units for pressure (p_o=1 atm) and temperature (T_o= 277 K). The diagram, computed through application of the s-ensemble method to one of the standard atomistic models of water, is illustrates the first systematic simulation of the far-from-equilibrium high-density and low-density amorphous solids of water, HDA and LDA, respectively. [Adapted from Ref. 18.]

Recent DOE Supported Research Publications

1. Varilly, P., A. J. Patel and D. Chandler, "Improved coarse grained model of solvation and the hydrophobic effect," *J. Chem. Phys.* **134**, 074109.1-15 (2011).

2. Patel, A. J., P. Varilly, S. N. Jamadagni, H. Acharya, S. Garde and D. Chandler, "Hydrophobic effects in interfacial environments," *Proc. Natl. Acad. Sci. USA* **108**, 17678-17683 (2011).

3. Patel, A. J., P. Varilly, S. Garde and D. Chandler, "Quantifying density fluctuations in volumes of all shapes and sizes using indirect umbrella sampling," *J. Stat. Phys.* **145**, 265-275 (2011).

4. Patel, A. J., P. Varilly, S. N. Jamadagni, H. Acharya, S. Garde and D. Chandler. "Extended surfaces modulate hydrophobic interactions of neighboring solutes" *Proc. Natl. Acad. Sci. U.S.A.* **108**, 17678-17683 (2011).

5. Limmer, D.T., and D. Chandler, "The Putative Liquid-Liquid Transition is a Liquid-Solid Transition in Atomistic Models of Water," *J. Chem. Phys.* **135,** 134503.1-10 (2011). Addendum discussing issues of equilibration and proper sampling techniques is found in the Appendix to the arXiv version of this paper: arXiv:1107.0337v2.

6. Keys, A.S., L.O. Hedges, J.P. Garrahan, S.C. Glotzer, and D. Chandler, "Excitations are localized and relaxation is hierarchical in glass-forming liquids," *Phys. Rev. X* **1**, 021013.1-15 (2011).

7. Jack, R. L., L. O. Hedges, J. P. Garrahan, and D. Chandler, "Preparation and relaxation of very stable glassy states of a simulated liquid" *Phys. Rev. Lett.* **107**, 275702.1-4 (2011).

8. Rotenberg, B., A. J. Patel, and D. Chandler, "Molecular explanation for why talc surfaces can be both hydrophilic and hydrophobic" *J. Am. Chem. Soc.* **113**, 20521-20527 (2011).

9. Patel A. J., P. Varilly, S. N. Jamadagni, M. Hagan, D. Chandler and S. Garde, "Sitting at the edge: How biomolecules use hydrophobicity to tune their interactions and function" *J. Phys. Chem. B* **116**, 2498-2503 (2012).

10. Speck, T., and D. Chandler, "Constrained dynamics of localized excitations causes a non-equilibrium phase transition in an atomistic model of glass formers" *J. Chem. Phys*. **136**, 184509.1-9 (2012).

11. Limmer, D. T., and D. Chandler, "Phase diagram of supercooled water confined to hydrophilic nanopores," *J. Chem. Phys.* **137**, 045509.1-11 (2012).

12. Limmer, D. T., A. P. Willard, P. A. Madden and D. Chandler, "Hydration of metal surfaces can be dynamically heterogeneous and hydrophobic," *Proc. Natl. Acad. Sci. USA* **110**, 4200-4205 (2013).

13. Varilly, P., and D. Chandler, "Water evaporation: a transition path sampling study," *J. Phys. Chem. B* **117**, 1419-1428 (2013).

14. Keys, A. S., J. P. Garrahan, and D. Chandler, "Calorimetric glass transition explained by hierarchical dynamic facilitation," *Proc. Natl. Acad. Sci. USA* **110**, 4482-4487 (2013).

15.Willard, A. P., D. T. Limmer, P. A. Madden and D. Chandler, "Characterizing heterogeneous dynamics at hydrated electrode surfaces," *J. Chem. Phys.* **138**, 184702 (2013)

16. Limmer, D. T., and D. Chandler, "The putative liquid-liquid transition is a liquid-solid transition in atomistic models of water, Part II, *J. Chem. Phys.***138**, 214504.1-15 (2013).

17. Limmer, D. T., and D. Chandler, "Corresponding states for mesostructure and dynamics of supercooled water," arXiv: 1305.1382. To appear in *Faraday Discussions.*

18. Limmer, D.T., and D. Chandler, "Theory of amorphous ices," arXiv:1306.4728. Under review at *Physical Review Letters.*

19. Limmer, D.T., C. Merlet, M. Salanne, D. Chandler, P.A. Madden, R. van Roij, B. Rotenberg, "Charge fluctuations in nano-scale capacitors," arXiv:1306.6902. To appear in *Physical Review Letters*.

Kinetics of charge transfer in a heterogeneous catalyst-reactant system: the interplay of solid state and molecular properties

Tanja Cuk
D46 Hildebrand Hall, Chemistry Department, University of California, Berkeley 94720
tanjacuk@berkeley.edu

I. Program Scope

One of the greatest challenges in the design of efficient and selective catalysis technologies is the limited fundamental understanding of how interfacial properties at solid state/reactant interfaces guide catalytic reactions. The central research question is to determine how molecular properties of reactants influence charge dynamics in solid state catalysts, and conversely, how these charge dynamics induce molecular changes; likely, it is this synergy that results in catalytic efficiency and high turnover rates. There are two perspectives on the solid state catalyst/reactant interface. From the solid state perspective, interfacial properties are described by band alignment and Fermi levels; from the molecular perspective, interfacial properties are described by oxidation states and reactant adsorption. The characterization of catalytic materials has either focused on molecular changes such as adsorption, dissociation, and new bond formations occurring on the reactant side of the interface or the changes in interfacial band alignment and passivation of surface states on the solid state side. While these properties are useful for understanding catalytic performance, a causal link between the changes observed on each side of the interface is lacking. What is needed is to directly follow the trajectory of how charge carriers in solid state catalysts initiate interfacial charge capture by reactant molecules—from the creation of the charge carrier in the bulk, to its accumulation at the interface, and to the moment at which a reactant molecule transforms and, in the process, consumes the charge carrier. It is a goal of this program to develop these approaches. In photoinitated heterogenous catalysis, the charge carrier is injected via a photodiode, photovoltaic, or Schottky junction. Rather than focusing on the excitonic features of an electron-hole pair, this proposal concentrates on the already well-separated charges to understand the detailed balance between the flow of charge carriers to catalyst-reactant interfaces and the dynamics of interfacial charge capture by reactant molecules. Understanding these interfacial dynamics from both the chemical and solid state perspective will reveal the interplay between molecular changes and the heterogeneous catalyst surface, leading to both better catalyst design and more intelligent control of the catalytic environment.

II. Recent Progress

Recent progress uses surface sensitive, *in-situ* transient optical spectroscopy to measure the rate of interfacial charge transfer by monitoring holes generated within the transition metal oxide that drive the water oxidation reaction at the catalyst/reactant interface. These experiments aim to resolve whether the initial, ultrafast steps of the reaction differentiate between the turnover rates in an high overpotential catalyst (~2V, 1000 O_2/site-s) and low over potential catalyst (0.3V, 1 O_2/site-s).

Interfacial Charge Transfer at the n-$SrTiO_3$/H_2O Interface with a large overpotential

A measurement that distinguishes the interfacial charge transfer rate from recombination kinetics and drift within the material requires a sample with a high quantum efficiency for separating electron-hole pairs and an experimental configuration with sufficient surface sensitivity. An n-type semiconductor/liquid interface is well described by a Schottky barrier that separates electron-hole pairs generated with the depletion layer of the semiconductor with efficiency approaching unity. The UV driven water oxidation catalyst, n-$SrTiO_3$, has a quantum efficiency

for O_2 evolution approaching 70% for 300 nm excitation. This high quantum efficiency comes from the fact that at 300nm, the depletion width of the electric field matches the penetration depth of the UV light. The surface sensitivity in our configuration comes simply from the fact that we measure the transient signal in reflectance. The effective probe depth of a reflectance measurement is guided by the real, rather than the imaginary, part of the index of refraction, $\alpha_{Reflectance} = \lambda/4\pi n$. In a setup probing the reflectance at the n-$SrTiO_3$/H_2O interface, the three parameters—the depletion width, the penetration depth of the exciting light, and the penetration depth of the probe light are all equal to ~25 nm. Essentially, this is what allows for us to distinguish interfacial charge transfer from recombination and drift using transient optical spectroscopy.

While high intensity, high peak power laser excitation can in principle change this picture, we maintain a high quantum efficiency with ~150 fs, 0.1 mJ/cm^2 excitation due to the high rate of drift in the depletion region and the well matched excitation wavelength. High intensity laser excitation, combined with the high quantum efficiency also creates a large bath of holes at the interface within the ~150 fs pulse— 10^{19}/cm^2, much higher than the number of sites available for catalysis (10^{15}/cm^2). If these holes are not consumed by the water oxidation reaction fast enough, they can lead to other side reactions that damage the catalyst surface. While we have observed damage to the catalyst surface under our excitation conditions, we have been able to control it enough to take reproducible data by taking the data at fresh sample spots and alternating between open and closed circuit conditions in the electrochemical cell.

The transient reflectance results on n-$SrTiO_3$ in an in-situ electrochemical cell, shown in Figure 1, exhibit a marked change in kinetics between open circuit (no current/no reaction) and closed circuit conditions (current flowing/reaction proceeding). Moreover, these kinetics speed up with applied voltage in a voltage region that does not change the quantum efficiency of the reaction, showing that the measured kinetics reflect interfacial charge transfer rather than the competition between drift and recombination. Given that holes are transferred in oxidative conditions, we can attribute the kinetics to holes that accumulate at the interface and then decay as a result of charge transfer to adsorbed water species. Further, the voltage dependence of the kinetics suggests that the applied voltage in the cell changes the potential of the VB at the interface, leading to a larger over-potential for the reaction. In a usual Schottky barrier model of the n-type semiconductor/liquid interface, the VB and CB are pinned at the interface and the applied voltage only changes the band-bending. However, under the high charge injection conditions that we have here, the band edges can be unpinned via majority carrier inversion. Indeed, the ~10^{19} holes/cm^3 generated by the laser just exceeds the n-type doping of the 0.1% Nb-$SrTiO_3$ sample.

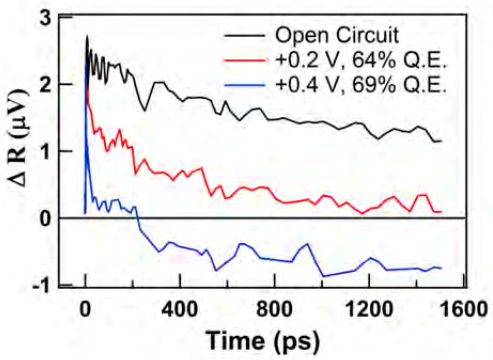

Figure 1: Kinetics of hole decay at n-$SrTiO_3$/H_2O interface upon 300nm excitation, probed at 800nm in reflectance.

These results show that we can both monitor and manipulate the interfacial charge transfer kinetics by an n-type semiconductor/liquid interface, where the manipulation of the VB edge likely comes from carrier inversion. They provide a testing ground for modeling Marcus Theory at the solid/liquid interface. Furthermore, they will determine the initial rate constants of

the heterogeneous water oxidation reaction that enable a large turnover rate (~ 1000's O_2/site-s) in an overdriven catalyst (1.6 V vs. Ag/AgCl).

Efficient charge injection into a low over potential WOC: an n-p GaAs/Co_3O_4 photodiode

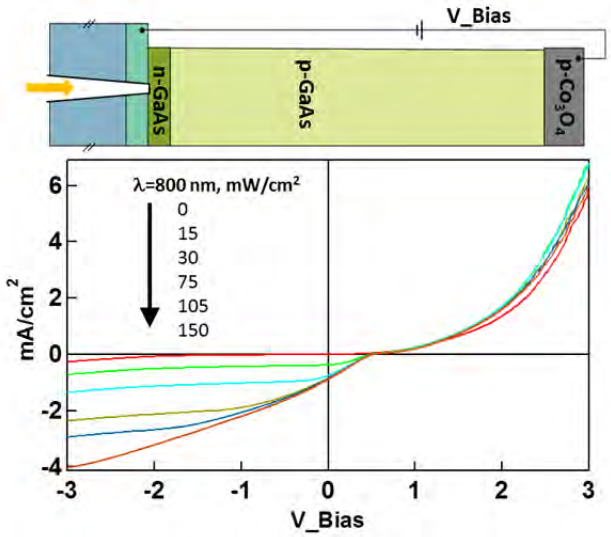

Figure 2: n-p GaAs/Co_3O_4 design and I-V curves measured under 800 nm excitation.

In order to investigate the interfacial charge transfer kinetics defining low overpotential, lower turnover rate (~1's O_2/site-s) catalysts, we have created a layered device where an underlying n-p GaAs junction is used as a photodiode to inject charges into a Co_3O_4 overlayer. For these initial studies, we have chosen Co_3O_4—an earth abundant catalyst with low over potential for the water oxidation reaction (~0.1-0.3V vs. Ag/AgCl) and reasonable turnover rates (0.1 O_2/site-s).

Imitating the properties that lead to high quantum efficiency in n-$SrTiO_3$, the n-p GaAs photodiode is designed such that the penetration depth of the exciting light matches the depletion width of the electric field. While a longer, lightly doped p-type region in combination with a short, highly doped n-type region can accomplish efficient charge separation, charge injection into the Co_3O_4 interface can be complicated by recombination at the interface and creating proper contacts to the GaAs junction. However, by operating the GaAs junction in reverse bias conditions (as a photodiode rather than photovoltaic), we were able to avoid these complications to achieve an overall quantum efficiency of charge separation and charge injection into Co_3O_4 of ~6% at an ultrafast timescale. While this quantum efficiency is not nearly as high as for the n-$SrTiO_3$, the kinetics at the Co_3O_4 surface are independent of the charge separation step occurring at the embedded heterojunction. So the Q.E. only needs to be high enough to inject enough charges to detect. Figure 2 shows the design of the device and the I-V curves.

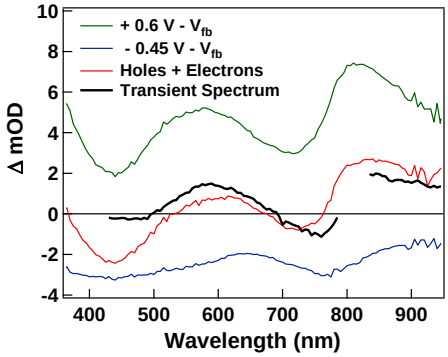

Figure 3: Transient optical spectrum of Co_3O_4 compared with spectral changes observed by injecting electrons and holes electrochemically.

There are two distinct advantages that such a device offers for the study of interfacial charge transfer over a high quantum efficiency, n-type semiconductor/liquid interface: (1) any type of transition metal oxide catalyst can be studied, regardless of its ability to separate electron-hole pairs. (2) Since the charge separation step happens at the embedded interface, the VB of the catalyst, and the over-potential of the light driven reaction, can be manipulated with a voltage applied directly to the transition metal oxide.

Using transient grating spectroscopy to generate and monitor a gradient of holes in the device, we have found that the kinetics changes with the addition of the Co_3O_4 overlayer, suggesting that we are sensitive to the interfacial properties of the device.

Spectral signatures of electrons and holes traps in photoexcited Co_3O_4

Another project reports on the spectral signatures of electron and hole traps in photoexcited Co_3O_4. While transient grating spectroscopy can follow diffusion and recombination kinetics, energetically defining the position of electron and hole traps in the material that influence the interfacial kinetics requires interpretation of a transient optical spectrum over an extended probe wavelength region. We have therefore used transient optical absorption, in combination with spectroelectrochemistry, to define the nature of these traps in Co_3O_4.

Figure 3 shows that the UV-VIS transient absorption spectrum of photoexcited Co_3O_4 can be well modeled by changes to the ground state spectrum that result from either electron or hole carriers, injected electrochemically. Voltages positive of the flat-band potential inject holes into Co_3O_4 and lead to the prominent absorption peaks in the transient spectrum. These absorption peaks grow continuously from the flat band potential, suggesting that the holes are created near the VB edge and that the transient absorptions to them arise from deeper in the VB band. Voltages negative of the flat-band potential inject electrons into Co_3O_4 and lead to bleaches in the transient spectrum. Unlike the absorptions, the bleaches only occur at an onset potential beyond the flat band indicating that they come from electron filling of higher lying states above the VB edge. A likely interpretation is that the electrons fill the mid-gap d-manifold of Co_3O_4, approximately 1 eV above the VB. This mid-gap d-manifold results from the partially filled d states of transition metal oxides and would molecularly correspond to on-site d-d transitions. Further evidence of this interpretation comes from the transient absorption spectrum of photoexcited Co_3O_4 in the near IR region, where the spectrum exhibits a bleach of this d-manifold that mirrors the shape of the ground state spectrum, indicating that the d-manifold is filled upon photoexcitation. In conjunction with the efficient GaAs/Co_3O_4 photodiode above, these results open the path for investigating how these electron and hole traps influence kinetics at the liquid interface.

III. Future Plans

Ultrafast Infrared Transient Spectroscopy of the n-$SrTiO_3$/H_2O Interface Future plans aim to correlate the ultrafast kinetics of holes observed on the solid state side of the n-$SrTiO_3$/H_2O interface with changes in the molecular bonding of adsorbates on the liquid side of the interface. In order to do this, we will apply ultrafast infrared spectroscopy in the vapor phase. We will conduct these experiments in a vapor phase that allows for facile infrared measurements and maintains high O_2 evolution. Previous work by Somorjai shows that a vapor phase leads to similar O_2 evolution as in an electrochemical cell, by deliquescing dried electrolyte on the surface of n-$SrTiO_3$. These experiments will be the first that investigate ultrafast kinetics of bond changes at the catalyst surface that are initiated by direct charge transfer, rather than heating.

Interfacial Charge Transfer at the Co_3O_4/H_2O interface Future plans aim to investigate the interfacial charge transfer kinetics of holes over a large over-potential range, such that we can answer an important question in heterogeneous catalysis—at what over-potential do the *initial* rates of the reaction associated with interfacial charge transfer kinetics begin to influence the overall turnover rate of the catalyst. We plan to investigate this using the GaAs/Co_3O_4 photodiode in an *in-situ* electrochemical cell with both transient grating and transient reflectance spectroscopy, where a separate voltage applied to the Co_3O_4 interface tunes the over-potential.

Publications: "The role of d-d excitations in transition metal oxides: Spectral Signatures of Mid-Gap Electron Traps in Co_3O_4" M. Waegele, H. Doan, T. Cuk, *J. Phys. Chem. C.*, in-review (2013).

Molecular Mechanism of Water Exchange around Aqueous Ion

Liem X. Dang
Physical Sciences Division
Pacific Northwest National Laboratory
Richland, WA 93352
liem.dang@pnnl.gov

Background and Significance

The study of thermodynamic and kinetic properties of ions in water by statistical mechanics or computer simulation techniques has provided molecular-level details that have advanced our understanding of the chemistry and physics of solvation. Specifically, the kinetics and thermodynamics of water exchange around aqueous ions have been subjects of considerable theoretical, computational, and experimental interest in recent years. Much of this interest results from the roles of these properties in aqueous chemistry and the assumption that the exchange process is believed to be associated with activation volume ($\Delta V^{\ddagger}$), which is the key indicator of the water-exchange mechanism. For example, the exchange process is an associative mechanism when the activation volume is negative and a dissociative mechanism when the activation volume is positive. Our work differs from these early efforts in that we include polarization effects into potential models as well as additional comparative studies between the RF and the Grote-Hynes (GH) theory methods. We demonstrate that the barrier heights for water exchange obtained from our computed potentials of mean force (PMF) and the corresponding transmission coefficients are significantly larger than those obtained from classical non-polarizable force fields. The mechanistic properties associated with the water-exchange process, such as PMFs, time dependent transmission coefficients, and the corresponding rate constants, were examined using TST, the RF method, and GH treatments of the dynamic response of the solvent. Characterization of this influence on the rate results and $\Delta V^{\ddagger}$ is the primary focus of this work. Our work using polarizable models predicted a larger free energy barrier heights and the transmission coefficients compared to studies using non-polarizable potentials. We are interested in expanding our current method to studies of ion solvation at interfaces due to their ability to respond to the local, non-homogeneous environment. We expect that the response will be different. Future research effort will focus on understanding the influence of nuclear quantum mechanical effects on the kinetics properties of ions in aqueous solution.

With the growing interest in RTIL and co-solvent mixtures, our intent in this study was to provide a molecular-level understanding of ion association between RTIL ions in water. To accomplish this, we used a PMF approach to study the molecular mechanism of ion-association processes. We studied four different imidazolium-based RTILs. Combinations of ions were chosen to study the effects of anion and cation chain length on the pairing processes. We also conducted kinetic studies of ion-pair association using various rate theories. We concluded that the computed rate results significantly deviated from results obtained from TST because it does not account for dynamical solvent effects. In addition, our analysis of rotational dynamics of cations shows that the time scales for molecular reorientation are longer for cations with longer alkyl tails.

Recent Progress and Future Plans

Computational Studies of Water Exchange around Aqueous Li^+ with Polarizable Potential Models

We describe molecular dynamics (MD) simulation studies performed on extended empirical models in which solvent molecules are treated explicitly using polarizable potential models. This approach allows us to examine solvent and polarization effects on the computed properties, which are expected to have a significant influence on the mechanism and rates of exchange process. We present our rate theory results on the water-exchange mechanism around aqueous Li^+, such as PMF, friction coefficients, and the corresponding rate constants obtained using TST, the RF method, and GH treatments of the dynamic response of the solvent. Pressure effects on these aqueous systems are of particular interest because of their relevance in aqueous chemistry to determine the activation volume. We also compare our computed rate theory results with results from previous corresponding studies that used non-polarizable force fields. Future research effort will focus on understanding the influence of nuclear quantum mechanical effects on the kinetic properties of ions in aqueous solution. Our primary goal in this work was to develop a molecular model that describes the

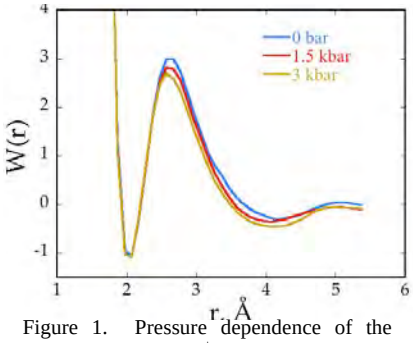

Figure 1. Pressure dependence of the PMFs and W(r) of Li^+-H_2O systems.

thermodynamics and the kinetics of the water-exchange process around aqueous Li^+. To compute the PMFs for the process, we used a constrained mean force approach that includes polarization effects, and then, we estimated the rate constant using TST. Next, we used the RF method to calculate the rate constant as a function of time and the corresponding transmission coefficients, κ_{RF}. Finally, we used the GH theory to compute the transmission coefficients, k_{GH}, for this exchange process. Subsequently, we evaluated the pressure dependence of rate constants and the corresponding $\Delta V^{\ddagger}$ for the exchange process. Figure 1 shows the computed PMFs obtained at 300 K for the three pressures, normalized to the contact Li^+-water pair free energy minimum at the pressure of 0 bar. As expected, the shapes of the computed PMFs are very similar, and the changes are rather small but are noticeable. We observe two effects: 1) increasing the pressure destabilizes the contact ion-water pair and 2) the free energy barrier for escaping the first hydration shell decreases from 4.07 kcal/mol at 0 bar to 3.77 kcal/mol at 3 kbar. These changes are accompanied by a small change in the transition-state distance from 2.67 Å to 2.57 Å. In their pioneering work of the same system, Rey and Hynes reported a barrier height of 3 kcal/mol at 2.70 Å at 0 pressure. In subsequent work, Rustad and Stack reported that the pressure dependence for the free energy barrier ranges from 2.93 to 2.65 kcal/mol at 0 bar and 2 kbar, respectively. Thus, our finding of a trend in barrier height changes as pressure changes is consistent with the findings reported by Rustad and Stack. The only major difference is the magnitude of the free energy barrier heights.

In Figure 2, we present the computed time dependent *k(t)* at three different pressures. It is clear that the results have converted well, and we observed that the rate constants increase with pressure. The transmission coefficients κ_{RF}, estimated as outlined above are 0.22, 0.23 and 0.24. The activation volume using the computed κ_{RF} is -4.1 cm^3/mol, which is greater that the value extracted using k^{TST}. Thus, we conclude that the pressure dependence of both the barrier height and the transmission coefficient contribute to the activation volume. As mentioned by Rustad and Stack, we also note that the exact contributions of the barrier height and transmission coefficient to the activation volume would vary with the chosen reaction coordinate.

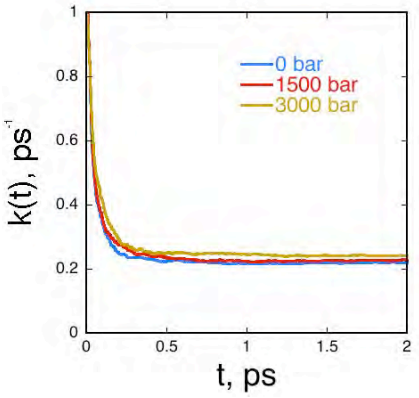

Figure 2. Pressure dependence of the transmission coefficients, *k(t)*, of Li^+-H_2O systems.

Figure 3, we show plots of un-normalized, time-dependent friction kernels of Li^+-H_2O in water for the three pressures. In all cases, there are two distinct decay time scales that show first an initial rapid decay lasting for about 0.07 ps and then a longer time decay that lasts for a few picoseconds. We can conclude from these data that the oscillating $\zeta(t)$ reflects the barrier heights of the computed PMFs. The computed values for κ_{GH} using these results are 0.37, 0.23 and 0.02. These results are in contrast to the actual transmission coefficients computed using the RF method. Thus, we can conclude from these data that, at lower pressure, the GH theory provides a good approximation of the transmission coefficient, but it is not that accurate at higher pressure. The performance of GH theory for our system is consistent with the result reported by Spangberg et al. obtained with their potential models (κ_{RF} = 0.14±0.02, κ_{GH} = 0.42), presumably under conditions corresponding to a pressure of around 0 bar. They attributed the poor performance to the re-crossing trajectories that make large excursions from *r**, which violates the assumptions of GH theory. In summary, to enhance our understanding of the mechanism of water exchange around the aqueous Li^+, we carried out a systematic study using MD simulations with polarizable potential models. We computed the PMFs, time dependent transmission coefficients, and the corresponding rate constants using TST, the RF method, and GH theory treatments of the dynamic response of the solvent. Our computed barrier heights for water exchange are significantly larger than those from classical non-polarizable force fields. The computed residence times of the water around Li^+ using the RF method are 191, 140, and 120 ps at 0, 1.5 and 3 kbar, respectively. Our computed value of 191 ps at 0 bar compares well with the value of 201 ps at 0 bar reported by Rustad and Stack using a similar approach.

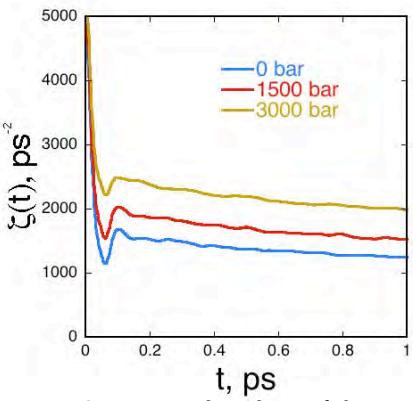

Figure 3. Pressure dependence of the time dependence friction kernels, $\zeta(t)$ of Li^+-H_2O systems.

We are interested in expanding our current study/method into studies of ion solvation at the interfaces. We believe that, based on experience gained during past studies, the computed transmission coefficients and the

corresponding residence times using the RF method with polarizable potential models will be more reliable and different from the corresponding fixed charge models. Our future research effort will focus on understanding the influence of nuclear quantum mechanical (QM) effects on the properties of ions in aqueous solution such as the water-exchange rate and the corresponding transmission coefficients using ring polymer MD techniques. The exact performance of GH theory for this problem is not that critical. Ring polymer MD rate theory is a straightforward quantum generalization of the Bennett-Chandler method that we have used to calculate the correct classical transmission coefficient (i.e., the RF method); therefore, we will simply use this method. We are not certain how large the QM effects will be. However, because the reduced mass of the Li^+-H_2O coordinate is close to the mass of the Li^+ ion, it is quite possible that there will be a QM enhancement of the rate owing to zero point energy in this coordinate, and perhaps also some tunneling through the barrier. Studies of these phenomena are underway.

Iodide adsorption at the liquid/air interfaces of water-methanol mixtures

Water and methanol mixtures are very important in many areas of chemistry, biochemistry, and electrochemistry. Also, from a chemical physics perspective, these systems are very interesting as water-methanol mixtures are basic and simple model systems that can be used to understand the balance of hydrophilic and hydrophobic interactions. Here we report our recent studies on the molecular mechanism of iodide transport across the liquid/air interface of water and methanol mixtures. We used MD simulations and the PMF approach to evaluate the free energy profile associated with the transfer of an ion from bulk into the vapor phase. In Figures 4 and 5 we show the PMFs for mixed solvents at different compositions of water and methanol. Clearly the surface propensity of iodide ion decreases with the methanol composition in the mixture. Contrary to the expectation, the decrease in free energy minima is not linear as is illustrated in the Figure 6. We analyze the computed density profiles and hydration numbers as a function of concentrations and ion positions with respect to the interface to further explain the observed phenomenon. The methanol/air interfacial region is composed of methyl groups pointing out at the interface. Because I^- has stronger interactions with the hydroxyl group, it does not show a significant preference for the surface. Though the density profiles at X_m = 0.25 indicate the surface activity of methanol, but the first solvation shell of iodide is significantly dominated by the water. Therefore we determined that the free energy minima for pure water and the mixture at X_m = 0.25 are almost equal. Noticeable differences in free energy minima start at X_m = 0.50. We observe that the free-energy minima values for X_m= 0.50 and X_m= 0.75 also are the same. This study indicates that caution should be taken when predicting the ion behavior at the interfaces of mixed solvents. Our analysis also indicates that the induced dipole moment of I^- is larger and more aligned at the interface of pure water. The strong alignment and enhancement of induced dipoles at the interface gradually decrease with increase of methanol composition in the mixture. In Figure 7 we show the PMF at 300 K for pure water along with the entropic and energetic components. The reduced entropy at the interface only partially compensates the energetic minimum. Therefore, the net PMF for iodide, that is a sum of these two components, shows a minimum at the interface.

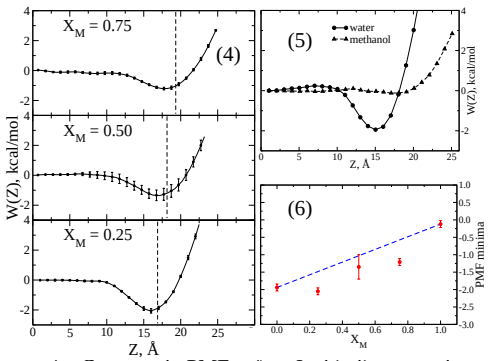

Figure 4. Computed PMFs for I^- binding to the liquid/vapor interface of water and methanol mixtures at various concentrations. Figure 5. PMFs for the pure systems. Figure 6. Free energy minima obtained from PMFs are plotted against the methanol concentration in the mixtures. The black line connecting the pure solvents represents an expected linear behavior

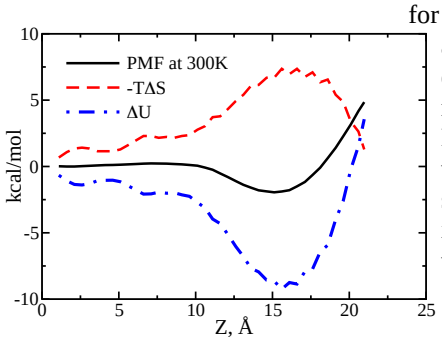

Figure 7. Partition of free-energy profile along the reaction coordinate into entropic and energetic contributions.

Pairing Mechanism among Ionic Liquid Ions in Aqueous Solutions

Room temperature ionic liquids (RTILs) are becoming important components in advanced processes and devices with various applications. Because a large number of RTILs with varying physical properties can be made by combining various cations and anions, they often are referred to as tailor-made designer materials. However, the high viscosities of RTILs are a problem in some processes. One solution to this problem is mixing ionic liquids and conventional solvents. We intend to provide a fundamental understanding how the co-solvents affect the association between various RTIL ions. To this end, we first chose to study the effect of water. We used MD simulations and

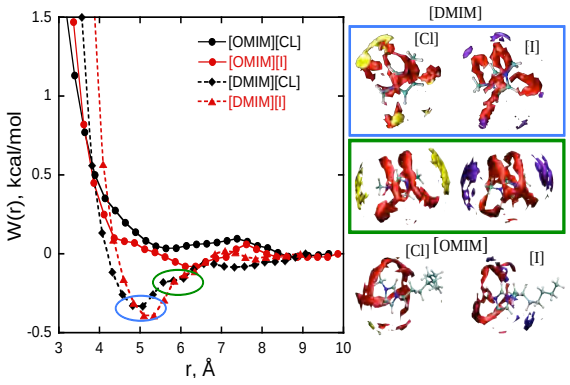

Figure 8: Left: Computed PMFs for all the RTIL pairs in aqueous solutions. Right: Spatial distribution of water and anion around the cation at the free energy minima. Water in red, Chloride in yellow and iodide in violet.

evaluated the free energy profiles along the center of mass separation between the ions. We studied the association mechanism four different RTIL ion-pair systems ([dmim][Cl], [dmim][I], [omim][Cl], and [omim][I]) in water. In Figure 8 we show the PMF plots as function of center of mass separation between ions. The PMFs for [dmim] containing systems has deeper minima compared to the [omim] indicating stronger association for the cations with shorter alkyl tails. The RTIL pairs involving [omim] have shallow minima. Comparing [dmim][Cl] vs. [dmim][I], we notice that the PMF for [dmim][I] has slightly deeper minima. This trend is in contrast to what we have noticed in gas phase interaction plots, where we observed a significantly deeper minimum for [dmim][Cl]. Similarly, [[omim][I] has deeper minima compared to [omim][Cl]. This higher affinity of iodide for both the cations agree with the Collins empirical law of matching affinities. Collins law states that the relative affinity among ion pairs in water depends on the similarity of cation and anion in terms of their size and charge densities. The spatial distribution plots shown in Figure 8 provide insight into how the water arranges around the ion pair along the reaction coordinate. The [dmim] systems have two minima that are color coded in blue and green circles. The anion coordination with the cation at these two minima positions is quite different.

References to publications of DOE sponsored research (2011-Present)

1. Computational Study of Ion Distributions at the Air/Liquid Methanol Interface. Sun, Xiuquan; Wick, Collin; Liem X. Dang, *J. Phys. Chem*. A 115, 5767-5773 (**2011**).
2. Computational Study of Hydrocarbon Adsorption in Metal–Organic Framework Ni_2(dhtp). Sun XQ, Wick CD, Thallapally PK, Liem X. Dang; McGrail, Benard, *J. Phys. Chem*. B, 115, 2842-2849 **(2011)**.
3. Molecular Mechanism of Hydrocarbons Binding to the Metal-Organic Framework. Sun XQ, Wick CD, Thallapally, PK, Liem X. Dang; McGrail, Benard, *Chemical Physics Letters*, 501, 455-460 **(2011)**.
4. Molecular Mechanism of Gas Adsorption into Ionic Liquids: A Molecular Dynamics Study. Liem X. Dang and Chang, Tsun-Mei, *J. Phys. Chem. Letters*, 3, 175-181 (**2012**).
5. Molecular Mechanism of Specific Ion Interactions between Alkali Cations and Acetate Anion in Aqueous Solution: A Molecular Dynamics Study. Annapureddy Harsha V. R.; Liem X. Dang, *J. Phys. Chem.* 116, 7492-7498 (**2012**).
6. Note: Interionic Potentials of Mean Force for Ca^{2+}-Cl^- in Polarizable Water. Liem X. Dang; Tai Ba Truong; Ginovska-Pangovska Bojana, *J. Chem. Phys.*, 136, 126101 (**2012**).
7. Quantitative Analysis of Aqueous Nanofilm Rupture by Molecular Dynamic Simulation. Peng Tiefeng; Nguyen Anh V.; Peng Hong; Tsun-Mei Chang and Liem X. Dang, *J. Phys. Chem.* B, 116, 1035-1042 (**2012**).
8. Development of Ions-TIP4P-Ew Force Fields for Molecular Processes in Bulk and at the Aqueous Interface using Molecular Simulations. Tiefeng Peng, Tsun-Mei Chang, Xiuquan Sun, Anh V. Nguyen, Liem X. Dang, *J. Mol. Liqs.* 173, 47–54 (**2012**).
9. Molecular Mechanism of the Adsorption Process of an Iodide Anion into Liquid-Vapor Interfaces of Water-Methanol Mixtures. Harsha V. R. Annapureddy and Liem X. Dang, *J. Chem. Phys.*, 137, 214705 (**2012**).
10. Understanding ion-ion interactions in bulk and aqueous interfaces using molecular simulations. Liem X. Dang, Sun, Xiuquan; Ginovska-Pangovska, Bojana; et al. Faraday Discussions 160, 151-160 (**2013**).
11. Pairing Mechanism among Ionic Liquid Ions in Aqueous Solutions. A Molecular Dynamics Study, Harsha V. R. Annapureddy and Liem X. Dang, *J. Phys. Chem. B*, 117, 8555 *(***2013**).
12. Computational Studies of Water Exchange around Aqueous Li^+ with Polarizable Potential Models. Liem X. Dang and Harsha V. R. Annapureddy, *J. Chem. Phys.*, (in Press, **2013**).

Transition Metal-Molecular Interactions Studied with Cluster Ion Infrared Spectroscopy

DE-FG02-96ER14658

Michael A. Duncan

Department of Chemistry, University of Georgia, Athens, GA 30602

maduncan@uga.edu

Program Scope

Our research program investigates gas phase metal clusters and metal cation-molecular complexes as models for heterogeneous catalysis, metal-ligand bonding and metal cation solvation. The clusters studied are molecular sized aggregates of metal or metal oxides. We focus on the bonding exhibited by "physisorption" versus "chemisorption" on cluster surfaces, on metal-ligand interactions with species such as benzene or carbon monoxide, and on solvation interactions exemplified by complexes with water, acetonitrile, etc. These studies investigate the nature of the metal-molecular interactions and how they vary with metal composition and cluster size. To obtain size-specific information, we focus on ionized complexes that can be mass selected. Infrared photodissociation spectroscopy is employed to measure the vibrational spectroscopy of these ionized complexes. The vibrational frequencies measured are compared to those for the corresponding free molecular ligands and with the predictions of theory to reveal the electronic state and geometric structure of the system. Experimental measurements are supplemented with calculations using density functional theory (DFT) with standard functionals such as B3LYP.

Recent Progress

The main focus of our recent work has been infrared spectroscopy of transition metal cation-molecular complexes with carbon monoxide, carbon dioxide, and benzene. These species are produced by laser vaporization in a pulsed-nozzle cluster source, size-selected with a specially designed reflectron time-of-flight mass spectrometer and studied with infrared photodissociation spectroscopy using an IR optical parametric oscillator laser system (OPO). In studies on complexes of a variety of transition metals, we examine the shift in the frequency for selected vibrational modes in the adsorbate/ligand/solvent molecule that occur upon binding to the metal. The number and frequencies of IR-active modes reveal the structures of these systems, while sudden changes in spectra or dissociation yields reveal the coordination number for the metal ion. In some systems, new bands are found at a certain complex size corresponding to intra-cluster reaction products. In small complexes with strong bonding, we use the method of rare gas "tagging" with argon or neon to enhance dissociation yields. In all of these systems, we employ a close interaction with theory to investigate the details of the metal-molecular interactions that best explain the spectroscopy. We perform density functional theory (DFT) calculations (using Gaussian 03W or GAMESS) and when higher level methods are required, we collaborate with theorists. Our infrared data on these metal ion-molecule complexes provide many examples of unanticipated structural and dynamical information. A crucial aspect of these studies is the infrared laser system, which is an infrared

optical parametric oscillator/amplifier system (OPO/OPA; Laser Vision). This system covers the infrared region of 600-4500 cm^{-1} with a linewidth of ~1.0 cm^{-1}.

Transition metal carbonyls provide classic examples of metal-ligand bonding, and carbon monoxide is the classic probe molecule for surface science and catalysis. We have investigated transition metal cation carbonyls to compare these to corresponding neutral carbonyls known to be stable. The stability of these systems is conveniently explained with the 18-electron rule, and this is a guiding principle for our cation work. We studied the $Co^+(CO)_n$ complexes, for which the n=5 species is isoelectronic to neutral $Fe(CO)_5$, and the $Mn^+(CO)_n$ system, for which the n=6 complex is isoelectronic to $Cr(CO)_6$. In both cases, the cation complexes had a filled coordination at the expected n=5 and 6 complexes, respectively, and they had the same structures as the corresponding neutrals (trigonal pyramid and octahedral). However, the frequencies of the CO stretch vibrations, which are strongly red-shifted in the neutrals, were hardly shifted at all for the cations. This trend was attributed to the reduced π back-bonding in the cation systems. We also studied the $Cu^+(CO)_n$ complexes, for which the n=4 species is isoelectronic to neutral $Ni(CO)_4$. Again, the n=4 complex has a closed coordination, with the expected tetrahedral structure. Unlike the nickel complex, but similar to the gold system, the copper complex has a blue-shifted carbonyl stretch, consistent with the behavior for so-called "non-classical" carbonyls.

A longstanding goal in inorganic chemistry has been to test the limits of the 18-electron rule in situations requiring unusual coordination numbers. Newer studies have extended this work to the early transition metals, which have fewer d electrons and require more CO ligands to achieve an 18-electron configuration. Specifically, we looked at the group IV transition metals titanium, zirconium and hafnium. As cations, each of these has an odd number of electrons and carbonyl complexes could conceivably have 15, 17 or 19 electrons for 6, 7,or 8 carbonyl complexes. Surprisingly, we found that each of these complexes form six-coordinate complexes with octahedral structures. The red shifts of the C–O stretches were among the largest yet seen, and these increased for the heavier metals. The group III metals scandium and yttrium have fewer-still electrons, and would form 18-electron complexes only if they have eight carbonyl ligands. We found that the coordination of the scandium complexes was only seven, but that yttrium did indeed form the unusual eight-coordinate carbonyls.

Although rhodium is isoelectronic to cobalt, $Rh(CO)_n^+$ complexes were found to have a primary coordination number of four, with a square-planar structure for the n=4 species. We found the same structure and coordination for the nitrogen complexes of rhodium, i.e., $Rh(N_2)_n^+$. In both cases, the bonding has a large component of electrostatics, which yields a blue-shifted carbonyl stretch, but a red-shifted N–N stretch.

Extending the metal carbonyl work, we examined metal *oxide* carbonyls, i.e., $VO^+(CO)_n$, $VO_2^+(CO)_n$ and $VO_3^+(CO)_n$. We found that the coordination of VO^+ is five CO's, while that of VO_3^+ is three. The carbonyl stretching frequencies in these systems are less shifted than in the V^+ carbonyl complex. The VO^+ system has a CO stretch that is virtually unshifted with respect to free CO, while the VO_2^+ and VO_3^+ carbonyl stretches are blue shifted. Increased oxidation apparently leads to reduced available *d* electron density and consequently less back-bonding. In these systems we could also compare the V–O stretches to those of the corresponding VO_n^+ cations without carbonyl ligands. In each case, the presence of the carbonyl ligands induced a

red-shift on the corresponding metal-oxygen stretches. In a further extension of the carbonyl work, we studied metal dimer carbonyl of copper and vanadium.

Previous work in our lab had identified intracluster reactions in several metal ion complexes with CO_2, i.e., $M^+(CO_2)_n$ (M=V, Ni, Al) Vibrational bands in the asymmetric stretch region of CO_2 (near 2350 cm^{-1}) were assigned to coordinated CO_2 in the small clusters (n=1-4) and other bands were assigned to second sphere ligands in the slightly larger clusters (n=5-7). In larger clusters still, however, new bands grew in suggesting that the core ion identity had somehow changed, producing a different environment for some CO_2 ligands. We speculated that the reaction might be the formation of an oxide-carbonyl species, which would have the same mass as the selected $M^+(CO_2)_n$ species, but at that time we could not scan the lower frequency region of the spectrum to investigate this further. Recently, using the new longer wavelength coverage of our IR system, we scanned this region for the $V^+(CO_2)_n$ system. We also intentionally produced the oxide carbonyl species of the form $VO^+(CO)_n$ (see above) to see where the carbonyl and oxide stretches for these systems would come. The lower frequency region of the spectrum also had new bands appearing at the same critical cluster size seen before, but the bands were not those of an oxide carbonyl. Instead, we found that the intracluster reaction had produced an oxalate species in the cluster by coupling two CO_2 molecules in the second sphere (remote from the metal). Similar chemistry on nickel complexes are underway.

In a study of benzene complexes, we investigate aluminum-benzene cations with up to four benzenes. Spectra in the fingerprint region reveal the nature of benzene ring vibrations and how they are affected by metal complexation. Computational studied indicate that aluminum forms a tri-benzene complex rather than a di-benzene sandwich as its completed coordination, but the infrared data is inconclusive on this point.

Future Plans

Continuing the work above, metal-benzene and metal-CO_2 studies will employ the long wavelength laser coverage to examine higher resolution spectroscopy in these systems and to further elucidate the intracluster reaction systems for other metals.

Publications (1/2011–present) for this Project

1. P. D. Carnegie, B. Bandyopadhyay and M. A. Duncan, "Infrared spectroscopy of $Sc^+(H_2O)$ and $Sc^{2+}(H_2O)$ via argon complex predissociation: The charge dependence of cation hydration," *J. Chem. Phys.* **134**, 014302-1 to 014302-9 (2011). **DOI:** 10.1063/1.3515425

2. M. A. Duncan, "IR spectroscopy of gas phase metal carbonyl cations," *J. Mol. Spec.* **266**, 63-74 (2011) (invited feature article; cover art). **DOI:**10.1016/j.jms.2011.03.006

3. B. Bandyopadhyay, P. D. Carnegie, and M. A. Duncan, "Infrared spectroscopy of $Mn^+(H_2O)_n$ and $Mn^{2+}(H_2O)$ complexes via argon complex predissociation," *J. Phys. Chem. A* **115**, 7602-7609 (2011). **DOI:** 10.1021/jp203501n.

4. A. M. Ricks, L. Gagliardi and M. A. Duncan, "Oxides and superoxides of uranium detected by IR spectroscopy in the gas phase," *J. Phys. Chem. Lett.* **2**, 1662-1666 (2011). **DOI:** 10.1021/jz2006868.

5. A. D. Brathwaite, Z. D. Reed and M. A. Duncan, "Infrared spectroscopy of copper carbonyl cations," *J. Phys. Chem. A* **115**, 10461-10469 (2011). **DOI:** 10/1021/jp206102z.

6. J. D. Mosley, T. C. Cheng, S. Hasbrouck, A. M. Ricks and M. A. Duncan, "Electronic Spectroscopy of Co^+-Ne via Mass-selected Photodissociation," *J. Chem. Phys.* **135**, 104309-1 to 104309-6 (2011). **DOI:** 10.1063/1.3633472.

7. A. D. Brathwaite and M. A. Duncan, "Infrared spectroscopy of $Si(CO)_n^+$ complexes: Evidence for asymmetric coordination," *J. Phys. Chem. A* **116**, 1375-1382 (2012). **DOI:** 10.1021/jp211578t.

8. R. Garza-Galindo, M. Castro and M. A. Duncan, "Theoretical study of nascent hydration in the $Fe^+(H_2O)_n$ system," *J. Phys. Chem. A* **116**, 1906-1913 (2012). **DOI:** 10.1021/jp2117533l.

9. B. Bandyopadhyay and M. A. Duncan, "Infrared spectroscopy of $V^{2+}(H_2O)$ complexes," *Chem. Phys. Lett.* **530**, 10-15 (2012). **DOI:** 10.1016/j.cplett.2012.01.048.

10. M. A. Duncan, "Laser Vaporization Cluster Sources," *Rev. Sci. Instrum.* **83**, 041101/1-19 (2012)(invited review). Selected for April 23, 2012 issue of *Virtual Journal of Nanoscale Science & Technology*, published by AIP.

11. A. M. Ricks, A. D. Brathwaite, M. A. Duncan, "Coordination and spin states of $V^+(CO)_n$ clusters revealed by IR spectroscopy," *J. Phys. Chem. A* **117**, 1001–1010 (2013). (Peter Armentrout Festschrift) **DOI:** 10.1021/jp301679m.

12. A. D. Brathwaite and M. A. Duncan, " Infrared photodissociation spectroscopy of saturated group IV (Ti, Zr, Hf) metal carbonyl cations," *J. Phys. Chem. A*, in press. (Curt Wittig Festschrift) **DOI:** 10.1021/jp400793h.

13. B. Bandyopadhyay, K. N. Reishus and M. A. Duncan, " Infrared spectroscopy of solvation in small $Zn^+(H_2O)_n$ Complexes," *J. Phys. Chem. A*, in press. **DOI:** 10.1021/jp4046676

14. A. D. Brathwaite and M. A. Duncan, "Infrared Spectroscopy of Vanadium Oxide Carbonyl Cations," *J. Phys. Chem. A*, in press. **DOI:** 10.1021/jp4068697

15. M. Castro, R. Flores Mena, and M. A. Duncan, "Theoretical Study of Nascent Solvation in $Ni^+(Benzene)_m$, m=3 and 4, Clusters," *J. Phys. Chem. A*, submitted.

Time Resolved Optical Studies on the Plasmonic Field Effects on Bacteriorhodopsin Proton Pump Function and Other Light-Harvesting Systems

Mostafa A. El-Sayed
School of Chemistry and Biochemistry, Georgia Institute of Technology
Atlanta, GA 30332
melsayed@gatech.edu

Program Scope

Plasmonic metal nanoparticles (Ag & Au) are known to support collective coherent oscillatory excitation modes of their conduction band electrons upon coupling to resonant electromagnetic light fields. These are known as the localized surface plasmons.[12] Electromagnetic fields of resonant frequencies (e.g. those of the sun) can induce these modes in the plasmonic nanoparticles. The plasmonic nanoparticle has a much more enhanced electromagnetic field than that of the light source falling on it. This large increase in the rate of absorption of molecular systems (e.g. a dye) or semiconductors (e.g. a Si wafer) occurs if the incident light is in resonance with the surface plasmon oscillation. The enhanced surface plasmon field on the nanoparticle surface decays by two mechanisms, enhanced light scattering processes and enhanced light absorption. The intensity of the scattered radiation is of very high intensity, the reason why plasmonic nanoparticles are used in imaging applications. The mechanism of the conversion into heat involves electron-phonon relaxation processes which occur in ~1 ps as well as phonon-phonon relaxation processes occurring in ~100 ps.[2, 13]

In our work, we have utilized plasmonic fields to enhance the proton photo-current production in bacteriorhodopsin (bR), the other photosynthetic system found in nature, by enhancing the rate of absorption of the blue light during the photocycle which increases the proton production.[5] We are currently working towards enhancing the performance of this and other light-harvesting systems with plasmonic nanoparticles. Ongoing efforts in colloidal chemistry are producing mechanically-stable, wavelength-tunable nanoparticles with stronger electric fields than most known plasmonic nanoparticles. We are currently exploring the transfer of the plasmonically produced heat from the nanoparticles to their environment.

Highlights and findings from some of the recent work include:

- Synthesis and comparison of Au and Ag nanorods (AuNRs and AgNRs,) with wide tunability of the localized surface plasmon resonance (LSPR) wavelength, with AgNRs being superior for surface-enhanced Raman spectroscopy (SERS) than the more studied AuNRs.[3]
- Using the double beam optical femtosecond transient absorption technique, we have determined the symmetric breathing vibration frequencies of plasmonic gold and silver nanocages and nanocubes[13] excited in the process of converting the plasmonic electronic energy into phonon energy involved in the conversion of the plasmonic energy into heat.[2] We have used the vibration frequencies as a measure of the nanoparticles' mechanical stability. These vibrations are found to correlate with the Young's modulus of the nanomaterials. Coating the plasmonic nanocages with stiffer material such as platinum or palladium nanoshells makes these nanocages mechnically more stable (having higher breathing vibration frequencies) by amounts that depend on the Young's modulus of the nanoshell.[12]
- We also studied the last step in the conversion of the plasmonic energy into heat. This occurs via the energy transfer processes between the "hot" plasmonic nanoparticles and the substrate on which they reside through coherent phonons.[2]

Comparison of Silver and Gold Nanorods (AgNRs and AuNRs) in Their Plasmonic Applications

For plasmonic nanoparticles to influence a light-harvesting system or be used in sensing, both field intensity and tunability of the LSPR spectrum are extremely important properties. One also needs to know the fraction of energy that is absorbed and not scattered, and how to adjust this for a particular application. Gold nanorods, a well-studied material,[12] have a longitudinal LSPR that redshifts into the near-infrared (NIR) as the aspect ratio increases. We successfully synthesized AgNRs[3] and performed a systematic comparison, using both theory and experiment, of their plasmonic properties with those of the more studied AuNRs. A seedless method is used to produce AgNRs with different aspect ratios, redshifting the LSPR by different amounts compared to Ag nanospheres to up to a maximum value of over 400 nm (**Figure 1, left**). Similar to AuNRs, the longitudinal LSPR wavelength of AgNRs is a simple linear function of the aspect ratio with nearly similar slopes.

Both types of nanorods are used in the SERS measurement of adsorbed molecules (**Figure 1, center**), with AgNRs giving an enhancement factor which is two orders of magnitude higher than that of AuNRs. Calculations (**Figure 1, right**) using the discrete dipole approximation (DDA) show those for nanorods of different materials but the same aspect ratio, AgNRs produce an electric field intensity which is 5 times greater than that of AuNRs. This is in agreement with the experimental results. The calculations also revealed that AuNRs scatter a larger fraction of the incident light at the wavelength of the longitudinal LSPR mode compared to AgNRs. Thus, in both nanorods, the absorption-to-scattering ratio and the LSPR wavelength can be tuned by the nanoparticle synthesis to produce a nanorod tailored specifically to the application at hand.

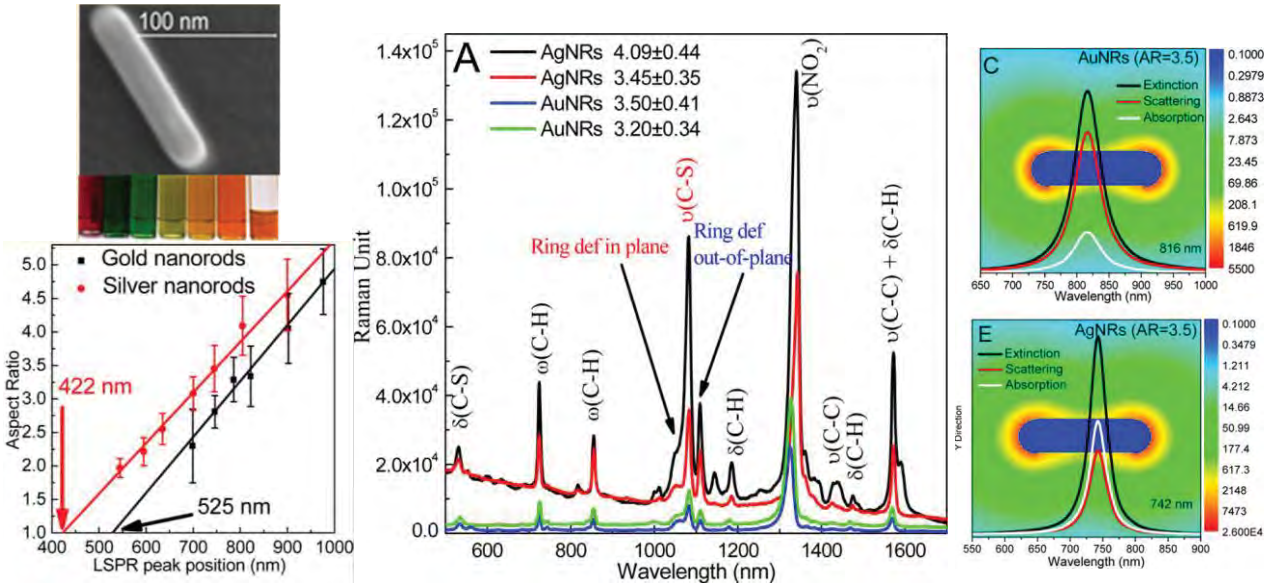

Figure 1. Left: Properties and images of AuNRs and AgNRs, with their LSPR peak positions varying with the aspect ratio. Center: Raman spectra of 4-nitrothiophenol absorbed on AuNRs and AgNRs of different aspect ratios, with AgNRs giving greater SERS enhancement. Right: Calculations of nanorods of 22 nm diameter and aspect ratio 3.5, performed by the DDA method, showing 5-fold greater field intensity and a smaller scattering-to-absorption ratio in the AgNRs.

The Fate of the Absorbed Energy in Plasmonic Nanocage Nanoparticles

Transient absorption (TA) dynamics experiments on plasmonic nanoparticles give information on how electronic excitation of the plasmonic oscillations decay first by being transferred to the metal lattice vibrations and, ultimately, to the environment as heat. These experiments have revealed a unique property of these materials, that the collective vibrations of atoms in the nanoparticle lattice may be observed

through time-dependent oscillations in the visible-to-NIR absorption spectrum.[14, 15] These oscillations are due to a varying electron density caused by changes in the particle volume. The LSPR shifts in energy in a periodic fashion, which is observed as sinusoidal behavior in the time-dependent absorption monitored at a single fixed wavelength.

We used TA to examine totally symmetric breathing vibrational modes of silver nanocubes (AgNCs), gold nanocages (AuNCs), and Au–Pd and Au–Pt double-shell nanocages (AuPdNCs and AuPtNCs, respectively).[2, 13] The hollow AuNCs are made by the galvanic replacement method[16, 17] starting from solid AgNCs as a template. The double-shell nanocages are formed by further galvanic replacement of residual Ag to add a layer of a second metal.[16] The shape and composition of the different nanocages gives a tunable LSPR in the NIR region. The breathing mode gave a measure of the mechanical stability of the nanoparticle and correlated well with the Young's modulus of the transition metal shell.[13]

The nanoparticles were deposited as monolayers on transparent substrates by the Langmuir-Blodgett (L-B) method. Dynamics measurements were performed by exciting with 400-nm, ~50-fs pulses of light and probing with white light (formed by focusing 800-nm light into sapphire or CaF_2 crystal). Different parts of the monolayer film were measured by mounting the sample holder to a continuously-translating X-Y stage.

Nanocages adsorbed as a monolayer have higher vibrational frequencies compared to the same particles in solution.[13] The stiffness of the substrate mechanically stabilizes the hollow nanoparticles, increasing the vibrational force constant, a beneficial effect for adsorbed nanoparticles used in applications such as sensing and catalysis. However, the dynamics of adsorbed nanocages have a longer-lived, lower-frequency oscillation component that is not seen for the same nanoparticles in a disordered solution environment (**Figure 2A**). We observed the same behavior for solid AgNCs (**Figure 2B**), so it is a general phenomenon, with the later dynamics depending on the substrate material.[2]

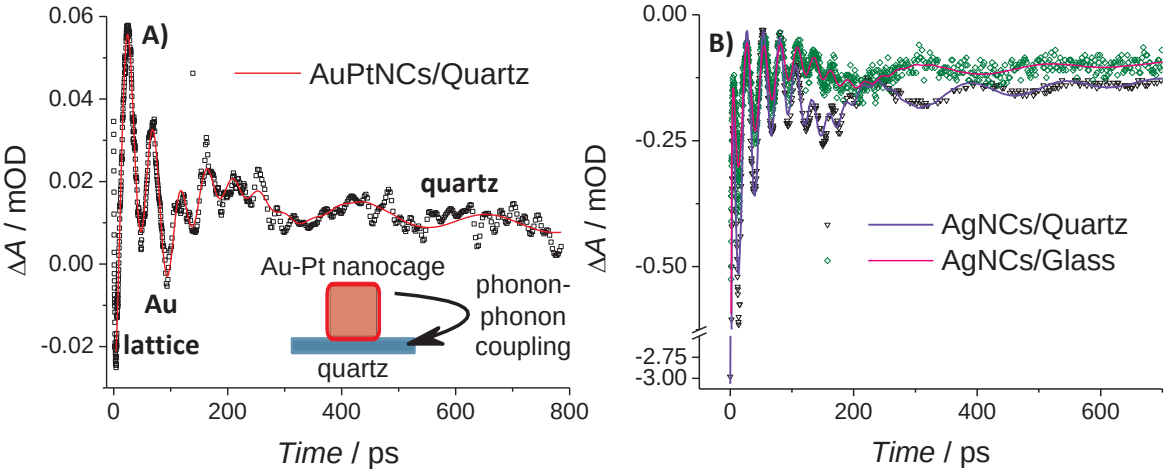

Figure 2. **A**) Transient absorption (pump 400 nm, probe 800 nm) of an L-B monolayer of AuPtNCs on quartz. Oscillations on different time scales are assigned to the vibrations of different parts of the system, with coupling between them as shown in the cartoon. **B**) Transient absorption (pump 400 nm, probe 440 nm) of L-B monolayers of AgNCs on different substrates. While the early dynamics (Ag lattice vibrations) are similar in both cases, the later dynamics (substrate vibrations) are different for the 2 systems.

The lower-frequency oscillations persist for hundreds of ps, the time scale of phonon–phonon coupling. This, along with the dependence on the substrate, is strong evidence that we are observing coherent energy transfer between the nanoparticles and the substrate. The excitation of coherent vibrations within the substrate beneath the nanoparticles causes periodic changes in the dielectric environment, which we observe experimentally through oscillations in the LSPR spectrum. Thus, we can directly monitor the fate

of the absorbed energy, both the efficiency of thermal energy transfer and its influence on the interface between the nanoparticle and the substrate. Ours is the first observation of this behavior for nanoparticles synthesized through colloidal chemistry with their native capping ligands still present. With the L-B technique, we are not limited by the complications or expense of lithography to produce supported nanoparticle monolayers.

Future Plans

Our laboratory is continuing the development of new plasmonic nanoparticles, with both hollow and solid shapes and new compositions such as bimetallic and core-shell structures, and studying their properties and potential applications. We are currently investigating the influence of these nanoparticles on their environment, including novel organic chromophores and substrates of different materials. Applications such as sensors (based on SERS, LSPR shift, etc.), catalysis, and plasmonic solar cells are being considered. Our optical, vibrational, and time-resolved spectroscopies are complemented with measurements of photocurrent and quantum yield. All of these tools will help us move towards our ultimate goal of understanding the role that plasmonic nanoparticles can play in the field of energy production, or the keys to achieving superior device performance.

Publications during the Past Period

1. Shaheen, B. S.; Salem, H. G.; El-Sayed, M. A.; Allam, N. K., Thermal/Electrochemical Growth and Characterization of One-Dimensional ZnO/TiO_2 Hybrid Nanoelectrodes for Solar Fuel Production. *J. Phys. Chem. C* **2013**, DOI: 10.1021/jp405515v.
2. Szymanski, P.; Mahmoud, M. A.; El-Sayed, M. A., The Last Step in Converting the Surface Plasmonic Energy into Heat by Nanocages and Nanocubes on Substrates. *Small*, **2013**, DOI: 10.1002/smll.201300233.
3. Mahmoud, M. A.; El-Sayed, M. A., Different Plasmon Sensing Behavior of Silver and Gold Nanorods. *J. Phys. Chem. Lett.* **2013**, *4* (9), 1541-1545.
4. Szymanski, P.; El-Sayed, M. A., Some recent developments in photoelectrochemical water splitting using nanostructured TiO_2: a short review. *Theor. Chem. Acc.* **2012,** *131* (6).
5. Yen, C.-W.; Hayden, S. C.; Dreaden, E. C.; Szymanski, P.; El-Sayed, M. A., Tailoring Plasmonic and Electrostatic Field Effects To Maximize Solar Energy Conversion by Bacteriorhodopsin, the Other Natural Photosynthetic System. *Nano Lett.* **2011,** *11* (9), 3821-3826.
6. Allam, N. K.; Yen, C.-W.; Near, R. D.; El-Sayed, M. A., Bacteriorhodopsin/TiO_2 nanotube arrays hybrid system for enhanced photoelectrochemical water splitting. *Energy Environ. Sci.* **2011,** *4* (8), 2909-2914.
7. Allam, N. K.; Poncheri, A. J.; El-Sayed, M. A., Vertically Oriented Ti–Pd Mixed Oxynitride Nanotube Arrays for Enhanced Photoelectrochemical Water Splitting. *ACS Nano* **2011,** *5* (6), 5056-5066.
8. Hesabi, Z. R.; Allam, N. K.; Dahmen, K.; Garmestani, H.; A. El-Sayed, M., Self-Standing Crystalline TiO_2 Nanotubes/CNTs Heterojunction Membrane: Synthesis and Characterization. *ACS Appl. Mater. Interfaces* **2011,** *3* (4), 952-955.
9. Chu, L. K.; Yen, C. W.; El-Sayed, M. A., Bacteriorhodopsin-based photo-electrochemical cell. *Biosens. Bioelectron.* **2010,** *26* (2), 620-626.
10. Hayden, S. C.; Allam, N. K.; El-Sayed, M. A., TiO_2 Nanotube/CdS Hybrid Electrodes: Extraordinary Enhancement in the Inactivation of Escherichia coli. *J. Am. Chem. Soc.* **2010,** *132* (41), 14406-14408.
11. Allam, N. K.; Alamgir, F.; El-Sayed, M. A., Enhanced Photoassisted Water Electrolysis Using Vertically Oriented Anodically Fabricated Ti−Nb−Zr−O Mixed Oxide Nanotube Arrays. *ACS Nano* **2010,** *4* (10), 5819-5826.

Additional References

12. Jain, P. K.; Huang, X.; El-Sayed, I. H.; El-Sayed, M. A., Noble Metals on the Nanoscale: Optical and Photothermal Properties and Some Applications in Imaging, Sensing, Biology, and Medicine. *Acc. Chem. Res.* **2008**, *41*, 1578-1586.
13. Mahmoud, M. A.; Szymanski, P.; El-Sayed, M. A., Different Methods of Increasing the Mechanical Strength of Gold Nanocages. *J. Phys. Chem. Lett.* **2012**, *3*, 3527-3531.
14. Huang, W.; Qian, W.; El-Sayed, M. A., The Optically Detected Coherent Lattice Oscillations in Silver and Gold Monolayer Periodic Nanoprism Arrays: The Effect of Interparticle Coupling. *J. Phys. Chem. B* **2005**, *109*, 18881-18888.
15. Hartland, G. V., Optical Studies of Dynamics in Noble Metal Nanostructures. *Chem. Rev.* **2011**, *111*, 3858-3887.
16. Mahmoud, M. A.; El-Sayed, M. A., Metallic Double Shell Hollow Nanocages: The Challenges of Their Synthetic Techniques. *Langmuir* **2012**, *28*, 4051-4059.
17. Sun, Y. G.; Xia, Y. N., Shape-controlled synthesis of gold and silver nanoparticles. *Science* **2002**, *298*, 2176-2179.

Statistical Mechanical and Multiscale Modeling of Catalytic Reactions

Jim Evans (PI) and Da-Jiang Liu
Ames Laboratory – USDOE and Departments of Physics & Astronomy and Mathematics,
Iowa State University, Ames, IA 50011
evans@ameslab.gov

PROGRAM SCOPE:

This theoretical Chemical Physics project at Ames Laboratory pursues molecular-level modeling of **heterogeneous catalysis and other complex reaction phenomena** at surfaces and in mesoporous materials. This effort incorporates *electronic structure analysis, non-equilibrium statistical mechanics, and coarse-graining or multi-scale modeling*. The *electronic structure* component includes DFT-VASP analysis of chemisorption and reaction energetics on metal surfaces, and *ab-initio* QM studies in collaboration with Mark Gordon. The *non-equilibrium statistical mechanical and related studies* of reaction-diffusion phenomena include Kinetic Monte Carlo (KMC) simulation of atomistic models, coarse-graining, and heterogeneous multi-scale formulations. We explore: (i) interplay between anomalous transport and catalytic reaction in functionalized mesoporous materials in collaboration with Ames Lab experimentalists; (ii) chemisorption and heterogeneous catalysis on metal surfaces, including steady-state bifurcation analysis, connecting atomistic to spatiotemporal mesoscale behavior, and fluctuation effects in nanoscale catalyst systems and for higher pressures; (iii) general statistical mechanical models for reaction-diffusion processes exhibiting non-equilibrium phase transitions, metastability, critical phenomena, etc.. (iv) diffusion, self-organization, reaction,… on non-conducting surfaces

RECENT PROGRESS:

CATALYTIC REACTIONS IN FUNCTIONALIZED NANOPOROUS MATERIALS

Recent efforts have focused on catalytic conversion reactions occurring inside linear nanopores where passing of reactants and products is strongly inhibited [3,4,11,13,15]. These studies are motivated by experiments at Ames Laboratory, e.g., of esterification reactions and conversion of PNB to an aldol compound in functionalized mesoporous silica nanospheres (MSN). The reaction and reactants tend to be concentrated near the pore openings, with the interior primarily populated by "trapped" product. Despite extensive analyses of such systems (mostly for catalysis in zeolites), there is limited understanding of basic issues such as the scaling of reactivity with key parameters, the form of reactant concentration profiles, etc. Mean-field reaction-diffusion equation (RDE) treatments fail to describe behavior, as do "hydrodynamic" treatments neglecting fluctuations in adsorption-desorption and diffusion at the pore openings.

In contrast, we have developed a "generalized hydrodynamic" treatment which for the case of comparable mobility of reactant and product species precisely captures reaction-diffusion behavior in these systems as assessed by "exact" KMC simulation studies [15]. The key requirements are appropriate description of inhibited transport, and incorporation of fluctuation effects. Our theory utilizes: (i) an exact relation between chemical diffusion fluxes appearing in the RDE and a tracer diffusion coefficient, D_{tr}, and (ii) a generalized D_{tr} which is enhanced near pore openings. The first approach to obtain D_{tr} was based on analysis of the random walk of tagged particles starting a certain distance from the pore opening. We are exploring an alternative based on analysis of concentration profiles for counter-diffusion modes. This theory provides a powerful tool to elucidate behavior, e.g., varying multiple experimental parameters.

Other work was motivated by esterification studies at Ames Laboratory which indicated that multi-functionalization to make the pore hydrophobic, i.e., to make it unfavorable for the reaction product H_2O, can enhance yield. Model refinement to account for varying pore-product interactions (by adjusting the product re-adsorption rate) reveals that yield can actually increase during conversion of reactant to product for single-file diffusion [15] ! We can identify both thermodynamic and kinetic contributions to this variation in yield.

CHEMISORPTION AND HETEROGENEOUS CATALYSIS ON METAL SURFACES

Chemisorption and complex formation. Detailed and precise characterization of chemisorption processes is key for modeling of catalytic reactions, e.g., to describe reactant ordering, possible chemisorption-induced restructuring and dynamics of metal surfaces, and poisoning and/or promotion by impurities such as sulfur (S). Our previous DFT analyses explored formation of "small" metal-S complexes and related enhanced decay of Ag nanoclusters on Ag(111) and Ag(100) [2,7,8]. The decay kinetics are distinct for these systems and we continue appropriate model development. Recently, we used DFT analysis to elucidate STM observations of an entire family of "larger" rod-like Ag-S complexes on Ag(100) [14].

Diffusion plays a ubiquitous role in chemisorption, catalysis, and self-assembly processes on surfaces. We continue analysis both for complex local environments on metal surfaces, and for species on non-conducting surfaces utilizing high-level quantum chemistry with Gordon [6].

Realistic multi-site lattice-gas (msLG) modeling of complete catalytic reaction processes. A long-standing goal for surface science has been to develop realistic molecular-level models for catalytic reaction processes on metal surfaces (incorporating adsorption, desorption, diffusion, and reaction). We have continued development and application of realistic msLG models and efficient KMC simulation algorithms to describe CO-oxidation on unreconstructed metal surfaces. Specifically, we developed the first realistic models for CO+O on Ir(100) and Pt(100) for typical operating regimes with significant coverage where the surface is unreconstructed. In particular, this includes description on n×1 O-ordering on bridge sites which is observed for pure O-adlayers and during reaction. In addition, reactive steady-states are impacted by dynamics, so we continue development more realistic treatments for CO-adsorption subject to steering and funneling, and especially for dissociative oxygen adsorption. For the latter, we find that the classic Brundle-Behm-Barker 8-site model for constrained dissociation on diagonal neighboring hollow sites does not apply. Instead activated dissociation occurs on neighboring vicinal br sites for Pd(100), with variations of this picture applying for other metals. Results have been incorporated into a comprehensive review on msLG modeling [16].

FUNDAMENTAL PHENOMENA IN FAR-FROM-EQUILIBRIUM REACTION SYSTEMS

An understanding of discontinuous non-equilibrium phase transitions (such as catalytic poisoning transitions) and associated metastability and criticality at a level comparable to that for equilibrium systems constitutes a ***BESAC Science Grand Challenges*** *(Cardinal Principles of Behavior beyond Equilibrium)*. We continue related statistical mechanical studies for a version of Schloegl's second model for autocatalysis, also comparing behavior with mean-field predictions [5,9,10,16]. Despite the occurrence of "generic two-phase coexistence", metastablity and nucleation phenomena appear similar to thermodynamic systems. Our previous nucleation studies developed an understanding of critical droplet size. However, a greater challenge is to develop a theory for the nucleation rate for these non-equilibrium systems in the absence of the usual free-energy framework. We have proposed a formulation mimicking the usual

thermodynamic treatment but assuming the existence of a free-energy type Lyapunov functional (which is only obvious for single-variable mean-field type models). Predicted behavior is consistent with simulation studies of nucleation kinetics. Other work has focused on mean-field type treatments of critical droplet behavior based on discrete reaction-diffusion equations.

FUTURE PLANS:

CATALYTIC REACTIONS IN FUNCTIONALIZED MESOPOROUS MATERIALS

We are working toward the development of more detailed system-specific models for catalytic conversion reactions in mesoporous materials including MSN. To elucidate the dependence of reactivity on pore diameter (as observed at Ames Lab for PNB conversion to an aldol), we are assessing the passing propensity for suitably shaped reactant and product molecules inside narrow pores, and plan to incorporate this behavior into coarse-grained models describing the overall reaction process. We are implementing stochastic Langevin dynamics to describe such passing phenomena, and will compare behavior with that predicted by an equivalent Fokker-Planck formulation. Also, further development of our generalized hydrodynamic treatment is needed for these systems, e.g., to describe greatly differing reactant/product mobilities, cooperativity in reaction kinetics (e.g., as reflected in the observed concentration-dependence of certain diasteroselective reactions at Ames Lab), more complex reaction mechanisms, etc..

There is also motivation to model catalytic nanomaterials themselves. We are exploring bond-switching MC algorithms for a Continuous Random Network model providing atomistic-level description of amorphous materials such as MSN. There is interest in describing the reaction-limited formation of semiconductor nanoclusters used in photocatalysis studies at Ames Lab.

CHEMISORPTION AND HETEROGENEOUS CATALYSIS ON METAL SURFACES

Atomistic msLG models of catalytic reactions on metal surfaces. We continue our core goal of developing realistic and predictive atomistic-level models and KMC simulation algorithms for catalytic reactions on various metal (111) and (100) surfaces. Recent PEEM studies (by Suchorski, Schloegl, et al.) provide detailed characterization of catalytic ignition for oxidation reactions which our models are uniquely positioned to elucidate. Of particular interest is enhanced fluctuations effects and more complex reaction kinetics (e.g., multistability) for higher pressures due to higher reactant coverages. There are also multiphysics and multiscale modeling challenges, e.g., concentration variations across polycrystalline catalysts surface as used in recent PEEM studies; mass-transport limited behavior at higher pressures requiring coupling of CFD for reactor flow. Both applications can utilize our HCLG multiscale modeling approach [16].

Chemisorbed adlayer and metal surface dynamics. We are interested in exploring ordering and dynamics in chemisorbed layers, formation of metal complex and metal surface dynamics. Target systems are: halogens, chalcogens, H_2S and H_2O on on coinage metals (with Thiel); diffusion in high-density adlayers, e.g., O adlayers on Pt(111) in EPOC studies (with Imbihl).

AB-INITIO STUDIES OF SURFACE ADSORPTION, DIFFUSION AND REACTION

We plan to continue exploring high-level QM analysis with Gordon of key surface diffusion and reaction processes (results of which can be incorporated into molecular-level KMC modeling, and potentially also into coarse-grained modeling). QM/MM can help address the limitations of DFT-based analysis of energetics on non-conducting surfaces. Also ab-initio QM performed for small clusters can correct DFT estimates of chemisorption energies for those systems. Then, suitable extrapolation yields more precise estimates for extended metal surfaces.

FUNDAMENTAL PHENOMENA IN FAR-FROM-EQUILIBRIUM REACTION SYSTEMS

Analysis will continue of non-equilibrium 1st-order phase transitions, especially issues of metstability and nucleation, in a variety of statistical mechanical reaction-diffusion models. We are extending these analyses to various ZGB-type surface reaction models, which although too simplistic to describe standard low-pressure reaction behavior, may provide a valuable paradigm for high-pressure high-coverage low-effective-surface-mobility fluctuation-dominated reactions.

PUBLICATIONS SUPPORTED BY USDOE CHEM. SCIENCES FOR 2011-PRESENT:

[1] *Boundary conditions for Burton-Cabrera-Frank type step-flow models: coarse-graining of discrete deposition-diffusion equations*, D.M. Ackerman, J.W. Evans, SIAM Multiscale Model. Sim. **9**, 59 (2011)

[2] *Adsorption of sulfur on Ag(100)*, S.M. Russell, M.M. Shen, D.-J. Liu, et al., Surf. Sci. **605**, 520 (2011).

[3] *Catalytic conversion reactions mediated by single-file diffusion in linear nanopores...,* D.M. Ackerman, J. Wang, J.H. Wendel, D.-J. Liu, M. Pruski, J.W. Evans, J. Chem. Phys. **134**, 114107 (2011).

[4] *Interplay between anomalous transport & catalytic reaction in single-file mesoporous systems*, D.-J. Liu, J. Wang, D. Ackerman, I. Slowing, M. Pruski, H. Chen, V. Lin, J.W. Evans, ACS Cat. **1**, 751 (2011).

[5] *Schloegl's second model for autocatalysis on a cubic lattice: Analysis via mean-field discrete reaction-diffusion equations*, C.-J. Wang, X. Guo, D.-J. Liu, J.W. Evans, J. Stat. Phys. **144**, 1308 (2011).

[6] *Adsorption and diffusion of Gallium Adatoms on the Si(100) -2x1 reconstructed surface: An MCSCF study using surface clusters*, L. Roskop, J.W. Evans, M.S. Gordon, J. Phys. Chem. C, **115**, 23488 (2011).

[7] *Comment on sulfur-induced reconstruction of Ag(111) surface studied by DFT*, M. Shen, D.-J. Liu, C.J. Jenks, P.A. Thiel, J. Phys. Chem. C **115**, 23651 (2011).

[8] *Destabilization of Ag nanoislands on Ag(100) by adsorbed sulfur*, M. Shen, S.M. Russell, D.-J. Liu, P.A. Thiel, J. Chem. Phys. **135**, 154701 (2011).

[9] *Tricriticality in generalized Schloegl models for autocatalysis: Lattice-gas realization with particle diffusion*, X. Guo, D.K. Unruh, D.-J. Liu, J.W. Evans, Physica A **391**, 633 (2012).

[10] *Schloegl's second model for autocatalysis on hypercubic lattices: Dimension-dependence of generic two-phase coexistence*, C.-J. Wang, D.-J. Liu, J.W. Evans, Phys. Rev. E, **85**, 041109 (2012).

[11] *Conversion reactions in surface-functionalized mesoporous materials*, J. Wang, D. Ackerman, K. Kandel, I.I. Slowing, M. Pruski, and J.W. Evans, MRS Proc. Symp. RR F11 (MRS, Pittsburgh, 2012).

[12] *Morphological evolution during growth and erosion on vicinal Si(100) surfaces: From electronic structure to atomistic and coarse-grained modeling*, D.-J. Liu, D.M. Ackerman, X. Guo, M.A. Albao, L. Roskop, M.S. Gordon, and J.W. Evans, MRS Proc. Symp. EE Fall 2011 (MRS, Pittsburgh, 2012).

[13] *Generalized hydrodynamic treatment of interplay between restricted transport & catalytic reactions in nanoporous materials*, D.M. Ackerman, J. Wang, J.W. Evans, Phys. Rev. Lett., **108**, 228301 (2012).

[14] *Structure, Formation, and Equilibration of Ensembles of Ag-S Complexes on an Ag Surface*, S. Russell, Y. Kim, D.-J. Liu, J.W. Evans, and P.A. Thiel, J. Chem. Phys., 138, 071101 (2013). (Cover)

[15] *Controlling reactivity in nanoporous catalysts by tuning reaction product – pore interior interactions: statistical mechanical modeling*, J. Wang, D.M. Ackerman, V.S.-Y. Lin, M. Pruski and J.W. Evans, J. Chem. Phys. 138, 134705 (2013).

[16] *Realistic multisite lattice-gas modeling and KMC simulation of catalytic surface reactions: Kinetics and multiscale spatial behavior for CO-oxidation on metal(100) surfaces,* D.-J. Liu and J.W. Evans, Progress in Surface Science, review submission approved by editor (2013).

Confinement, Interfaces, and Ions: Dynamics and Interactions in Water, Proton Transfer, and Room Temperature Ionic Liquid Systems (DE-FG03-84ER13251)

Michael D. Fayer
Department of Chemistry, Stanford University, Stanford, CA 94305
fayer@stanford.edu

Water and processes that occur in water rarely take place in pure bulk water. In most situations that occur in nature and in technological applications, water is interacting with interfaces and ions, and it is frequently confined in structures that have nanometer dimensions. We are investigating the dynamics of water and other molecules in complex systems using a variety of ultrafast methods, particularly infrared methods including 2D IR vibrational echo spectroscopy and polarization selective IR pump-probe experiments. These experimental methods provide information on the dynamics and interactions of water and other molecules in complex systems.[1,3,4,5,7,9,10,11,15]

Aqueous salt solutions and interactions of water with ions are ubiquitous. They occur inside living cells, the ocean, polyelectrolyte fuel cell membranes and in many industrial chemical processes. The physical changes in structure and dynamics that ions exert on aqueous solutions are central to understanding and controlling processes. The ability of water to form up to four hydrogen bonds gives it unique liquid properties. Water hydrogen bonds are not static, but continually break and reform in an extended network of concerted motions encompassing at least the first and second solvation shells. When the water molecules interact with other species, they are unable to form hydrogen bonds in the same manner as bulk water. Understanding the dynamics of water in complex environments is important for understanding many physical and biological processes, such as proton transport in fuel cell membranes and protein folding, but it is also challenging because the dynamics of the water structure occur on the hundreds of femtoseconds to picoseconds scale. Thus, ultrafast mid-infrared spectroscopy is utilized to probe the dynamics of these systems.

Water hydrogen bond dynamics in concentrated salt solutions were studied using polarization-selective IR pump-probe spectroscopy and 2D IR vibrational echo spectroscopy performed on the OD hydroxyl stretching mode of dilute HOD in H_2O/salt solutions.[14] The OD stretch is studied to eliminate vibrational excitation transfer, which interferes with the dynamical measurements. We studied a wide range of ion pairs, e.g., NaBr, $MgBr_2$, Na_2SO_4, $MgSO_4$, and many others. Though previous research suggested that only the anion affected dynamics in aqueous solution, we have shown that the cation plays a role as well. From FT-IR spectra of the OD stretch, it was observed that replacing either ion of the salt pair causes a shift in absorption frequency relative to that of the OD stretch absorption in bulk pure water. This shift becomes pronounced with larger, more polarizable anions or smaller, high charge-density cations. The vibrational lifetime of the OD hydroxyl stretch in these solutions is a local property and is primarily dependent on the nature of the anion and whether the OD is hydrogen bonded to the anion or to the oxygen of another water molecule. However, the cation still has a small effect. Time dependent anisotropy measurements showed that reorientation dynamics in these concentrated solutions is a highly concerted process. While the lifetime, a local probe, displays an ion-associated and a bulk-like component in concentrated solutions, the orientational relaxation does not have two subensemble dynamics as demonstrated by the lack of wavelength dependence. The orientational relaxation of the single ensemble was found to be dependent on the identity of both the cation and anion. The 2D IR vibrational echo experiments measure spectral diffusion that is caused by structural evolution of the system. The vibrational echo measurements yield the frequency-frequency correlation function (FFCF). The results

also showed that the structural dynamics of the water in concentrated salt solutions are dependent on the cation as well as the anion.

Extensive previous work in this program has examined in detail the influence of interfaces and nanoscopic environments on the dynamics of water. Systems that have been very useful in these studies use the surfactant AOT, which forms well defined reverse micelles and lamellar structures, as well as other ordered phases. We have examined the dynamics of water at the interfaces of AOT reverse micelles and AOT lamellae. The experiments using 2D IR and IR pump-probe methods have shown that water at interfaces has dynamics that are strongly influenced by the interface and that the nanoscopic dimensions of such systems is very important. Although we and other researchers have obtained a great deal of information about water at surfactant interfaces, until now there has been no information on the fast structural dynamics of the molecules that make up the interface. We have begun systematic studies to understand the dynamics inside of bilayers with water at the bilayer exterior interfaces. The first experiments are on AOT lamellae and other phases, but the experiments will be extended to other bilayer forming molecules as planar bilayers and as vesicle bilayers of different sizes, and therefore radii of curvature.

The dynamics inside the organic regions of AOT/water mixtures in the lamellar mesophase, bicontinuous cubic (BC) phase, and in an analogous molecule without the charged sulfonate head group were investigated by observing spectral diffusion, orientational relaxation and population relaxation using 2D-IR and IR pump-probe experiments on the asymmetric CO stretch of a vibrational probe, tungsten hexacarbonyl ($W(CO)_6$).[17] The water layer thickness between the bilayer planes in the lamellar phase was varied. For comparison, the dynamics of $W(CO)_6$ in the normal liquid bis(2-ethylhexyl) succinate (EHS), which is identical to AOT but has no charged sulfonate head group, were also studied. The 2D IR experiments measured spectral diffusion, which results from the structural evolution of the system. Spectral diffusion was quantified by frequency-frequency correlation function (FFCF). In addition to a homogeneous component, the FFCFs were found to be biexponential decays with fast and slow time components of ~12.5 ps and ~150 ps in the lamellar phase. Both components of the FFCF were determined to be independent of the number of water molecules per head group for the lamellae. Thus, the dynamics inside of the bilayers in the alkyl chain regions away from the head groups are independent of the number of water molecules solvating the head groups. However, a phase transition to the BC phase, which modifies the internal structure of the bilayers, does change the internal dynamics, with the structural dynamics becoming slower. The dynamics in the ordered phases are in sharp contrast to the dynamics in EHS, which displayed fast and slow components of the FFCF of 5 ps and 80 ps, respectively. So far the take home message is that the dynamics of the organic interior of bilayer structures depends on the details of the structure and are very different from a disordered liquid even when the individual molecule structure is the same.

Thin films and molecular monolayers are of fundamental interest and importance in science and technology. Molecular monolayers are used to control surface properties and reactions in a variety of scientific and technological fields including micro-electrical-mechanical systems, chemical sensors, and micro-electronics. Functionalized molecular monolayers are also an important class of systems for performing molecular heterogeneous catalysis. In many of the practical uses of molecular monolayers, functionalized surfaces come into contact with different chemical environments, e.g. solvents. Understanding how functionalized surface properties are different from the same chemical species in bulk and how surface properties including dynamics of the molecular surface layer change with exposure to different chemical conditions is

important for building a more complete understanding of these ubiquitous physical and chemical systems.

Monolayers functionalized with tricarbonyl (1,10)-phenanthroline rhenium chloride ($RePhen(CO)_3Cl$) were studied in the presence of a variety of polar organic solvents (chloroform, tetrahydrofuran, dimethylformamide, acetonitrile), hexadecane, and water. $RePhen(CO)_3Cl$ is a photocatalyst that takes CO_2 to CO or other products.[6,12] The head group of the functionalized surfaces, $RePhen(CO)_3Cl$, is soluble in the bulk polar organic solvents but not in hexadecane or water. The surface structural dynamics were studied using IR absorption, 2D IR vibrational echoes, and heterodyne-detected transient gratings (HDTG). The application of 2D IR and other nonlinear IR methods to monolayers is a major advance because of the exceedingly small number of molecules that give rise to the signals from a monolayer. The head group was also studied in the bulk solvents. Immersion in solvent changes the environment of the surface bound $RePhen(CO)_3Cl$ as was shown by a solvent-dependent symmetric CO stretch absorption frequency and line shape. The 2D IR spectroscopy is sensitive to spectral diffusion, which reports on the structural time dependence. In the absence of solvent (bare surface), the 2D IR measurements showed that spectral diffusion takes place on a 37 ± 4 ps timescale. However, in the presence of THF, MeCN or $CHCl_3$ spectral diffusion occurred in 25 ± 6 ps. When the surface was immersed in DMF, the spectral diffusion time constant was 15 ± 3 ps. In hexadecane the spectral diffusion slowed to 77 ± 15 ps, slower than the bare surface. In D_2O, the spectral diffusion was also slower than the bare surface. Therefore, there is a distinct difference in surface dynamics for solvents that can dissolve the head group in bulk solution and solvents in which the head group is insoluble.

Multidimensional visible spectroscopy using pulse shaping to produce pulses with stable controllable phases and delays has emerged as an elegant tool to acquire electronic spectra faster and with greatly reduced instrumental and data processing errors. Recent migration of this approach using acousto-optic modulator (AOM) pulse shaping to the mid-infrared region has proved useful for acquiring 2D IR vibrational echo spectra. The measurement of spectral diffusion in 2D IR experiments hinges on obtaining accurate 2D line shapes. Until our recent work, pulse shaping 2D IR has not been used to study the time-dependent spectral diffusion of a vibrational chromophore. We have compared the spectral diffusion data obtained from a standard non-collinear 2D IR spectrometer using delay lines to the data obtained from an AOM pulse shaper based 2D IR spectrometer.[13] The pulse shaping experiments were performed in stationary, partially rotating, and fully rotating reference frames and were the first in the infrared to produce 2D spectra collected in a fully rotating frame using a phase controlled pulse sequence. Rotating frame experiments provide a dramatic reduction in the number of time points that must be measured to obtain a 2D IR spectrum, with the fully rotating frame giving the greatest reduction. Experiments were conducted on the transition metal carbonyl complex tricarbonylchloro(1,10-phenanthroline)rhenium(I) in chloroform. The time dependent data obtained from the different techniques and with different reference frames were shown to be in agreement. These experiments have established the ability of pulse shaping 2D IR to make accurate measurements of spectral diffusion. We are now applying this method to a variety of systems including the study of the interior of AOT bilayers as briefly discussed above.

Publication from DOE Sponsored Research 2010 – present

(1) "Analysis of Water in Confined Geometries and at Interfaces," M. D. Fayer and Nancy E. Levinger Ann. Rev. Analytical Chem. 3, 89-107 (2010).

(2) "Room Temperature Ionic Liquids–Lithium Salts Mixtures: Optical Kerr Effect Dynamical Measurements," Bruno G. Nicolau, Adam Sturlaugson, Kendall Fruchey, Mauro C. C. Ribeiro, and M. D. Fayer J. Phys. Chem. B 114, 8350-8356 (2010).

(3) "Water Dynamics in Small AOT Reverse Micelles in Two Solvents: 2D IR Vibrational Echoes with 2D Background Subtraction," Emily E. Fenn, Daryl B. Wong, and M.D. Fayer J. Chem. Phys. 134, 054512 (2011).

(4) "Extracting 2D IR Frequency-Frequency Correlation Functions from Two Component Systems," Emily E. Fenn and M. D. Fayer J. Chem. Phys. 135, 07450 (2011).

(5) "Dynamics of Water at the Interface in Reverse Micelles: Measurements of Spectral Diffusion with 2D IR Vibrational Echoes," Emily E. Fenn, Daryl B. Wong, Chiara H. Giammanco, and M. D. Fayer J. Phys. Chem. B 115, 11658-11670 (2011).

(6) "Structural Dynamics of a Catalytic Monolayer Probed by Ultrafast 2D IR Vibrational Echoes," Daniel E. Rosenfeld, Zsolt Gengeliczki, Brian J. Smith, T. D. P. Stack, and M. D. Fayer Science 334, 634-639 (2011).

(7) "Water in a Crowd," M. D. Fayer Physiology 26, 381-392 (2011).

(8) "Investigation of Nanostructure in Room Temperature Ionic Liquids using Electronic Excitation Transfer," Kendall Fruchey and M. D. Fayer J. Phys. Chem. B 116, 3054-3064 (2012).

(9) "Dynamics of Water Interacting with Interfaces, Molecules, and Ions," M. D. Fayer Acc. of Chem. Res. 45, 3-14 (2012).

(10) "Orientational Dynamics of Room Temperature Ionic Liquid/Water Mixtures: Evidence for Water-Induced Structure and Anisotropic Cation Solvation," Adam L. Sturlaugson, Kendall S. Fruchey, and M. D. Fayer J. Phys. Chem. B 116, 1777-1787 (2012).

(11) "Water Dynamics in Water/DMSO Binary Mixtures," Daryl B. Wong, Kathleen P. Sokolowsky, Musa I. El-Barghouthi, Emily E. Fenn, Chiara H. Giammanco, Adam L. Sturlaugson, and Michael D. Fayer J. Phys. Chem. B 116, 5479-5490 (2012).

(12) "Dynamics of Functionalized Surface Molecular Monolayers Studied with Ultrafast Infrared Spectroscopy," Daniel E. Rosenfeld, Jun Nishida, Chang Yan, Zsolt Gengeliczki, Brian J. Smith, and Michael D. Fayer J. Chem. Phys. C 116, 23428-23440 (2012).

(13) "Measured Spectral Diffusion in Rotating Frames Using Pulse Shaping and in the Stationary Frame Using the Standard Method," S. K. Karthick Kumar, A. Tamimi, and M. D. Fayer J. Chem. Phys. 137, 184201 (2012).

(14) "Water Dynamics in Divalent and Monovalent Concentrated Salt Solutions," Chiara H. Giammanco, Daryl B. Wong, and Michael D. Fayer J. Phys. Chem. B 116, 13781-13792 (2012).

(15) "The Dynamics of Isolated Water Molecules in a Sea of Ions in a Room Temperature Ionic Liquid," Daryl B. Wong, Chiara H. Giammanco, Emily E. Fenn, Michael D. Fayer J. Phys. Chem. B 117, 623-635 (2013).

(16) "Structural Dynamics at Monolayer-Liquid Interfaces Probed by 2D IR Spectroscopy," Daniel E. Rosenfeld, Jun Nishida, Chang Yan, S. K. Karthick Kumar, Amr Tamimi, and Michael D. Fayer J. Phys. Chem. C 117, 1409-1420 (2013).

(17) "Dynamics in the Interior of AOT Lamellae Investigated with 2D IR Spectroscopy," S. K. Karthick Kumar, A. Tamimi, and Michael D. Fayer J. Am. Chem. Soc. 135, 5118-5126 (2013).

Chemical Kinetics and Dynamics at Interfaces

Fundamentals of Solvation under Extreme Conditions

John L. Fulton

Chemical and Materials Sciences Division
Pacific Northwest National Laboratory
902 Battelle Blvd., Mail Stop K2-57
Richland, WA 99354
john.fulton@pnl.gov

Collaborators: M. Baer, M. Balasubramanian, E. J. Bylaska, N. Govind, T. Hutwelker, C. J. Mundy, G. K. Schenter, J. H. Weare

Program Scope

The primary objective of this project is to describe, on a molecular level, the solvent/solute structure and dynamics in fluids such as water under extremely non-ideal conditions. The scope of studies includes solute–solvent interactions, clustering, ion-pair formation, and hydrogen bonding occurring under extremes of temperature, concentration and pH. The effort entails the use of spectroscopic techniques such as x-ray absorption fine structure (XAFS) spectroscopy, high-energy x-ray scattering, coupled with theoretical methods such as molecular dynamics (MD-XAFS), and electronic structure calculations in order to test and refine structural models of these systems. In total, these methods allow for a comprehensive assessment of solvation and the chemical state of an ion or solute under any condition. The research is answering major scientific questions in areas related to energy-efficient separations, hydrogen storage and sustainable nuclear energy (aqueous ion chemistry and corrosion). This program provides the structural information that is the scientific basis for the chemical thermodynamic data and models in these systems under non-ideal conditions.

Recent Progress

Cation-anion interactions in aqueous phases. The interaction of anions with cations in aqueous solutions underlies broad areas of biochemistry, geochemistry and atmospheric chemistry. To this day, there is an incomplete understanding of the interaction of simple salts such as Na^+ with Cl^- or of Li^+ with Cl^- dissolved in water. The electrostatic attractive interactions between counter ions are modulated by a delicate balance of different hydration effects that are not yet fully understood. Using XAFS, HEXS, and DFT-MD we explored the interaction of chloride (Cl-) with cations from the Group IA (Li^+, Na^+, K^+, Rb^+) and IIA (Be^{2+}, Mg^{2+}, Ca^{2+}, Sr^{2+}) elements. The method primarily involves XAFS spectroscopy at the Cl K-edge using a new, low-Z cell that incorporates 200 nm thick Si_3N_4 x-ray transmission windows. The same series of salts were also studied by high energy x-ray diffraction (HEXS at APS) to derive their longer range structure.

For the monovalent cations, XAFS shows the degree of contact ion pair (CIP) formation increases with increasing ionic radius leading to a remarkably simple relationship shown in Figure 1 that relates the ion charge/radius ratio to the formation of either the CIP or the solvent-separated ion pair (SSIP). For small ions, that have the highest local electrostatic potential, the strong ion-water interactions displace the anion into the second shell. The ability to capture the entire series of ions using a single method (Cl EXAFS) has provided the first unified insight into this process and clarifies an inconsistent set of previous literature studies on individual salts.

Complimentary HEXS studies show the existence of the longer-range, solvent-separated ion pairs (SSIP) for the divalent cations.

The hydrated structure of Al^{3+}: EXAFS and ab initio MD Simulations. The hydrated structures of Al^{3+} and Mg^{2+} have not previously been measured by EXAFS because of the challenges of working at low x-ray energies. We have again utilized the special low-Z x-ray cell to determine the hydration structure of these ions and to evaluate the reported existence of the Al^{3+} - Cl^- contact ion pair.

Both EXAFS and HEXS show an Al^{3+}-H_2O bond distance that is appreciably shorter than recent literature results from ab initio MD simulations (1.85 Å vs 1.93 Å, respectively). This led to a reexamination of the MD approach (E. Balaska) showing that only the more computationally-demanding version of DFT using exact exchange (PBE0) recovers the shorter bond length measured experimentally.

We also previously found that ab initio-MD simulations (CPMD PBE0) *quantitatively* reproduce EXAFS structure for a series of 6 different transition metal cations. To our knowledge, this is the first time that any simulation method has quantitatively modeled the hydration structure to this level of detail.

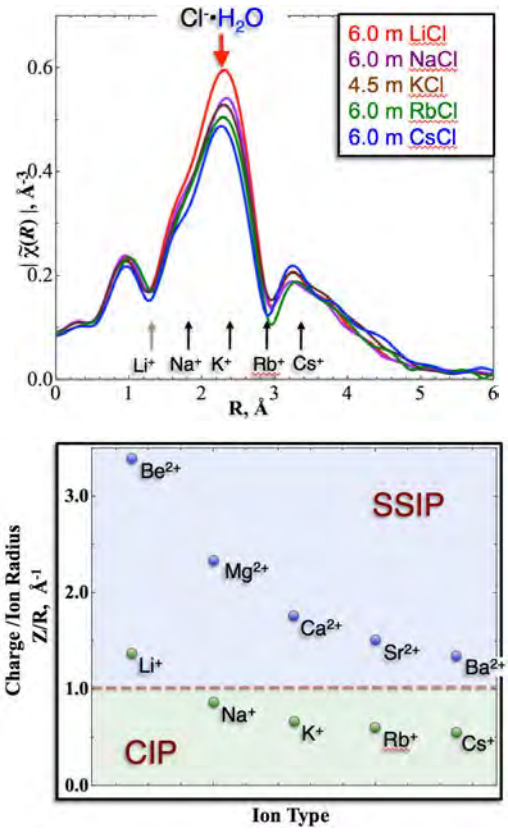

Figure 1. Cl K-edge XAFS spectra for a series of salt solutions showing positions of the detected backscattering signal from the cations(top). Contact- (CIP) and solvent-separated (SSIP) ion pair regimes (bottom).

In these earlier studies we found that it was necessary to include a higher accuracy pseudopotential description of the atomic potential using core polarization and a reduced core radius. This is another example where the high structural resolution available in EXAFS provides a necessary benchmark for the DFT-based simulations of ions in aqueous systems leading to significant revisions in the standard theoretical treatment.

In a related study, very recent DFT-MD results point to the formation of a contact ion pair between Al^{3+} and Cl^- (InorgChem 51, 10856, 2012). We embarked upon very extensive effort to confirm this structure however results from Cl and Al EXAFS (and from HEXS) definitively show that Al^{3+}-Cl^- CIP does not form up to the saturation concentration. In contrast, our results for Al^{3+} are consistent with the relationship we established in Figure 1 in which, for high charge/radius cations, only SSIP are formed. The challenge for the DFT-MD methods then appears to be reaching the cation/anion/water equilibrium in a system where the first-shell ligands have very long lifetimes. Improvements to the simulated equilibrated structure are being explored that include various types of free-energy optimizations. (E. Bylaska) The implications of these findings have far reaching consequences on how DFT-MD is employed in describing aqueous ions in chemistry.

Al $KL_{II\&III}$ -edge XANES and EXAFS spectra for the double electron excitation. In the course of our low-Z EXAFS studies of the Al K-edge we discovered a prominent feature residing at about 100 eV above the K-edge that we have assigned to the multielectron, Al $KL_{II\&III}$ -edge. These multi-electron edges are known to occur in higher Z atoms and they have been the subject of several studies in our own work with ions as well as by others in other chemical systems. The process involves a single-photon double electron excitation of ls and 2p states. These new, high-quality Al XANES spectra (Figure 3) have led to two important new findings. First, we found to our surprise that this edge contains *extended* x-ray absorption features. This observation confirms theoretical predictions of John Rehr from 35 years ago. (PhysRevB, 17, 560, 1978). The second and perhaps more important discovery is that the $KL_{II\&III}$ edge height and spectral features are dependent upon the ligand symmetry about the absorber. This is contrary to the foundation underlying the K-edge spectroscopy. This means that the Al $KL_{II\&III}$ edge provides an independent set of information about the chemical and electronic state of the core atom (Al). Most successful theoretical treatments of the K-edge XANES involve variations of time-dependent DFT. We have started TD-DFT calculations (Niri Govind) to determine the electronic transitions and cross sections for both the single- and double-electron excitations of several different model Al systems including aqueous Al^{3+} (using MD-XANES), α-alumina (octahedral) and sodium aluminate (tetrahedral). A full description of the $KL_{II\&III}$ transition has the potential to expand our understanding of aqueous Al^{3+}, Al hydroxides, and Keggin ions and the structure and chemistry of the Al- Brønstead acid sites in zeolites.

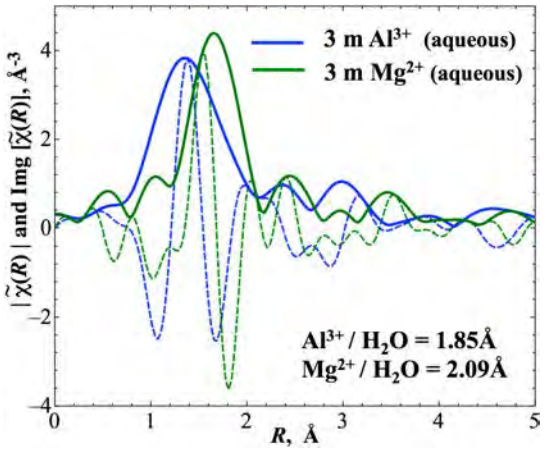

Figure 2. EXAFS spectra of aqueous Al^{3+} and Mg^{2+}.

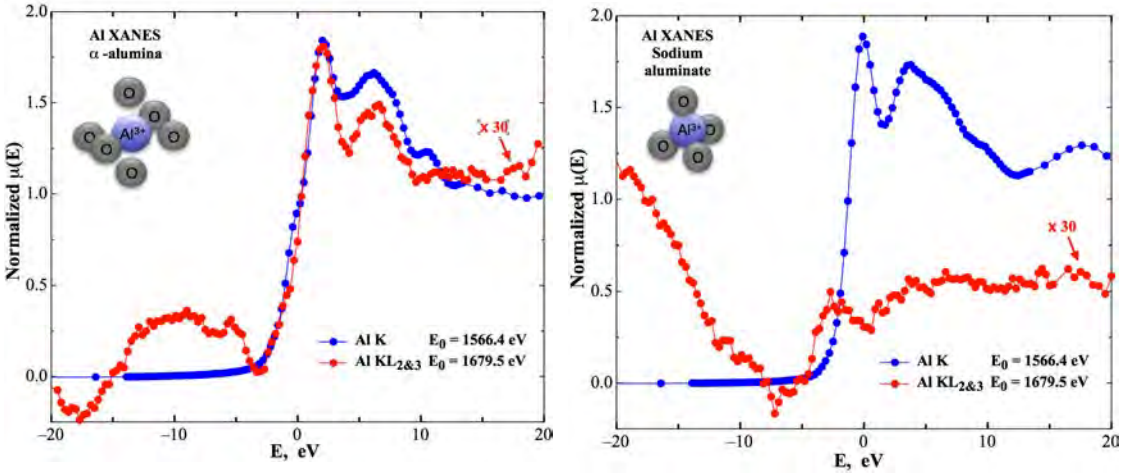

Figure 3. Comparison of the Al K-edge single electron with the $KL_{II\&III}$ multi-electron excitation spectra for α-alumina and sodium aluminate.

Future Plans

The objective is to gain a fundamental understanding of the molecular structure that provides the basis for understanding ion chemistry and dynamics. We propose exploring ion-water structure for systems in which the local structure has not yet been measured or the structure is not yet fully understood. Our goal is to identify the underlying structural factors that govern the macroscopic properties of ions that have so far eluded a comprehensive theoretical treatment. The proposed work also involves a comprehensive study of ion pairing in concentrated solutions and at high temperatures. The objective is to describe how the ion pair structure is governed by a range of different types of solvent interactions.

References to publications of DOE sponsored research (Oct. 1, 2010 - present)

1. J. L. Fulton, G. K. Schenter, M. D. Baer, C. J. Mundy, L. X. Dang and M. Balasubramanian, "Probing the Hydration Structure of Polarizable Halides: A Multiedge XAFS and Molecular Dynamics Study of the Iodide Anion." **J. Phys. Chem. B** 114 (40), 12926-12937 (2010).
2. G. S. Li, D. M. Camaioni, J. E. Amonette, Z. C. Zhang, T. J. Johnson and J. L. Fulton, "[CuCln](2-n) Ion-Pair Species in 1-Ethyl-3-methylimidazolium Chloride Ionic Liquid-Water Mixtures: Ultraviolet-Visible, X-ray Absorption Fine Structure, and Density Functional Theory Characterization." **J. Phys. Chem. B** 114 (39), 12614-12622 (2010).
3. M. Baer, V.-T. Pham, J. L. Fulton, G. K. Schenter, M. Balasubramanian, C. J. Mundy, "Is Iodate a Strongly Hydrated Cation?" **J. Phys. Chem. Letters**, 2, 2650–2654, (2011)
4. J. L. Fulton, E. J. Bylaska, S. Bogatko, M. Balasubramanian, E. Cauët, G. K. Schenter, J. H. Weare, "Near quantitative agreement of model free DFT- MD predictions with XAFS observations of the hydration structure of highly charged transition metal ions." **J. Phys. Chem. Lett.**, 3, 2588–2593 (2012)
5. V.-T. Pham, J. L. Fulton, "Ion-pairing in aqueous $CaCl_2$ and RbBr solutions: simultaneous structural refinement of XAFS and XRD data.", **J. Chem. Phys.**, 138, 044201, (2013)
6. J. Fulton, M. Balasubramanian, V.-T. Pham, G. S. Deverman, "A variable, ultra-short pathlength solution cell for XAFS transmission spectroscopy of the light elements", **J. Synchrotron Radiation**, 19, 949,(2012)
7. S. Bogatko, E. Cauet, E. Bylaska, G. K. Schenter, J. L. Fulton, J. H. Weare, "Hydration Structure and Dynamics of Aqueous Ca^{2+} using Ab Initio Molecular Dynamics: Comparison with Zn^{2+}, Fe^{3+}, and Al^{3+}." **Chemistry: A European Journal**, 19, 3047, (2013)

Probing Chromophore Energetics and Couplings for Singlet Fission in Solar Cell Applications

DE-FG02-13ER16393

Etienne Garand

Department of Chemistry, University of Wisconsin-Madison, Madison, WI 53706
egarand@chem.wisc.edu

Program scope

The goal of this project is to provide a molecular-level understanding of paths for improving alternative sources of energy, including an improved efficiency of dye-sensitized solar cells. Here, the mechanisms and molecular requirements for efficient exciton multiplication through singlet fission (SF) are explored by using high-resolution anion photoelectron spectroscopy to probe clusters and covalently-bonded dimers of organic chromophores. The experiments are capable of observing directly the singlet, triplet, and charge transfer states involved in singlet fission and determining precisely their energetics, vibrational structures and couplings. More specific aims are (1) to probe the evolution of the electronic structure as a function of cluster size in order to understand singlet fission in crystals, (2) to explore the relationship between the nature of linkers and the electronic structure in covalently-bonded chromophore dimers, and (3) to highlight the differences, including exciton delocalization and the effects of solvent interactions, between the crystalline species and the isolated covalently-bonded dimers.

Progress

The electronic states of organic chromophore clusters and covalently-bonded dimers will be probed via photoelectron (PE) spectroscopy of mass-selected radical anion precursors. Specifically, starting with the radical anion with a doublet ground state, all the low-lying singlet and triplet states of the neutral molecule that involve removal of a single electron can be accessed in the one-photon experiments. Therefore, with the exception of the doubly excited state, all the electronic states relevant to SF will be accessible. Using anions also provides the added advantage of mass selection, which is crucial for studying the behavior of SF as a function of size. However, conventional PE spectroscopy is often limited in terms of energy resolution, and in order to extract precise information about the electronic state spacings and couplings, it is important to obtain well-resolved spectra. This will be achieved by recording the PE spectra using a combination of velocity-map imaging (VMI) detection and tunable photodetachment light source, known as the slow electron velocity-map imaging (SEVI) technique. The proposed experiment will also avoid such temperature related resolution limitations by collisionally

cooling the anions to ~10 K in a cryogenic radio-frequency ion trap prior to laser photodetachment.

Since the beginning of this program in July 2013, we have started to design and build the cryogenic SEVI setup shown schematically in the figure below. The radical anion monomers and clusters will be generated using previously established methods consisting of a combination of oven heating, supersonic expansion, and electron beam bombardment. Alternatively, the

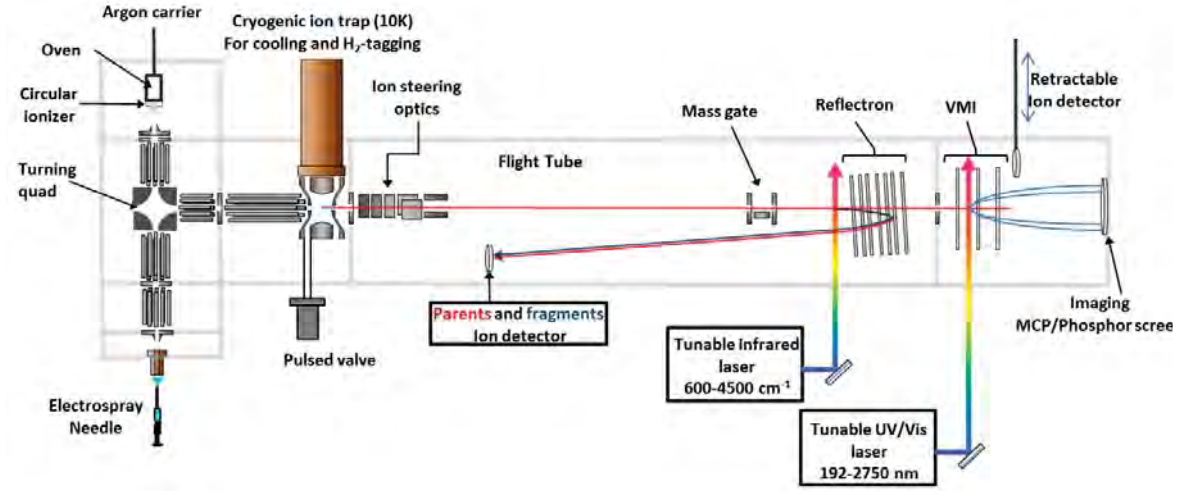

Figure 1. Schematic of the experimental setup in construction, which includes two different anion sources, a cryogenic ion trap for cooling and tagging, a two stage TOF mass-spectrometer for mass-selection and CIVS, and a slow photoelectron VMI detector.

covalently-bonded dimers of chromophore, which might be too fragile or have insufficient vapor pressure for the oven, will be generated by electrospray ionization from a solution containing proper electron transfer agents, similar to what have been used to form doubly negatively charged fullerene in the gas-phase. The experimental setup will therefore be equipped with both anion sources, after which ion guides and a turning quad will send the ions into a cryogenic ion trap. The quadrupole ion trap, cooled and held at 4-10K by a closed-cycle helium cryostat, will be similar to the design of Wang and coworkers. Short burst (~1 ms) of helium buffer gas will be introduced through a pulsed valve, facilitating the collisional cooling of the trapped ions. The ions will be held in the trap for 50-90 ms to ensure temperature equilibrium before they are gently extracted into a time-of-flight mass spectrometer. A mass-gate will allow only anions with a specific mass into the VMI region where they intersect the gently focused output of a tunable laser. Photoelectrons will be mapped onto a detector assembly consisting of imaging quality micro-channel plates and a phosphor screen. The resulting images will be captured by a charge-coupled device camera connected to a computer. The SEVI images provide both the conventional PE spectra via angular integration, as well as anisotropy information on the individual transitions.

Analysis of PE spectra requires knowing the structure of the anion state from which photodetachment occurred. This is especially true for clusters in which several structural

isomers are possible, complicating the resulting PE spectrum. To facilitate the analysis, the experimental apparatus will have an additional probing ability, enabling the direct characterization of the anion via cryogenic ion vibrational spectroscopy (CIVS). In CIVS, the trap temperature is held at 10K and the buffer gas consists of ~10% H_2 in a balance of helium. Under these conditions, H_2 condenses on the anion, forming weakly-bound adducts suitable for infrared single-photon dissociation. The H_2-tagged ions are intersected with the output of a tunable infrared laser (Laservision OPO/OPA). If the photon energy is resonant with a molecular transition, absorption of a single photon can dissociate the H_2. A switchable reflectron, placed between the mass-gate and the VMI region, will be used to provide a secondary mass-selection stage to separate the parent and photofragment ions. By monitoring the intensity of the photofragment as a function of laser wavelength, linear absorption infrared spectra in the 600-4000 cm^{-1} range can be obtained, providing direction information on the geometry of the anion precursor.

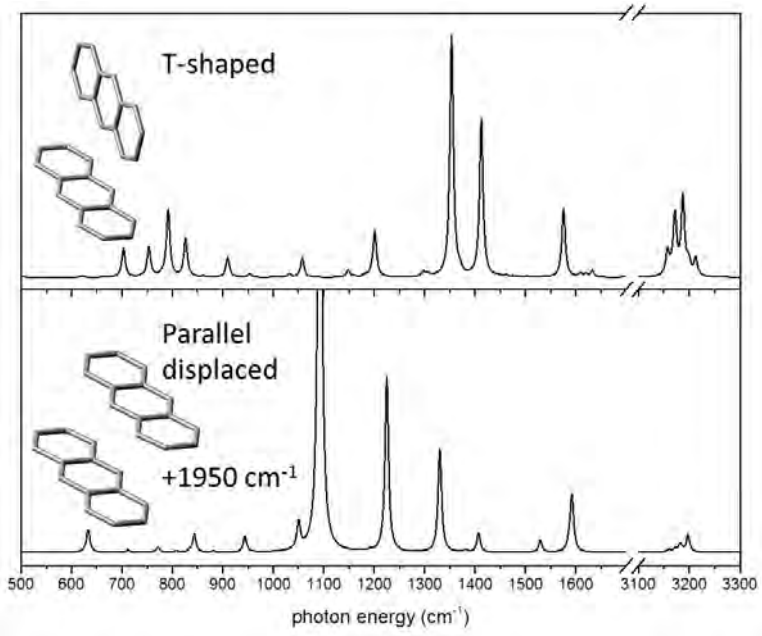

Figure 2. Calculated (cam-B3LYP/6-31g+(d,p) structure and infrared spectra of the two lowest energy isomers of anthracene anion dimer.

In parallel with the building of the experimental apparatus, we have started an extensive DFT study of polyacenes anion clusters. The goal of this study is to identify the expected anion cluster motifs that will be the initial state for the anion photoelectron spectroscopy. Because of the size of these chromophores, we started our search with the smaller naphthalene and anthracene species. For the dimers, we have identified two possible close-lying structures: T-shaped and parallel displaced. These structures are shown in Figure 2, along with their calculated infrared spectrum. Surprisingly, they have very distinctive features between 600 cm^{-1} and 1600 cm^{-1} which will allow them to be easily differentiated in our CIVS experiments. We found that the T-shaped arrangement of the individual monomer persists in the trimer and tetramer.

Once these results are confirmed by infrared predissociation spectroscopy, we will use them to constrain and facilitate the conformer search for the larger tetracene and pentacene anion clusters which are relevant to singlet fission. These structures will also be the basis for the calculations of the neutral cluster geometries accessible through photodetachment.

We also started to investigate the formation of the polyacene radical anion directly from electrospray ionization. These experiments are conducted on a separate already operational cryogenic ion vibrational spectrometer. We successfully produced the anthracene anion monomer by using adding a reducing agent in the electrospray solution. We are currently experimenting with source conditions to see if we can form clusters with the same approach.

Future plans

Our immediate plan in the next year is to complete the building and testing of the cryogenic SEVI apparatus. We will use our existing CIVS machine to continue testing the electrospray source conditions and to start acquiring infrared spectrum of polyacene anion clusters. These, in conjunction with DFT calculations will clarify the structure of the starting geometry for the photodetachment experiments. We anticipate being able to start the SEVI experiments by the next summer.

Ion Solvation in Nonuniform Aqueous Environments

Principal Investigator
Phillip L. Geissler
Faculty Scientist, Chemical Sciences, Physical Biosciences, and Materials Sciences Divisions

Mailing address of PI:
Lawrence Berkeley National Laboratory
1 Cyclotron Road
Mailstop: HILDEBRAND
Berkeley, CA 94720

Email: plgeissler@lbl.gov

Program Scope

Research in this program applies computational and theoretical tools to determine structural and dynamical features of aqueous salt solutions. It focuses specifically on heterogeneous environments, such as liquid-substrate interfaces and crystalline lattices, that figure prominently in the chemistry of energy conversion. In these situations conventional pictures of ion solvation, though quite accurate for predicting bulk behavior, appear to fail dramatically, e.g., for predicting the spatial distribution of ions near interfaces. We develop, simulate, and analyze reduced models to clarify the chemical physics underlying these anomalies. We also scrutinize the statistical mechanics of intramolecular vibrations in nonuniform aqueous systems, in order to draw concrete connections between spectroscopic observables and evolving intermolecular structure. Together with experimental collaborators we aim to make infrared and Raman spectroscopy a quantitative tool for probing molecular arrangements in these solutions.

Recent Progress

Our past work in this program has revealed that selective ion adsorption at the air-water interface involves as essential ingredients several previously underappreciated microscopic factors, for instance the fluctuating roughness of the liquid's boundary. Recent work has been focused in two complementary areas: (1) construction of an analytically tractable microscopic model for ions at liquid-vapor interfaces that respects the physical understanding we have gained from computer simulations, and (2) further exploring by simulation the molecular underpinnings of adsorption selectivity, e.g., the preferential solvation of anions at the interface.

Long-standing debates over the surface propensities of small ions were reinvigorated a decade ago by computer simulations demonstrating that charged model solutes can adsorb strongly to the air-water interface. From the perspective of classic theories of ion solvation in bulk polar solvents, this behavior is quite counterintuitive. Despite a significant amount of experimental and theoretical work in this area, a deep appreciation

of the structure and fluctuations that distinguish interfacial solvation from bulk scenarios has remained outstanding.

We have found in molecular simulations that capillary waves (mesoscopic undulations in topography of a soft interface) can be a key contributor to the thermodynamics of ion adsorption. This observation greatly enriches solvation scenarios at liquid interfaces, but also complicates the task of determining a successful theory. In the past year, we have taken an important step in this direction by establishing the details of a lattice model that is capable of accurately describing liquid density fluctuations at all relevant length scales. This approach builds on pioneering work by David Chandler and coworkers, who devised Ising-like descriptions of the hydrophobic effect. They recognized that accommodating volume-excluding objects in liquid water involves an interplay between short-wavelength response (governed by Gaussian distributed density fields) and larger-scale fluctuations that manifest the proximity of ambient conditions to liquid-vapor coexistence. Models based on this understanding were used to clarify many fundamental aspects of hydrophobic assembly; but their detailed treatment of coarse density fluctuations was not formulated to capture the statistical mechanics of capillary waves, to which our attention has been focused by the phenomenon of interfacial ion adsorption.

We have shown that careful consideration of capillary fluctuations can be straightforwardly incorporated into such a coarse-grained description, with the surprising result of simplifying its form. Drawing from and extending classical theories of surface roughness, we derived an approximate relationship between the microscopic cohesive energy ε of a lattice gas and its emergent surface tension γ. This connection ($\varepsilon^2 \propto \gamma$) is different in form from the low-temperature argument ($\varepsilon \propto \gamma$), which had been previously used to parameterize lattice gas models. As a practical matter, this result suggests a re-parameterization of Ising-like models that are intended to represent liquid density fluctuations near an interface. Physically, it emphasizes the essential contributions of surface undulations to the emergent mechanics of an interface.

This re-parameterization improves remarkably the accuracy of reduced lattice descriptions of hydrophobicity in even their simplest forms. Taking as input only the radial distribution function for oxygen atoms in water (and with no adjustable parameters), subtle material properties of the air-water interface can be captured quantitatively, in particular the Tolman length and effective elastic properties like spontaneous curvature. These mechanical details, which might appear to reflect geometric intricacies of hydrogen bonding, are in fact encoded by couplings between the simplest measure of microscopic structure, the pair correlation function, and the interfacial physics dictated by the surface tension.

Establishing reduced models for solvation of generic solutes near fluctuating interfaces constitutes a first step towards a predictive understanding for ion adsorption. The *specificity* of this phenomenon, however, has eluded even rudimentary understanding. Experiments and simulations indicate that an ion's affinity for the surface is extremely sensitive to the details of the ion itself. Perhaps the most dramatic example of this selectivity is the asymmetry between anions and cations: Merely switching the sign of

the charge of a model ion can modulate its density at the surface by a factor of 100. This behavior (which ultimately originates in the charge asymmetry of water molecules themselves) is often attributed to liquid water's nonzero surface potential. In the past year, we have scrutinized this proposition and found it to be unsatisfactory. Conventionally defined as the electrostatic potential averaged over all points in the liquid (including the interior of solvent molecules), the surface potential has no direct bearing on solvation of real ions (which of course cannot explore the volume-excluding interior of a water molecule). More importantly, we have found that the statistics of solvent potential depend in a very nonlinear way on an ion's charge. This result echoes our previous findings that solvent polarization near the interface is not linearly responding to a good approximation, likely a consequence of coupling between dipole and density fluctuations due in part to capillary waves. As an alternative origin of specificity, we have found that anions interact more favorably with nearby solvent molecules when they reside near the interface than when they are in bulk; cations show the opposite behavior.

Finally, we have made strides towards calculating solvent response within dielectric continuum theory for solutes that exclude volume near an interface. Assessing this fundamental behavior poses a technical challenge associated with boundary conditions, which are defined over an infinite surface yet involve important local features due both to the solute and to microscopic fluctuations in surface topography. Our approach treats these two effects in separate ways, resulting in an exact integral equation to be solved over the local boundary. We have successfully implemented this method for simple solute geometries.

Future Plans

A major goal for the next few years is to continue constructing a predictive theory for ions' spatial distributions near a liquid-vapor interface. Our previous work has set the stage for this development, pointing to essential physical ingredients missing in previous approaches. With this knowledge we are poised to formulate a tractable mathematical description of this phenomenon, capable of predicting density profiles, thermodynamic driving forces, and key experimental control parameters.

Among the challenges we face in this goal is extending the lattice model of density fluctuations described above to include as well a description of electrostatic interactions with charged and generally hydrophilic species. In the simplest approach, which is underway, a dielectric continuum representation could be appended to the coarse-grained density field. The resulting model, however, cannot capture adsorption specificity, as it lacks charge asymmetry. More detailed information about local molecular orientations is required; these might be captured by a measure of local tetrahedral order, or else Steinhardt-Nelson order parameters. Further insight from simulations may be required to properly couple essential coarse-grained fields together.

Our focus thus far has been on understanding properties of single ions in solution. In particular, we have aimed to predict free energy profiles in the microscopic vicinity of a liquid-vapor interface. While this quantity is well-defined at infinite dilution, many

macroscopic properties require attention to correlations among ions. Energy applications often involve sufficiently high ionic strength that such correlations cannot be neglected. Moreover, SHG studies by Saykally's group indicate that finite-concentration effects on adsorption appear at relatively low concentration. In previous theoretical work Debye-Hückel calculations have been performed in attempt to gauge these effects. As with conventional applications of dielectric continuum theory, however, this approach neglects many aspects of interfacial physics we now know to be important.

We aim to begin characterizing multi-ion correlations in the interfacial environment. The screening effects described by Debye-Hückel theory are of course an important component. But the adsorption mechanisms we have revealed suggest other, rather different consequences of ions' association. For example, the thermodynamics of interfacial pinning could favor clustering of two or more solutes, since one localized interfacial constraint is likely to be less costly than pinning at many dispersed sites. Similar mechanisms of solute aggregation have been discussed in the context of large molecules embedded in an elastic membrane. In addition, it is not clear how the energetics of excluding volume in the interfacial zone will depend upon solutes' spatial arrangement. We plan to explore these behaviors in computer simulations, both of detailed molecular models and of the reduced models we have described.

Recent Publications

S.J. Byrnes, P.L. Geissler, and Y.R. Shen, "Ambiguities in Surface Nonlinear Spectroscopy Calculations," *Chem. Phys. Lett. Frontiers*, **516**, 115 (2011).

D. E. Otten, P. R. Shaffer, P. L. Geissler, and R. J. Saykally, "Elucidating the Mechanism of Selective Ion Adsorption to the Liquid Water Surface," *Proc. Natl. Acad. Sci.,* **109**, 701 (2012).

S. Vaikuntanathan, P. R. Shaffer, and P. L. Geissler, "Adsorption of solutes at liquid-vapor interfaces: insights from lattice gas models," *Faraday Discuss.*, **160**, 63 (2013).

P. L. Geissler, "Water interfaces, solvation, and spectroscopy," *Ann. Rev. Phys. Chem.*, **64**, 317 (2013).

S. Vaikuntanathan and P. L. Geissler, "Putting water on a lattice: The importance of long wavelength density fluctuations in theories of hydrophobic and interfacial phenomena," arXiv, 1302.6323 (2013).

Program Title: Theoretical Developments and Applications to Surface Science, Heterogeneous Catalysis, and Intermolecular Interactions

Principal Investigator: Mark S. Gordon, 201 Spedding Hall, Iowa Sate University and Ames Laboratory, Ames, IA 50011; mark@si.msg.chem.iastate.edu

Program Scope. Our research effort combines new theory and code developments with applications to a variety of problems in surface science and heterogeneous catalysis, as well as the investigation of intermolecular interactions, including solvent effects in ground and excited electronic states and the liquid-surface interface. Many of the surface science studies are in collaboration with Dr. James Evans. Much of the catalysis effort is also in collaboration with Drs. Evans, Marek Pruski and Igor Slowing.

Recent Progress. Chemical processes on and with the Si(100) surface have been one research focus. The diffusion of Al on Si(100) was studied using an embedded cluster model and multi-reference electronic structure methods, including CASSCF explorations of the doublet and quartet potential energy surfaces and improved energies with multi-reference perturbation theory. The details of the potential energy surfaces depend critically on the presence of the bulk that is represented by molecular mechanics (MM). Only when edge effects are minimized by embedding the quantum mechanics (QM) region in a much larger MM region, using our SIMOMM method, does a consistently realistic picture emerge. Similar results are obtained in our studies of Ga on Si(100). It appears that both Al and Ga can form metal wires on the Si(100) surface. The etching and diffusion of O atoms on the Si(100) surface was also studied with the QM/MM model and both multi-reference methods and the cluster-in-molecule (CIM) CR-CC(2,3) coupled cluster method developed by the Piecuch group. The latter method combines a coupled cluster method, CR-CC(2,3), that is able break single bonds and account for the diradical character that is inherent in the Si(100) surface) with a novel method (CIM) for greatly speeding up accurate coupled cluster calculations. The CIM method enables the calculation of large clusters that can diminish the need for the MM part of the embedding scheme. Two complementary approaches for increasing the sizes of clusters that can be studied with accurate QM methods are the occupation restricted multiple active space (ORMAS) and the fragment molecular orbital (FMO) methods. The ORMAS method divides a large, intractable active space into chemically sensible subspaces, thereby making a very difficult calculation feasible. The utility of the ORMAS method has been demonstrated with Si(100) clusters of increasing size. The FMO method divides a large species into fragments to facilitate accurate QM calculations on very large systems. A fully analytic FMO/Hartree-Fock gradient has been derived and implemented in GAMESS, to enable geometry optimizations and molecular dynamics simulations. We have shown that one can do ab initio MD simulations with periodic boundary conditions and that fully analytic gradients are absolutely essential. Mesoporous silica nanoparticles (MSN) have received increasing attention due to their catalytic capabilities. Because the MSN species are very complex, we have implemented the ReaxFF force field into GAMESS and are exploring the possibility of using this method to study catalytic processes in MSN species. A combined ReaxFF/NMR study, in collaboration with the

Pruski group, demonstrated that the ReaxFF method can produce structural data that are consistent with the temperature-dependent NMR data.

The effective fragment potential (EFP) method, a sophisticated model potential designed to accurately describe intermolecular interactions, has been interfaced with the FMO method, so that low-cost explicit solvent effects can be incorporated into FMO studies. Both FMO-EFP energies and analytic gradients are now available. EFP interfaces have also been derived and implemented for configuration interaction with single excitations (CIS), multi-reference, multi-state perturbation theory, and equations-of-motion (EOM) coupled cluster theory. These interfaces provide an array of tools that are available to study solvent effects on electronic spectra and photochemistry. Initial studies have addressed the aqueous solvation of the n-π^* and π–π^* excitations in uracil. These are by far the most accurate calculations on this topic. The EFP method was also applied to the study of aqueous solvation of several anions, including bihalide ions and the nitrate ion. The latter study was particularly important, because it demonstrated that, contrary to predictions from simulations with (mostly inadequate) simple model potentials, only a modest number of water molecules are needed to force the anion to the interior. New advances in the EFP method include the development of a general approach to damping the various contributions to the potential and the development and implementation of the QM-EFP exchange repulsion. We have used the EFP code in GAMESS to demonstrate the an approach to inter-operability among existing high performance electronic structure codes. A GAMESS-NWChem EFP interface was successfully constructed.

Time-dependent density functional theory (TDDFT) is in principle a good compromise between accuracy and computational cost for studying electronic excited states. However, because DFT, and therefore TDDFT, is at it core a single determinant method, there are some phenomena that are very difficult to address with TDDFT. One very important phenomenon is the conical intersections that occur when two or more potential energy surfaces cross. Conical intersections are ubiquitous, and therefore very important, in photochemistry and photobiology. We have implemented the Krylov spin-flip approach with TDDFT and have demonstrated for ethylene, and most recently stilbene, that the new combined method can correctly describe conical intersections and the associated detailed structural information. This SF-TDDFT method has now been interfaced with the EFP method, so solvent effects on conical intersections and non-adiabatic interactions can be studied.

“Composite” methods refer to the use of multiple levels of theory to predict accurate thermodynamic properties of molecules. Most composite methods can predict very accurate thermochemistry, but are not reliable for the prediction of reaction mechanisms, barrier heights and (therefore) kinetics. We have recently developed a new composite method, called ccCA-CC(2,3), based on the Piecuch CR-CC(2,3) method, that can predict both thermodynamics and reaction mechanisms with very high accuracy.

Advances have also been made in high performance computational chemistry. An INCITE grant has enabled us to have access to the BlueGene /P at Argonne, where we

have demonstrated that the FMO method allows essentially perfect scaling to the petascale (more than 131,000 processors).

Future Plans. The development of the FMO and CIM-CR-CC(2,3) methods will allow us to explore fully quantum studies of heterogeneous catalysis, in which we can minimize edge effects, because these methods will allow us to expand the size of the QM region in a computationally efficient manner. A combined CIM-FMO method is now under development, so we can take advantage of the best features of both methods. We are also developing a new embedded cluster method SIMOMM-Rx that replaces the Tinker force field with ReaxFF. Fully analytic FMO/DFT gradients will be developed. The CIM-CR-C(2,3) method will be applied to studies of phenomena on the Si(100) surface, such as more extensive studies of diffusion of Ga and In. We will explore the use of ORMAS-PT2 for the adsorption of substrates on conducting metals, since QM/MM embedded cluster methods are not appropriate for such problems. Preliminary FMO studies have been performed on model MSN species at the Hartree-Fock level of theory with a minimal basis set. The agreement with the fully ab initio method is excellent, so we will now apply FMO with higher levels of theory and reliable basis sets. The EFP-QM exchange repulsion analytic gradients have been derived, and these will now be implemented so that any solvent can be studied. Related to this, we will work with the ReaxFF developers to obtain improved parameters for silica and silica-X, where X represents atoms in the important substrates.

References to publications of DOE sponsored research 2010-present

1. D.D. Kemp and M.S. Gordon, "Aqueous Solvation of Bihalide Ions", J. Phys. Chem. A, 114, 1298 (2010).
2. D.D. Kemp, J. Rintelman, M.S. Gordon, and J.H. Jensen, "Exchange Repulsion between Effective Fragment Potentials and *Ab Initio* Molecules", Theor. Chem. Accts., 125, 481 (2010).
3. Y. Ge, M.S. Gordon, F. Battaglia, and R.O. Fox, "Theoretical Study of the Pyrolysis of Methyltrichlorosilane in the Gas Phase. 3. Reaction Rate Constants", J. Phys. Chem. A, 114, 2384 (2010).
4. A. Asadchev, V. Allada, J. Felder, B.M. Bode, T.L. Windus, and M.S. Gordon, "Uncontracted Rys Quadrature Implementation of up to g Functions on Graphical Processing Units", J. Comp. Theor. Chem., 6, 696 (2010).
5. P. Arora, L.V. Slipchenko, S.P. Webb, A. DeFusco, and M.S. Gordon, "Solvent-Induced Frequency Shifts: Configuration Interaction Singles combined with the Effective Fragment Potential Method, J. Phys. Chem. A, 114, 6742 (2010).
6. P. Arora, W. Li, P. Piecuch, J.W. Evans, M. Albao, and M.S. Gordon, "Diffusion of atomic oxygen on the Si(100) surface", J. Phys. Chem. C, 114, 12649 (2010).
7. D. Ghosh, D. Kosenko, V. Vanovschi, C.F. Williams, J.M. Herbert, M.S. Gordon, M.W. Schmidt, L.V. Slipchenko, and A.I. Krylov, "Non-covalent interactions in extended systems described by the Effective Fragment Potential method: Theory and application to nucleobase oligomers", J. Phys. Chem. A, 114, 12739 (2010).
8. T Nagata, D.G. Fedorov, K. Kitaura, and M.S. Gordon, "A combined effective fragment potential-fragment molecular orbital method. II. Analytic gradient and

application to the geometry optimization of solvated tetraglycine and chignolin", J. Chem. Phys., 134, 034110 (2011).
9. T. Nagata, K. Brorsen, D.G. Fedorov, K. Kitaura, and M.S. Gordon, "Analytic energy gradient in the fragment molecular orbital method", J. Chem. Phys., 134, 124115 (2011).
10. A. DeFusco, J. Ivanic, M.W. Schmidt, and M.S. Gordon, "Solvent-Induced Shifts in the Electronic Spectra of Uracil", J. Phys. Chem. A, 115, 4574 (2011).
11. S. Nedd, C.-H. Tsai, I.I. Slowing, M. Pruski, and M.S. Gordon, "Using a Reactive Force Field to Correlate Mobilities Obtained from Solid-State ^{13}C NMR on MesoporousSilica Nanoparticle Systems", J. Phys. Chem. C, 115, 16333 (2011).
12. A. Devarajan, T.L. Windus, and M.S. Gordon, "Implementation of Dynamical Nucleation Theory Effective Fragment Potentials (DNTEFP) method for modeling aerosol chemistry", J. Phys. Chem. A, 115, 13987 (2011).
13. L. Roskop, J.W. Evans, and M.S. Gordon, "The adsorption and diffusion of gallium adatoms on the Si(100)-2x1 reconstructed surface: An MCSCF study utilizing molecular surface clusters", J. Phys. Chem. C, 115, 23488 (2011).
14. M.S. Gordon, D.G. Fedorov, S.R Pruitt, and L.V. Slipchenko, "Fragmentation Methods: A Route to Accurate Calculations on Large Systems", Chem. Rev, 112, 632 (2012) (INVITED).
15. G.D. Fletcher, D.G. Fedorov, S.R. Pruitt, T.L. Windus and M.S. Gordon, "Large-Scale MP2 Calculations on the Blue Gene Architecture Using the Fragment Molecular Orbital Method", J. Comp. Theor. Chem., 8, 75 (2012).
16. S. Nedd, N.J. DeYonker, A.K. Wilson, P. Piecuch, and M.S. Gordon, "Incorporating a Completely Renormalized Coupled Cluster Approach into a Composite Method for Thermodynamic Properties and Reaction Paths", J. Chem. Phys., 136, 144109 (2012).
17. S. Markutsya, Y. Kholod, A. Devarajan, T.L. Windus, M.S. Gordon, and M.H. Lamm, "A coarse-grained model for β-D-glucose based on force matching", Theor. Chem. Accts., 131, 1 (2012).
18. D.-J. Liu, D.M. Ackerman, X. Guo, M.A. Albao, L. Roskop, M.S. Gordon, and J.W. Evans, "Morphological Evolution during Growth and Erosion on Vicinal Si(100) Surfaces: From Electronic Structure Analyses to Atomistic and Coarse-Grained Modeling", Mater. Res. Soc. Symp. Proc., 1411 (2012)
19. A. Gaenko, T.L. Windus, M. Sosonkina and M.S. Gordon, "Design and Implementation of Scientific Software Components to Enable Multi-scale Modeling: The Effective Fragment Potential (QM/EFP) Method", J. Chem. Comp. Theory, 9, 222 (2012).
20. K.Brorsen, N. Minezawa, F. Xu, T.L. Windua, and M.S. Gordon, "Fragment molecular orbital dynamics with the fully analytic gradient.", J. Chem. Comp. Theory, 8, 5008 (2012).
21. D. Rios, G. Schoendorff, M.J. Van Stipdonk, M.S. Gordon, T.L. Windus, J.K. Gibson, and W. A. de Jong, "Roles of Acetone and Diacetone Alcohol In Coordination and Dissociation Reactions of Uranyl Complexes", Inorg. Chem., 51, 12768 (2012).

Dynamics of Electrons at Interfaces on the Ultrafast Timescale

Charles B Harris P.I.
Chemical Sciences Division
Lawrence Berkeley National Lab
1 Cyclotron Road, Mail Stop Latimer
Berkeley, CA 94720
CBHarris@berkeley.edu

Program Scope:

The interface between two materials defines the behavior of electronic devices. In the case of organic photovoltaic cells, the interface between donor and acceptor type materials drives charge separation. In the case of supercapacitors, charge is stored by molecular reorganization at the metal-solvent interface. The physical phenomena governing electronic properties at surfaces and interfaces are unique from the bulk solid; the reduced dimensionality of these surfaces leads to characteristics that are often poorly understood. Our research aims to explore the molecular mechanisms governing energy levels and dynamics of electrons at the metal-molecule interface.

We use femtosecond time- and angle- resolved two-photon photoemission spectroscopy (TPPE) to probe the energy and momentum of electrons in thin film adlayers on a metal surface. Briefly, a pump pulse excites an electron from below the Fermi level of the substrate into a previously unoccupied state below the vacuum level. After a variable time delay, a probe pulse photoemits the electron into a time-of-flight detector. The low energy electrons generated in this process gives TPPE high surface sensitivity and high energy resolution. Angle resolved measurements allow TPPE to collect electronic spectra as a function of momentum. Momentum is conserved upon photoemission, and by changing the angle of the surface relative to the detector, momentum resolved band-structure can be determined. Localization can be determined by the curvature and intensity of the measured band structure. Our work has investigated several cases where delocalized electrons collapse into localized states on the femtosecond timescale.

Our work can be broadly divided into two areas. The first area concerns the static modification of the interfacial electronic states upon the deposition of films. This was recently explored in studies of phthalocyanine thin films in terms of the band folding, and then later extended into looking at the effect of graphene on the image potential states above the silicon carbide surface, which has been investigated in its use in high frequency electronics. The second area concerns dynamic processes such as the localization and solvation of electrons in thin films supported by the metal surface; this line of work originated with our pioneering work on polaron formation in alkane thin films, and continues today with studies of the solvation response of room temperature ionic liquids and the trapping of conduction band electrons in alkali halide insulating ultrathin films. All of these studies inform and complement our ongoing work which attempts to monitor excitonic states in organic semiconductors relevant to organic photovoltaics.

Recent and Ongoing Work:

Electron Solvation and Phase Changes at the Room Temperature Ionic Liquid/Electrode Interface:

Room temperature ionic liquids (RTILs) are composed of charge separated ions that, for steric and entropic reasons, exist in the liquid phase at room temperature. Due to their unique properties, RTILs have been used in applications ranging from lubricants to liquid conductors in photovoltaic Gratzel cells. We studied one such RTIL system, 1-methylpyrrolidinium bis(trifluoromethylsulfonyl)-imide ($[Bmpyr]^+[NTf_2]^-$), with the aim of investigating the solvation response of the RTIL to a photoinjected electron. Due to the intrinsically low vapor pressure of ionic liquids, we were able to use standard surface science techniques to control and characterize the RTIL on a Ag(111) crystal. An electron affinity (EA) state was observed in thin films of the RTIL, and this feature was the main focus of our studies. The EA state was assigned based on angle- and time-resolved measurements that showed it being localized at all delay times, a characteristic property of molecular states. Utilizing an extension of the Heisenberg

uncertainty principle as applied to TPPE momentum resolved intensity data, we estimated that the state was spatially localized to 11±5 Å, indicating that the state overlaps with one or a few ions.

Using time-resolved TPPE, substantial solvation of the photoinjected electron was observed as a downward shift in the EA peak as a function of time. The solvation kinetics are found to be temperature independent within the error of our measurement, and, due the absence of discrete states, solvation appears to be a continuous process. Rise and decay times for different energy slices corresponding to different stages of the solvation process showed that the time dependent shift of the EA peak was associated with solvation and not a simple energy-dependent decay rate based on the state's position in the band gap. Though temperature did not have an effect on EA state lifetime, lowering the temperature resulted in both a factor of two decrease in solvation energy and a ~200 meV decrease in sample work function. The work function shift and change in solvation magnitude was assigned to a phase transition at around 250K; it is likely that these changes are due to a collective reorientation of the ions at the interface. This study serves to both further the understanding of these unique liquids and to lay the groundwork for future investigations of RTIL response to injected electrons.

Electron Localization in Ultrathin Alkali Halide Films on Ag(100):

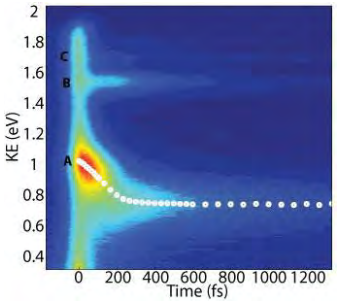

In recent years, thin films of alkali halides on metal surfaces have attracted much attention due their decoupling properties and to serve as a model of metal/insulator properties. These interfaces have been used by the scanning probe community to directly image molecular wavefunctions of organic semiconductors. Furthermore, these systems have been proposed as potential materials in nanoelectronics. To date, there have been few time resolved studies of alkali halide/metal interfaces and their properties. Our group has recently used TPPE to study the electronic properties of thin films of NaCl on Ag(100). Our results show that an electron excited to the delocalized conduction band of NaCl becomes localized on the femtosecond time scale due to small polaron formation or trapping at a defect, as displayed in the Figure. Here, **A** corresponds to the conduction band (CB) of NaCl and **B** and **C** are assigned to image potential states. The white circles guide the eye to the peak center of mass, revealing that an electron excited to the CB undergoes a trapping energy of ~300 meV within 200 femtoseconds. This property is not specific to NaCl on Ag(100). Qualitatively similar behavior has been observed by our group of NaCl on Ag(111) and a number of other alkali halides on Ag(100). Our studies additionally reveal a layer thickness and temperature dependence on the magnitude of trapping energy, and also the rate of an electron becoming trapped in the conduction band and its lifetime. We believe these results will add to a deeper understanding of dynamic processes at the metal/insulator interface, and be of interest to the emerging community that uses these materials.

The Corrugation of the Interfacial Potential at the Phthalocyanine/Metal Interface:

TPPE has expanded from studying model small molecules, such as pentanes and benzene, to larger, more device relevant molecules, such as those used in organic photovoltaic materials. These materials have lattice constants on the same length scale as low energy electrons at the surface, meaning that the organization of the molecules at the interface can substantially affect the electronic structure of free-electron like states at the interface. Previous work in our group studied the modification of the image state band structure using well characterized and device relevant metallated phthalocyanine monolayers. Recently, we extended those studies to the non-metallated phthalocyanine ligand on both the Ag(100) and Ag(111) surfaces in an attempt to better understand what causes the corrugation of the interfacial potential. Somewhat surprisingly, it was found that the magnitude of the corrugation in the interfacial potential was comparable to that in the metallated phthalocyanines. This appears incongruous with the interfacial charge transfer that is known to occur between the silver surface and the phthalocyanine metal center. Density functional calculations are being performed in an attempt to gain a detailed understanding of the nontrivial charge transfer and back donation that is likely occurring in this system. These studies

will extend our understanding of the band-folding phenomenon and inform our future studies of device relevant molecules, allowing us to disentangle the effects of the lattice constant and symmetry of the system from the effects derived from molecular origins.

Modification of the Shockley Surface State via the Adsorption of Organic Monolayers:

The use of organic layers in optoelectronic devices necessitates an understanding of the electronic energy levels at the metal/molecule interface. Frequently, the resulting electronic states are assumed to be a perturbed superposition of the bare metal and free molecule electronic states. In some cases, however, it is known that the metal and organic states can hybridize substantially, changing the spatial extent, carrier mobility and excited state lifetime. This was exemplified in the case of 3,4,9,10-perylenetetracarboxylic dianhydride (PTCDA)/Ag(111) where the Shockley surface state and the LUMO+1 of the organic layer hybridize into a state that is spatially overlapped with the LUMO+1 of the PTCDA molecule, but retains the free electron like character of the metal surface state. Our work demonstrates that the hybridization phenomenon is not unique to this system, by observing the existence of the metal/organic hybrid state for the phthalocyanine class of molecules. Our two-photon photoemission experiments have observed this interface state and confirmed its nature from lifetime and dispersion data. In addition to demonstrating the existence of the interface state, we are able to monitor the relative overlap of the metal state with the organic state by measuring the lifetime of the state for different molecular configurations. These results are being supported by density functional calculations that can show the hybridization process in detail. This work will extend our understanding of the hybridization that can occur at metal/organic interfaces which can define how charges move parallel to and across the interface.

The Nature of Image Potential States at the Silicon Carbide/Graphene Interface:

Characteristics such as their ambipolar field effect and extremely high carrier mobility suggest that graphene or graphene-like materials may be integral in developing the next generation of electronic devices. A detailed understanding of surfaces and interfaces is essential to the development and optimization of novel devices. In order to better understand the behavior of these unique materials, we studied few layer graphene on silicon carbide (SiC). It has been well documented that graphene can be readily formed from atoms within a SiC sample by a series of heating steps, where the second to last of these steps leads to the formation of a carbon rich $(6\sqrt{3} \times 6\sqrt{3})R30^{o}$ reconstruction.The first graphene layer forms directly on top of this reconstruction, which is commonly referred to as the "buffer layer." ARPES studies compared the occupied electronic structure of both the $(6\sqrt{3} \times 6\sqrt{3})R30^{o}$ buffer layer and a monolayer of graphene, finding apparent similarities in the nature of sigma bonding and marked differences in pi bonding. We take a different approach, instead focusing on the behavior of the image potential state (IPS) series for the two different systems. We characterized samples of both buffer layer and 'true' graphene using TPPE. We observed the first 3 IPSs in both systems, and find their behavior to be remarkably similar, the main difference being an increased lifetime of all states in the graphene sample. Our results imply that the buffer layer supports IPSs in the absence of graphene. This is an interesting result considering that the image states were not observed for the SiC substrate itself suggesting that the buffer layer itself substantially modifies the image force felt by an electron at the surface. Further work will focus on exactly how the carbon rich buffer layer can support its own IPS series.

Future Work:

Observing Molecular Mechanisms of Solvation in Room Temperature Ionic Liquids:

Room temperature ionic liquids (RTILs) have attracted attention in recent years, notably due to their intrinsic conductivity in the absence of solute molecules. These materials find use in supercapacitors, batteries, catalysis, and photovoltaic Gratzel cells as well as being used as novel solvents and lubricants. Using TPPE, we have already characterized the solvent response and the temperature-dependent phase transition of a simple RTIL at the interface of a metal electrode. Our goal is now to expand on these

results, first by studying a variety of different RTIL systems in an attempt to link dynamical behavior to structural differences. Furthermore, the introduction of a thin spacer layer, inserted between the RTIL and metal electrode, should serve to change the interaction between the RTIL molecules and the metal. By using a series of different spacers, we will directly investigate the effect of the RTIL/electrode interaction on solvent response and phase changes in the ionic liquid layer. Our goal is to make a direct link between spacer size/structure and the solvent response and/or structure of the RTIL. These results will further shed light on the precise nature of response and structure in RTILs as a whole and may even provide clues as to how the behavior of an RTIL system could be directly controlled.

Band Structure Effects on the Electronic States in Ultrathin Alkali Halide Films:

To date, the majority of studies of electronic states at alkali halide/metal interface have been carried out by Scanning Tunneling Spectroscopy (STS). This method is neither time-resolved, nor momentum-resolved, and therefore makes electronic state determination difficult to interpret. TPPE is ideally suited to map out the band structure of the interfacial states of alkali halide/metal interface due to its time- and momentum- resolved capabilities. Our work will aim to correlate conduction band alignment to anion and cation chemical identity and the relative insulating and decoupling properties of different alkali halides. These results will be valuable to the potential use of alkali halides in nanoelectronics.

Molecular Excitations in Organic Semiconductors:

Thin films of organic semiconductors (OSC) remain a large study of ongoing research for their potential as materials in photovoltaics, organic light emitting diodes (OLED), and organic field effect transistors (OFET). Organic based electronics are promising because of their ease of fabrication, cheaper and more abundant materials, and easily tunable to match the solar spectrum. Unfortunately, organic based electronics are less efficient than inorganic based materials. TPPE is ideally suited to model these devices and their interfaces, which determine device efficiency with device relevant materials. However, studying electronic properties of thin films of OSCs on metal substrates has proven difficult because the metal's density of states broadens molecular orbitals and renders molecular excitations invisible. The group's recent progress with growth and studies of alkali halides will allow us to study excitations in OSCs. By growing OSCs on top of thin films alkali halide, the problem of molecular orbital broadening and excitation quenching can be prevented. Once the exciton of OSC has been efficiently decoupled from the metal and characterized, we can then grow in an acceptor molecule and study the rate and energetics of exciton splitting to charge transfer and charge separated states, which largely determine the efficiency of devices.

Articles Supported by DOE Funding from 2011-Present:

[1] E.A. Muller, M.L. Strader, J.E. Johns, A. Yang, B.W. Caplins, A.J. Shearer, D.E. Suich, C.B. Harris. "Femtosecond Electron Solvation at the Ionic Liquid/Metal Electrode Interface", J. Am. Chem. Soc., 135(29), 10646, (2013).

[2] E.A. Muller, J.E. Johns, B.W. Caplins, C.B. Harris. "Quantum Confinement and Anisotropy in Thin Film Molecular Semiconductors", Phys. Rev. B., 83(16), 165422, (2011).

[3] E.A. Muller "Electron Dynamics and Symmetries at the Metal-Molecule Interface Probed by Two Photon Photoemission", *LBNL Thesis*

Program Title: "SISGR: Ultrafast Molecular Scale Chemical Imaging"
(DOE Grant Number: DE-FG02-09ER16109)

PI: Mark C. Hersam, Professor of Materials Science and Engineering, Chemistry, and Medicine; Northwestern University, 2220 Campus Drive, Evanston, IL 60208-3108;
Phone: 847-491-2696; Fax: 847-491-7820; E-mail: m-hersam@northwestern.edu;
WWW: http://www.hersam-group.northwestern.edu/

Co-PIs: Jeffrey R. Guest (Argonne National Lab), Nathan P. Guisinger (Argonne National Lab), Saw Wai Hla (Argonne National Lab), George C. Schatz (Northwestern University), Tamar Seideman (Northwestern University), Richard P. Van Duyne (Northwestern University)

1. Program Overview

This SISGR program utilizes newly developed instrumentation and techniques including integrated ultra-high vacuum tip-enhanced Raman spectroscopy/scanning tunneling microscopy (UHV-TERS/STM) and surface-enhanced femtosecond stimulated Raman scattering (SE-FSRS) to advance the spatial and temporal resolution of chemical imaging for the study of photoinduced dynamics of molecules on plasmonically active surfaces. An accompanying theory program includes modeling of charge transfer processes using constrained density functional theory in addition to modeling of SE-FSRS, thereby providing a detailed description of the excited state dynamics. Over the past year, significant experimental and theoretical progress has been made on several topics including ultrafast UHV-TERS/STM, chemically modified graphene on plasmonic substrates, and optically active adsorbates.

2. Recent Progress

2.1. Ultrafast UHV-TERS/STM

The SISGR team has actively pursued its goal of developing UHV-TERS/STM that is capable of molecular spatial resolution while femtosecond laser pulses are focused at the tip-sample junction. Towards that end, we have employed SE-FSRS to probe the interactions between molecules and plasmonic nanomaterials on the ultrafast time scale. This work has shown that plasmonic nanoparticles and adsorbed molecules are strongly coupled due to the appearance of Fano-like lineshapes, which result from the interaction between the narrow-band molecular vibrational coherences and the broadband plasmon resonances. This coupling does not shorten the lifetime of the vibrational coherence dephasing, which suggests that plasmonically enhanced photovoltaic and photocatalytic systems can effectively make use of vibrational coherences lasting for over a picosecond, potentially increasing their efficiency.

In parallel, TERS has been advanced to an unprecedented level in the past year. Although TERS has the ability to probe spectroscopic and topographic information below the diffraction limit, this field has only utilized continuous wave excitation in the past. In contrast, we have shown that TERS spectra can be reliably obtained using picosecond excitation, thereby suggesting the possibility of molecularly resolved TERS with ultrafast time resolution. In parallel, UHV-TERS/STM has been used to characterize thermally sublimed rhodamine 6G (R6G) molecules on Ag (111). To decrease the surface diffusion of R6G at sub-monolayer coverage, we cooled the sample down to 19 K. Under these conditions, single R6G molecules are observed using STM. In addition, TERS vibrational modes for R6G on Ag (111) are resolved concurrently with molecular resolution STM. In comparison with TERS at room temperature, the TERS peaks are significantly sharpened are 19 K, which allows new features to be resolved including site-specific chemical information about the adsorbed molecules.

2.2. Chemically Modified Graphene on Plasmonic Substrates

Graphene plasmonics is an emerging field that combines the near-field optical properties of metallic nanostructures with the superlative electronic and chemical properties of graphene to realize architectures capable of extreme light concentration and manipulation, highly efficient photoconversion, and single molecule detection. While the unique electronic structure and chemical stability of graphene make it an ideal platform for studying and exploiting light-matter interactions, current graphene plasmonic devices are limited by the non-pristine processing steps that are required to interface exfoliated or chemical vapor deposition (CVD) transferred graphene on metal substrates. Over the past year, we have overcome these limitations by demonstrating the direct epitaxial growth of graphene on a single crystal Ag(111) substrate, resulting in an atomically clean graphene-silver substrate that is free of organic residue and other contaminants. The growth is achieved in ultra-high vacuum at a substrate temperature of ~700° C via the evaporation of atomic carbon from a graphite source. Since this growth method requires relatively low temperatures, it presents opportunities for integrating graphene with other low melting point substrates.

In addition to graphene growth on plasmonic substrates, methods for chemically functionalizing graphene have been concurrently pursued. For example, we have achieved the formation of well-defined one-dimensional organic nanostructures on graphene via the self-assembly of 10,12 pentacosadiynoic acid (PCDA) in UHV. Molecular resolution UHV STM images confirm the one-dimensional ordering of the as-deposited PCDA monolayer and show domain boundaries with symmetry consistent with the underlying graphene lattice. In an effort to further stabilize the monolayer, in situ ultraviolet photopolymerization induces covalent bonding between neighboring PCDA molecules in a manner that maintains one-dimensional ordering as verified by UHV STM and ambient atomic force microscopy.

Beyond PCDA, we have also extended our previous results with C_{60} acceptor molecules on graphene to the donor molecule pentacene. With C_{60}, we were able to demonstrate that the molecules were effectively decoupled both structurally and electronically from graphene and the underlying SiC substrate. Similarly, we have recently shown that pentacene is also isolated from the supporting substrate as evidenced by sharp isolated molecular states in scanning tunneling spectra. Furthermore, the large measured HOMO-LUMO gap (3.6 eV) indicates that we can measure a molecular scale ‘transport gap’ in the pentacene molecule.

2.3. Optically Active Adsorbates

Interactions between light and matter are vital for many natural phenomena as well as for applications such as solar energy conversion. For example, β-carotene is found in photosynthetic reaction centers and has great potential to be used in plant-based solid-state solar cells for energy harvesting applications. Over the past year, low temperature STM studies have successfully imaged β-carotene molecules, thus allowing the identification of five different conformations: all-trans (trans), 15-cis (cis), 12-13,12'-13'-di-cis (twist), 14-15,14'-15',15-15',10-11,10''-11''-penta-cis (V-twist), and 13,14'-15''-di-cis (V-shape) on the Au(111) surface. We have also investigated the chlorophyll-a and β-carotene mixed molecular system. Low temperature STM images reveal the co-existence of β-carotene and chlorophyll-a. In the mixed region, β-carotene is found in five different conformations that match the single molecule studies described above. Interestingly, β-carotene molecules mostly position next to chlorophyll-a molecules, indicating a tendency for charge transfer between the two molecular systems. The cis and V-twist structures appear to be the largest portions of the observed structures inside the mixed molecular clusters.

2.4. Theory/Modeling

Due to the complexity of the ongoing experimental work, theory and modeling play a critical role in helping define productive experiments and interpreting freshly gathered data. In the area of electronic structure studies of SERS and TERS, new theories have been developed in which electronic structure theory is coupled with classical electrodynamics to describe plasmon enhanced spectroscopic processes. In particular, we have developed the ability to determine resonance Raman spectra for open shell molecules using the AOResponse module of NWChem.

Electronic structure theory and molecular dynamics/mechanics have also been employed to determine the structures of molecules and clusters on graphene surfaces. For example, the semiempirical electronic structure method PM6 was used to model the structure of PCDA on graphene before and after photopolymerization, enabling accurate interpretation of the STM measurements described above. In addition, ongoing work is focused on developing models of the preparation of ZnO clusters on graphene using atomic layer deposition. Here, we are performing electronic structure calculations to determine bond energies of the diethyl-zinc precursors as well as the oxidized clusters that result.

Theoretical effort has also been devoted to the strong coupling that exists between molecular excited states and surface plasmon modes of a slit array in a thin metal film. The coupling manifests itself as an anti-crossing behavior of the two newly formed polaritons. As the coupling strength grows, a new mode emerges, which is attributed to long range molecular interactions induced by the plasmonic field. This molecular-like mode repels the polariton states, and leads to an opening of energy gaps both below and above the free molecule energy.

3. Future Plans

In future work, we intend to utilize the knowledge and momentum gained from the aforementioned accomplishments to advance the following project objectives:

(1) *Ultrafast UHV-TERS/STM*: We plan to use picosecond excitation SERS/TERS in UHV to avoid decay of the TERS signal for molecules that is observed in ambient conditions due to reaction in the enhancing region by O_2 and H_2O. We will then investigate the charge transfer dynamics of adsorbates on thin insulating layers supported by single crystal metal substrates (e.g., MgO on Ag). Femtosecond pump – picosecond probe SERS/TERS (using a femtosecond pump pulse and a delayed picosecond probe pulse) will be utilized to study the effect of buffer layers and surface defects on the mechanism, yield, and rate of charge-transfer dynamics at the 1-100 ps time scale.

(2) *Development of plasmonic substrates for UHV-TERS/STM*: We intend to expand our graphene on silver synthesis capabilities to other 2-D van der Waals materials such as silicene, germanene, and MoS_2. In contrast to graphene, these alternative 2-D materials are expected to be chemically reactive and thus have the potential to serve as an effective template for covalent molecular attachment to plasmonic Ag substrates. A variety of atomic adsorbates (e.g., hydrogen and oxygen) and molecular adsorbates (e.g., olefins and thiols) will be explored with UHV-TERS/STM.

(3) *Light-induced charge transfer process in photosynthetic molecules*: We will study optically driven charge transfer processes between adsorbed carotene and chlorophyll molecules. In particular, spatially resolved scanning tunneling spectroscopy (STS) will be acquired at different energies with and without laser irradiation. The changes in the STS maps as a function of optical irradiation will quantify light-induced charge transfer processes at the sub-molecular scale. Related measurements will also be pursued on metallo-organic molecular networks (e.g., Co-porphyrin and Co-salen based molecules).

4. Publications

[1] Q.H. Wang, M.C. Hersam, *Nano Lett.*, **11**, 589 (2011).
[2] Q.H. Wang, M.C. Hersam, *MRS Bulletin*, **36**, 532 (2011).
[3] J.D. Emery, Q.H. Wang, M. Zarrouati, P. Fenter, M.C. Hersam, M.J. Bedzyk, *Surf. Sci.*, **605**, 1685 (2011).
[4] Md.Z. Hossain, J.E. Johns, K.H. Bevan, H.J. Karmel, Y.T. Liang, S. Yoshimoto, K. Mukai, T. Koitaya, J. Yoshinobu, M. Kawai, A.M. Lear, L.L. Kesmodel, S.L. Tait, M.C. Hersam, *Nature Chemistry*, **4**, 305 (2012).
[5] N. Jiang, E.T. Foley, J.M. Klingsporn, M.D. Sonntag, N.A. Valley, J.A. Dieringer, T. Seideman, G.C. Schatz, M.C. Hersam, R.P. Van Duyne, *Nano. Lett.*, **12**, 5016 (2012).
[6] A. Deshpande, C.-H. Sham, J.M.P. Alaboson, J.M. Mullin, G.C. Schatz, M.C. Hersam, *J. Am. Chem. Soc.*, **134**, 16759 (2012).
[7] E.A. Pozzi, M.D. Sonntag, N. Jiang, J.M. Klingsporn, M.C. Hersam, R.P. Van Duyne, *ACS Nano*, **7**, 885 (2013).
[8] H.J. Karmel, M.C. Hersam, *Appl. Phys. Lett.*, **102**, 243106 (2013).
[9] J. Cho, L. Gao, J. Tian, H. Cao, W. Wu, Q. Yu, J.R. Guest, Y.P. Chen, N.P. Guisinger, *ACS Nano*, **5**, 3607 (2011).
[10] J.A. Smerdon, M. Bode, N.P. Guisinger, J.R. Guest, *Phys. Rev. B*, **84**, 165436 (2011).
[11] J. Cho, J. Smerdon, L. Gao, Ö. Süzer, J.R. Guest, N.P. Guisinger, *Nano Lett.*, **12**, 3018 (2012).
[12] J. Tian, H. Cao, W. Wu, Q. Yu, N.P. Guisinger, Y.P. Chen, *Nano Lett.*, **12**, 3893 (2012).
[13] E.V. Iski, E.N. Yitamben, L. Gao, N.P. Guisinger, *Adv. Funct. Mater.*, **23**, 2554 (2013).
[14] J.A. Smerdon, R.B. Rankin, J.P. Greeley, N.P Guisinger, J.R. Guest, *ACS Nano*, **7**, 3086 (2013).
[15] J.M. Mullin, J. Autschbach, G.C. Schatz, *Comp. Theor. Chem.*, **987**, 32 (2012).
[16] J.M. Mullin, G.C. Schatz, *J. Phys. Chem. A*, **116**, 1931 (2012).
[17] J.M. McMahon, S.K. Gray, G.C. Schatz, *J. Phys. Chem. C*, **114**, 15903 (2012).
[18] R.R. Frontiera, A.-I. Henry, N.L. Gruenke, R.P. Van Duyne, *JPCL*, **2**, 1199 (2011).
[19] M.G. Blaber, A.-I. Henry, J.M. Bingham, G.C. Schatz, R.P. Van Duyne, *J. Phys. Chem. C*, **116**, 393 (2012).
[20] M.D. Sonntag, J.M. Klingsporn, L.K. Garibay, J.M. Roberts, J.M. Dieringer, T. Seideman, K. Scheidt, L. Jensen, G.C. Schatz, R.P. Van Duyne, *J. Phys. Chem. C*, **116**, 478 (2012).
[21] J.M. Mullin, N. Valley, M.G. Blaber, G.C. Schatz, *J. Phys. Chem. A*, **116**, 9574 (2012).
[22] N. Valley, N. Greeneltch, R.P. Van Duyne and G.C. Schatz, *JPCL*, **4**, 2599 (2013).
[23] M.G. Reuter, M.C. Hersam, T. Seideman, M.A. Ratner, *Nano Lett.*, **12**, 2243 (2012).
[24] M.G. Reuter, M.A. Ratner, T. Seideman, *Phys.Rev. A*, **86**, 013426 (2012).
[25] Z. Hu, M.A. Ratner, T. Seideman, *J. Chem. Phys.*, **137**, 204111 (2012).
[26] B. Fainberg, T. Seideman, *Chem. Phys. Lett.*, **576**, 1 (2013).
[27] S.L. Kleinman, R.R. Frontiera, A.-I. Henry, J.A. Dieringer, R.P. Van Duyne, *Phys. Chem. Chem. Phys.*, **15**, 21 (2013).
[28] R.R. Frontiera, N.L. Gruenke, R.P. Van Duyne, *Nano. Lett.*, **12**, 5989 (2012).
[29] B. Sharma, R.R. Frontiera, A.-I. Henry, E. Ringe, R.P. Van Duyne, *Materials Today*, **15**, 16 (2012).
[30] S.L. Kleinman, E. Ringe, N. Valley, K.L. Wustholz, E. Phillips, K.A. Scheidt, G.C. Schatz, R.P. Van Duyne, *J. Am. Chem. Soc.*, **133**, 4114 (2011).

Chemical Kinetics and Dynamics at Interfaces

Laser induced reactions in solids and at surfaces

Wayne P. Hess (PI) and Alan G. Joly

Chemical and Materials Sciences Division
Pacific Northwest National Laboratory
P.O. Box 999, Mail Stop K8-88,
Richland, WA 99352, USA
wayne.hess@pnnl.gov

Additional collaborators include A.L. Shluger, P.V. Sushko
P.Z. El-Khoury, W.D. Wei, S.J. Peppernick, V.A. Apkarian

Program Scope

The chemistry and physics of electronically excited solids and surfaces is relevant to the fields of photocatalysis, radiation chemistry, and solar energy conversion. Irradiation of solid surfaces by UV, or higher energy photons, produces energetic species such as core holes and free electrons, that relax to form electron-hole pairs, excitons, and other transient species capable of driving surface and bulk reactions. The interaction between light and nanoscale oxide materials is fundamentally important in catalysis, microelectronics, sensor technology, and materials processing. Photostimulated desorption studies, of atoms or molecules, provide a direct window into these important processes and are particularly indicative of electronic excited state dynamics. Greater understanding is gained using a combined experiment/theory approach. We therefore collaborate with leading solid-state theorists who use *ab initio* calculations to model results from our laser desorption and photoemission experiments. The interaction between light and metal nano objects can lead to intense field enhancement and strong optical absorption through excitation of surface plasmon polaritons. Such plasmon excitation can be used for a variety of purposes such as ultrasensitive chemical detection, solar energy generation, or to drive chemical reactions. Large field enhancements can be localized at particular sites by careful design of nanoscale structures. Similar to near field optics, field localization below the diffraction limit can be obtained. The dynamics of plasmonics excitations is complex and we use finite difference time domain calculations to model field enhancements and optical properties of complex structures including substrate couplings or interactions with dielectric materials.

Approach:

We are developing a combined PEEM two-photon photoemission approach to probe plasmonic nanostructures such as solid metal particles or lithographically produced nanostructures such as such as gratings or nanohole arrays. We then correlate PEEM images with scanning electron microscopy or surface enhanced Raman spectroscopy (or the spatially resolved tip-enhanced implementation). Finite difference time domain (FDTD) calculations are used to interpret the field enhancements measured by the electron and optical techniques. The effects of extreme electric field enhancement on Raman spectra is investigated using plasmonic nanostructures constructed from a metal nanoparticles or metal covered atomic force microscopy (AFM) tips on flat metal substrates. The Raman scattering from molecules adhered between these structures show greatly enhanced scattering and often highly perturbed spectra depending on nanogap dimensions or whether a conductive junction is created between tip and substrate. In photodesorption studies, photon energies are chosen to excite specific surface structural features

that lead to particular desorption reactions. The photon energy selective approach takes advantage of energetic differences between surface and bulk exciton states and probes the surface exciton directly. We measure velocities and state distributions of desorbed atoms or molecules from ionic crystals using resonance enhanced multiphoton ionization and time-of-flight mass spectrometry. Application of this approach to controlling the yield and state distributions of desorbed species requires detailed knowledge of the atomic structure, optical properties, and electronic structure. We have demonstrated surface-selective excitation and reaction on alkali halides and generalized our exciton model to oxide materials and shown that desorbed atom product states can be selected by careful choice of laser wavelength, pulse duration, and delay between laser pulses.

Recent Progress

Very intense photoelectron emission has been observed from localized points on nanostructured metal surfaces following UV femtosecond (fs) laser excitation. The regions of intense emission, dubbed 'hot spots', are due to collective charge oscillations, termed localized surface plasmons (LSPs). The intensity of the incident electric field can be amplified several orders of magnitude when resonantly coupled with the LSP mode of the nanostructure. The electromagnetic (EM) field amplification is largely responsible for non-linear phenomena such as surface enhanced Raman scattering (SERS) although SERS intensities are a convolution of both electronic and chemical Raman enhancement factors. While the EM contribution is believed to dominate the overall SERS signal, obtaining a quantitative measure of individual chemical and EM contributions, from a single molecule or hot spot, has proved challenging. It is possible to measure the field enhancement due to a nanoparticle LSP using PEEM. By applying a two-photon excitation scheme, using fs laser pulses, isolated EM enhancements can be examined and photoemission yields can be correlated with detailed structural images from complementary microscopic techniques such as scanning electron microscopy (SEM).

Solid silver nanoparticles (average diameters of 34, 75 and 122 nm) were deposited on an atomically flat mica substrate and covered with a 50 nm Ag thin film. The enhancement in photoelectron yield of single nanoparticles illuminated with femtosecond laser pulses (400 nm, ~3.1 eV) is found to be a factor of 10^2 to 10^3 times greater than that produced by the adjacent flat silver thin film. High-resolution, multi-photon PEEM images of single silver nanoparticles reveal that the greatest enhancement in photoelectron yield is localized at distinct regions of the nanoparticle whose magnitude and spatial extent is dependent on the incident electric field polarization. In conjunction with correlated scanning electron microscopy (SEM), nanoparticles that deviate from nominally spherical shapes are found to exhibit irregular spatial distributions in the multi-photon PEEM images that are correlated with unique particle shape or topology. Furthermore, we determined that Enhancement Factors, within each nanoparticle size range, exhibit a large spread of values indicative of the exact geometry and local environment unique to each individual nanoparticle.

PEEM is a charged particle (photoelectrons) imaging technique and has therefore been applied almost exclusively to conducting materials and in particular metals. We have found, however, that wide-gap semiconductors and even insulating materials, in some cases, yield high quality PEEM images. We have imaged 3 μm diameter polystyrene spheres supported on a thin metal substrate illuminated by 400 nm (~ 3.1 eV) and 800 nm (~ 1.5 eV) femtosecond (fs) laser pulses. Intense photoemission is generated by microspheres even though polystyrene is an insulator and its ionization threshold is well above the photon energies employed. We observe the most intense photoemission from the far side (the side opposite the incident light) of the illuminated microsphere that is attributed to light focusing within the microsphere. The light focused though the microsphere then propagates to the thin film surface where photoemission from the metal substrate can be imaged. For the case of p-polarized, 800 nm fs laser pulses, we observe

photoemission exclusively from the far side of the microsphere and additionally resolve sub-50 nm hot spots in the supporting Pt/Pd thin film that are located only within the focal region of the microsphere. We find that the fs PEEM images at both 400 and 800 nm can be modeled using FDTD electrodynamic simulations. The FDTD calculations predict light focusing in the optically transparent microsphere and subsequent focusing of the transmitted field on the supporting metal surface. The ability to obtain high resolution and high contrast PEEM image from an insulator is attributed to photoinduced conductivity of the polystyrene microspheres.

Future Plans

Time-resolved two-photon PEEM is an experimental method which offers both nanometer spatial and fs time resolution. We have conducted proof-of-principle studies for an initial set of plasmonic nanostructures, specifically, hexagonal and prism shaped gold particles using this technique. These initial studies capture spatially resolved field enhancement, and subsequent decay dynamics, following 800 nm fs laser excitation. Using PEEM we have measured plasmonic enhancement factors, without the presence of a molecular emitter as in surface enhanced Raman scattering (SERS). We now have the tools needed to correlate field enhancement with SERS response and by adding time-resolved PEEM (stabilized using a recently constructed Mach-Zhender interferometer) the path opens to an entirely new set of measurements capable of correlating structure and dynamics of a variety of designer plasmonic hotspots (e.g. the nano-gaps of particle aggregates or in gaps between nanowires). The inclusion of helium ion lithography into our arsenal, in the coming year, will allow sub 10 nm structures to be fabricated at will.

Future plans include femtosecond PEEM to study plasmon resonant photoemission from noble metal nanostructures and time-resolved PEEM to probe dynamics of metal and hybrid (metal:metal-oxide) nanostructures. We will interrogate such metal-insulator systems using a variety of advanced techniques including: x-ray and ultraviolet photoelectron spectroscopy (XPS, UPS) femtosecond 2PPE, PEEM, SERS and the tip enhanced version (TERS) for spatially-resolved Raman spectroscopy. Femtosecond time-resolved PEEM can reveal spatially resolved ultrafast dynamics and is a powerful tool for studying the near-surface electronic states of nanostructures or plasmonic devices. We will explore the formation of interfacial polarons on a sample of nanoscale insulator (either alkali halides or metal oxides) islands on Cu (111) and possibly other metal substrates. Our goal is to resolve the temporal and spatial evolution of electron emission and the dynamics of small interfacial polarons using the combined PEEM and 2PPE approach. We are also presently developing capabilities to perform energy-resolved two-photon photoemission using a hemispherical analyzer XPS instrument. In combination we expect these two techniques will provide spatially-resolved electronic state dynamics of nanostructured metal-insulator materials.

By generalizing the exciton based desorption model to metal oxides, we can pursue selective excitation of specific surface sites, on an atomic scale, for a general class of technologically important materials. We note that the higher valence of oxides requires a more complex mechanism. With the aid of DFT calculations we have developed a “hole plus exciton” mechanism that relies on the combination of a surface exciton with a three-coordinated surface-trapped hole. In every instance we have studied, a hyperthermal O-atom KE distribution can be linked to an electronic surface excited state desorption mechanism. In contrast, a thermal O-atom KE distribution clearly indicates a bulk derived origin for desorption. In analogy to alkali halide thermal desorption, we have considered a bulk-based thermal desorption mechanism involving trapping of two holes at a three-coordinated site (a “two-hole localization” mechanism). Our calculations, however, do not indicate that two-hole localization is likely without invoking a dynamical trapping process. Since extensive calculations have not yielded an enduring theoretical model for thermal desorption we are exploring possible nonthermal mechanisms that yield low

kinetic energy particle desorption in the "thermal energy" range. Initial experiments on CsBr thin films suggest intriguing possibilities of near-thermal desorption from surface molecular anion centers (H centers). We will therefore study low energy desorption from thin films of CsBr, CsI, and perhaps RbI grown on insulators and metals. We also plan to grow and study oxide thin films, such as ZrO_2, BaO, and ZnO, on well-characterized metal surfaces.

References to publications of DOE BES sponsored research (2010 to present)

1. K.M. Beck, A.G. Joly, and W.P. Hess, "Effect of Surface Charge on Laser-induced Neutral Atom Desorption." *Appl. Phys. A*, **101**, 61 (2010).

2. G. Xiong, R. Shao, S.J. Peppernick, A.G. Joly, K.M. Beck, W.P. Hess, M. Cai, J Duchene, J.Y. Wang W.D. Wei "Materials Applications of Photoelectron Emission Microscopy," *J. Metals*, **62**, 90 (2010).

3. S.J. Peppernick, A.G. Joly, K.M. Beck, W.P. Hess "Plasmonic Field Enhancement of Individual Nanoparticles by Correlated Scanning and Photoemission Electron Microscopy" *J. Chem. Phys.* **134**, 034507 (2011).

4. P.V. Sushko, A.L. Shluger A.G. Joly, K.M. Beck, and W.P. Hess, "Exciton-driven highly-hyperthermal O-atom desorption from nanostructured CaO" *J. Phys. Chem. C*. **115**, 692 (2011).

5. S.J. Peppernick, A.G. Joly, K.M. Beck, and W.P. Hess "Near-Field Focused Photoemission from Polystyrene Microspheres Studied with Photoemission Electron Microscopy", *J. Chem. Phys.* **137**, 014202 (2012).

6. S.J. Peppernick, A.G. Joly, K.M. Beck and W.P. Hess, J. Wang, Y.C. Wang and W.D. Wei, "Two-Photon Photoemission Microscopy of a Plasmonic Silver Nanoparticle Trimer," *Appl. Phys. A* **112**, 35 (2013).

7. A. Polyakov, C. Senft, K. F. Thompson, J. Feng, S. Cabrini, P. J. Schuck, H. A. Padmore, S. J. Peppernick, and W. P. Hess, "Plasmon enhanced photocathode for high brightness and high repetition rate x-ray sources" Phys. Rev. Lett.**110**, 076802 (2013).

8. P.Z. El-Khoury, S.J. Peppernick, D. Hu, A.G. Joly, and W.P. Hess, "The Origin of Surface-Enhanced Raman Scattering of 4,4'-Biphenyldicarboxylate on Silver Substrates" *J. Phys. Chem. C*, **117**, 7260 (2013).

9. S.J. Peppernick, A.G. Joly, K.M. Beck, and W.P. Hess "Plasmon-Induced Optical Field Enhancement studied by Correlated Scanning and Photoemission Electron Microscopy", *J. Chem. Phys.* **138**, 154701 (2013).

10. P.Z. El-Khoury, D. Hu, V.A. Apkarian and W.P. Hess, "Raman Scattering at Plasmonic Junctions Shorted by Conductive Molecular Bridges" *Nano Lett*. **13**, 1858 (2013).

11. M.T.E. Halliday, A.G. Joly, W.P. Hess, P.V. Sushko and A.L. Shluger, "Photodesorption of Br-atoms from crystalline CsBr thin films grown on LiF and KBr(100)," *J. Phys. Chem. C*, **117**, 1302 (2013).

12. P.Z. El-Khoury, W.P. Hess, "A Theoretical Investigation of Raman from a Single 1,3-Propanedithiol Molecule." *Chem. Phys. Lett*. **581**, 57 (2013).

Spectroscopic Imaging of Molecular Functions at Surfaces

Wilson Ho

Department of Physics & Astronomy and Department of Chemistry
University of California, Irvine
Irvine, CA 92697-4575 USA

wilsonho@uci.edu

Program Scope:

This project is concerned with the experimental challenge of reaching single molecule sensitivity with atomic scale spatial resolution in spectroscopic imaging. These experiments would lead to an understanding of the inner machinery of single molecules that are not possible with other approaches, including the electronic, vibrational, and structural properties, as well as the relation of these properties to the molecular functions. Results from these studies will provide the scientific basis for understanding the unusual properties, processes, and phenomena in chemical and physical systems at the atomic scale that would carry over to larger length scales. The experiments rely on the unique properties of the scanning tunneling microscope (STM) and additionally its coupling to optical techniques to overcome diffraction limited spatial resolution. Tunneling electron induced light emission from nanoclusters yields information on the radiative decay channel and the role of plasmonics in photocatalytic reactions on oxide supported metal clusters. Results from the investigation of single molecules, nanoclusters, and nano-optics provide the basis for surface chemistry, photocatalysis, solar energy, environmental processes, and electron transport through molecules.

Recent Progress:

The most recent results will be highlighted in this report and involve the spectroscopic imaging of the molecular structure and its relation to molecular functions. The composition and arrangement of atoms in a molecule determine its physical and chemical properties. The scanning tunneling microscope previously has provided spatially resolved electronic and vibrational signatures of single molecules. However, the spatial distributions of these signatures do not relate directly to the geometric structures of the molecules. When a CO-terminated tip is scanned over a cobalt phthalocyanine (CoPc) molecule, the energy, intensity, and line shape of the lowest energy hindered translational mode of CO vary over each atom, bond, and lone electron pair in the molecule. These variations in the CO vibration are detected by inelastic electron tunneling spectroscopy and reveal chemical sensitivity. Spatial imaging at a selected vibrational energy of CO yields direct visualization of the skeletal structure of the molecule. The combined capabilities of the scanning tunneling microscope suggest the possibility to relate structure and function in chemistry at the single molecule level.

In the August 28, 2009 issue of Science, Leo Gross, Fabian Mohn, Nikolaj Moll, Peter Liljeroth, and Gerhard Meyer at IBM Zürich imaged the molecular structure of pentacene with the atomic force microscope (AFM) and a CO-terminated tip. Since then a few papers have been

published by Meyer's group and others, notably in the June 21, 2013 issue of Science led by the UC Berkeley groups. In all these papers the authors note the inability of the scanning tunneling microscope (STM) to achieve structural resolution, e.g. "Structural identification using STM, however, is limited by the microscopic contrast arising from the electronic local density of states (LDOS), which is not always easily related to chemical structure."

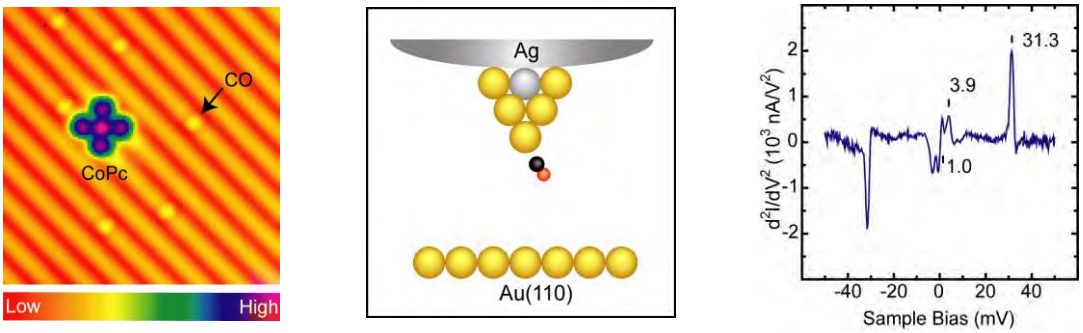

Fig. 1: (Left) Topographic image of CO coadsorbed with cobalt phthalocyanine (CoPc) on Au(110)-1×2 surface, recorded with a bare Au-covered Ag tip. (Middle) Schematic illustrating a CO-terminated tip. (Right) Vibrational spectrum for a single CO molecule on the tip taken by inelastic electron tunneling spectroscopy at 600 mK, revealing hindered translation mode at 3.9 meV and hindered rotational mode at 31.3 mV.

Here we show that molecular structures can be imaged by the STM. Specifically individual atoms and bonds, as well as lone electron pairs are resolved, and the width of a bond is determined to better than 0.34 Angstroms. We have developed a new approach by picking up a CO molecule on the tip and monitor its low energy (about 4 meV), hindered translational vibrational mode as the CO-terminated tip is scanned over the molecule. We show that the energy, intensity, and line shape of the CO vibration are sensitive to the elemental composition and bonds in the molecule (cobalt phthalocyanine: 57 atoms and 68 bonds). The CO vibration senses the skeletal structure differently than elsewhere, and is detected by inelastic electron tunneling spectroscopy with the STM (STM-IETS). This inelastic tunneling probe (*it*Probe) is expected to be generally applicable to other molecules.

The CO-terminated tip has proven to be crucial for both the AFM and *it*Probe to resolve molecular structures. For the AFM, the CO-terminated tip provides a well-defined tip apex structure and the interactions in the tip-molecule junction can be sensed by a macroscopic oscillator with high sensitivity to obtain the required contrast for imaging the molecular structure. The *it*Probe also benefits from the well-defined tip apex structure provided by the CO. However, in contrast to the AFM the environmental perturbations to a molecular vibration of the CO (by scanning the CO-terminated tip over different parts of the molecule) are monitored by STM-IETS signals which directly result in the structural imaging contrast and furthermore elemental discrimination.

The ability of the STM to image molecular structure is an important addition to its previously shown capabilities for manipulation and the determination of the electronic and vibrational properties. The results presented in this manuscript suggest opportunities to relate structure and function in chemistry at the single molecule level.

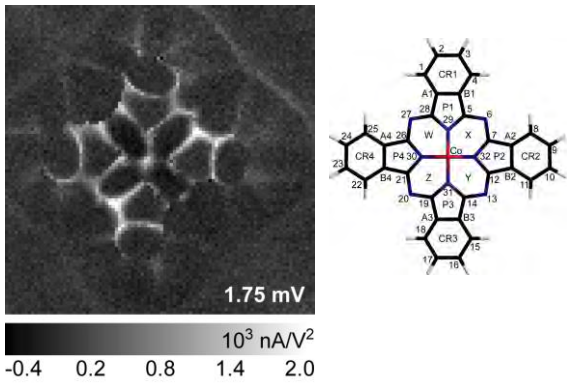

Fig. 2: (Left) Image of the skeletal structure of cobalt phthalocyanine (CoPc) adsorbed on Au(110)-1×2 surface obtained by the *it*Probe at 1.75 mV sample bias and 600 mK. The imaged area is 21.1×21.1 Å^2 (96×96 pixels). Different parts of the molecular structure are highlighted at different bias voltages. All 57 atoms and 68 bonds can be imaged. (Right) Schematic diagram showing atoms, bonds, and regions in the CoPc molecule. Comparison the image with the schematic structure reveals distortion in the molecule due to the bonding; the molecule has the shape of an inverted bowl with the four outer six-membered carbon rings bent toward and bonded to the Au substrate.

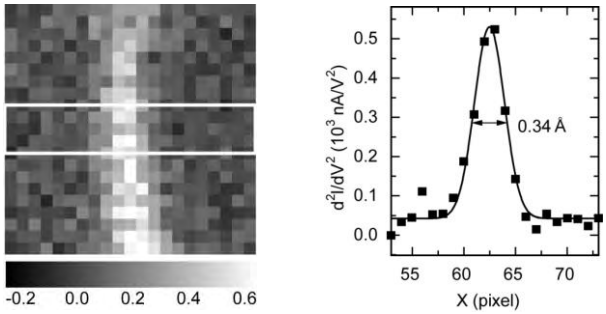

Fig. 3: (Left) Zoom in image of a C-C bond shared by the five-membered pyrrole ring and the six-membered carbon ring in CoPc. The imaged area is 2.31×2.31 Å^2 (21×21 pixels). (Right) Cross sectional cut through the C-C bond, showing the spatial resolution of the width of the bond to be 0.34 Å. Each point is an average of 4 vertical pixels in the rectangular area shown in the zoom in image. The C-C bond is the one on the right side of the image in Fig. 2.

Future Plans:

The functions of a molecule depend on its composition, structure, and environment. The composition is determined by identifying the atoms in the molecule. The arrangement of the atoms gives its structure. The changes that the molecule undergoes are in response to its environment, such as temperature, light, charge, and other chemical species. Future research seeks an understanding of molecular functions by relating them to the composition, structure, and environment with low temperature scanning tunneling microscopes (STM), in combination with electronic and vibrational spectroscopies and manipulation. The relationships between structure and bonding are central for understanding chemistry. The focus of the future plans includes four key problems in chemistry: 1. imaging molecular structure, 2. nature of hydrogen bonding, 3. mechanism of tautomerism, and 4. molecular responses to environmental changes.

References to Publications of DOE Sponsored Research:

[1] "Submolecular control, spectroscopy, and imaging of bond-selective chemistry in single functionalized molecules", Ying Jiang, Qing Huan, Laura Fabris, Guillermo C. Bazan and Wilson Ho, Nature Chemistry **5**, 36-41 (2013). This article was selected as highlights by:

- Chemistry World, Simon Hadlington, Royal Society of Chemistry, 11 November 2012.
- Peking University News, Ji Fang and Zhang Jiang, Nov. 19, 2012.
- Institute of Physics, Chinese Academy of Sciences News Updates, Nov. 30, 2012.
- Foresight Institute, Stephanie Corchnoy, March 11, 2013.

[2] "Real-Space Imaging of Molecular Structure and Chemical Analysis by Single-Molecule Inelastic Tunneling Probe", Chi-lun Chiang, Chen Xu, Zhumin Han, and W. Ho, Science, submitted (2013).

THEORY OF THE REACTION DYNAMICS OF SMALL MOLECULES ON METAL SURFACES

Bret E. Jackson

Department of Chemistry
104 LGRT
710 North Pleasant Street
University of Massachusetts
Amherst, MA 01003
jackson@chem.umass.edu

Program Scope

Our objective is to develop realistic theoretical models for molecule-metal interactions important in catalysis and other surface processes. The dissociative adsorption of molecules on metals, Eley-Rideal and Langmuir-Hinshelwood reactions, recombinative desorption and sticking are all of interest. To help elucidate the experiments that study these processes, we examine how they depend upon the nature of the molecule-metal interaction, and experimental variables such as substrate temperature, beam energy, angle of impact, and the internal states of the molecules. Electronic structure methods based on Density Functional Theory (DFT) are used to compute the molecule-metal potential energy surfaces. Both time-dependent quantum scattering techniques and quasi-classical methods are used to examine the reaction dynamics. Effort is directed towards developing improved quantum methods that can accurately describe reactions, as well as include the effects of temperature (lattice vibration) and electronic excitations.

Recent Progress

The dissociative chemisorption of methane on a Ni catalyst is the rate-limiting step in the chief industrial process for H_2 production. This reaction has a high barrier and a correspondingly small dissociative sticking probability that increases exponentially with collision energy below saturation. The reaction has an unusually strong dependence on the temperature of the substrate, and is also enhanced by vibrational excitation of the methane, but in a non-statistical fashion. Most of our recent work has focused on the dissociative chemisorption of methane on metals, in an attempt to understand how methane reactivity varies with the temperature of the metal, the translational and vibrational energy in the molecule, and the properties of the metal surface. Initial studies of methane dissociation on Ni(111) used DFT to compute the barrier height and explore the potential energy surface (PES) for this reaction, with an emphasis on how it changes due to lattice motion. At the transition state for dissociation, we found that if the metal lattice is allowed to relax, the Ni atom over which the molecule dissociates puckers out of the surface by a few tenths of an Å. Put another way, thermal motion of this Ni atom causes the barrier to dissociation to change, which should lead to a strong variation in the reactivity with temperature. High dimensional quantum scattering calculations which allowed for the inclusion of several key methane degrees of freedom (DOF), as well as the motion of the metal atom over which the reaction occurs, found that the reaction probability was significantly larger than for a static lattice, and strongly increased with temperature. Studies of how lattice motion effects methane dissociation led to the development of sudden models, where quantum calculations were implemented for several frozen lattice configurations, Monte Carlo sampled at the substrate temperature. These approaches reproduced the results of quantum treatments, and because motion of the heavy metal atom was not explicitly included in the wave function, several orders of magnitude less computer time were required. These models have proven to be very useful in

our more recent studies. We find that lattice motion modifies the energetics of methane dissociation in a similar fashion on Ni(100), Ni(111), Pt(100), Pt(111) and the stepped Pt(110)-(1x2) surface.

Exciting the vibrational modes of methane can increase the reaction probability. This increase, relative to that from putting the same amount of energy into translational motion, the so-called efficacy, is different for different vibrational modes, as well as for the same mode on different metal surfaces. We have made significant progress in understanding this mode-selective chemistry, using a formulation based on the Reaction Path Hamiltonian (RPH). Assuming only that the PES is harmonic for displacements away from the reaction (or minimum energy) path, we use DFT to compute a reasonably accurate PES that includes all 15 molecular DOF. We computed the RPH for methane dissociation on Ni(100), and then derived close-coupled equations by expanding the total wavefunction in the adiabatic vibrational states of the molecule. This approach was then used to compute full 15-DOF dissociative sticking probabilities for methane dissociation on Ni(100), using sudden models to average over surface impact sites and to introduce the effects of lattice motion [1]. These were the first calculations, based entirely on *ab intio* data, which could be compared directly with experimental studies of methane dissociative adsorption. We showed that the ν_1 mode (symmetric stretch), which significantly softens at the transition state, is strongly coupled to the reaction coordinate. As a result there is a large vibrational efficacy for this mode, as observed by two experimental groups. We demonstrated how the efficacies for vibrational enhancement are related to transitions from higher to lower energy vibrationally adiabatic states, or to the ground state, with the excess energy going into motion along the reaction path, increasing the reaction probability. Agreement with experiment was good, in terms of both the magnitude of the reactivity over a broad range of incident energies, and the efficacies of the different vibrational modes for promoting reaction [1]. More importantly, our approach made it possible to follow the flow of energy within the molecule as it dissociates, providing a detailed understanding of how translational, vibrational and lattice energy contribute to reactivity.

We have now applied this approach to methane reactions on two other metal surfaces. Studies on Ni(111) were motivated by experiments from the Utz group (Tufts), where they were able to measure methane dissociative sticking probabilities over a wide range of surface temperatures. This was the first real test of the models we developed for including lattice motion effects in these reactions. Not only did our *ab initio* methods accurately reproduce the observed variation with temperature, they were able to explain why the variation in reactivity with temperature was strong for certain energies and weak for others [2]. In addition, we were able to model and explain the variation in reactivity with nozzle temperature in terms of contributions to sticking from vibrationally excited molecules. Another set of studies focused on Pt(110)-(1x2), where the missing-row reconstruction leads to a very large surface corrugation, making this an excellent model for real (rough) catalysts [3]. Our focus was on comparing the reactivity and the molecule-phonon coupling at the step edges with that on the terrace sites of smooth Pt(111) and Pt(100) surfaces, as well as comparing with experimental work from the Beck group (EPFL). We found that the edge sites were more reactive, as expected, but that the effects of lattice motion were not any larger than on smoother surfaces, even though the phonon coupling was far more complicated, involving the motion of several lattice atoms. This coupling increases the dissociative sticking probability by about an order of magnitude when the surface temperature increases from 400 K to 600 K, in agreement with the experiments [3].

Recent experimental studies of CH_4 dissociation on Pt(111) by the Beck group show that the saturation coverage of CH_3 on the surface increases with both the translational energy and

vibrational excitation of the incident molecule. We used DFT to examine how the dissociation barrier is modified by the presence of chemisorbed H and CH_3 fragments, and find that this barrier increases as the surface coverage of reaction products increases. Using our DFT results, we developed kinetic models that were able to reproduce and explain the saturation behavior observed in the experimental uptake curves. Our work, along with the experimental findings, has been submitted for publication. In another recently completed study, we used a purely classical RPH to examine methane reactions on Ni(100) and Ni(111). First, we showed that the perturbative assumptions made in our quantum RPH model are valid. Second, we showed that classical trajectory methods based on the RPH could reproduce in a reasonable fashion the behavior observed in the experiments, including differing vibrational efficacies. However, while these classical methods did a good job at describing the reactions of vibrationally excited molecules, they consistently overestimated the reaction probability of molecules in the ground vibrational state. Our studies suggest that this is due to a non-conservation of zero point energy. The amount of vibrational zero point energy in the molecule is large, about 1.2 eV, and in classical mechanics this energy can lead to reactive trajectories at energies below the zero point energy-corrected activation energy; i.e., in the classically forbidden region. We have published a book chapter discussing the effects of lattice motion on gas-surface reactions [4]. The primary focus is on our methane studies, where the molecule-phonon coupling is unusually strong. Another book chapter is in press [5]. This book is aimed at a more general audience, and focuses on quantum effects in reactions. The focus of our contribution is again our methane work.

In recent years we have studied H-graphite reactions, important in the formation of molecular Hydrogen on graphitic dust grains in space, the etching of graphite walls in fusion reactors, and the modification of the electronic properties of graphene. Two recent studies examined the physisorption of H. We have developed a powerful approach to these types of problems based on the reduced density matrix, which allows us to evolve a quantum system weakly coupled to a bath over relatively long times. Thus, we can not only compute, quantum mechanically, the scattering into free and bound states, we can observe the eventual relaxation and/or desorption from these states. In a study of H physisorption on graphite, we showed that sticking is enhanced at low energies by diffraction mediated trapping states, and examined the adsorption and subsequent desorption of H on graphite in great detail. We compared our reduced density approach with more traditional wavefunction-based approaches, and demonstrated the utility and accuracy of these various methods [6]. More recently, these wavefunction-based close coupling approaches were used to examine H sticking on single-layer graphene at very low energies. We showed that support of graphene on a substrate, or suspension of graphene over a hole in a substrate modifies the dispersion properties of the lattice vibrations, stabilizing the two-dimensional structure. This in turn modifies the H-graphene phonon coupling, leading to anomalously large sticking probabilities at very low temperatures [7].

A collaboration with the Kroes group (Leiden) used AIMD, *ab initio* molecular dynamics, to study H_2 dissociation on Cu(111). In AIMD, one computes the instantaneous forces on the particles "on the fly", using DFT in our case. This eliminates the need to construct approximate many-dimensional PESs, which is extremely difficult when lattice motion is involved. Our studies showed that lattice motion and temperature could effect some aspects of H_2-Cu(111) scattering, particularly the quadrupole alignment parameter [8].

Future Plans

An on-going project involves methane chemisorption on Pt(111), which we compared with Ni(111) in an early low-dimensional study. While we found the Pt surface to be more reactive than the Ni, experiment suggests that the difference is much larger than our study found.

On both metals, the transition state is over the top site. However, on Ni, the methyl group moves towards a hollow site during the reaction, while on Pt the methyl remains at the top site. This behavior, if included in the model, should lead to a further lowering of the reactivity for Ni relative to Pt, as the heavy methyl group does not tunnel as effectively as the H. This motion is now included in our full 15-DOF RPH study of Ni(111) [2], and we plan to do a similar study on Pt(111), now that the coverage effects on the barrier height have been elucidated. This barrier height variation may also play a role in the discrepancy. We will also use our RPH approach to examine CD_3H dissociation on Pt(111), as part of a three-way collaboration with the Beck group, who are doing the corresponding experiments, and the Kroes group in Leiden, currently implementing AIMD studies.

In a second project, a relatively new study, we are examining the dissociative chemisorption of H_2O on Ni(111). This is motivated by recent experimental results from the Beck group, who are the very first to measure dissociative sticking probabilities for water on a metal surface. Mode-selective chemistry is also observed. We have located the transition state, and are applying our RPH methods to this problem. Finally, we have a third ongoing project examining H-Ag interactions, motivated by experiments in the Wodtke group (MPI, Göttingen). In particular, we are examining scattering, subsurface penetration and thermal desorption, in collaboration with the Lemoine group in Toulouse, and Sven Nave in Orsay.

References

[1] B. Jackson and S. Nave, "The dissociative chemisorption of methane on Ni(100): Reaction path description of mode-selective chemistry" J. Chem. Phys. 135, 114701 (2011).

[2] B. Jackson and S. Nave, "The dissociative chemisorption of methane on Ni(111): The effects of molecular vibration and lattice motion" J. Chem. Phys. 138, 174705 (2013).

[3] D. Han, S. Nave and B. Jackson, "Dissociative chemisorption of methane on Pt(110)-(1x2): Effects of lattice motion on reactions at step edges" J. Phys. Chem. A (in press).

[4] B. Jackson, "The effects of lattice motion on gas-surface reactions", in *Dynamics of Gas-Surface Interactions: Atomic-level Understanding of Scattering Processes at Surfaces,* Springer Series in Surface Sciences, vol. 50, 2013, R. D. Muiño and H. F. Busnengo, eds.

[5] C. Diaz, A. Gross, B. Jackson and G.-J. Kroes, "Elementary molecule-surface scattering processes relevant to heterogeneous catalysis: Insights from quantum dynamics calculations", in *Molecular Quantum Dynamics*, Springer Series: Physical Chemistry in Action, (in press).

[6]. B. Lepetit, D. Lemoine, Z. Medina, and B. Jackson, "Sticking and desorption of hydrogen on graphite: a comparative study of different models," J. Chem. Phys. 134, 114705 (2011).

[7] B. Lepetit and B. Jackson, "Sticking of hydrogen on supported and suspended graphene at low temperature," Phys. Rev. Lett. 107, 236102 (2011).

[8] Effect of surface motion on the rotational quadrupole alignment parameter of D_2 reacting on Cu(111), F. Nattino, C. Díaz, B. Jackson, and G.J. Kroes, Phys. Rev. Lett. 108, 236104 (2012).

DE-FG02-07ER15889: **Probing catalytic activity in defect sites in transition metal oxides and sulfides using cluster models: A combined experimental and theoretical approach**

Caroline Chick Jarrold and Krishnan Raghavachari
Indiana University, Department of Chemistry, 800 East Kirkwood Ave.
Bloomington, IN 47405
cjarrold@indiana.edu, kraghava@indiana.edu

I. Program Scope

Our research program combines experimental and computational methods to study well-defined cluster models of heterogeneous catalytic materials. The focus of our studies has been transition metal oxide and sulfide clusters in non-traditional oxidation states (surface defect models) and their chemical and physical interactions with water and CO_2. The applications that are being modeled are H_2 production from photocatalyic decomposition of water, and photocatalytic CO_2 reduction using Group 6 (Mo and W) oxides and sulfides. The experiments and calculations are designed to probe fundamental, cluster-substrate molecular-scale interactions that are governed by charge state, peculiar oxidation states, and unique physical structures.

The general strategy of our studies continues to be as follows: (1) Determine how the molecular and electronic structures of transition metal suboxide and subsulfide clusters evolve as a function of oxidation state by reconciling anion photoelectron spectra of the bare clusters with high-level DFT calculations. Anions are of particular interest because of the propensity of metal oxide and sulfides to accumulate electrons in applied systems. (2) Measure and analyze the kinetics of cluster reactivity with water or CO_2. (3) Dissect possible reaction mechanisms computationally, to determine whether catalytically relevant interactions are involved. (4) Verify these challenging computational studies by spectroscopic investigation of observed reactive intermediates. (5) Probe the effect of local electronic excitation on bare clusters and cluster complexes, to evaluate photocatalytic processes. The overarching goal of this project is to identify particular defect structures that balance structural stability with electronic activity, both of which are necessary for a site to be simultaneously robust and catalytically active, and to find trends and patterns in activity that can lead to improvement of existing applied catalytic systems, or the discovery of new systems.

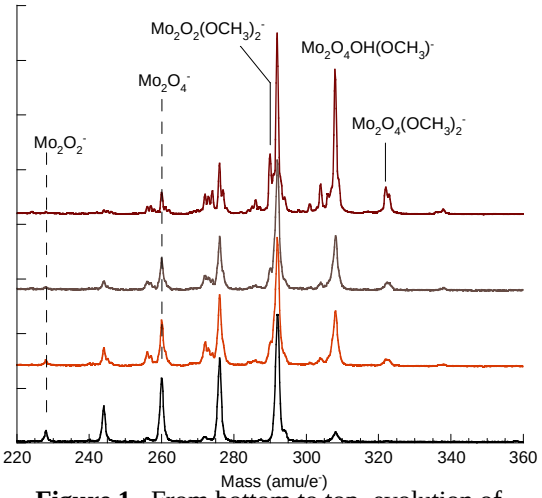

Figure 1. From bottom to top, evolution of products of $^{98}Mo_2O_y^-$ + CH_3OH reactions. Certain peaks illustrating both dissociative CH_3OH addition and double CH_3OH with H_2

II. Recent Progress

A. Alcohol reduction by $M_xO_y^-$ clusters (M = Mo, W)

One of the more important findings in our previous studies of $M_xO_y^-$ + water → $M_xO_{y+1}^-$ + hydrogen reactions was that several trapped intermediates observed for M = Mo reactions were not observed in M = W reactions, which has been explained (below) as the result of disparate barrier heights for proton mobility in –OH groups formed upon water addition to the metal oxide cluster anions. In an effort to test this finding, alcohol reactivity studies were done in an effort to determine how replacing one of the hydrogens with a relatively immobile –R group would affect the reaction rates or prevalence of trapped intermediates in the $M_xO_y^-$ + ROH → $M_xO_{y+1}^-$ + RH reaction.

Interestingly, ROH reactivity studies revealed that H_2 elimination, in addition to RH elimination and $M_xO_yROH^-$ traps could occur. H_2 elimination is achieved by addition of two ROH molecules, with the observation of $M_xO_y(OR)_2^-$ species as evidence. Figure 1

shows a typical series of mass spectra of $^{98}Mo_2O_y^-$ clusters generated in pure He (bottom trace) and with increasing MeOH concentration in the reaction channel, reaching a maximum 0.2% for the top trace. These double addition products were observed for both methanol and ethanol, in addition to single addition trapped intermediates that are analogous with the water addition products. This observation supports the computational results that proton mobility figures importantly in the rate of H_2 evolution, since the alcohol reaction products reached a higher oxidation state than the water reaction products via the two-reactant channel, indicating that the $M_xO_yROH^-$ intermediates are longer lived than the $M_xO_yHOH^-$ intermediates. [S.E. Waller and C.C. Jarrold, "Hydrogen Evolution from ROH reactions with $M_xO_y^-$ (M = Mo, W; $x = 1 - 4$, $y \leq 3x$), *in preparation*.]

Methanol, with mass equal to two oxygen atoms, presents a unique problem for mass spectrometry-based reactivity studies. Because the mass spectrometer used in these studies also has the capability of mass-selected anion photoelectron spectroscopy, we are able to separate species with coincident masses by their PE spectra. Using this technique, we learned that (single) ROH addition products have analogous structures to water addition products. An example of the trapped $Mo_3O_5^-$ + water/methanol product is shown in Figure 2. [S.E. Waller and C.C. Jarrold, "Photoelectron spectroscopic determination of product identity in ROH reactions with $M_xO_y^-$ (M = Mo, W; $x = 1 - 4$, $y \leq 3x$), *in preparation*.]

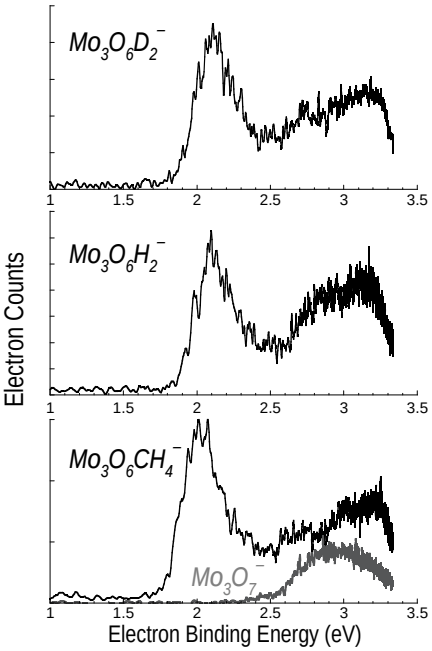

Figure 2. PE spectra of analogous trapped intermediates formed in the $Mo_3O_5^-$ + D_2O, H_2O, and CH_3OH reactions. $Mo_3O_6CH_4^-$ and $Mo_3O_7^-$, but their different PE spectra allow us to ascertain that methanol adds to $Mo_3O_5^-$ in the same way as water.

B. Reaction rate and product irregularities in the $Mo_xO_y^-$ + H_2O reaction

The rate of sequential oxidation of tungsten oxide cluster anions decreases with an increase in cluster size. This was not the case for molybdenum oxide clusters, an affect that could be attributed to the lower symmetry of molybdenum oxide clusters. [M. Ray, S.E. Waller, A. Saha, C.C. Jarrold and K. Raghavachari, "Comparative Study of Water Reactivity to $Mo_2O_y^-$ and $W_2O_y^-$ Clusters: A Combined Experimental and Theoretical Investigation," *in preparation.*] The structural asymmetry can further be linked to the particular stability of the +4 oxidation state of Mo. Interestingly, with improvements in resolution of the mass spectrometer used in our experiments, we were able to identify MoO_3H^-, which would be the conjugate base of a suboxide form (MoO_3H_2) of molybdic acid (MoO_4H_2) in which Mo is found in a +4 oxidation state. Our spectra and calculations indicate that the anion is planar and electronically stable. [S.E. Waller, M. Ray, and C.C. Jarrold, "A Simple Relationship Between Oxidation State and Electron Affinity in Gas-phase Metal-oxo complexes," *in preparation*.]

C. Computational studies Hydrogen Evolution from Water through Metal Sulfide catalysis

We have conducted a careful computational study of the structures, electronic states, and reactivity of metal sulfide cluster anions $M_2S_X^-$ (M = Mo and W, X = 4 to 6) using density functional theory. Detailed structural analysis shows that these metal sulfide anions have ground state isomers with two bridging sulfide bonds, notably different in some cases from the corresponding oxides with the same stoichiometry. This is partly due to the fact that the *M*–O–*M* angle in the metal oxides is much more strained than the *M*–S–*M* angle in the metal sulfides. Mo–S bond lengths are significantly larger than the Mo–O bond lengths, allowing the metal sulfides to have more strain free bridging sulfur bonds with less repulsion. The chemical reactivity of these metal sulfide anions with water has also been carried out. After a thorough search on the reactive potential energy surface, we propose several competitive, energetically favorable, reaction pathways that lead to the evolution of hydrogen. Selectivity in the initial

water addition and subsequent hydrogen migration are found to be the key steps in all the proposed reaction channels. As illustrated in Figure 3, initial adsorption of water is most favored involving a terminal sulfur atom in $Mo_2S_4^-$ isomers whereas the most preferred orientation for water addition involves a bridging sulfur atom in the case of $W_2S_4^-$ and $Mo_2S_5^-$ isomers. In all the lowest energy H_2 elimination steps, the interacting hydrogen atoms involve a metal hydride and a metal hydroxide (or thiol) group. We have also observed an unusual higher energy reaction channel where the interacting hydrogen atoms in the H_2 elimination step involve a thiol (–SH) and a hydroxyl (–OH) group. For all the reaction pathways, the Mo sulfide reactions involve a higher barrier than the corresponding W analogues. We observe for both metals that reactions of $M_2S_4^-$ and $M_2S_5^-$ clusters with water to liberate H_2 are exothermic and involve modest free energy barriers. However, the reaction of water with $M_2S_6^-$ is highly endothermic with a considerable barrier due to saturation of the local bonding environment. [A. Saha and K. Raghavachari, "Hydrogen Evolution from Water through Metal Sulfide Catalysis", Submitted to J. Chem. Phys., July 2013.]

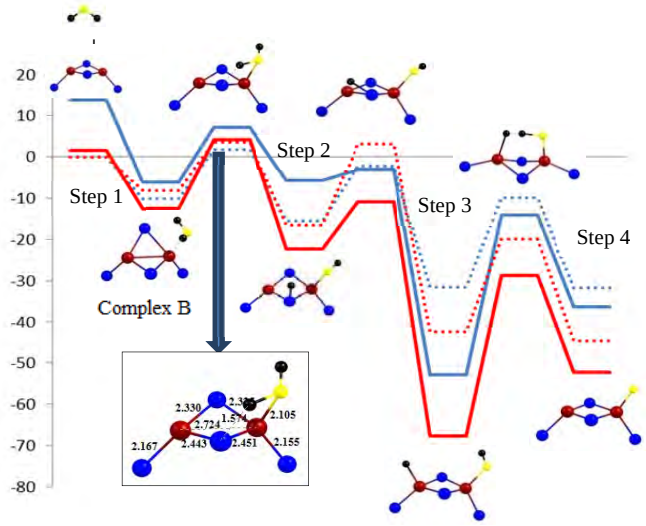

Figure 3. Reaction energy profile for one possible reaction pathway for $M_2S_4^-$ cluster with water. Blue line denotes Mo and red lines denotes W. Solid line represents the doublet profile & dotted line represents the quartet profile. Quartet surface has been taken as the origin of the reaction energy coordinate

D. New Insights on Photocatalytic H_2 Liberation from Water using Transition Metal Oxides: Lessons from Cluster Models of Molybdenum and Tungsten Oxides

We have finalized an extensive investigation into the chemical reactions of $W_3O_5^-$ and $Mo_3O_5^-$ clusters with water that throw light on a variety of key factors central to H_2 generation. Our computational results explain why experimentally, $Mo_3O_5^-$ forms a unique kinetic-trap in its reaction, while $W_3O_5^-$ undergoes a facile oxidation to form the lowest energy isomer of $W_3O_6^-$ and liberates H_2. Mechanistic insights on the reaction pathways that occur, as well as the reaction pathways that do not occur, are point to the pivotal roles of (a) differing metal-oxygen bond strengths, (b) the initial electrostatic complex formed and (c) the geometric factors involved in the release of H_2. The most important factor leading toward the different reaction outcomes appears to be the stronger W–O bond energy compared to Mo–O. However, the discovery of the importance of fluxionality of the proton on the reaction complex drove more recent studies on ROH reactions (above). [R.

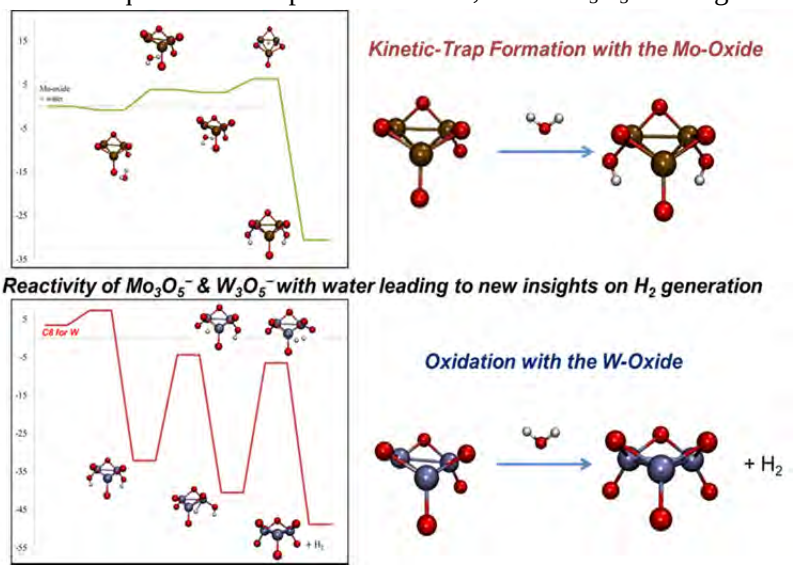

Ramabhadran, J.E. Mann, S.E. Waller, D.W. Roghgeb, C.C. Jarrold and K. Raghavachari, "New Insights on Photocatalytic H_2 Liberation from Water using Transition Metal Oxides: Lessons from Cluster Models of Molybdenum and Tungsten Oxides," submitted to JACS, July, 2013.]

III. Future Plans

A continuing strength of the research program is the synergistic interplay between theory and experiment. We have been working toward achieving a generalized description of the chemical reactivity of the transition metal oxides resulting in H_2 evolution. Other newer directions include modeling full-cycle catalysis by identifying a desirable sacrificial reagent that will be oxidized during the course of water (or alcohol) reduction. Past studies on CH_4 reactivity suggested that under high-energy conditions, CH_4 could compromise Mo-O-Mo bridge bonds. When a suboxide cluster is oxidized by water, it is vibrationally very hot due to the sudden increase in internal energy. The high internal energy may facilitate reactions with CH_4. Encouraging preliminary studies indicate that under room temperature conditions, CH_4 will react with $Mo_xO_y^-$ clusters ONLY in the presence of water. Calculations on CH_4 and several other potential sacrificial reagents are ongoing.

In addition, temperature-dependence studies of reaction kinetics are currently underway in an effort to benchmark calculated reaction barriers, and efforts to generate isotopically pure $^{98}Mo_xS_y^-$ and $^{186}W_xO_y^-$ clusters have been initiated.

IV. References to publications of DOE sponsored research that have appeared in 2009–present or that have been accepted for publication (5 manuscripts currently are either in the late stages of revision or submitted)

1. "Properties of Metal Oxide Clusters in non-Traditional Oxidation States," J. E. Mann, N. J. Mayhall and C. C. Jarrold, Chem. Phys. Lett. **525-6**, 1-12 (2012).
2. "Fluxionality in the Reactions of Transition-Metal Oxide Clusters: The Role of Metal, Spin-state and the Reacting Small Molecule," R. O. Ramabhadran, E. L. Becher, III, A. Chowdhury, and K. Raghavachari, J. Phys. Chem. A **116**, 7189-7196 (2012).
3. "Study of Nb_2O_y (y = 2-5) anion and neutral clusters using photoelectron spectroscopy and DFT calculations," J. E. Mann, S.E. Waller, D.W. Rothgeb and C. C. Jarrold, J. Chem. Phys. **135**, 104317 (2011).
4. "Structures of trimetallic molybdenum and tungsten suboxide cluster anions," D. W. Rothgeb, J. E. Mann, S. E. Waller and C. C. Jarrold, J. Chem. Phys. **135**, 104312 (2011).
5. "Molybdenum Oxides versus Molybdenum Sulfides: Geometric and Electronic Structures of $Mo_3X_y^-$ (X = O, S and y = 6, 9) Clusters," N.J. Mayhall, E.L. Becher, A. Chowdhury, and K. Raghavachari, J. Phys. Chem A, **115**, 2291-2296 (2011).
6. "Resonant two-photon detachment of WO_2^-," J.E. Mann, S.E. Waller, D.W. Rothgeb and C.C. Jarrold, Chem. Phys. Lett. **506**, 31-36 (2011).
7. "Proton Hop Paving the Way for Hydroxyl Migration: Theoretical Elucidation of Fluxionality in Transition-Metal Oxide Clusters," R.O. Ramabhadran, N.J. Mayhall, and K. Raghavachari, J. Phys. Chem. Lett. **1,** 3066-3071 (2010).
8. "Electrochemistry of Substituted Salen Complexes of Nickel(II):Nickel(I)-catalyzed Reduction of Alkyl and Acetylenic Halides," M. P. Foley, P. Du, K. J. Griffith, J. A. Karty, M. S. Mubarak, K. Raghavachari, and D. G. Peters, J. Electroanal. Chem. **647**, 194-203 (2010).
9. "Electrochemical Reduction of 5-Chloro-2-(2,4-Dichlorophenoxy)Phenol (Triclosan) in Dimethylformamide," K. N. Knust, M. P. Foley, M. S. Mubarak, S. Skljarevski, K. Raghavachari, and D. G. Peters, J. Electroanal. Chem. **638**, 100-108 (2010).
10. "H_2 production from reactions between water and small molybdenum suboxide cluster anions," D.W. Rothgeb, J.E. Mann, and C.C. Jarrold, J. Chem. Phys. **133**, Article 054305 (2010).
11. "CO_2 reduction by group 6 transition metal suboxide cluster anions," E. Hossain, D.W. Rothgeb, and C.C. Jarrold, J. Chem. Phys. **133**, Article 024305 (2010).

Critical evaluation of theoretical models for aqueous chemistry and CO_2 activation in the temperature-controlled cluster regime

DE-FG02-00ER15066 and DE-FG02-06ER15800

K. D. Jordan (jordan@pitt.edu), Dept. of Chemistry, University of Pittsburgh, Pittsburgh, PA 15260

M. A. Johnson (mark.johnson@yale.edu), Dept. of Chemistry, Yale University, New Haven, CT 06520

Program Scope

Our program exploits size-selected clusters as a medium with which to unravel molecular level pictures of key transient species in condensed phase and interfacial chemistry. These systems are relevant to mediation of radiation damaged biomolecules as well as to catalytic activation of CO_2 for conversion into transportable solar fuels. Much of this work involves trapping labile free radicals created using negatively charged molecular clusters as powerful reducing agents.

Recent Progress

For aqueous species, the negatively charged water clusters have been particularly useful as they undergo fast electron scavenging reactions that are gas-phase analogues to those of the hydrated electron, a ubiquitous intermediate in radiation chemistry. An important aspect of electron-induced aqueous chemistry is the nature of the interaction between a diffuse electron and its associated water network, and in 2012 we completed our analysis of the distorted "Fano" lineshapes arising from interaction of vibrational levels of the supporting water network with the electron cloud. That work was carried out with Yale colleague and fellow CPIMS PI John Tully, and reported in Ref. [1]. We also completed our efforts initiated under the previous grant to understand how this electron is transported to scavengers like CO_2 by water network fluctuations, reported as a feature article in Ref. [2]. Beyond aqueous processes, we were able to extend our theoretical and experimental methodologies to characterize free radicals generated by electron attachment to multidentate H-bond bridges such as those found in double-

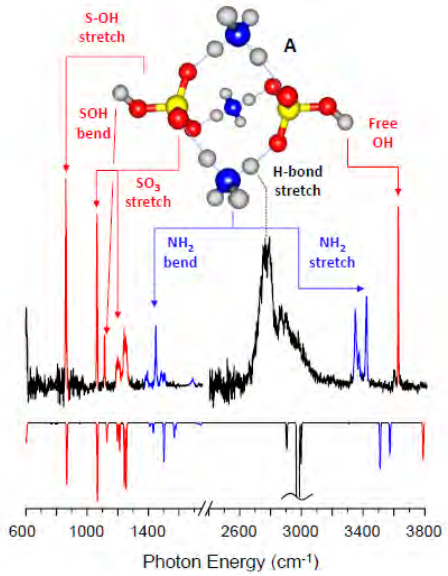

Figure 1: Vibrational predissociation spectrum of D_2-tagged $(NH_4^+)_3(HSO_4^-)_2$ along with a comparison to the calculated (harmonic) spectrum (inverted) of the best-fitting structure at the top. Bisulfate-localized modes are colored in red, and ammonium-localized modes are blue. Signature vibrations are highlighted with arrows.

stranded DNA. Our joint work on the archetypal formic acid dimer anion was reported in Refs. [3,4].

In an important recent experimental advance, we dramatically broadened the scope of the chemistry that we can study by incorporating ion sources that not only provide universal access to both aqueous and non-aqueous species, but do so in a temperature-controlled fashion. This was carried out in close consultation with Profs. L.-S. Wang and X. Wang using methods they developed at PNNL and first reported at a CPIMS meeting. We are particularly interested in the structures of complexes invoked to explain the advantages of ionic liquids (IL) as media for CO_2 chemistry. To initiate this new aspect of our program, we first demonstrated the production, isolation and D_2 molecule "tagging" of salt clusters involving alkyl ammonium and bisulfate ions, thought to play the key role of seed species in the growth of atmospheric aerosols. We then obtained highly resolved vibrational spectra of these ionic clusters, with a typical spectrum shown in Figure 1 for $(NH_4^+)_3(HSO_4^-)_2$. The discrete transitions are the unique spectroscopic signatures of their anionic and cationic constituents. Furthermore, we find that the characteristic vibrational bands of much larger ammonium bisulfate particles (1000s of molecules) are already emergent for clusters of only a handful of molecules. These studies (reported in Ref. (5)) provide firm experimental benchmarks for ongoing computational studies of the aerosol nucleation problem.

We note that in our spectroscopic study of the aerosols, we encountered the situation that the bands associated with the ionic hydrogen bonds are typically very broad envelopes spanning hundreds of wavenumbers (H-bond stretch in Figure 1). We demonstrated how such broadening can be recovered in a related system through incorporation of cubic terms in the potential surface, which is reported in Ref. [6].

ILs have attracted considerable attention because of their small Henry's law constants for CO_2 uptake (i.e., high solubility), their potential use as green solvents (in part due to the low vapor pressures), and their favorable catalytic activity in electrochemical production of CO_2. In imidazolium-based ILs (such as those based on 1-ethyl-3-methyl imidizolium [emim] cations), it has been reported that the CO_2 activity is mostly correlated with the chemical nature of the anionic component (e.g, BF_4^-, Tf_2N^-, PF_6^-, acetate, etc.), prompting many theoretical studies of the intermolecular CO_2 interactions with various anionic partners. To this end, we obtained our first vibrational spectrum of a cold, tagged cation complex prepared by electrospray ionization of an IL. The preliminary experimental and calculated (harmonic) spectra of the $[emim^+]_2[BF_4^-]$ ion is presented in Fig. 2, and is very encouraging indeed, as sharp bands are observed throughout the fingerprint region that are, as in the case in the aerosol clusters, readily assigned to the ionic

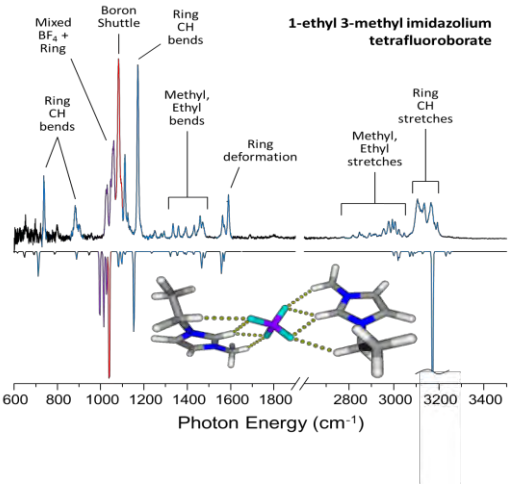

Figure 2. Comparison of experimental and calculated (inverted) vibrational spectra of 1-ethyl 3-methyl imidazolium tetrafluoroborate $[emim^+]_2[BF_4^-]$, with the best-fitting computed structure inset. [emim]-localized modes are colored in blue, local BF stretching modes are red, and purple denotes modes including motion of both species. Modes assignable (tentatively) to specific functional groups are labeled.

constituents. Refinement of the theoretical method required to accurately recover the observed band positions and inclusion of anharmonic corrections will be a primary focus for the Pittsburgh team in the coming year.

The well-resolved peaks apparent in the spectrum shown in Fig. 2 provide an excellent basis for characterization of the structural changes induced by the fundamental interactions between ionic liquid constituents and CO_2 during activation. To accomplish this, we have spent considerable effort in this first year of the grant to establish a general means with which to condense CO_2 onto any ion extracted from solution. This required empirical variation of trap temperature and buffer gas compositions to achieve maximal condensation while minimizing destructive sticking of CO_2 onto the trap and cryostat surfaces. We now have a robust protocol for preparing relatively large CO_2 adducts of ions injected at room temperature, with a typical result displayed in Fig. 3 for the case of a classic Ni(cyclam) CO_2 reduction catalyst. The next phase of the project will involve attachment of CO_2 to various compositions of ILs to monitor the extent to which CO_2 is perturbed upon contact with both the cationic and anionic constituents.

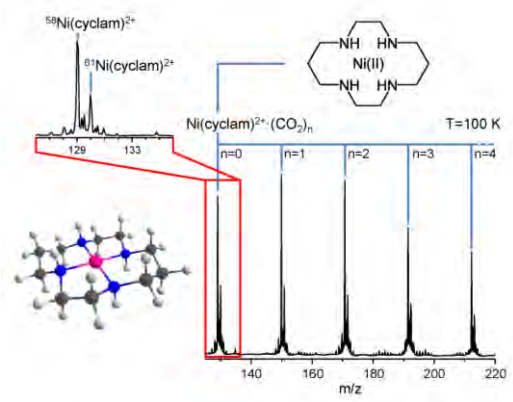

Figure 3. Mass spectrum demonstrating the condensation of CO_2 onto Ni(cyclam)$^{2+}$. Addition of CO_2 onto the organometallic complex was achieved by collecting the ions in an ion trap maintained at a temperature of 100 K by a buffer gas consisting of ~1% CO_2 in He.

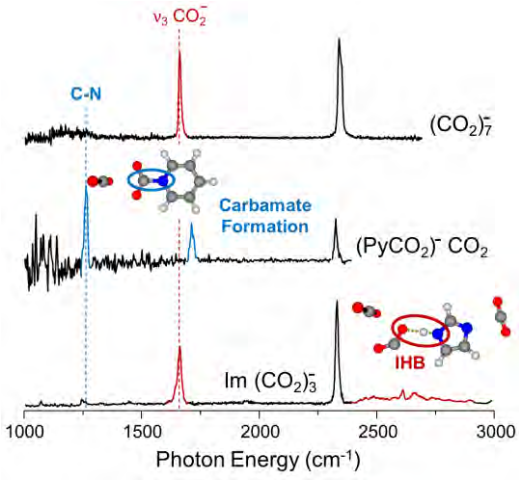

Figure 4. Predissociation spectra of CO_2 adducts involving radical anions of two Schiff base heterocyclic rings: pyridine and imidazole. While CO_2^- makes a covalent bond with pyridine to form the key carbamate intermediate, the complex with imidazole involves an H-bonded complex between the neutral imidazole and the CO_2^- radical anion.

Future Plans

An important aspect of our work on CO_2 activation is to understand the degree to which a CO_2 molecule is altered upon attachment to various local binding sites of catalysts. In the previous grant period, we demonstrated how pyridine, a current candidate for photoelectrocatalysis, can strongly interact with CO_2 in a reductive environment to yield a carbamate radical ion (Ref [7]). We have already extended this work to explore whether this attachment motif is a general property of Schiff bases, with preliminary results comparing the behavior of pyridine and imidazole in Fig. 4. Interestingly, carbamate formation is completely suppressed in the radical anion adduct to imidazole as the CO_2^- is stabilized in an anionic H-bonded arrangement.

Recently, Musgrave and coworkers [*J. Am. Chem. Soc.*, **135**, 142, 2013] have proposed a water-mediated proton transfer mechanism for the electrochemical reduction of CO_2 to HCO_2^- by a neutral pyridinium radical. Thus, we intend to extend this work to explore the reactions between $(H_2O)_n^-$ clusters and [pyridine·$(CO_2)_m$] complexes. Exploratory experimental and theoretical studies have been initiated on these reactions, with the main discovery being that for the larger water clusters, there is spontaneous proton transfer to the pyridine to create the critical pyridinium radical.

Papers since October 1, 2010 under CPIMS DOE support

1. **"Vibrational Fano resonances in dipole-bound anions,"** Stephen T. Edwards, Mark A. Johnson, and John C. Tully, *J. Chem. Phys.*, **136**, 154305, 2012.

2. **"Bottom-up view of water network-mediated CO_2 reduction using cryogenic cluster ion spectroscopy and direct dynamics simulations,"** Kristin J. Breen, Andrew F. DeBlase, Timothy L. Guasco, Vamsee K. Voora, Kenneth D. Jordan, Takashi Nagata, and Mark A. Johnson, *J. Phys. Chem. A*, **116**, 903, 2012.(Cover article)

3. **"Structural characterization of electron-induced proton transfer in the formic acid dimer anion, $(HCOOH)_2^-$, with vibrational and photoelectron spectroscopies,"** Helen K. Gerardi, Andrew F. DeBlase, Christopher M. Leavitt, Xiaoge Su, Kenneth D. Jordan, Anne B. McCoy, and Mark A. Johnson, *J. Chem. Phys.*, **136**, 134318, 2012.

4. **"Unraveling the Anomalous Solvatochromic Response of the Formate Ion Vibrational Spectrum: An Infrared, Ar-Tagging Study of the HCO_2^-, DCO_2^-, and $HCO_2^-\cdot H_2O$ Ions,"** Helen K. Gerardi, Andrew F. DeBlase, Xiaoge Su, Kenneth D. Jordan, Anne B. McCoy, and Mark A. Johnson," *J. Phys. Chem. Lett.*, **2**, 2437, 2011.

5. **"Structures and fragmentation pathways of size-selected, D_2-tagged ammonium/methylammonium bisulfate clusters,"** Christopher J. Johnson and Mark A. Johnson, *J. Phys. Chem. A*, *Accepted,* 2013, DOI: 10.1021/jp404244y.

6. "**Origin of the diffuse vibrational signature of a cyclic intramolecular proton bond: anharmonic analysis of protonated 1,8-disubsituted naphthalene ions,"** Andrew F. DeBlase, Steven Bloom, Thomas Lectka, Kenneth D. Jordan, Anne B. McCoy, and Mark A. Johnson, *J. Chem. Phys.*, **139**, 024301, 2013.

7. "Vibrational predissociation spectrum of the carbamate radical anion, $C_5H_5N\text{-}CO_2^-$, generated by Reaction of pyridine with $(CO_2)_m^-$," Michael Z. Kamrath, Rachael A. Relph, and Mark A. Johnson, *J. Am. Chem. Soc.*, **132**, 15508, 2010.

8. "Vibrational manifestations of strong non-Condon effects in the $H_3O^+\cdot X_3$(X = Ar, N_2, CH_4, H_2O) complexes: A possible explanation for the intensity in the "association band" in the vibrational spectrum of water," Anne B. McCoy, Timothy L. Guasco, Christopher M. Leavitt, Solveig G. Olesen, and Mark A. Johnson, *Phys. Chem. Chem. Phys.*, **14**, 7205, 2012.(Cover article)

Nucleation Chemical Physics

Shawn M. Kathmann
Physical Sciences Division
Pacific Northwest National Laboratory
902 Battelle Blvd.
Mail Stop K1-83
Richland, WA 99352
shawn.kathmann@pnl.gov

Program Scope

The objective of this work is to develop an understanding of the chemical physics governing nucleation. The thermodynamics and kinetics of the embryos of the nucleating phase are important because they have a strong dependence on size, shape and composition and differ significantly from bulk or isolated molecules. The technological need in these areas is to control chemical transformations to produce specific atomic or molecular products without generating undesired byproducts, or nanoparticles with specific properties. Computing reaction barriers and understanding condensed phase mechanisms is much more complicated than those in the gas phase because the reactants are surrounded by solvent molecules and the configurations, energy flow, electric fields, and ground and excited state electronic structure of the entire statistical assembly must be considered.

Recent Progress and Future Directions

Charge and Field Fluctuations in Aqueous NaCl

The observations of luminescence during crystallization suggest that the process of crystallization may not be purely classical but also involves an essential electronic structure component. Strong electric field fluctuations may play an important role in this process by providing the necessary driving force for the observed electronic structure changes (see Figure 1 – top). The importance of electric field fluctuations driving electron transfer has been a topic of intense research since the seminal work of Marcus. The main objective of this work is to provide basic understanding of the fluctuations in charge, electric potentials, and electric fields for concentrated aqueous NaCl electrolytes. Our charge analysis reveals that the water molecules in the 1st solvation shell of the ions serve as a sink for electron density originating on Cl^- (see Figure 1 – bottom). We find that the electric fields inside aqueous electrolytes are extremely large (up to several V/Å) and thus may alter the ground and excited electronic states in the condensed phase (see Figure 2). Furthermore, our results show that the potential and field distributions are largely independent of concentration. We also find that the field component distributions to be Gaussian for the ions and non-Gaussian for the O and H sites (computed in the lab frame of reference), however, these non-Gaussian distributions are readily modeled via an orientationally averaged non-zero mean Gaussian plus a zero mean Gaussian. These calculations and analyses provide the first steps toward understanding the magnitude and fluctuations of charge, electric potentials and

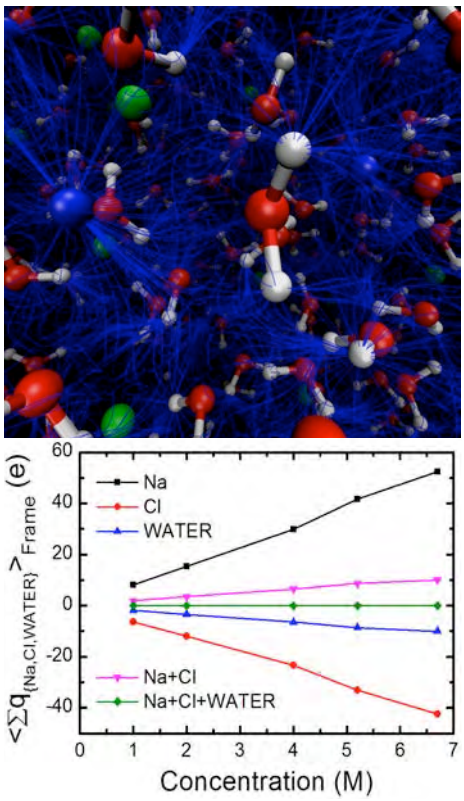

Figure 1. Electric fields in 6.7M NaCl (top), charge redistribution as a function of concentration (bottom).

fields in aqueous electrolytes and what role these fields may play in driving charge redistribution/transfer during crystalloluminescence.

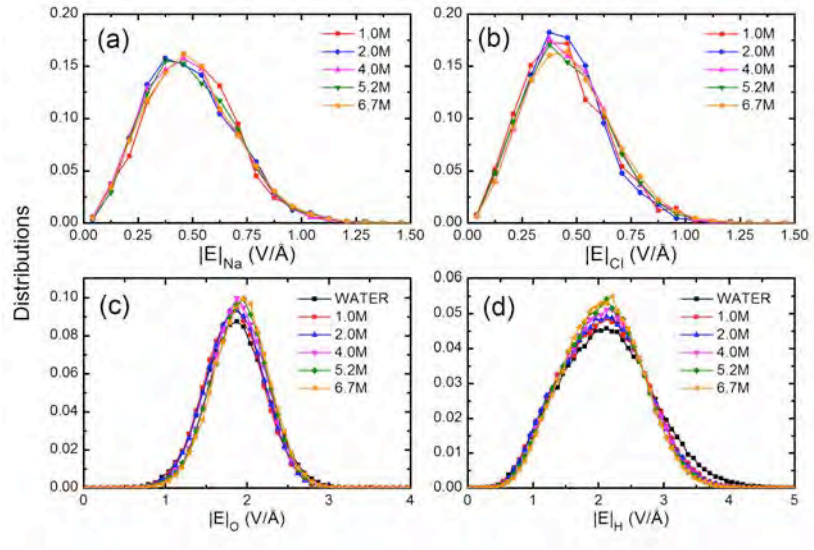

Figure 2. Distributions of the magnitude of the electric field P(E) at the Na^+, Cl^-, O, and H sites. The electric field distributions on Na^+ and Cl^- are nearly concentration independent with the distributions for O and H showing a slight concentration dependence and having larger fields (by a factor of 4) and broader distributions (factor of 2) than those on Na^+ and Cl^-.

Homogeneous and Heterogeneous Ice Nucleation

It is surprisingly difficult to freeze water. Almost all ice that forms under "mild" conditions (temperatures > −40◦C) requires the presence of a nucleating agent - a solid particle that facilitates the freezing process - such as clay mineral dust, soot or bacteria. In a computer simulation, the presence of such ice nucleating agents does not necessarily alleviate the difficulties associated with forming ice on accessible timescales. Nevertheless, in this work we present results from molecular dynamics simulations in which we systematically compare homogeneous and heterogeneous ice nucleation, using the atmospherically important clay mineral kaolinite as our model ice-nucleating agent (see Figure 3). From our simulations, we do indeed find that kaolinite is an excellent ice nucleating agent but that contrary to conventional thought, non-basal faces of ice can nucleate at the basal face of kaolinite. We see that in the liquid phase, the kaolinite surface has a drastic effect on the density profile of water, with water forming a dense, tightly bound first contact layer. Monitoring the time evolution of the water density reveals that changes away from the interface may play an important role in the nucleation mechanism. The findings from this work suggest that heterogeneous ice nucleating agents may not only enhance the ice nucleation rate, but also alter the macroscopic structure of the ice crystals that form. Current and future work will understand the role of surface chemistry, reconstruction, defects, as well as the near and far-field interfacial electric effects.

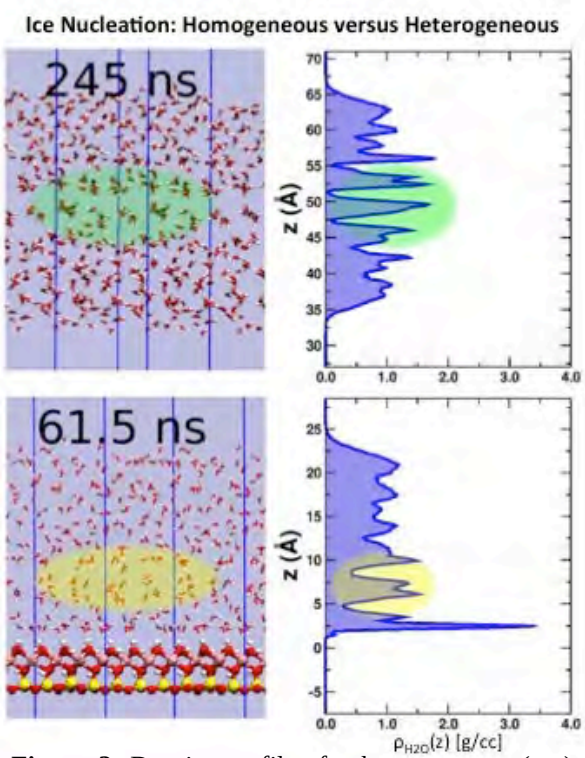

Figure 3. Density profiles for homogeneous (top) and heterogeneous (kaolinite) ice nucleation. Note that ice is forming away from the interface.

Zero-Point Motion in Sulfuric Acid-Water Clusters

The nucleation of particles from trace gases in the atmosphere is an important source of cloud condensation nuclei (CCN), and these are vital for the formation of clouds in view of the high supersaturations required for homogeneous water droplet nucleation. The methods of quantum chemistry have increasingly been employed to model nucleation due to their high accuracy and efficiency in calculating configurational energies; and nucleation rates can be obtained from the associated free energies of particle formation. However, even in such advanced approaches, it is typically assumed that the nuclei have a classical nature, which is questionable for some systems. The thermodynamics and kinetics of H_2SO_4-H_2O clusters are complicated by the facile motion of the protons associated with the dissociation of H_2SO_4 in the presence of several H_2O molecules. The importance of zero-point motion in modelling small clusters of sulfuric acid and water is tested here using the path integral molecular dynamics (PIMD) method at the density functional theory (DFT) level of theory. We observe a small zero-point effect on the equilibrium structures of certain clusters. One configuration is found to display a bimodal behaviour at 300 K in contrast to the stable ionised state suggested from a zero temperature classical geometry optimization (see Figure 4). The general effect of zero-point motion is to promote the extent of proton transfer with respect to classical behaviour.

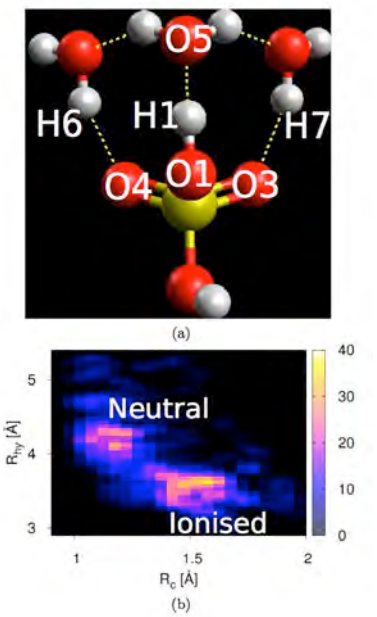

Figure 4. (a) H_2SO_4•$(H_2O)_3$. (b) Probability density as a function of R_c = O1-H1 and R_{hy} = O4-H6 + O3-H7.

Some ongoing work includes: (1) performing *ab initio* MD in addition to using *ab initio* methods to resample the classical potential to study charge transfer, (2) using QM/MM hydrid DFT functionals to obtain distributions of excited (singlet and triplet) states to ground state singlet photon energies as well as spin-orbit interactions and oscillator strengths for the concentrated electrolytes, (3) use the Hartree potential analysis to compute the surface potentials of various aqueous electrolytes as functions of concentration as well as investigate the electrical properties of the crystal-aqueous phase interfaces to compare with available experiments, and (4) computing potentials of mean force for ions in solutions from the *ab initio* MD to use in accelerated dynamics to model crystallization kinetics.

Direct PNNL collaborators on this project include Marat Valiev, G.K. Schenter, C.J. Mundy, Xuebin Wang, John Fulton, Liem Dang and Postdoctoral Fellows Bernhard Sellner and Marcel Baer. Outside collaborations with the University College London include Stephen Cox and Angelos Michaelides on ice nucleation (Chemistry), Jake Stinson and Ian Ford on sulfuric acid-water nucleation (Physics), and Andrew Alexander (Chemistry) at the University of Edinburgh, Scotland.

Acknowledgement: This research was performed in part using the DOE NERSC facility. Battelle operates PNNL for DOE.

Publications of DOE Sponsored Research (2011-present)

Cover Article – S.M. Kathmann, I-FW. Kuo, C.J. Mundy, and G.K. Schenter, "Understanding the Surface Potential of Water." *Journal of Physical Chemistry B*, **115**, 4369 (2011).

G. Murdachaew, M. Valiev, S.M. Kathmann, and X. Wang, "Study of Ion Specific Interactions of Alkali Cations with Dicarboxylate Dianions", *Journal of Physical Chemistry A*, **116**, 2055 (2012).

Communication – S.J. Cox, S.M. Kathmann, J.A. Purton, M.J. Gillan, and A. Michaelides, "Non-hexagonal ice at hexagonal surfaces: the role of lattice mismatch", *Physical Chemistry Chemical Physics*, **14**, 7944 (2012).

Communication – H. Wen, G.L. Hou, S.M. Kathmann, M. Valiev, and X.B. Wang, "Solute anisotropy effects in hydrated anion and neutral clusters", *Journal of Chemical Physics*, **138**, 031101 (2013).

S.J. Cox, Z. Raza, S.M. Kathmann, B. Slater, and A. Michaelides, "The Microscopic Features of Heterogeneous Ice Nucleation May Affect the Macroscopic Morphology of Atmospheric Ice Crystals", *Faraday Discussions*, in press (2013).

S.M. Kathmann, B. Sellner, A.J. Alexander, and M. Valiev, "Beyond Classical Theories", Proceedings of the 19th International Conference on Nucleation and Atmospheric Aerosols, (2013).

J.L. Stinson, S.M. Kathmann, and I.J. Ford, "Investigating the significance of zero-point motion in small molecular clusters of sulphuric acid and water", *Journal of Chemical Physics*, in press (2013).

Cover Article – B. Sellner, M. Valiev, and S.M. Kathmann, "Charge and Electric Field Fluctuations in Aqueous NaCl Electrolytes", *Journal of Physical Chemistry B*, in press (2013).

Chemical Kinetics and Dynamics at Interfaces

Structure and Reactivity of Ices, Oxides, and Amorphous Materials

Bruce D. Kay (PI), R. Scott Smith, and Zdenek Dohnálek
Chemical and Materials Sciences Division
Pacific Northwest National Laboratory
P.O. Box 999, Mail Stop K8-88
Richland, Washington 99352
bruce.kay@pnnl.gov

Additional collaborators include P. Ayotte, P. J. Feibelman, G. A. Kimmel, J. Knox, J. Matthiesen, R. A. May, G. S. Parkinson, and N. G. Petrik

Program Scope

The objective of this program is to examine physiochemical phenomena occurring at the surface and within the bulk of ices, oxides, and amorphous materials. The microscopic details of physisorption, chemisorption, and reactivity of these materials are important to unravel the kinetics and dynamic mechanisms involved in heterogeneous (i.e., gas/liquid) processes. This fundamental research is relevant to solvation and liquid solutions, glasses and deeply supercooled liquids, heterogeneous catalysis, environmental chemistry, and astrochemistry. Our research provides a quantitative understanding of elementary kinetic processes in these complex systems. For example, the reactivity and solvation of polar molecules on ice surfaces play an important role in complicated reaction processes that occur in the environment. These same molecular processes are germane to understanding dissolution, precipitation, and crystallization kinetics in multiphase, multicomponent, complex systems. Amorphous solid water (ASW) is of special importance for many reasons, including the open question over its applicability as a model for liquid water, and fundamental interest in the properties of glassy materials. In addition to the properties of ASW itself, understanding the intermolecular interactions between ASW and an adsorbate is important in such diverse areas as solvation in aqueous solutions, cryobiology, and desorption phenomena in cometary and interstellar ices. Metal oxides are often used as catalysts or as supports for catalysts, making the interaction of adsorbates with their surfaces of much interest. Additionally, oxide interfaces are important in the subsurface environment; specifically, molecular-level interactions at mineral surfaces are responsible for the transport and reactivity of subsurface contaminants. Thus, detailed molecular-level studies are germane to DOE programs in environmental restoration, waste processing, and contaminant fate and transport.

Our approach is to use molecular beams to synthesize "chemically tailored" nanoscale films as model systems to study ices, amorphous materials, supercooled liquids, and metal oxides. In addition to their utility as a synthetic tool, molecular beams are ideally suited for investigating the heterogeneous chemical properties of these novel films. Modulated molecular beam techniques enable us to determine the adsorption, diffusion, sequestration, reaction, and desorption kinetics in real-time. In support of the experimental studies, kinetic modeling and simulation techniques are used to analyze and interpret the experimental data.

Recent Progress and Future Directions

The release of trapped gases from amorphous solid water films. "Top-down" crystallization-induced crack propagation probed using the molecular volcano Amorphous solid water (ASW) is a kinetically metastable form of water which is created when water vapor impinges on a substrate below 130 K. When heated, or allowed to sit for a fantastically long time, ASW converts to thermodynamically stable crystalline ice. Crystallization of ASW can result in structural changes in the film. For example, when an inert gas (CCl_4, Ar, CO_2, Kr , Xe, CO, N_2, O_2, and others) is deposited underneath an ASW overlayer, the inert gas desorption is delayed until crystallization of the ASW overlayer. We have termed the episodic release of trapped gases from ASW the "molecular volcano". The observed abrupt desorption is likely due to the formation of cracks that accompany the crystallization kinetics and form a

connected release pathway.

Recently, we have revisited the "molecular volcano" phenomenon and have used it to characterize the length and distribution of crystallization-induced cracks. In this work composite films were created by depositing 1 ML of the gas of interest and then capping it with various overlayer thicknesses of ASW. The films were heated and the desorption of the underlayer was monitored. At low overlayer thicknesses (< 100 ML), nearly all of the inert gas underlayer desorbs in a molecular volcano event. However as the overlayer thickness is increased, an increasing fraction of the inert gas does not desorb in a volcano event but instead desorbs at higher temperature when the ASW film itself desorbs. We refer to the desorption at higher temperature as the "trapped" fraction. A plot of the "trapped" faction versus the ASW overlayer coverage yields a sigmoidal-like curve that plateaus near 600 ML. Below 200 ML, the trapped fraction increases slowly, implying that most of the crystallization-induced cracks span the entire overlayer thickness, opening a path for all of the gas to desorb. Above 200 ML, the trapped fraction increases rapidly until all the gas is trapped at thicknesses above 600 ML. The rapid increase in trapped fraction indicates that increasing numbers of cracks are unable to span the thicker ASW films, thus increasing the amount of trapped gas. The vertical length distribution of crystallization-induced cracks through ASW was determined by taking the derivative of the trapped faction versus overlayer thickness curve. We found that the crack length distribution is independent of the trapped gas (Ar, Kr, Xe, CH_4, N_2, O_2, or CO) with an average length of 306 ± 9 ML for a heating rate of 1 ML/s. We also observed that the trapped fraction increased with heating rate indicating a competition between crack propagation and healing.

The volcano peak was also used to determine the crystallization induced crack propagation mechanism. In this case an inert gas layer was deposited at various positions in the ASW film. We found that the closer to the top of the film the layer was deposited, the earlier in temperature (time) the volcano desorption peak occurred. Through a series of experiments we were able to show conclusively that the direction of crack formation begins at the ASW/vacuum interface and moves downward into the film. Isothermal desorption experiments where the overlayer thickness was varied were used to measure the crack propagation rate. The results revealed that after an induction period, cracks propagate linearly in time with an Arrhenius temperature dependent velocity and an activation energy of 54 kJ/mol. This value is consistent with the crystallization growth rates reported by others and establishes a direct connection between crystallization growth rate and the crack propagation rate. A two-step kinetic model in which nucleation and crystallization occurs in an induction zone near the top of the film followed by the propagation of a crystallization/crack front into the film is in good agreement with the temperature programmed desorption results. (This work is described in publication #13 below).

The release mechanism studied here is due to structural changes in the ASW overlayer as a result of crystallization. As a consequence, for 1 ML underlayer coverages, the results are independent of the specific gas. Below we describe the appearance of additional pre-crystallization desorption pathways that become available when the underlayer thicknesses are larger than 1 ML.

The release of trapped gases from amorphous solid water films. "Bottom-up" induced desorption pathways The trapping and retention of volatile gases by ASW is important to understanding a wide array of astrophysical processes including the abundance of molecules in the interstellar medium and the possibility that many types of gases were originally brought to earth by comets. Above we described a mechanism whereby gas release is controlled by crystallization-induced cracks formed in the ASW overlayer. In that work, where the underlayer thicknesses were 1 ML, the results were largely independent of the particular gas. Here we focus on the high coverage regime where new desorption pathways become accessible prior to ASW crystallization. In contrast to the results for the low coverage regime, the release mechanism is a function of the multilayer thickness and composition, displaying dramatically different behavior between Ar, Kr, Xe, CH_4, N_2, O_2, and CO.

Two primary pre-crystallization desorption pathways are observed. The first occurs between 100 and 150 K and manifests itself as sharp, extremely narrow desorption peaks. Temperature programmed desorption shows that these abrupt desorption bursts are due to pressure induced structural failure of the ASW overlayer. The second pathway occurs at low temperature (typically <100 K) where broad

desorption peaks are observed. Desorption through this pathway is attributed to diffusion through pores formed during ASW deposition. The extent of desorption and the line shape of the low temperature desorption peak are dependent on the substrate on which the gas underlayer is deposited. Angle dependent ballistic deposition of ASW is used to vary the porosity of the overlayer and strongly supports the hypothesis that the low temperature desorption pathway is due to porosity that is templated into the ASW overlayer by the gas underlayer during deposition.

The two pre-crystallization desorption mechanisms are both dependent on the particular underlayer species and as such represent "bottom-up" mechanisms. This work provides a physical, mechanistic explanation for the previous observational reports of gas release. It is clear that relatively small changes in the ASW overlayer (density, porosity) can give rise to dramatic differences in the release kinetics of the gaseous underlayer. This is an important factor to consider when interpreting the experimental studies of gaseous release from laboratory analogs of astrophysical ices. (This work is described in publication #14 below). Future work will focus on the surface structure of the underlayer and how it may induce porosity in the ASW overlayer.

Mobility of supercooled liquid toluene, ethylbenzene, and benzene near their glass transition temperatures investigated using inert gas permeation Glasses and other noncrystalline solids are utilized in a variety of scientific and applied fields and are important in diverse disciplines ranging from art and architecture to catalysis and drug delivery. However, it is experimentally difficult to measure the kinetic processes involved in creating these materials. Part of the difficulty is due to the inherent drive to crystallize as the temperature of the supercooled liquid approaches the glass transition. Recently, we have developed a technique in which the permeation rate of inert gases is used to determine the diffusivity of the supercooled liquid. In this technique, a layer of an inert gas (e.g., Ar, Kr, and Xe) is deposited beneath the amorphous solid overlayer. When the amorphous solid transforms into a supercooled liquid, the gas begins to permeate through the supercooled liquid. Desorption of the gas can be measured and is related to the diffusivity of the supercooled liquid itself.

We have applied this technique to investigate the mobility of supercooled liquid toluene, ethylbenzene, and benzene near their respective glass transition temperatures (Tg). For toluene and ethylbenzene the onset of inert gas permeation is observed at temperatues near Tg. Diffusivities of 10^{-14} to 10^{-9} cm^2/s were determined from 115 to 135 K, respectively. The diffusivities in toluene and ethylbenzene were the same over this temperature range, which is consistent with the behavior of their higher temperature liquids. The temperature dependence of the diffusivity approaching Tg was non-Arrhenius and was equally well-fit by either a VFT or the Corresponding States quadratic equation proposed by David Chandler and colleagues. At these temperatures, the relationship between the diffusivities and the viscosity did not obey the Stokes−Einstein equation but instead was well-fit by the fractional Stokes−Einstein equation with an exponent of ∼0.66. The diffusivity in neat supercooled benzene could not be determined using inert gas permeation due to the onset of crystallization at temperatures well below Tg. Mixtures of benzene and ethylbenzene were used to shift the benzene crystallization to higher temperature. A 50/50 mixture shifted the benzene crystallization to ∼120 K, but even at this temperature, the inert gas desorption spectra were far too complicated to extract meaningful diffusivities. (This work is described in publication #15 below).

Future work will focus on expanding the inert gas permeation method to other systems and expanding the range of probe molecules used to further understand how their interactions with the material of interest alters the measured diffusivity.

References to Publications of DOE sponsored Research (October 2010- present)

1. R. S. Smith, J. Matthiesen, and B. D. Kay, *"Measuring diffusivity in supercooled liquid nanoscale films using inert gas permeation. I. Kinetic model and scaling methods"*, Journal of Chemical Physics **133**, 174504 (2010).
2. J. Matthiesen, R. S. Smith, and B. D. Kay, *"Measuring diffusivity in supercooled liquid nanoscale films using inert gas permeation. II. Diffusion of Ar, Kr, Xe, and CH_4 through Methanol"*, Journal of Chemical Physics **133**, 174505 (2010).
3. J. Matthiesen, R. S. Smith, and B. D. Kay, *"Mixing It Up: Measuring Diffusion in Supercooled Liquid Solutions of Methanol and Ethanol at Temperatures near the Glass Transition"*, Journal of Physical Chemistry Letters **2**, 557 (2011).
4. P. J. Feibelman, G. A. Kimmel, R. S. Smith, N. G. Petrik, T. Zubkov, and B. D. Kay, *"A unique vibrational signature of rotated water monolayers on Pt(111): Predicted and observed"*, Journal of Chemical Physics **134**, 204702 (2011).
5. R. S. Smith, J. Matthiesen, J. Knox, and B. D. Kay, *"Crystallization Kinetics and Excess Free Energy of H_2O and D_2O Nanoscale Films of Amorphous Solid Water"*, Journal of Physical Chemistry A **115**, 5908 (2011).
6. D. W. Flaherty, N. T. Hahn, R. A. May, S. P. Berglund, Y. M. Lin, K. J. Stevenson, Z. Dohnálek, B. D. Kay, and C. B. Mullins, *"Reactive Ballistic Deposition of Nanostructured Model Materials for Electrochemical Energy Conversion and Storage"*, Accounts of Chemical Research **45**, 434 (2012).
7. P. Ayotte, P. Marchand, J. L. Daschbach, R. S. Smith, and B. D. Kay, *"HCl Adsorption and Ionization on Amorphous and Crystalline H_2O Films below 50 K"*, Journal of Physical Chemistry A **115**, 6002 (2011).
8. R. A. May, R. S. Smith, and B. D. Kay, *"Probing the interaction of amorphous solid water on a hydrophobic surface: dewetting and crystallization kinetics of ASW on carbon tetrachloride"*, Physical Chemistry Chemical Physics **13**, 19848 (2011).
9. R. S. Smith, N. G. Petrik, G. A. Kimmel, and B. D. Kay, *"Thermal and Nonthermal Physiochemical Processes in Nanoscale Films of Amorphous Solid Water"*, Accounts of Chemical Research **45**, 33 (2012).
10. R. A. May, R. S. Smith, and B. D. Kay, *"The Molecular Volcano Revisited: Determination of Crack Propagation and Distribution During the Crystallization of Nanoscale Amorphous Solid Water Films"*, Journal of Physical Chemistry Letters **3**, 327 (2012).
11. R. S. Smith and B. D. Kay, *"Breaking Through the Glass Ceiling: Recent Experimental Approaches to Probe the Properties of Supercooled Liquids near the Glass Transition"*, Journal of Physical Chemistry Letters **3**, 725 (2012).
12. J. Matthiesen, R. S. Smith, and B. D. Kay, *"Probing the mobility of supercooled liquid 3-methylpentane at temperatures near the glass transition using rare gas permeation"*, Journal of Chemical Physics **137**, 064509 (2012).
13. R. A. May, R. S. Smith, and B. D. Kay, *"The release of trapped gases from amorphous solid water films. I. "Top-down" crystallization-induced crack propagation probed using the molecular volcano"*, Journal of Chemical Physics **138**, 104501 (2013).
14. R. A. May, R. S. Smith, and B. D. Kay, *"The release of trapped gases from amorphous solid water films. II. "Bottom-up" induced desorption pathways"*, Journal of Chemical Physics **138**, 104502 (2013).
15. R. A. May, R. S. Smith, and B. D. Kay, *"Mobility of Supercooled Liquid Toluene, Ethylbenzene, and Benzene near Their Glass Transition Temperatures Investigated Using Inert Gas Permeation"*, Journal of Physical Chemistry A, dx.doi.org/10.1021/jp403093e (2013).

Chemical Kinetics and Dynamics at Interfaces

Non-Thermal Reactions at Surfaces and Interfaces

Greg A. Kimmel (PI) and Nikolay G. Petrik

Chemical and Materials Sciences Division
Pacific Northwest National Laboratory
P.O. Box 999, Mail Stop K8-88
Richland, WA 99352
gregory.kimmel@pnnl.gov

Program Scope

The objectives of this program are to investigate 1) thermal and non-thermal reactions at surfaces and interfaces, and 2) the structure of thin adsorbate films and how this influences the thermal and non-thermal chemistry. Energetic processes at surfaces and interfaces are important in fields such as photocatalysis, radiation chemistry, radiation biology, waste processing, and advanced materials synthesis. Low-energy excitations (e.g. excitons, electrons, and holes) frequently play a dominant role in these energetic processes. For example, in radiation-induced processes, the high energy primary particles produce numerous, chemically active, secondary electrons with energies that are typically less than ~100 eV. In photocatalysis, non-thermal reactions are often initiated by holes or (conduction band) electrons produced by the absorption of visible and/or UV photons in the substrate. In addition, the presence of surfaces or interfaces modifies the physics and chemistry compared to what occurs in the bulk.

We use quadrupole mass spectroscopy, infrared reflection-absorption spectroscopy (IRAS), and other ultra-high vacuum (UHV) surface science techniques to investigate thermal, electron-stimulated, and photon-stimulated reactions at surfaces and interfaces, in nanoscale materials, and in thin molecular solids. Since the structure of water near interface plays a crucial role in the thermal and non-thermal chemistry occurring there, a significant component of our work involves investigating the structure of aqueous interfaces. A key element of our approach is the use of well-characterized model systems to unravel the complex non-thermal chemistry occurring at surfaces and interfaces. This work addresses several important issues, including understanding how the various types of low-energy excitations initiate reactions at interfaces, the relationship between the water structure near an interface and the non-thermal reactions, energy transfer at surfaces and interfaces, and new reaction pathways at surfaces.

Recent Progress

Adsorption Geometry of CO versus Coverage on TiO_2(110) from s- and p-polarized Infrared Spectroscopy

For molecules adsorbed on surfaces, the adsorption geometry is one of the most fundamental pieces of information needed to characterize the interactions. For example, the adsorption geometry typically affects other important properties such as the adsorption energy and chemical reactivity. Surface science experiments on well-characterized, single crystals in ultrahigh vacuum have proved particularly useful for gaining detailed information about adsorbate interactions with surfaces, including adsorption geometries. While most surface science experiments have historically focused on metals and semiconductors, research on metal oxides has been rapidly increasing, particularly for titanium dioxide. The interest in TiO_2 is driven by its broad range of applications and potential applications.

We have investigated the adsorption of CO on reduced TiO_2(110) using IRAS. For s-polarized light, the electric field is parallel to the surface and perpendicular to the azimuth containing the IR beam. Thus on a dielectric substrate, the s-polarized spectra are sensitive to vibrations that have a projection parallel to the surface. For p-polarized light, the spectra are sensitive to vibrations with components perpendicular and parallel to the surface. As a results, detailed information regarding the adsorption

geometry of the CO as a function of CO coverage, θ_{CO}, can be obtained from IRAS experiments utilizing s- and p-polarized light directed along the [001] and $[1\bar{1}0]$ azimuths.

When θ_{CO} is comparable to the vacancy concentration (θ_V) a peak at ~2179 cm^{-1} is observed in IRAS that has previously been assigned to CO adsorbed near the vacancies. For $\theta_{CO} > \theta_V$, a peak associated with CO adsorbed at "normal" Ti_{5c} sites (i.e. not related to the vacancies) appears at ~ 2188 cm^{-1} in the p-polarized spectra for both azimuths. This peak becomes more intense and shifts to lower frequency as θ_{CO} increases to 1 ML. However, no signal is observed for s-polarized light, indicating that CO adsorbs at Ti_{5c} sites perpendicular to the surface (i.e. $\Theta \sim 0°$) for $\theta_{CO} \leq 1$ ML (see Fig. 1, right side). Analysis of the signal to the noise level in the s-polarized spectra suggests that angle between the surface normal and the CO adsorbed at Ti_{5c} sites is $0° \pm 10°$ for $\theta_{CO} \leq 1$ ML. The perpendicular adsorption geometry for CO on Ti_{5c} sites is consistent with a (1×1) structure for the CO adlayer observed in previous He scattering experiments, but not with calculations.

For 1 ML $< \theta_{CO} \leq 1.5$ ML, a new peak appears at 2136 cm^{-1} for s-polarized light along the [001] azimuth (Fig. 1, green line). The intensity of this peak increases linearly with coverage for 1 ML $< \theta_{CO} \leq$ 1.5 ML. In contrast, no absorption for s-polarized light is observed for the other crystal orientation (Fig. 1, blue line).

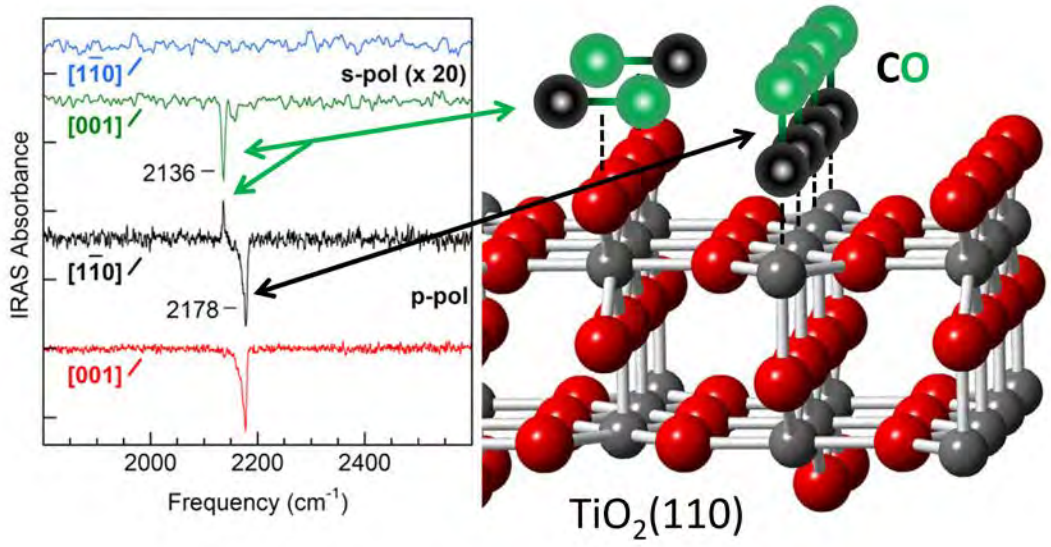

Fig. 1. Left side: s- and p-polarized IRAS spectra for 1.5 ML CO adsorbed on TiO_2(110). Right side: Schematic of CO adsorption geometry on TiO_2(110). For $\theta_{CO} \leq 1.5$ ML, CO adsorbs normal to the surface at Ti_{5c} sites. For 1 ML $< \theta_{CO} \leq 1.5$ ML, additional CO adsorbs at bridging oxygen sites parallel to the surface and perpendicular to the bridging oxygen rows.

For p-polarized IR and 1 ML $< \theta_{CO} \leq 1.5$ ML, the peak at 2178 cm^{-1} decreases slightly and the spectra broaden for both azimuths. In addition, the absorbance at 2136 cm^{-1} is seen as a *positive* peak for the p-polarized spectra, but only along the $[1\bar{1}0]$ azimuth (Fig. 1, black line). These results show that for 1 ML $\leq \theta_{CO} \leq 1.5$ ML, the CO in the second monolayer adsorb at O_b sites, perpendicular to the bridging oxygen rows, and parallel to the surface (see Fig. 1). Since for s-polarized IR the signal is only observed along the [001] azimuth, the projection of the molecules in the plane of the surface must be perpendicular to the O_b rows (i.e. along the $[1\bar{1}0]$ azimuth). The positive peak at 2136 cm^{-1} for p-polarized spectra along the $[1\bar{1}0]$ azimuth also indicates that CO/O_b adsorbs *parallel* to the surface and *perpendicular* to the O_b rows. If these molecules had an appreciable component of their transition dipole moment normal to the

surface then the absorbance at 2136 cm^{-1} would be negative *and* it would also be observed as a *negative* absorbance peak in the p-polarized spectra along the [001] azimuth, where no absorbance is seen (Fig. 1, red line).

These results provide the first experimental evidence that CO adsorbs parallel to the surface at O_b sites, and demonstrate the utility of polarization- and azimuthally-resolved IRAS for investigating adsorption geometries on transition metal oxides such as TiO_2(110). This work is published in reference 6.

Multiple Non-Thermal Reaction Steps for the Photooxidation CO to CO_2 on Reduced TiO_2(110)

TiO_2 is a widely used photocatalyst. Its ability to oxidize organic contaminants makes it useful, for example, in air and water purification systems and as a thin-film coating for self-cleaning surfaces. As a result of titanium oxide's practical applications and its potential use in photocatalytic water spitting, it has been the subject of a tremendous amount of research. Because it is a prototypical photocatalytic reaction, the photooxidation of CO to CO_2 has received considerable attention, and some of the most detailed information has come from investigations of the reactions of CO and O_2 on single-crystal TiO_2(110).

Previous experiments have shown that the CO_2 photon-stimulated desorption (PSD) yield increased abruptly at the beginning of the UV irradiation and then monotonically decreased as the irradiation proceeds (see Fig. 2a). Similar kinetics are also observed for the CO_2 electron-stimulated desorption (ESD) yield when energetic electrons are used to create electron-hole pairs in the TiO_2 instead of UV photons. It has been proposed that the photooxidation of CO on TiO_2(110) proceeds in a single step via electron attachment, $CO + O_2^- + e^- \rightarrow CO_2 + O_b^{2-}$, and this mechanism is consistent with the observed kinetics. However, the typical time resolutions in the earlier experiments have been ~0.1 s, precluding investigation of the reaction kinetics at earlier times.

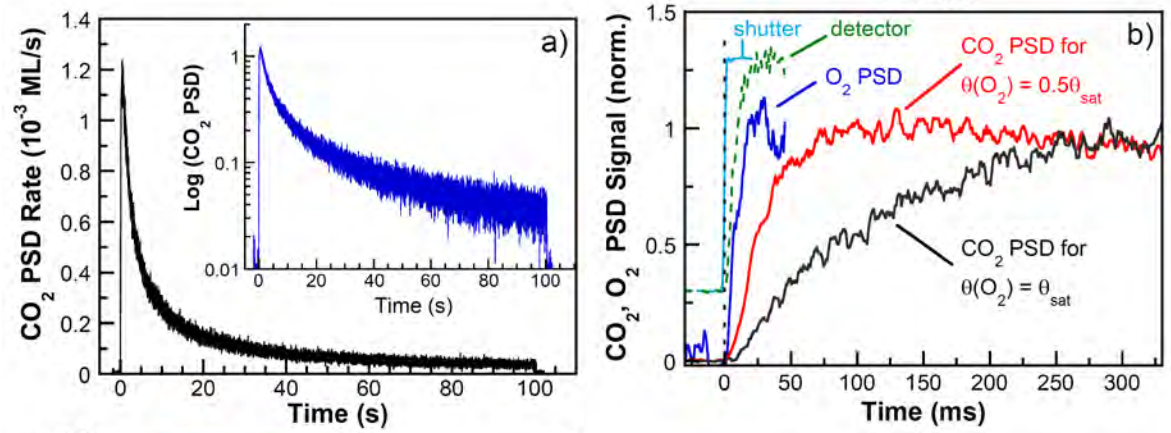

Figure 2. CO_2 and O_2 PSD signals versus time during UV irradiation of co-adsorbed O_2 and CO on TiO_2(110). a) On a longer timescale, the CO_2 PSD signal appears to increase abruptly when the UV light is switched on at t = 0 s, and then decays with complicated (non-exponential) kinetics. b) On a millisecond timescale, the CO_2 PSD signals (red and black lines) increase gradually from zero, reach a maximum and then decay at longer times. In contrast, the O_2 PSD signal (blue line) increases with the response time of the mass spectrometer detection system (green line).

We have investigated the photooxidation of CO adsorbed on reduced, rutile TiO_2(110) with an emphasis on the initial reaction kinetics on a millisecond timescale. For a saturation coverage of chemisorbed O_2 and half that coverage, we find that the CO_2 PSD signal is initially zero and gradually increases to a maximum value after several tens of milliseconds (Fig. 1b). The initial CO_2 PSD signal increases more quickly for the smaller O_2 coverage, but reaches approximately the same maximum value

at intermediate times for both O_2 coverages. The results show that the photooxidation of CO on TiO_2(110) requires two or more non-thermal reaction steps and involves a metastable intermediate species. It is likely that both a hole and an electron are involved in the reactions, e.g. $CO + O_2^{2-} \xrightarrow{h^+} (CO \cdot O_2)^- \xrightarrow{e^-} O_b^{2-} + CO_2(gas)$. Alternatively, the order of the electron- and hole-mediated steps could be reversed. (Our results do not distinguish between the two possibilities.) The results also suggest that a non-thermal reaction involving this intermediate species is responsible for the non-cosine angular distribution of desorbing CO_2 that we have previously reported. This work is published in reference 6.

Future Directions:

Important questions remain concerning the factors that determine the structure of thin water films on various substrates. We plan to continue investigating the structure of thin water films on non-metal surfaces, such as oxides, and on metals where the first layer of water does not wet the substrate. For the non-thermal reactions in water films, we will use IRAS to characterize the electron-stimulated reaction products and precursors. We will also continue our investigations into the photochemistry of small molecules on TiO_2(110).

References to publications of DOE-sponsored research (FY 2011 – present)

[1] Nikolay G. Petrik and Greg A. Kimmel, "Electron- and hole-mediated reactions in UV-irradiated O_2 adsorbed on reduced rutile TiO_2(110)," *J. Phys. Chem. (C)*, **115**, 152 (2011).

[2] Peter J. Feibelman, Greg A. Kimmel, R. Scott Smith, Nikolay G. Petrik, Tykhon Zubkov, and Bruce D. Kay, "A unique vibrational signature of rotated water monolayers on Pt(111): Predicted and observed," *J. Chem. Phys.,* **134**, 204702 (2011).

[3] Nikolay G. Petrik and Greg A. Kimmel, "Oxygen Photochemistry on TiO_2(110): Recyclable, Photoactive Oxygen Produced by Annealing Adsorbed O_2," *J. Phys. Chem. Lett,* **2**, 2790 (2011)**.**

[4] R. Scott Smith, Nikolay G. Petrik, Greg A. Kimmel, and Bruce D. Kay, "Thermal and non-thermal physiochemical processes in nanoscale films of amorphous solid water," *Accounts of Chemical Research*, **45,** 33 (2012).

[5] G. A. Kimmel, M. Baer, N. G. Petrik, J. VandeVondele, R. Rousseau, and C. J. Mundy, "Polarization- and azimuth-resolved infrared spectroscopy of water on TiO_2(110): Anisotropy and the hydrogen-bonding network, " *J. Phys. Chem. Lett,* **3**, 778 (2012).

[6] Nikolay G. Petrik and Greg A. Kimmel, "Adsorption geometry of CO versus coverage on TiO_2(110) from s- and p-polarized infrared spectroscopy," *J. Phys. Chem. Lett,* **3**, 3425 (2012) (DOI: 10.1021/jz301413v)**.**

[7] Nikolay G. Petrik and Greg A. Kimmel, "Multiple Non-Thermal Reaction Steps for the Photooxidation CO to CO_2 on Reduced TiO_2(110)," *J. Phys. Chem. Lett,* **4**, 344 (2013) (DOI: 10.1021/jz302012j).

Radiolysis of Aromatic Compounds

Jay A. LaVerne
Notre Dame Radiation Laboratory, University of Notre Dame
Notre Dame, IN 46556
laverne.1@nd.edu

Program Scope

Aromatic compounds have long been thought to be radiation inert, but recent studies from our laboratories have shown that aromatic compounds can in fact undergo extensive radiolytic decomposition under certain conditions. [1-3] Our program seeks to understand the mechanism underlying how aromatic compounds decompose when exposed to radiation and to identify the final products formed. Characterization of the conditions under which aromatic compounds are likely to be sensitive to radiation is an important part of this effort. In addition, probes of what particular characteristic of an aromatic compound makes it susceptible to radiation damage are being explored. Such compounds are found throughout the DOE complex. They are vital components of resins used in radioactive waste separations and the polymers used in construction components and waste storage containers. Aromatic entities are found in many of the solvents used in extraction processes including the newer "designer solvents" made from ionic liquids. Many building blocks of cells including DNA contain aromatic components so this research is also important for radiation protection purposes. The research focuses on the radiation chemistry of a variety of aromatic liquids containing different heteroatoms or side chains. More complex aromatic compounds examined in this project include various polymers and resins. Molecular hydrogen production is the primary probe of radiation sensitivity, but a wide variety of spectroscopic and chromatographic techniques are also used. This effort differs substantially from the conventional radiation chemical approach in that heavy ion radiolysis makes up a substantial portion of the program.

Recent Progress

The program relies extensively on exploiting the detailed characteristics of the track structure of radiation to probe the mechanisms involved in the decomposition of organic liquids. Ionizing radiation deposits energy along its path in localized regions leading to a nonhomogeneous distribution of reactive species that constitutes the radiation track. The general effects of track structure on the radiolysis of materials in the condensed phase are reasonably well understood, especially in liquid water. [4] With increasing linear energy transfer (LET, equal to the stopping power, -dE/dx) the density of energy deposition becomes greater about the particle path. This increase in local energy density leads to higher concentrations of reactive species than are obtained using conventional fast electron or γ-radiolysis. Yields of products that are formed due to second order reactions will be enhanced with increasing LET while those due to first order processes will be unaffected. Therefore, the yield dependence on LET can be used as a convenient probe of mechanisms in radiolysis. These so-called track effects elucidate the dominant process from the many possible pathways for product formation in the radiolysis of organic compounds. Studies on benzene and its analogs found a substantial increase in the production of H_2 on increasing the LET of the incident radiation. [5,6] Organic radiolysis is primarily initiated by C-H bond breakage so the observation of H_2 implies that modification to the parent molecule must be occurring. However, until these studies were performed little information existed on the mechanism for H_2 formation.

The main products found in the radiolytic decomposition of simple aromatic

liquids are H_2 and the dimers or polymers from the parent molecule. However, these two products have very different dependences on LET, which suggests that the pathways to their formation are not common. Typical radical scavenging techniques show that the higher molecular weight product formation is consistent with simple C-H bond breakage followed by addition reactions. The mechanism for the production of H_2 remained elusive except that it was definitely due to a second order process. Additional studies using photon sources of various energies found that most of the H_2 is formed from highly excited states of the medium molecules. [3] Such a finding is contrary to contemporary thought that the lowest level excited states are responsible for radiolytic decomposition. The increase in local concentration of excited state species within the particle track is promoting a substantial amount of reaction between them before they normally decay to ground. The implication of this observation is that high energy states can undergo extensive chemistry, but that chemistry can be somewhat restricted because of the short lifetimes of these states. Heavy ion radiolysis, especially due to the alpha particles from radioactive waste decay, is common throughout the DOE complex and extensive decomposition of aromatic compounds can be expected in a variety of scenarios.

An effort was made to determine how an aromatic entity within a compound could control the overall radiolytic effect. This work proceeded by examining the decomposition of Amberlite, a strongly basic ion exchange resin used in the treatment of nuclear reactor cooling water. The resin is a quaternary ammonium salt on a cross-linked polystyrene backbone. The gamma radiolysis of Amberlite gives a very low yield of 0.07 molecules of H_2 per 100 eV of energy absorbed, but that yield increases substantially to 0.27 molecules/100 eV for 5 MeV He ions, chosen to represent alpha particles. Gamma radiolysis yield of H_2 from polyethylene, polystyrene, and benzene are 3.3, 0.03 and 0.04 molecules/100 eV, respectively. Clearly, the results are not averaged over the various components making up the molecules since one would expect the radiolytic yield of H_2 with polystyrene to be somewhere between that for polyethylene and benzene. Apparently, the presence of an aromatic entity completely dominates the radiolytic formation of H_2. The yields of H_2 formation from all of these compounds show the characteristic increase with increasing LET suggesting similar formation mechanisms. All resins and polymers examined to date show an increase in H_2 formation with increasing LET if the compound contains an aromatic component. Various yields are observed with gamma radiolysis depending on the relative aliphatic and aromatic makeup of the compound.

Future Plans

Much of the work on resins has been performed on the dry compounds in order to examine their fundamental decomposition mechanisms. Further studies will examine the influence of water associated with these compounds since almost all applications will involve an aqueous phase. In addition to the resins themselves, critical building blocks of each resin will be examined to determine if the aromatic entity always dominates radiolytic decomposition. Although the presence of an aromatic entity always leads to a low yield of H_2 in gamma radiolysis, there is little predictability of yields with aliphatic compounds and further studies will explore this problem.

The mechanism of H_2 formation in any aromatic compound is still in doubt. Higher energy light sources will be used to examine simple aromatic liquids to try to narrow down what states are responsible for H_2 production. Aliphatic compounds are known to have higher yields of H_2 than aromatic compounds so combinations of aromatic and aliphatic compounds will be examined. Simple mixtures such cyclohexane and benzene will be used to check the additivity of each component to H_2 production. Other studies will examine the variation of the side chains attached to a given aromatic compound, e.g. toluene, ethylbenzene, butylbenzene, etc.

References

(1) Roder, M. *Aromatic Hydrocarbons. In Radiation Chemistry of Hydrocarbons*; Elsevier: Amsterdam, 1981.
(2) La Verne, J. A.; Baidak, A. Track Effects in the Radiolysis of Aromatic Liquids. *Radiat. Phys. Chem.* **2012**, *81*, 1287-1290.
(3) Baidak, A.; Badali, M.; LaVerne, J. A. Role of the Low-energy Excited States in the Radiolysis of Aromatic Liquids. *J. Phys. Chem. A* **2011**, *115*, 7418-7427.
(4) LaVerne, J. A. Radiation Chemical Effects of Heavy Ions. In *Charged Particle and Photon Interactions with Matter*; Mozumder, A., Hatano, Y., Eds.; Marcel Dekker, Inc: New York, 2004; pp 403-429.
(5) Enomoto, K.; LaVerne, J. A.; Araos, M. S. Heavy Ion Radiolysis of Liquid Pyridine. *J. Phys. Chem. A* **2007**, *111*, 9-15.
(6) LaVerne, J. A.; Araos, M. S. Heavy Ion Radiolysis of Liquid Benzene. *J. Phys. Chem. A* **2002**, *106*, 11408-11413.

DOE Sponsored Publications in 20011-2013

Lousada, C. M.; La Verne, J. A.; Jonsson, M. Enhanced Hydrogen Formation During the Catalytic Decomposition of H_2O_2 on Metal Oxide Surfaces in the Presence of HO Radical Scavengers *Phys. Chem. Chem. Phys.* **2013**, *15*, 12674-12679.
El Omar, A. K.; Schmidhammer, U.; Balcerzyk, A.; La Verne, J. A.; Mostafavi, M. Spur Reactions Observed by Picosecond Pulse Radiolysis in Highly concentrated Bromide Aqueous Solutions. *J. Phys. Chem. A* **2013**, *117*, 2287-2293.
Dhiman, S.; La Verne, J. A. Radiolysis of Simple Quaternary Ammonium Salt Components of Amberlite Resin. *J. Nucl. Mater.* **2013**, *436*, 8-13.
Roth, O.; Dahlgren, B.; La Verne, J. A. Radiolysis of Water on ZrO_2 Nanoparticles. *J. Phys. Chem. C* **2012**, *116*, 17619-17624.
La Verne, J. A.; Baidak, A. Track Effects in the Radiolysis of Aromatic Liquids. *Radiat. Phys. Chem.* **2012**, *81*, 1287-1290.
Groenewold, G. S.; Elias, G.; Mincher, B. J.; Mezyk, S. P.; La Verne, J. A. Characterization of CMPO and its Radiolysis Products by Direct Infusion ESI-MS. *Talanta* **2012**, *99*, 909-917.
El Omar, A. K.; Schmidhammer, U.; Rousseau, B.; La Verne, J. A.; Mostafavi, M. Competition Reactions of $H2O^{\bullet+}$ Radical in Concentrated Cl^- Aqueous Solutions: Picosecond Pulse Radiolysis Study. *J. Phys. Chem. A* **2012**, *116*, 11509-11518.
Schmitt, C.; LaVerne, J. A.; Robertson, D.; Bowers, M.; Lu, W.; Collon, P. Target Dependence for Low-Z Ion Charge State Fractions *Nucl. Inst. Meth. Phys. Res. A* **2011**, *269*, 721-728.
Roth, O.; LaVerne, J. A. Effect of pH on H_2O_2 Production in the Radiolysis of Water. *J. Phys. Chem. A* **2011**, *115*, 700-708.
Roth, O.; Hiroki, A.; LaVerne, J. A. Effect of Al_2O_3 Nanoparticles on Radiolytic H_2O_2 Production in Water. *J. Phys. Chem. C* **2011**, *115*, 8144-8149.

LaVerne, J. A. Radiation Chemistry of Water with Ceramic Oxides. In *Charged Particle and Photon Interactions with Matter. Recent Advances, Applications, and Interfaces*; Hatano, Y., Katsumura, Y., Mozumder, A., Eds.; CRC Press, Taylor & Francis Group: Boca Raton, 2011; pp 425-444.

Balcerzyk, A.; LaVerne, J. A.; Mostafavi, M. Direct and Indirect Radiolytic Effects in Highly Concentrated Aqueous Solutions of Bromide. *J. Phys. Chem. A* **2011**, *115*, 4326-4333.

Baidak, A.; Badali, M.; LaVerne, J. A. Role of the Low-energy Excited States in the Radiolysis of Aromatic Liquids. *J. Phys. Chem. A* **2011**, *115*, 7418-7427.

Radiation Chemistry Underpinning Nuclear Power Generation

Jay A. LaVerne, David M. Bartels Daniel M. Chipman, Sylwia Ptasinska
Notre Dame Radiation Laboratory, University of Notre Dame, Notre Dame, IN 46556
laverne.1@nd.edu, bartels.5@nd.edu, chipman.1@nd.edu, ptasinska.1@nd.edu

Program Scope

The primary radiation chemical effects underlying a variety of applications in the field of nuclear energy are being investigated. The project builds on the NDRL strengths developed over many years in addressing fundamental radiation chemical topics by examining in detail a few specific challenges found in the field of nuclear power generation. Three broad areas are being addressed: reactor chemistry, fuel and waste processing, and waste storage that are linked by the common factor of the influence of interfaces. The focus of much of the research is water and aqueous media because of its ubiquitous nature throughout the nuclear industry. Important questions to be answered include how the radiolysis of water either modifies or is modified by a nearby interface. In reactor chemistry, specific topics to be addressed are rates of radical reactions at high temperature and the production and destruction of aqueous H_2O_2 at interfaces. The knowledge obtained aids in the management of existing reactors and in the development of next generation reactors. Specific topics investigated in separation systems include an examination of the stable products from various system components. Gas production in the radiolysis of resins, especially when associated with water, is being explored to aid in the management and development of waste separation streams. The third area of research focuses on the radiation chemistry associated with waste storage. This part examines the effects of water radiolysis on interfaces and the radiolysis of polymers used in waste storage. Both topics address the production of hazardous gases, which are especially important in the storage and transportation of waste in sealed containers.

Recent Progress and Future Plans

Hydrogen peroxide generation in the radiolysis of water is of grave concern to the nuclear power industry. This species is responsible for much of the radiation-induced corrosion of nuclear reactor components. The addition of H_2 is typically used to minimize H_2O_2 production by scavenging the OH radicals before they can combine to give H_2O_2. Reduction of H_2O_2 yields in this system is actually caused by a chain process that also involves H atoms. A reduction in the concentration of H atoms and OH radicals will lead to a cessation of the chain process with a corresponding loss in H_2O_2 protection. Radical concentrations may be lowered by an increase in LET (LET = linear energy transfer), which leads to a greater amount of radical combination reactions in the track. Experiments have shown that an LET of about 8 eV/nm corresponding to a 5 MeV proton is typically the breaking point. At lower proton energies the LET is sufficiently large that the escaping H atoms and OH radicals cannot sustain the chain process and the production of H_2O_2 increases with dose. However, dose rate can also affect the escape yields of radicals. This latter phenomenon is important because of the wide variation in dose rates from reactor cores to stored waste materials. High dose rates enhance radical combination reactions and can lower OH radical and H atom concentrations sufficiently to stop the chain process with added H_2. Accelerator based studies with 5 MeV protons did observe the dose rate effect; however, extremely high dose rates are necessary to sufficiently lower the radical yields and shut down the chain process. These dose rates will be obtained in reactor cores, but not in typical waste scenarios. Modeling studies will be included in this project to predict the onset of dose

effects and the expected outcomes. Almost all of the past studies have generally been in the low dose rate regime. Accelerator based electron radiolysis studies will be performed to push the upper limit on does rates. Further studies will also examine the role of interfaces on the production of H_2O_2 in water with added H_2.

Modeling of reactor core chemistry relies on accurate dosimetry and radiation yields (*G* values, or product amount/unit energy) to establish the boundary condition for kinetic modeling. Several years ago we participated in compilation of a review of the data that includes low-LET yields for gamma and electron radiolysis. In general, yields are a function of time after energy deposition due to recombination reactions. For the application to reactors, one wants to know the "escape" yields at very long (microsecond) time after all recombination has occurred. Unfortunately, most product yields are not measured under conditions of very low dose and scavenger concentration, which provide an accurate measure of the "escape" yields. Moreover, at elevated temperatures, the hydrated electron and H atom equilibrate on the same microsecond timescale as the spur recombination chemistry. The useful quantity is the sum of $G(H) + G(e^-_{aq})$. A project was carried out in the last year to provide these numbers for reactor conditions up to 350 °C. N_2O was used to scavenge hydrated electrons giving the N_2 product, which was determined by mass spectrometry.

$$e^-_{aq} + N_2O \rightarrow N_2 + O^- \quad (1)$$

The present series of measurements used 0.001 M KOH to convert the H atoms to e^-_{aq} and measure the sum of their yields.

$$H + OH^- \rightarrow H_2O + e^-_{aq} \quad (2)$$

To make a useful measurement with sufficient product, H_2O_2 production from OH radical recombination must be suppressed. Alcohols are unsuitable OH scavengers because the resulting reducing radicals reduce N_2O in a chain reaction at high temperature, giving excess N_2 product. Hydrocarbons in general are insufficiently soluble to scavenge the OH quickly enough. Acetate was chosen as a scavenger, which produces an oxidizing radical.

$$^{\bullet}OH + CH_3COO^-_{aq} \rightarrow H_2O + {}^{\bullet}CH_2COO^-_{aq} \quad (3)$$

The acetate radicals recombine to form malonate, which reacts much faster with H atom than acetate. The dose was carefully limited to avoid producing this product and avoid loss of H to other reaction channels. Preliminary results show rough agreement with the total yields from our review. The scatter in the measurement is unacceptably large, because the experiment was plagued by subtle drift of the accelerator focusing over the hours needed for the entire temperature series. A final run is in process of analysis.

As a cross-check of the 0.001 M hydroxide experiment, we also attempted a measurement of H_2 yield in slightly acidic (0.0001 M perchloric acid) THF solution. In this experiment, e^-_{aq} is converted to H atoms by the acid, and H atoms abstract hydrogen from THF giving H_2 product. Agreement with expectation is good up to 100 °C. At higher temperature a strong deviation from the expected trend is observed. Testing suggests that the THF must be unstable, probably producing an unsaturated product to which the H atoms "add". At higher temperature, the desired H abstraction may begin to win the competition for H atoms again, because of the

higher activation energy of this process. Systems suitable for scavenging H atoms at high temperature are being explored, which will then be followed up with measurements into the supercritical water regime.

Examination of polymeric materials has focused on polysiloxanes, which are proposed to be used to encase waste materials that cannot come into contact with metals. The simple polysiloxanes studied in this work contained methyl side chains with total molecular weights of 237, 1250, 14000 Da. These compounds are reasonable surrogates for the commercial silicones proposed for waste encapsulation. As expected with the abundant methyl groups, the main gaseous product is methane with a measured yield of about 1.8 molecules/100 eV which is nearly independent of polymer molecular weight. Molecular hydrogen is formed with about half the yield of that for methane. Both gaseous product yields are considerably reduced with the presence of air, presumably by scavenging of H atom precursors by the O_2. Commercial polysiloxanes have a variety of additives that greatly increases molecular hydrogen formation. FTIR studies show that gas production is associated with changes in the Si-O bonds. No new Si-Si bonds were formed indicating that crosslinking does not occur by this mechanism. Thermal gravimetric analysis, TGA, shows almost complete dissociation of the lower molecular weight polysiloxanes with some residual inert product formation with the higher molecular weight polymers. Radiolysis seems to form more of the inert material, which is presumably a highly cross linked compound. Future studies will examine different types of polysiloxanes and to identify the differences between the pure materials and commercial compounds.

Resins are used for separations and filtering throughout the nuclear power industry and their radiolytic decay is important for proper maintenance. An extensive examination of the H_2 production from amberlite resin was undertaken. The radiolytic response of resins to high LET radiation was observed to be very similar to that for simple organic liquids. Resins with an aromatic component like amberlite exhibit a large increase in H_2 yield with increasing LET. The first step to understand the underlying mechanism was to examine H_2 production from dry components of the amberlite resin. This research gives a good indication of the radiolytic response due to direct radiolysis of the resin. Resin decomposition in association with water may also occur by indirect processes due to reactions with water decomposition products. The radiolysis of various dry components of the amberlite resin shows that the presence of an aromatic entity in the compound completely dominates the radiolytic response. For instance, the H_2 yields are very nearly the same for amberlite as well as for its components: benzene, polystyrene, and benzyl trimethylamine. On the other hand, the H_2 yield from trimethylamine is almost two orders of magnitude greater that for these compounds. The results show how dominant the aromatic ring is in controlling the radiolytic H_2 yield. Several complementary studies on the radiolysis of dry amines show that the initial step in the formation of hydrogen is the breaking of the N-H bond followed by H atom abstraction. The significance of this process in the decomposition of amberlite is still being assessed. The next step will be to examine resins in the presence with various amounts of water as will typically be encountered in realistic scenarios.

Publications with BES support since 2011

Baidak, A.; Badali, M.; LaVerne, J. A. Role of the Low-energy Excited States in the Radiolysis of Aromatic Liquids. *J. Phys. Chem. A* **2011**, *115*, 7418-7427.

Balcerzyk, A.; LaVerne, J. A.; Mostafavi, M. Direct and Indirect Radiolytic Effects in Highly Concentrated Aqueous Solutions of Bromide. *J. Phys. Chem. A* **2011**, *115*, 4326-4333.

LaVerne, J. A. Radiation Chemistry of Water with Ceramic Oxides. In *Charged Particle and Photon Interactions with Matter. Recent Advances, Applications, and Interfaces*; Hatano, Y., Katsumura, Y., Mozumder, A., Eds.; CRC Press, Taylor & Francis Group: Boca Raton, 2011; pp 425-444.

Roth, O.; Hiroki, A.; LaVerne, J. A. Effect of Al_2O_3 Nanoparticles on Radiolytic H_2O_2 Production in Water. *J. Phys. Chem. C* **2011**, *115*, 8144-8149.

Roth, O.; LaVerne, J. A. Effect of pH on H_2O_2 Production in the Radiolysis of Water. *J. Phys. Chem. A* **2011**, *115*, 700-708.

Schmitt, C.; LaVerne, J. A.; Robertson, D.; Bowers, M.; Lu, W.; Collon, P. Target Dependence for Low-Z Ion Charge State Fractions *Nucl. Inst. Meth. Phys. Res. A* **2011**, *269*, 721-728.

Bartels, D. M.; Wu, W.; Kanjana, K.; Sims, H. E.; Henshaw, J. Laboratory and modeling studies in search of the critical hydrogen concentration. In *NPC2012 Proceedings*, 2012; pp 11p.

El Omar, A. K.; Schmidhammer, U.; Rousseau, B.; La Verne, J. A.; Mostafavi, M. Competition Reactions of $H_2O^{\bullet+}$ Radical in Concentrated Cl^- Aqueous Solutions: Picosecond Pulse Radiolysis Study. *J. Phys. Chem. A* **2012**, *116*, 11509-11518.

Groenewold, G. S.; Elias, G.; Mincher, B. J.; Mezyk, S. P.; La Verne, J. A. Characterization of CMPO and its Radiolysis Products by Direct Infusion ESI-MS. *Talanta* **2012**, *99*, 909-917.

La Verne, J. A.; Baidak, A. Track Effects in the Radiolysis of Aromatic Liquids. *Radiat. Phys. Chem.* **2012**, *81*, 1287-1290.

Roth, O.; Dahlgren, B.; La Verne, J. A. Radiolysis of Water on ZrO_2 Nanoparticles. *J. Phys. Chem. C* **2012**, *116*, 17619-17624.

Kanjana, K.; Haygarth, K. S.; Wu, W.; Bartels, D. M. Laboratory studies in search of the critical hydrogen concentration. *Radiat. Phys. Chem.* **2013**, *82*, 25-34.

Bartels, D. M.; Henshaw, J.; Sims, H. E. Modelling the critical hydrogen concentration in the AECL test reactor. *Radiat Phys. Chem.* **2013**, *82*, 16-24.

Dhiman, S.; La Verne, J. A. Radiolysis of Simple Quaternary Ammonium Salt Components of Amberlite Resin. *J. Nucl. Mater.* **2013**, *436*, 8-13.

Dhiman, S. B.; Goff, G. S.; Runde, W.; La Verne, J. A. Hydrogen Production in Aromatic and Aliphatic Ionic Liquids. *J. Phys. Chem. B* **2013**, *117*, 6782-6788.

El Omar, A. K.; Schmidhammer, U.; Balcerzyk, A.; La Verne, J. A.; Mostafavi, M. Spur Reactions Observed by Picosecond Pulse Radiolysis in Highly concentrated Bromide Aqueous Solutions. *J. Phys. Chem. A* **2013**, *117*, 2287-2293.

Lousada, C. M.; La Verne, J. A.; Jonsson, M. Enhanced Hydrogen Formation During the Catalytic Decomposition of H_2O_2 on Metal Oxide Surfaces in the Presence of HO Radical Scavengers *Phys. Chem. Chem. Phys.* **2013**, *15*, 12674-12679.

Single-Molecule Interfacial Electron Transfer

H. Peter Lu
Bowling Green State University
Department of Chemistry and Center for Photochemical Sciences
Bowling Green, OH 43403
hplu@bgsu.edu

Program Scope

We apply single-molecule high spatial and temporal resolved techniques to study molecular dynamics in condensed phase and at interfaces, especially, the complex reaction dynamics associated with electron and energy transfer rate processes. The complexity and inhomogeneity of the interfacial ET dynamics often present a major challenge for a molecular level comprehension of the intrinsically complex systems, which calls for both higher spatial and temporal resolutions at ultimate single-molecule and single-particle sensitivities. Combined single-molecule spectroscopy and atomic force microscopy (AFM) approaches are unique for heterogeneous and complex interfacial electron transfer systems because the static and dynamic inhomogeneities can be identified and characterized by studying one molecule at a specific nanoscale surface site at a time. Single-molecule spectroscopy reveals statistical distributions correlated with microscopic parameters and their fluctuations, which are often hidden in ensemble-averaged measurements. The goal of our project is to integrate and apply these spectroscopic imaging and topographic scanning techniques to measure the energy flow and electron flow between molecules and substrate surfaces as a function of surface site geometry and molecular structure. We have been primarily focusing on studying interfacial electron transfer under ambient condition and electrolyte solution involving both single crystal and colloidal TiO_2 and related substrates. The resulting molecular level understanding of the fundamental interfacial electron transfer processes will be important for developing efficient light harvesting systems and broadly applicable to problems in fundamental chemistry and physics.

Recent Progress

Probing Electric Field Effect on Covalent Interactions at a Molecule-TiO_2 Interface. Fundamental understanding of the energetic coupling properties of the molecule-semiconductor interface is of great importance. In this project, we have probed the change in the interface properties of alizarin-TiO_2 system as a result of the externally applied electric field by using single-nanospot microscopic surface-enhanced Raman spectroscopy (Figure 1), and we have also provided a theoretical model analysis of our experimental results by *ab initio* calculations (Figure 2). The energetic perturbation on the interfacial coupling chemical bonds, caused by the external potential, has been observed as a shift and two-peak occurrence at 648 cm^{-1} Raman peak, typical indicator of the strong coupling between alizarin and TiO_2. On the basis of our experimental results and supporting *ab initio* calculations, we suggest that the electric field has significant effects on vibrational coupling at the molecule-TiO_2 interface. This vibrational energy change plays a critical role in interfacial electron transfer process, which is crucial for interfacial electron transfer dynamics and mechanisms.

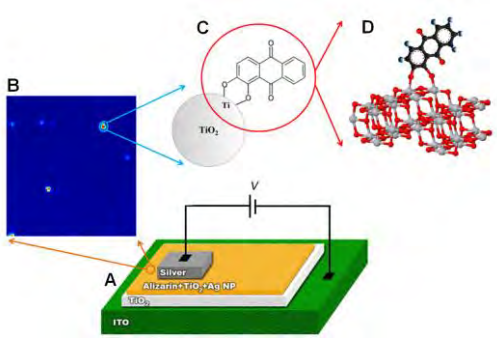

Figure 1. (A) Schematic representation of the experimental set-up. (B) Optical imaging of the sample surface (20 µm x 20 µm). (C) Schematic representation of the alizarin-TiO_2 system. (D) Crystal structure of alizarin on anatase TiO_2 surface (red - oxygen, grey - titanium, dark grey - carbon, and blue - hydrogen). During our potential measurements, it has been assumed that all layers experience the applied potential without any losses from layer to layer.

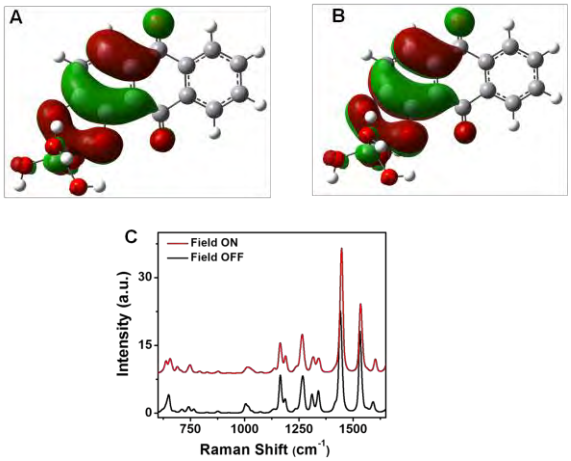

Figure 2. DFT calculations of alizarin-TiO_2 system (A) in the absence and (B) in the presence of potential and (C) calculated Raman spectra of corresponding structures.

Probing Ultrafast Interfacial Electron Transfer (ET) Dynamics by Combined Single-Molecule Photon-Stamping Spectroscopy and Femtosecond Transient Absorption Spectroscopy. Single-molecule spectroscopy and ensemble-averaged transient absorption measurements provide powerful "zoom-in" and "zoom-out" views of the interfacial ET dynamics. We have used the combined approach to study the interfacial forward and backward electron transfer (FET and BET) dynamics in the PF/TiO_2 system (9-phenyl-2,3,7-trihydroxy-6-fluorone: PF). The ultrafast ET processes deduced from the ensemble transient femtosecond absorption spectroscopy are precisely projected to a wide time window revealed by our single-molecule lifetime measurements. In the PF/TiO_2 system, the ET rate is dominated by the electronic coupling between PF and TiO_2, and the ultrafast FET corresponding to the strong coupling can be observed from ensemble transient absorption dynamics, and the relatively slower FET corresponding to the relatively weaker coupling can be demonstrated by single molecule fluorescence photon-stamping measurements. Based on the biexponential characteristics of the BET dynamics and the deduced two typical charge recombination processes, we propose a model consisting of two different interfacial ET channels to characterize the FET and BET reactions in the ET dynamics of the PF/TiO_2 system involving in both strong coupling and weak coupling. In the strong coupled state, under photon excitation, the electron

state of PF-TiO_2 is directly transferred into $PF^{\delta+}$-$TiO_2^{\delta-}$ charge separation state within 0.4 ps, which is similar to the intra-molecular forward electron transfer such as a charge separation in MLCT (metal to ligand charge transfer) processes. The 3.0 ps charge recombination time was obtained from the recovery of ground state bleaching and the decay of charge separation state. At single molecule level, the location of charge transfer state, charge transfer rate and charge recombination rate are inhomogeneous. In the weak coupled PF/TiO_2 system, the electron of PF is injected into the conduction band or energetically accessible surface state via its excited singlet state of PF. This forward electron injection takes picoseconds to nanoseconds time scale, depending upon the interaction of individual PF/TiO_2 events in which the excited state of PF. After injection, the electron presumably undergoes trapping and de-trapping, and non-Brownian motions or scattering in TiO_2 NP and then recombines with the cation $PF^{\delta+}$. The BET process takes tens of nanoseconds or up to sub-microseconds, which is demonstrated by our transient absorption spectroscopy.

Site-Specific Characterization of the Surface States involving in Interfacial Electron Transfer Rate Processes. Surface states play important roles in interfacial electron transfer process, regulating both the energetics and dynamics. The density and energy distributions of the associated surface states are often the critical parameters that affect the charge transfer pathways. Using an alizarin/TiO_2 interfaicial electron transfer system, a typical model system with strong electronic coupling, we have probed these parameters of the surface states. In this experiment, we used confocal and tip-enhanced high-resolution near-field luminescence and Raman imaging spectroscopy to analyze the interfacial charge transfer energetics down to the single site and single-molecule level, well beyond the spatial resolution of the optical diffraction limit. With laser excitation, electrons at the valence band can be excited to higher energy states, for example, trap states below the conduction band. Our results suggest that the single surface states are originated from the bridging oxygen vacancies. The physical nature of surface states has been attributed to bridging oxygen vacancies or interstitial Ti-atoms. We suggest that the single surface states revealed by our nanoscale imaging are originated from the bridging oxygen vacancies, which can be deduced from the donut-shape optical patterns under radial polarized mode laser excitation because only for quantum systems with a two dimensional transition dipole moment can give circular optical patterns. On the basis of a quantum-chemical calculation, O-vacancy formation in rutile Ti(110) surface results in two excess electrons occupying 3d orbitals on Ti atoms neighboring the vacancy, which can be identified and analyzed from the near-field optical imaging in our measurements.

Understanding single-molecule interfacial geminate electron-cation recombination dynamics. We have probe and analysed the interfacial electron-cation recombination in zinc-tetra (4-carboxyphenyl) porphyrin (ZnTCPP)/TiO_2 system by recording and analyzing photon-to-photon pair times of the ZnTCPP fluorescence. We have developed a novel approach to reveal the hidden single-molecule interfacial electron-cation recombination dynamics by analyzing the autocorrelation function and a proposed convoluted single-molecule interfacial electron-cation recombination model. Using our unique approach, we have probed and analyzed the single-molecule interfacial electron-cation recombination dynamics at a precise photon-to-photon pair time scale of sub-ms to □s time scales by single-molecule photo-stamping spectroscopy. The autocorrelated photon-to-photon pair times of an ET-active state, which conceals the real-time characteristics of the interfacial electron-cation recombination dynamics, has been revealed and applied to probe the BET dynamics of ZnTCPP/TiO_2 system. Based on a convoluted interfacial electron-cation recombination model, the BET time is deduced to be on a 10^{-5} s time scale, which is consistent with the ensemble-averaged measurements which demonstrate the BET time ranging from sub-nanosecond to millisecond time scale. Our approach not only can effectively probe the single-molecule interfacial electron-cation dynamics, but also can be applied to other single-molecule ground state regeneration dynamics at interfaces and in condensed phases. We are currently using a novel correlated electrochemical AFM tip scanning correlated single-molecule photon stamping spectroscopy analysis to investigate the

nature of molecule chemical interaction at the dye/TiO2 interface with single-molecule sensitivity and site specificity.

Future Research Plans

Interfacial ET dynamics strongly involves with and regulated by molecule-surface interactions. To decipher the underlying mechanism of the complex and inhomogeneous interfacial electron transfer dynamics, we plan to study interfacial electron transfer on single crystal TiO_2 surfaces by using ultrafast single-molecule spectroscopy and electrochemical AFM metal tip scanning microscopy. Our study will focus on understanding the interfacial electron transfer dynamics at specific crystal sites with high-spatially and temporally resolved topographic/spectroscopic characterization at individual molecule basis, characterizing single-molecule rate processes, reaction driving force, and molecule-substrate electronic coupling. One of the most significant characteristics of our approach is that we will interrogate the complex interfacial electron transfer dynamics by actively pin-point energetic manipulation of the surface interaction and electronic couplings, beyond the conventional excitation and observation. Our effort will also be focused on understanding the TiO_2 electron trap centers and surface states.

Publications of DOE sponsored research (FY2010-2013)

1. Papatya C. Sevinc, Yuanmin Wang, H. Peter Lu, "Probing Electric Field Effect on Covalent Interactions at a Molecule-Semiconductor Interface," submitted (2013).

2. X. Wang, D. Zhang, Y. Wang, P. Sevinc, H. Peter, Lu, A. J. Meixner, "Interfacial Electron Transfer Energetics Studied by High Spatial Resolution Tip-Enhanced Raman Spectroscopic Imaging," *Angewandte Chemie International Edition* **50**, (2011) A25-A29.

3. Yuanmin Wang, Papatya C. Sevinc, Yufan He, H. Peter Lu, "Probing Ground-State Single-Electron Self-Exchange Across a Molecule-Metal Interface," *J. Am. Chem. Soc.,* **133**, 6989-6996 (2011).

4. Sevinc, Papatya; Wang, Xiao; Wang, Yuanmin; Zhang, Dai; Meixner, Alfred; Lu, H. Peter, "Simultaneous Spectroscopic and Topographic Near-Field Imaging of TiO_2 Single Surface States and Interfacial Electronic Coupling," *Nano Letter*, **11**, 1490-1494 (2011).

5. H. Peter Lu, "Acquiring a Nano-View of Single Molecules in Actions," *Nano Reviews* **1**, 6-7 (2010).

6. Guo, Lijun; Wang, Yuanmin; Lu, H. Peter, "Combined Single-Molecule Photon-Stamping Spectroscopy and Femtosecond Transient Absorption Spectroscopy Studies of Interfacial Electron Transfer Dynamics," *J. Am. Chem. Soc.* **132**, 1999-2004 (2010) (Cover page).

Solution Reactivity and Mechanisms through Pulse Radiolysis

Sergei V. Lymar
Chemistry Department, Brookhaven National Laboratory, Upton, NY 11973-5000
e-mail: lymar@bnl.gov

Program Scope

This program applies pulse radiolysis for investigating reactive intermediates and inorganic reaction mechanisms. The specific systems are selected based on their fundamental significance or importance in energy and environmental problems.

The first project investigates physical chemistry of nitrogen oxides and their congeneric oxoacids and oxoanions. They play an essential role in environmental chemistry, particularly in the terrestrial nitrogen cycle, pollution, bioremediation, and ozone depletion. Nitrogen-oxygen intermediates are also central to the radiation-induced reactions that occur in nuclear fuel processing and within attendant nuclear waste. Redox and radical chemistry of the nitrate/nitrite system mediates the most of radiation-induced transformations in these environments. Equally important are the biological roles of nitrogen oxides. We apply time-resolved techniques for elucidation of the prospective reactions in terms of their thermodynamics, rates and mechanisms, focusing on the positive nitrogen oxidation states, whose chemistry is of the greatest current interest. The meeting presentation will be focused mainly on new results from this project.

The goal of the second project is to gain mechanistic insight into water oxidation catalysis through characterization of the catalyst transients involved in the catalytic cycle. Development of catalysts to carry out the four-electron water oxidation remains the greatest challenge in the solar energy utilization. Growing recent interest in this field has triggered the discovery of a wide variety of catalytic systems, both molecular and heterogeneous, but the reaction mechanisms remain to be established. The major impediment has been the difficulties in identification and characterization of the reaction intermediates. In this project, we use radiolysis techniques to generate and characterize the redox states of the catalyst involved in water oxidation.

Collaborators on these projects include M. Valiev (PNNL),[1-2] Shafirovich (NYU),[2-3] J. Hurst (WSU),[4-6] D. Polyansky (BNL),[4] and H. Schwarz (BNL, emeritus).[7]

Progress

Reductive chemistry of NO. Rapid one-electron reduction of NO is most readily accomplished through pulse radiolysis whereby the hydrated electron reacts with NO producing the nitroxyl anion ($^3NO^-$) in its triplet ground state. In contrast, the radiolytically-generated hydrogen atom adds to NO producing nitroxyl (^1HNO), whose ground state is singlet. Undoubtedly, $^3NO^-$ and ^1HNO are major species that mediate the radiation-induced transformations in nuclear fuel processing and in nuclear wastes, as evidenced by NO and N_2O emission by Hanford waste storage tanks. In our previous work, we have elucidated these processes and ensuing chemistry as shown to the right.[8] Salient features of this mechanism are the extremely slow spin-forbidden $^3NO^-$-^1HNO acid-base equilibration and the vastly different reactivities of $^3NO^-$ and ^1HNO toward hemicolligation with NO.

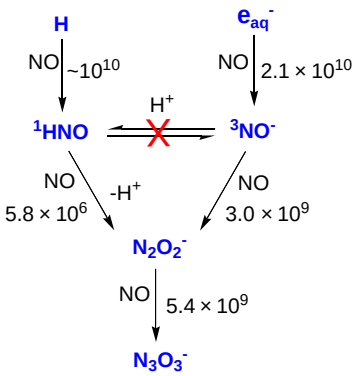

In search for other methods of nitroxyl generation, we have recently examined NO reactivity toward the strongly reducing C-centered radicals, $(CH_3)_2{}^{\bullet}COH$ and $^{\bullet}CO_2^-$. While NO reacts with the former radical through simple addition making the 2-nitroso-2-propanol product, the $^{\bullet}CO_2^-$ radical does reduce NO. Surprisingly however, the reduction product is not the expected $^3NO^-$ but the protonated ^1HNO species. This result unambiguously indicated the involvement of the solvent water molecule, and the two plausible reaction pathways are shown below. The addition pathway consists of the recombination of NO and $^{\bullet}CO_2^-$ radicals with the attendant formation of the nitroso-carboxyl adduct whose rapid hydrolysis results in the ^1HNO final product. The alternative pathway involves an electron transfer with the formation of NO^- in its singlet excited state, which is a very strong base and undergoes rapid protonation by H_2O. Experiments toward distinguishing between these pathways are currently under way.

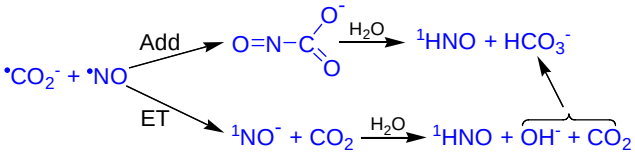

Although energetics of the nitroxyl species is germane for evaluating their reactivity, literature energy estimates involve significant, questionable assumptions.[9-13] The most important poorly known quantity is $\Delta_{form}G^0(^3NO^-)$, that defines the reduction potentials for NO. In order to evaluate this potential, we have investigated the redox equilibrium between $^3NO^-$ and a low potential bipyridinium derivative: $NO+TQ^{\bullet+} \underset{k_r}{\overset{k_f}{\rightleftharpoons}} {}^3NO^- + TQ^{2+}$, where TQ^{2+} stands for tetraquat that has $E^0(TQ^{2+}/TQ^{\bullet+})$ = -0.65 V vs NHE and is optically detectable in its radical cationic form. Forward and reverse rate constants have been measured through pulse radiolysis and flash photolysis, respectively, and the equilibrium constant $K_{eq} = k_f/k_r$ gives the first direct determination of $E^0(NO/^3NO^-)$ = -(0.85 ± 0.05) V.

Our computations at CCSD(T) theory level combined with COSMO approach for the evaluation of hydration energies reveals the highly unusual manifold of nitroxyl species spin states that is diagramed to the right. The diagram shows the existence of the higher energy tautomer of protonated NO^- with triplet ground state (^3NOH) and is drawn to scale using the relative computed energies for $^1HNO/^3HNO$ and $^3NOH/^1NOH$, the above described $E^0(NO/^3NO^-)$, and the previously estimated $\Delta_{form}G^0(^1HNO)$.[10] The pattern of energy levels engenders an expectation of the unique acid-base chemistry, which we have indeed observed in the nitroxyl species production through the photochemical decomposition of trioxodinitrate($N_2O_3^{2-}/HN_2O_3^-$), as shown in the scheme below.

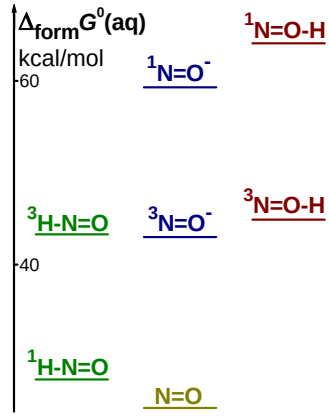

In variance with the long-held belief,[14] our CCSD(T)/COSMO computations clearly show that protonation of $N_2O_3^{2-}$ occurs on the lone terminal oxygen atom and not on the neighboring nitrogen atom. These finding has important implications for understanding our flash UV laser photolysis data. Counterintuitively, we find that only protonated ^1HNO nitroxyl species is produced from the fully deprotonated $N_2O_3^{2-}$ anion and observe a considerable amount of deprotonated $^3NO^-$

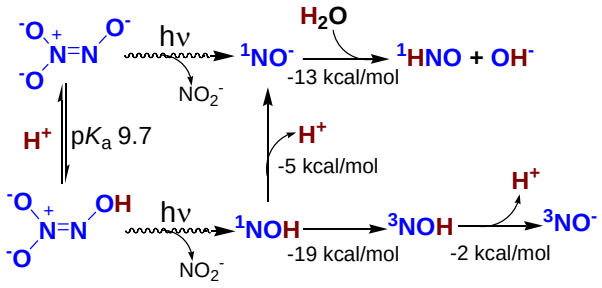

product from fully protonated $HN_2O_3^-$; in this case decomposition bifurcates between $^3NO^-$ and ^1HNO products. The most plausible interpretation of these findings is shown in the scheme above and involves a number of rapid, energetically favorable acid-base reactions along with the $^1HNO \rightarrow {}^3HNO$ intersystem crossing.

Intermediates in water oxidation catalysis. Research from several laboratories, have established that water oxidation catalysis by the *cis,cis*-$[(bpy)_2(H_2O)Ru\text{-}O\text{-}Ru(OH_2)(bpy)_2]^{4+}$ (known as the *blue dimer* **{3,3}**, whose structure is shown to the left and the numbers in parenthesis indicate oxidation states of the Ru atoms) involves its progressive oxidation with the attendant loss of protons to the ruthenyl **{5,5}** dimer.[15-17] Pulse radiolysis has figured prominently in two aspects of these studies, namely (1) the assignment of intermediary oxidation states formed upon sequential one-electron oxidation of the dimer[5] and (2) the potential role of bipyridine as a non-innocent ligand (a ligand that directly participate in the catalyst oxidation with the formation of the ligand-localized radical state) in the O_2-forming catalytic cycle.[16]

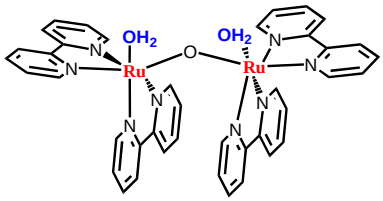

To gain insight into this latter process, we have investigated the reaction dynamics of $OH^\bullet$ with the blue dimer in its stable **{3,3}** and **{3,4}** oxidation states. Our pulse radiolysis data indicate that in both cases $OH^\bullet$ attack on the catalyst's aromatic ligands results in the diffusion-controlled formation of the OH-adducts. However, further transformations of these adducts depend on the Ru atom oxidation states; while the **{3,3}**-OH adduct expels OH^- and the net result is oxidation of **{3,3}** to **{3,4}**, the net result of the $OH^\bullet$ + **{3,4}** reaction is *reduction* of **{3,4}** to **{3,3}**. Although the reduction process is complex; is not yet completely understood, and will be studied in the future work, our observations strongly indicate that the catalyst in the **{4,4}** and higher states are susceptible to nucleophilic attack by H_2O or OH^-.

We have discovered that at high concentrations, the nitrate ion alters the dynamics of ruthenium "blue dimer"-catalyzed water oxidation by Ce^{4+} such that the oxidation rate is enhanced and a unique reaction intermediate accumulates.[6] This intermediate exhibits anomalous EPR and optical spectra, and new oxygen isotope-sensitive Raman band. Collectively, the data suggest that Ce – nitrate complexes are the causative agents. Use of ^{18}O-labeled and ^{15}N-labeled materials has established that: (i) the new Raman band involves the O atom coordinated to a Ru center; (ii) the O_2 product does not contain an O atom derived from nitrate, eliminating several pathways involving direct O-atom transfer to oxidized dimer. Although these results are surprising, similar phenomena have been reported for monomeric Ru complexes. The dramatic effects observed for the "blue dimer" make it an ideal candidate for further study.

Recently, we have demonstrated that a pH-controlled deposition of Co(II) on silica nanoparticles affords a novel, purely inorganic, and stable water oxidation catalyst.[3] The lower limit for the catalyst turnover frequency in oxygen evolution of ~300 s^{-1} attests to a very high catalytic activity. This catalyst is optically transparent in the entire UV-vis range and is thus suitable for mechanistic studies by time-resolved spectroscopic techniques that are planned.

Planned work will investigate:

- New pathways for generating nitroxyl species and their reactivity, including rate and mechanism of their self-decay.
- Spin-forbidden ground state bond breaking/making reactions involving $^1HNO/^3NO^-$.
- Thermodynamics of photochemical and spontaneous generation of $^1HNO/^3NO^-$ from trioxodinitrate ($HN_2O_3^-/N_2O_3^{2-}$).

- Redox and radical chemistry in the nitrite/nitrate system, including: formation pathways and thermodynamics of nitrate radical anion ($NO_3^{\bullet 2-}$); rates and mechanisms of its acid-catalyzed and redox reactions.
- Nature of catalyst states involved in water oxidation by the ruthenium "blue dimer", including reduction potential and decay mechanism for the Ru^{IV}-Ru^{IV} state and accessing Ru^{IV}-Ru^{V} and Ru^{V}-Ru^{V} states.
- Mechanistic studies of radiation-induced radical and redox reactions on solid/liquid interfaces. We will begin with the cobalt/silica system that represents a very efficient water oxidation catalyst and is of great current interest.

References (DOE sponsored publications in 2010-present are marked with asterisk)

(1*)Valiev, M.; Lymar, S. V. "Structural and Mechanistic Analysis through Electronic Spectra: Aqueous Hyponitrite Radical ($N_2O_2^-$) and Nitrosyl Hyponitrite Anion ($N_3O_3^-$),"*J. Phys. Chem. A* **2011**, *115*, 12004-12010.
(2*)Shaikh, N.; Shafirovich, V.; Valiev, M.; Lymar, S. V. "Decomposition of Amino Diazeniumdiolates (NONOates): Molecular Mechanisms," *J. Inorg. Biochem.*, (under revision).
(3*)Zidki, T.; Zhang, L.; Shafirovich, V.; Lymar, S. V. "Water Oxidation Catalyzed by Cobalt(II) Adsorbed on Silica Nanoparticles," *J. Am. Chem. Soc.* **2012**, *134*, 14275-14278.
(4*)Polyanskiy, D. E.; Hurst, J. K.; Lymar, S. V. "Application of Pulse Radiolysis to Mechanistic Investigations of Water Oxidation Catalysis," *Eur. J. Inorg. Chem.*, (in press).
(5)Cape, J. L.; Lymar, S. V.; Lightbody, T.; Hurst, J. K. *Inorg. Chem.* **2009**, *48*, 4400-4410.
(6*)Stull, J. A.; Britt, R. D.; McHale, J. L.; Knorr, F. J.; Lymar, S. V.; Hurst, J. K. "Anomalous Reactivity of Ceric Nitrate in Ruthenium "Blue Dimer"-Catalyzed Water Oxidation," *J. Am. Chem. Soc.* **2012**, *134*, 19973-19976.
(7*)Lymar, S. V.; Schwarz, H. A. "Hydrogen Atom Reactivity toward Aqueous *tert*-Butyl Alcohol," *J. Phys. Chem. A* **2012**, *116*, 1383-11389.
(8)Lymar, S. V.; Shafirovich, V.; Poskrebyshev, G. A. *Inorg. Chem.* **2005**, *44*, 5212-5221.
(9)Bartberger, M. D.; Fukuto, J. M.; Houk, K. N. *Proc. Natl. Acad. Sci. USA* **2001**, *98*, 2194-2198.
(10)Shafirovich, V.; Lymar, S. V. *Proc. Natl. Acad. Sci. USA* **2002**, *99*, 7340-7345.
(11)Bartberger, M. D.; Liu, W.; Ford, E.; Miranda, K. M.; Switzer, C.; Fukuto, J. M.; Farmer, P. J.; Wink, D. A.; Houk, K. N. *Proc. Natl. Acad. Sci. USA* **2002**, *99*, 10958-10963.
(12)Dutton, A. S.; Fukuto, J. M.; Houk, K. N. *Inorg. Chem.* **2005**, *44*, 7687-7688.
(13)Tossell, J. A. *Geochim. Cosmochim. Acta* **2005**, *69*, 5647-5658.
(14)Bonner, F. T.; Hughes, M. N. *Comments Inorg. Chem.* **1988**, *7*, 215-234.
(15)Meyer, T. J.; Huynh, M. H. V. *Inorg. Chem.* **2003**, *42*, 8140-8160.
(16)Hurst, J. K. *Coord. Chem. Rev.* **2005**, *249*, 313-328.
(17)Liu, F.; Concepcion, J. J.; Jurss, J. W.; Cardolaccia, T.; Templeton, J. L.; Meyer, T. J. *Inorg. Chem.* **2008**, *47*, 1727-1752.

Geminate Recombination in Tetrahydrofuran

Principal Investigators: John R. Miller and Andrew R. Cook

Department of Chemistry, Brookhaven National Laboratory, Upton, NY, 11973 USA

jrmiller@bnl.gov, acook@bnl.gov

Program Scope:

This program applies both photoexcitation and ionization by short pulses of fast electrons to investigate fundamental chemical problems relevant to the production and efficient use of energy and thus obtain unique insights not attainable with other techniques. These studies may play an important role in the development of safer, more effective, and environmentally beneficial processes for the chemical conversion of solar energy. Picosecond pulse radiolysis is employed to generate and study reactive chemical intermediates or other non-equilibrium states of matter in ways that are complementary to photolysis and electrochemistry and often uniquely accessible by radiolysis. This program also develops new tools for such investigations, applies them to chemical questions, and makes them available to the research community. Advanced experimental capabilities, such as Optical Fiber Single-Shot detection system, allow us to work on fascinating systems with 5-10 ps time-resolution that were previously prohibitive for technical reasons.

Recent Progress:

Charge recombination in THF: different fates for conjugated molecules.

Ionization of THF, one of the best solvents for conjugated polymers, produces free ions, which move independently of each other, and a somewhat larger amount of geminate (or spur) ions consisting of electrons and holes that are separated by 1-7 nm, but are bound by their mutual Coulomb attraction. When THF was used in past work to investigate electron transfer and the Marcus theory, the geminate ion-pairs presented only a minor problem because they annihilate upon recombination. Electrons in long conjugated molecules behave differently. Geminate recombination of positive and negative charge carriers was observed in THF. Pulse radiolysis gives rapid creation of solvated protons (RH_2^+) and anions ($M^{\bullet -}$) in THF. These were expected to recombine by diffusion within their mutual Coulomb potential. Such annihilations of the carriers are due to proton transfer(PT) from the donor, RH_2^+, to the acceptor, $M^{\bullet -}$.

In 1938, Onsager applied the Debye-Smoluchowski (DS) equation to the case in which positive ions and negative ions annihilate upon contact (infinite annihilation rate: ion annihilation is diffusion-controlled). He discussed ion recombination under influence of Coulomb potential, predicted the free ion yield (F_h) as a function of initial separation distance, and defined a critical radius (r_c), now often called the Onsager radius, at which the attractive Coulomb potential energy, $V(r_c)$, equals thermal energy, $V(r_c)=k_BT$. An ion thermalized at r_c from its geminate counter ion has a 50% probability to escape to become free ion and a 50% probability to escape. For the primary ion pairs, the probabilities of escape and recombination change with the initial distance. We will refer

to the free ion yield arising from escape by diffusion from their initial separation distances as the Type I free ion yield (F_h^I). Rice, Flannery, Hong, and Noolandi, extended Onsager's work to solve the DS equation for the case in which the rate of annihilation was not infinite, and suggested that an additional contribution to F_h could arise from ion-pairs that escape after coming together. We will refer this additional contribution as the Type II free ion yield (F_h^{II}).

The data indicate the two step nature of the recombination: Coulomb driven formation of ion pairs followed by proton transfer. With large driving force (ΔG^0=-0.3 to -1.6 eV) for PT reaction, some of ion pairs react rapidly ($k_{MPT} > 10^9\ s^{-1}$) but others react more slowly. For 17 molecules studied the amplitude of the long-lived homogenous (free) ion yield is constant at 0.356±0.03 of the total regardless of k_{MPT}, indicating no geminate ions escape to become free ions. For anions of oligo(9,9-dihexyl)fluorenes, $F_n^{\bullet-}$ (n=2-4), some of $F_n^{\bullet-}$ (n=2-4) do escape to become free ions. This escape suggests the ion's charge distribution is crucial for an ion to survive geminate recombination.

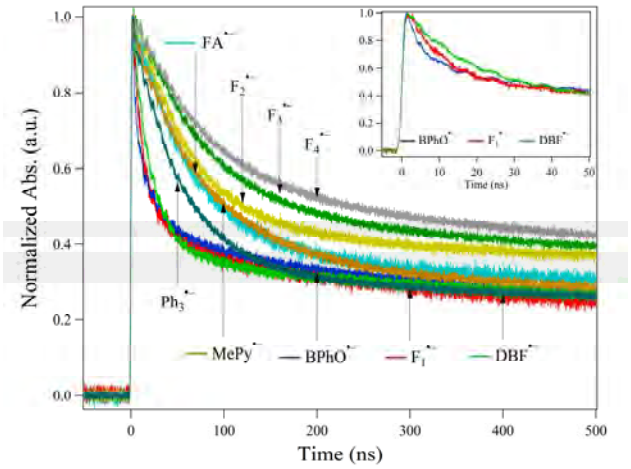

Electron Transfer by Excited Benzoquinone Anions: Slow Rates for Two-Electron Transitions. Electron transfer (ET) rate constants from the lowest excited state of the radical anion of benzoquinone, $BQ^{-\bullet *}$, were measured in THF solution. Rate constants for bimolecular electron transfer reactions typically reach the diffusion-controlled limit when the free-energy change, $\Delta G°$, reaches −0.3 eV. The rate constants for ET from $BQ^{-\bullet *}$ are one-to-two decades smaller at this energy and do not reach the diffusion-controlled limit until $-\Delta G°$ is 1.5−2.0 eV. The rates are so slow probably because a second electron must also undergo a transition to make use of the energy of the excited state. Similarly, ET, from solvated electrons to neutral BQ to form the lowest excited state, is slow, while fast ET is observed at a higher excited state, which can be populated in a transition involving only one electron. A simple picture based on perturbation theory can roughly account for the control of electron transfer by the need for transition of a second electron. The picture also explains how extra driving force ($-\Delta G°$) can restore fast rates of electron transfer.

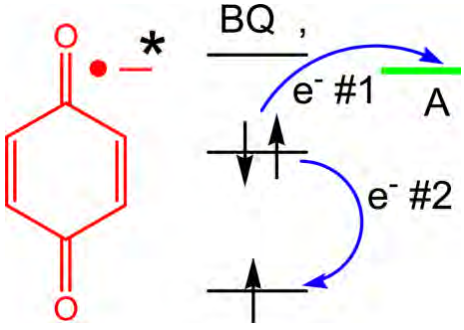

Rapid, "Step Capture" of Holes in Chloroform During Pulse Radiolysis. The fundamental process of hole capture in solution was investigated following pulse radiolysis with polyfluorene (pF) and 4-cyano-4''-pentyl-p-terphenyl (CPT) scavengers. Capture of holes was expected to be slow and occurring at rates typical for molecular diffusion, as the hole is typically thought to be localized on a solvent molecule. Contrary

to expectation, a large fraction of holes were captured in experimental time-resolution limited ~15 ps Steps, by a process much faster than diffusion of the initially formed solvent molecular cation. Yields of solute radical cations produced in 15 ps Steps as a function of the concentration of solute benzene rings is shown to the right. The data can be explained by capture of presolvated holes, analogous to presolvated electrons. Such a process for holes is not generally known in solution; however the observed Step capture as a function of solute volume or ring concentration is shown to be well explained by this model. The fits shown use the same exponential form as used for capture of presolvated electrons: $f = \exp(-[S]/C_{37}) = \exp(-q*[S])$, where f is the fraction of electrons that survive capture, C_{37} is the concentration at which 37% survive capture, and q is a quenching coefficient. The fit for the small molecule, CPT, gives a maximum yield (G_{max}) of solvent radical cations of 1.76 x 10^{-7} mol J^{-1}, with q = 2.5 M^{-1} / ring, while that for pF uses the same G_{max}, and finds q = 4.4 M^{-1} / ring. At the highest concentrations, 1.92 mM for a 52 unit long polyfluorene and 800 mM for 4-cyano-4''-pentyl-p-terphenyl, 66% and 99% respectively of the initially formed holes were captured by 20 ps.

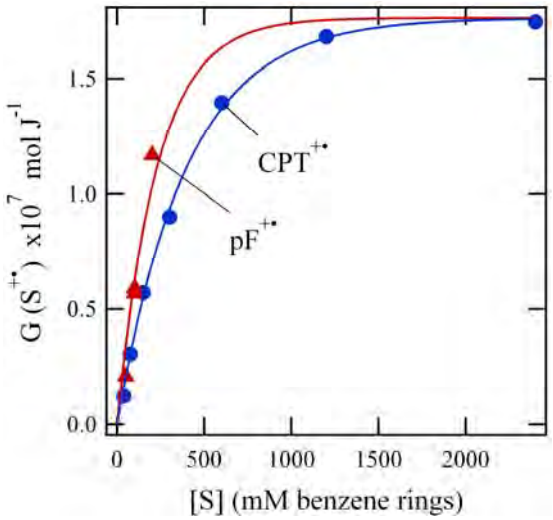

For [CPT] ≤ 100 mM and all pF samples, step yields are much too large to be accounted for by capture by encounter pairs, diffusion at short times, or direct ionization of solute molecules. However, at.the highest concentration of CPT up to ~70% of the Step yield is likely due to a combination of direct solute ionization and ionization of solute molecules neighboring CPT. The presolvated hole model gives an exponential dependence for capture in terms of solute volume in solution. Capture volumes are characterized by extended capture distances of 1.3 and 2.3 nm for CPT and pF respectively, across multiple intervening solvent molecules, as seen in the figure to the right for pF. Likely mechanisms for this capture at these distances in the first few picoseconds include initially delocalized solvent hole wavefunctions, highly mobile localized but shallowly trapped holes, or hole wavefunctions that have excess kinetic energy and can move through the solution coherently on short timescales.

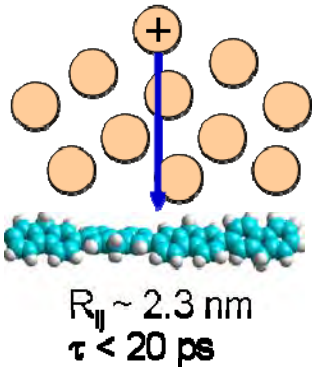

While the mechanism may not be clear, the large amount of oxidation within 20 ps is remarkable and has important implications for subsequent studies using these materials. Time resolution in pulse radiolysis experiments is often limited by the rate at which charges can be attached by diffusion, in particular for samples like the polymers that have limited solubility. Step capture provides a route to lift this limitation, allowing time resolution in subsequent reactions, such as charge transport to pendant trap groups, to be as short as the electron pulse, in this case 20 ps.

Future Plans:

The fast step capture of holes is presently contrary to our intuition. Like those for electron capture the mechanism is not clearly identified. The generality of this phenomenon is the subject of future studies. Experiments will utilize both polymers and small molecules in a variety of solvents with different IP's as well as mixtures to shed some light on the mechanism. A consequence of large amounts of hole capture appears to be large amounts of excited states produced from recombination also on very short times scales. This will be further explored.

Efforts will be made to observe electrons and holes attached to aggregates and crystallites, that may simulate the behavior of charges in films. We will also be seeking to investigate production of charges in actual films comprised of or containing conjugated polymers.

Publications of DOE sponsored research that have appeared since 10/1/2010:

1. Cook, A. R.; Sreearunothai, P.; Asaoka, S.; Miller, J. R. "Sudden, "Step" Electron Capture by Conjugated Polymers" *J. Phys. Chem. A* **2011**, *115*, 11615-11623. doi:10.1021/jp205790k.
2. Keller, J. M.; Glusac, K. D.; Danilov, E. O.; Mcilroy, S.; Sreearuothai, P.; Cook, A. R.; Jiang, H.; Miller, J. R.; Schanze, K. S. "Negative Polaron and Triplet Exciton Diffusion in Organometallic "Molecular Wires"" *J. Am. Chem. Soc.* **2011**, *133*, 11289-11298. doi:10.1021/ja202898p.
3. Sreearunothai, P.; Estrada, A.; Asaoka, S.; Kowalczyk, M.; Jang, S.; Cook, A. R.; Preses, J. M.; Miller, J. R. "Triplet Transport to and Trapping by Acceptor End Groups on Conjugated Polyfluorene Chains" *J. Phys. Chem. C* **2011**, *115*, 19569-19577. doi:10.1021/jp205828q.
4. Wishart, J. F.; Funston, A. M.; Szreder, T.; Cook, A. R.; Gohdo, M. "Electron Solvation Dynamics and Reactivity in Ionic Liquids Observed by Picosecond Radiolysis Techniques" *Faraday Discuss.* **2012**, *154*, 353-363. doi:10.1039/C1FD00065A.
5. Musat, R. M.; Cook, A. R.; Renault, J. P.; Crowell, R. A. "Nanosecond Pulse Radiolysis of Nanoconfined Water" *J. Phys. Chem. C* **2012**, *116*, 13104-13110. doi:10.1021/jp301000c.
6. Zaikowski, L.; Kaur, P.; Gelfond, C.; Selvaggio, E.; Asaoka, S.; Wu, Q.; Chen, H. C.; Takeda, N.; Cook, A. R.; Yang, A.; et al. "Polarons, Bipolarons, and Side-by-Side Polarons in Reduction of Oligofluorenes" *J. Am. Chem. Soc.* **2012**, *134*, 10852-10863. doi:10.1021/ja301494n.
7. Cook, A. R.; Bird, M. J.; Asaoka, S.; Miller, J. R. "Rapid "Step Capture" of Holes in Chloroform During Pulse Radiolysis" *J. Phys. Chem. A* **2013**, *In Press: Article ASAP*. doi:10.1021/jp405349u.
8. Zamadar, M.; Cook, A. R.; Lewandowska-Andralojc, A.; Holroyd, R.; Jiang, Y.; Bikalis, J.; Miller, J. R. "Electron Transfer by Excited Benzoquinone Anions: Slow Rates for Two-Electron Transitions" *J. Phys. Chem. A* **2013**, *In Press: Article ASAP*. doi:dx.doi.org/10.1021/jp403113u.

Spectroscopy of Organometallic Radicals

Michael D. Morse
Department of Chemistry
University of Utah
315 S. 1400 East, Room 2020
Salt Lake City, UT 84112-0850
morse@chem.utah.edu

I. Program Scope:

In this project, we seek to obtain fundamental physical information about unsaturated, highly reactive organometallic radicals containing open *d* subshell transition metal atoms. Gas phase electronic spectroscopy of jet-cooled transition metal molecules is used to obtain fundamental information about ground and excited electronic states of such species as the transition metal carbides, nitrides, and halides, and of organometallic species such as CrCCH, NiCCH, and CuCCH. Spectroscopic studies of small actinide molecules are also being pursued with the goal of understanding the electronic structure and chemical bonding in these molecules, which present severe challenges for computational chemistry. Ionic species will be available for investigation when the construction of our ion trap photodissociation spectrometer is complete.

II. Recent Progress: Optical spectroscopy of CrC, TaC, ZrF, ZrCl, OsN, CuCCH, VC, UN, VN, NiCCH, and TiC

During 2010-2013, we published papers on the resonant two-photon ionization spectroscopy of CrC, TaC, ZrF and ZrCl, OsN, CuCCH, VC, and UN. The work on CrC, TaC, ZrF, and VC were the first spectroscopic investigations of any kind for these molecules, and led to the determination of the ground electronic state symmetry and bond length. Our studies on ZrCl supplemented previous work on this molecule and identified a number of new spectroscopic transitions. Our work on OsN greatly increased our knowledge of the excited states of this molecule, leading to the identification of seven excited electronic states arising from the $1\sigma^2\ 2\sigma^2\ 1\pi^4\ 1\delta^3\ 3\sigma^1\ 2\pi^1$ and $1\sigma^2\ 2\sigma^2\ 1\pi^4\ 1\delta^2\ 3\sigma^2\ 2\pi^1$ electronic configurations. Because the studies of CrC, TaC, ZrF, ZrCl, and OsN have been published and have been described in previous abstracts, they will not be discussed further here.

More recently, we have published on the electronic structure and spectroscopy of CuCCH. This molecule has a closed shell $^1\Sigma^+$ ground state. Although not truly a radical, CuCCH is quite reactive and is important in organic synthesis, where copper acetylides form the basis of the Sonogashira cross-coupling reaction. Our work has identified three electronic band systems in the visible. The lowest energy system, the $\tilde{a}\ ^3\Pi_1 \leftarrow \tilde{X}\ ^1\Sigma^+$ system, is a spin-forbidden transition with an upper state lifetime greater than 100 μs. Nevertheless, we have succeeded in recording the spectrum and rotationally resolving the origin band at 20249 cm^{-1}. Further to the blue (23130 cm^{-1}) we have located a strongly allowed $\tilde{A}\ ^1\Sigma^+ \leftarrow \tilde{X}\ ^1\Sigma^+$ band system with an upper state lifetime of 450 ns. Finally, a third strongly allowed band system is observed at 24673 cm^{-1} ($\tau \approx 820$ ns), but we have not rotationally resolved this system. Based on a comparison to the closely related CuF, CuCl, CuBr, and CuI molecules, we believe that this is the strongly allowed $\tilde{B}\ ^1\Pi \leftarrow \tilde{X}\ ^1\Sigma^+$ band system. These studies have shown a close correspondence between the electronic structure of CuCCH and the copper halides, CuF, CuCl, CuBr, and CuI, and the Cu^+ atomic ion, and demonstrate that CuCCH can be understood as primarily an ionic molecule.

We have also continued our studies of the transition metal carbides, and have recently had success on the difficult molecule, VC. The molecule has been calculated to have a triply bound, $1\sigma^2\ 2\sigma^2\ 1\pi^4\ 1\delta^1$, $^2\Delta_{3/2}$ ground state with an exceptionally large dipole moment (about 7.3 D). Our studies have provided the first gas-phase spectra of any kind for VC and show that it does indeed have an $\Omega''=3/2$ ground state, consistent with the calculated $^2\Delta_{3/2}$ ground state. Our rotationally resolved studies also

provide r_0'' = 1.6180(3) Å, in reasonable agreement with the calculated value of r_e''=1.636 Å. We plan to pursue a collaboration with Prof. Tim Steimle at Arizona State University to measure the dipole moment of this unusual molecule, to see if the unusually large calculated value is correct.

While investigating the spectra of VC, we also observed spectroscopic transitions in the VN molecule, which was probably formed due to residual NH_3 in the instrument from a previous experiment on UN. Although this molecule has been well-studied, we nevertheless found several transitions that have not previously been observed. We anticipate that this will permit one or more new excited states of this VN to be identified.

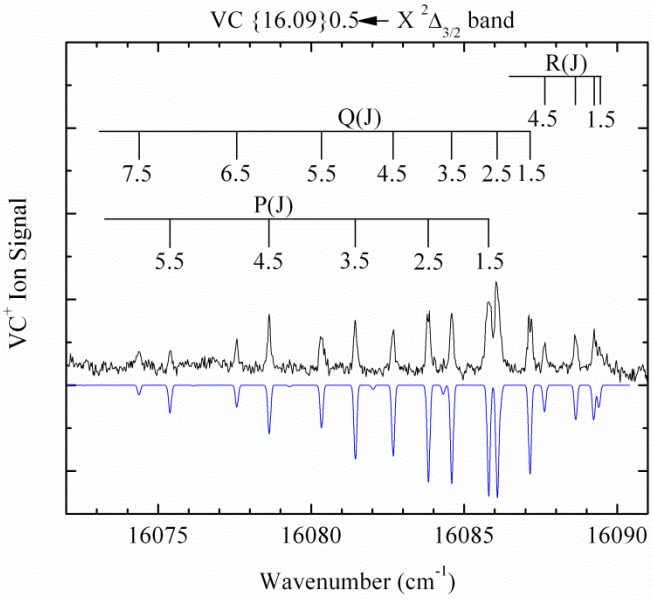

Figure 1. Rotationally resolved spectrum of the {16.09}0.5 ← X $^2\Delta_{3/2}$ band of VC, which allowed the bond length and ground state symmetry to be determined.

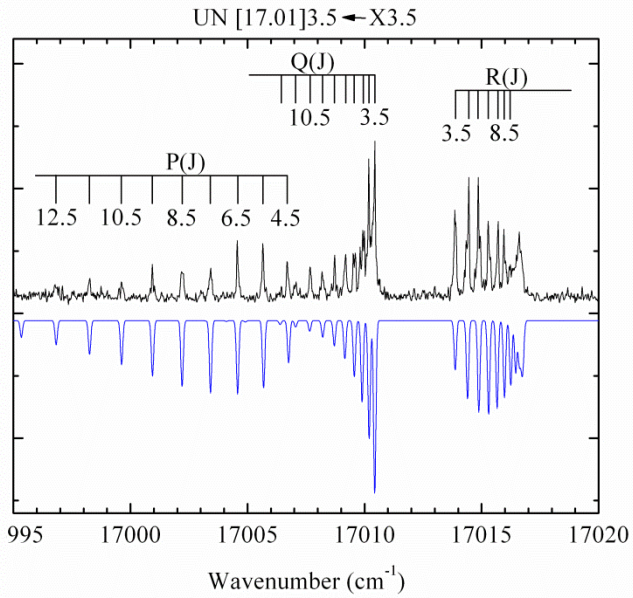

Figure 2. Rotationally resolved spectrum of the [17.01]3.5 ←X3.5 band of UN. In both figures the simulated spectrum is shown in blue.

We have also now completed an investigation of UN, the first of the actinide molecules to be studied in this group. The molecule has a complicated vibronic spectrum due to the exceptionally large number of electronic arrangements in the 5*f*, 6*d*, and 7*s* orbitals. Rotationally resolved work has shown that the molecule has a ground state with a projection of angular momentum along the axis of Ω= 3.5 and a bond length of 1.7650(12) Å. The most intriguing result of this study is that the ground state of UN differs from that of its isoelectronic counterpart, UO^+. Both of these molecules may be considered to be ionic, consisting of a U^{3+} ion bound to a closed shell N^{3-} or O^{2-} ligand. The ground state of atomic U^{3+} is the $5f^3$, $^4I_{9/2}$ level, which splits into Ω=4.5, 3.5, 2.5, 1.5, and 0.5 states in the field of the N^{3-} ion, with the Ω=4.5 level expected to lie lowest in energy. Although this description has been verified for the ground state of UO^+, our observation of an Ω=3.5 ground state for UN shows that this cannot be correct for the UN molecule. We believe that the increased negative charge on the N^{3-} ligand, as compared to O^{2-}, stabilizes the U^{3+} ion in its $7s^15f^2$ configuration, which has a ground atomic term of $^4H_{7/2}$. This leads to molecular states with Ω = 3.5, 2.5, 1.5, and 0.5. Of these, interaction with the negatively charged N^{3-} will stabilize the Ω=3.5 level, as found in our experimental data. The reason why the U^{3+}, $7s^15f^2$, $^4H_{7/2}$ atomic level emerges as the ground state in UN, but the $5f^3$, $^4I_{9/2}$ level is the ground state in UO^+ is that the ligand lies slightly inside the outermost electron density of the 7s orbital, causing the ligand to experience a U atom charge that is slightly greater than +3. The greater interaction between the N^{3-} ligand and this positive charge (as compared to the O^{2-} ligand and this positive charge) leads to a greater lowering of the

manifold of $7s^15f^2$ states in the case of UN than in UO^+. Although the $7s^15f^2$ manifold is lowered in both molecules, relative to the free ion, the greater magnitude of the effect in UN causes the $7s^15f^2$ configuration to emerge as the ground state.

In addition to these completed studies, we have conducted preliminary investigations of UC, ThC, and ThC_2, and have recorded vibrationally resolved spectra. In the upcoming year we plan to rotationally resolve these species and to deduce the symmetry of the ground and excited electronic states, and to measure the bond lengths. We have also recorded preliminary spectra of NiCCH and TiC. Diatomic TiC is of interest for comparison to the isovalent ThC molecule, for which relativistic effects are of far greater importance. In NiCCH, the location of the hole in the $3d^9$ Ni core is an open question.

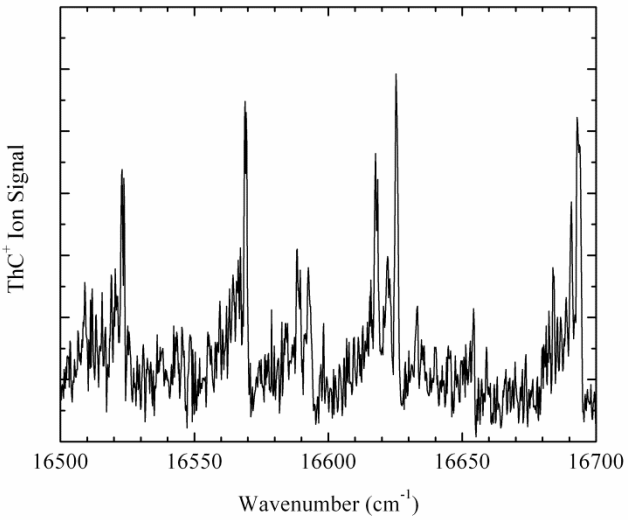

Figure 3. Vibrationally resolved spectrum of ThC, showing several good candidates for rotationally resolved studies.

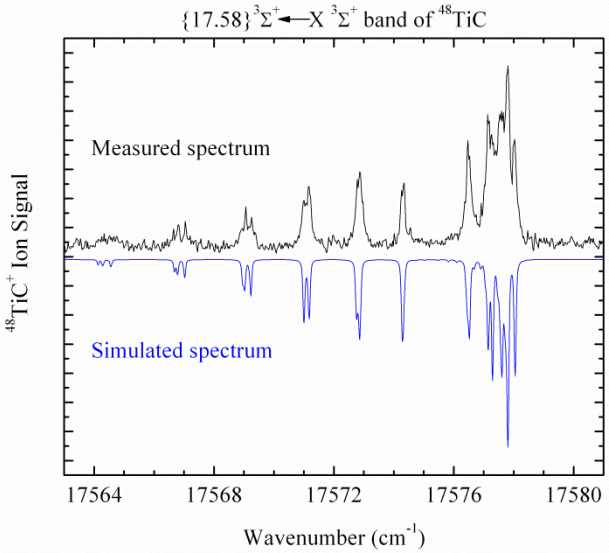

Figure 4. Rotationally resolved scan over a $^3\Sigma^+ \leftarrow {}^3\Sigma^+$ band of ^{48}TiC. Although the spin splitting has not been well-resolved, this spectrum shows that the ground state is $^3\Sigma^+$ with a bond length of approximately 1.90 Å.

III. Future Plans

A. R2PI and DF spectroscopy of transition metal carbides and radicals

Upcoming projects include: (1) Completion of spectral analysis for VN, CrCCH, NiCCH, TiC, and ThC, and publication of the results; (2) Studies of UC, UB, ThB, and ThC_2 ; (3) Collaboration with Prof. Steimle to measure the electric dipole moments of VC and UN; (4) completion of the construction of the ion trap photodissociation spectrometer (see below).

B. Photodissociation spectroscopy of cold, trapped ions

With DOE funding, we are building an ion photodissociation spectrometer that is designed to record photodissociation action spectra of cryogenically cooled transition metal and actinide ion complexes. The method will generate transition metal ion complexes that will be mass-selected, cooled in a cryogenic trap, irradiated, and photofragmented. The fragment ions will be selectively detected and the spectrum of the cold ion will be recorded by measuring the fragment ion signal as a function of the laser wavenumber. The electron impact ion source, first quadrupole mass filter, turning quadrupole, 22-pole ion trap, and Daly detector are now completed and function well. Using $Fe(CO)_5$ in the EI source, we have been able to trap 3400 mass-selected $FeCO^+$ ions, and this number is expected to increase with

further improvements in the trap. The second turning quadrupole and second mass-selective quadrupole, which will be tuned to transmit fragment ions, are mounted and ready for installation.

Among the first species we will investigate are the transition metal carbonyl cations $FeCO^+$, $CoCO^+$, $NiCO^+$, $CrCO^+$, and related species with larger numbers of ligands.

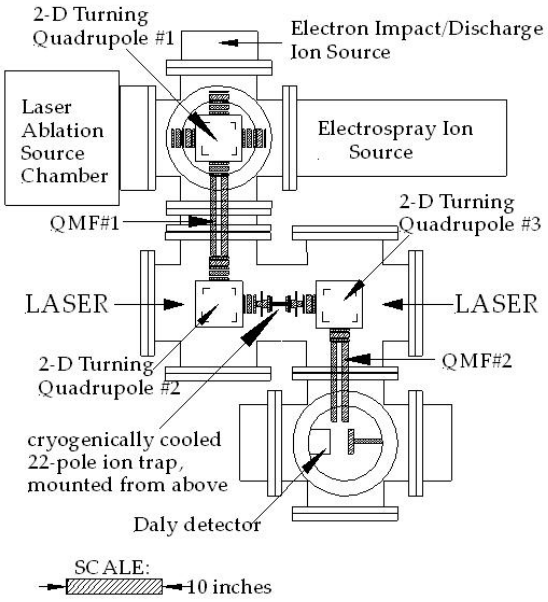

Figure 5. Design plan for the Utah ion trap photodissociation spectrometer.

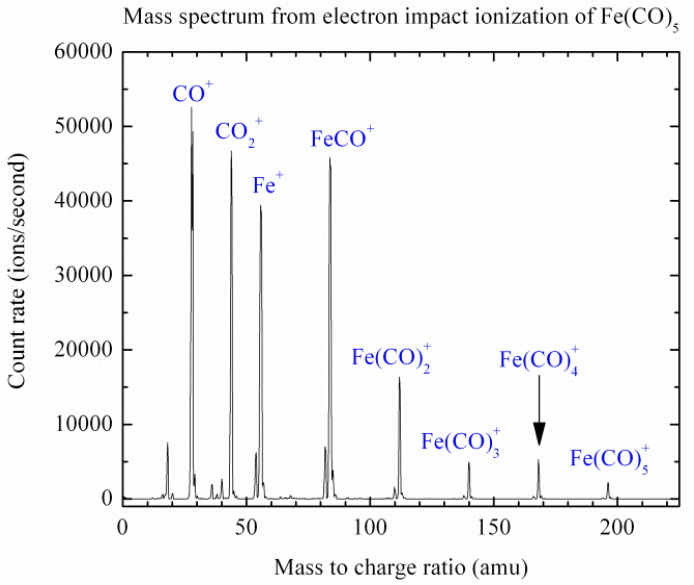

Figure 6. Mass spectrum obtained using EI ionization of $Fe(CO)_5$ in the instrument. Ion signals can be greatly increased if the isotopes of iron are not resolved.

IV. Publications from DOE Sponsored Research, 2010-present:

1. D. J. Brugh, M. D. Morse, A. Kalemos and A. Mavridis, "Electronic spectroscopy and electronic structure of diatomic CrC," J. Chem. Phys. **133**, 034303/1-8 (2010). http://dx.doi.org/10.1063/1.3456178
2. O. Krechkivska and M. D. Morse, "Resonant two-photon ionization spectroscopy of jet-cooled tantalum carbide, TaC," J. Chem. Phys. **133**, 054309/1-8 (2010). http://dx.doi.org/10.1063/1.3464486
3. A. Martinez and M. D. Morse, "Spectroscopy of diatomic ZrF and ZrCl: 760 - 555 nm," J. Chem. Phys. **135**, 024308/1-10 (2011). http://dx.doi.org/10.1063/1.3608055
4. M. A. Garcia and M. D. Morse, "Resonant two-photon ionization spectroscopy of jet-cooled OsN: 520-418 nm," J. Chem. Phys. **135**, 114304/1-12 (2011). http://dx.doi.org/10.1063/1.3633694
5. Maria A. Garcia and Michael D. Morse, "Electronic spectroscopy and electronic structure of copper acetylide, CuCCH," J. Chem. Phys. A, to appear in the Oka Festschrift: Celebrating 45 Years of Astrochemistry. (in press, available online) http://dx.doi.org/10.1021/jp312841q.
6. Daniel J. Matthew and Michael D. Morse, "Resonant two-photon ionization spectroscopy of jet-cooled UN: Determination of the ground state," J. Chem. Phys. **138**, 184303/1-7 (2013). http://dx.doi.org/10.1063/1.4803472
7. Olha Krechkivska and Michael D. Morse, "Electronic spectroscopy of diatomic VC," J. Phys. Chem. A, to appear in the T. A. Miller Festschrift. (in press, available online) http://dx.doi.org/10.1021/jp404710s

Ab initio approach to interfacial processes in hydrogen bonded fluids

Christopher J. Mundy
Physical Sciences Division
Pacific Northwest National Laboratory
902 Battelle Blvd, Mail Stop K1-83
Richland, WA 99352
chris.mundy@pnnl.gov

Program Scope

The long-term objective of this research is to develop a fundamental understanding of processes, such as transport mechanisms and chemical transformations, at interfaces of hydrogen-bonded liquids. Liquid surfaces and interfaces play a central role in many chemical, physical, and biological processes. Many important processes occur at the interface between water and a hydrophobic liquid. Separation techniques are possible because of the hydrophobic/hydrophilic properties of liquid/liquid interfaces. Reactions that proceed at interfaces are also highly dependent on the interactions between the interfacial solvent and solute molecules. The interfacial structure and properties of molecules at interfaces are generally very different from those in the bulk liquid. Therefore, an understanding of the chemical and physical properties of these systems is dependent on an understanding of the interfacial molecular structure. The adsorption and distribution of ions at aqueous liquid interfaces are fundamental processes encountered in a wide range of physical systems. In particular, the manner in which solvent molecules solvate ions at the interface is relevant to problems in a variety of areas. Another major focus lies in the development of models of molecular interaction of water and ions that can be parameterized from high-level first principles electronic structure calculations and benchmarked by experimental measurements. These models will be used with appropriate simulation techniques for sampling statistical mechanical ensembles to obtain the desired properties.

Progress Report

Ions at the air-water interface:

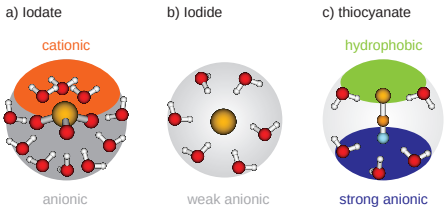

Figure 1: Schematic representations of the solvation of iodate, iodide, and thiocyanate. Iodate shows strong cationic and ionic solvation producing it's kosmostropic nature. Iodide has a more flexible anionic solvation shell making it a weak chaotrope. Thiocyanate depicts both a hydrophobic end (S) and a strong anionic part (N) giving it directionality in the vicinity of a broken symmetry and it's strong chaotropic behavior [4].

Our studies [2-5] have pointed to the specific ion effect as being a *local* effect, as opposed to an ions long-range effect on water's structure. Recently we have compared the first solvation shell of simple (I^-) and complex ions (IO_3^-) using the extended x-ray absorption fine structure (EXAFS) technique in conjunction with molecular dynamics (MD). In a head-to-head comparison of empirical polarizable models with DFT based interaction potentials it was found that DFT was able to account for subtle experimental features in EXAFS spectra leading to a picture of the solvation shell of I- that is less structured than that obtained with empirical polarizable interaction potentials [4]. Moreover, in the case of IO_3^-

DFT has provided unprecedented agreement with XAFS data supporting the surprising picture of IO_3^- as being a strong kosmotrope [4].

We can further push this concept and consider the role of the first solvation shell in determining interfacial propensity. To this end, we investigated three ions with similar polarizabilities but significantly different categorization with respect to the Hofmeister series. Specifically, we have studied IO_3^- (a strong kosmotrope), I^-, and SCN^- (a strong chaotrope) and examined the hydration structure under both bulk and interfacial conditions. Our results suggest that it is indeed the characterization of the hydration structure rather than the underlying polarizablility that is a strong indicator of surface propensity [4] (**see Figure 1).**

<u>Ion-pairing in concentrated electrolytes</u>

Establishing the role of the first solvation shell has far reaching implications for the precise balance of forces needed to explain anion adsorption. The use of *ab initio* based potentials over the empirical counter parts seems to be the most direct route towards elucidating the all important local structure that determines the thermodynamics of these important mixtures. Establishing the use of *ab initio* based potentials to study electrolytes at relevant concentrations is the next step towards our understanding of the importance of local structure on describing thermodynamics of complex systems. To this end, we examine the structure of a concentrated electrolyte, namely hydrochloric acid (HCl). A previous EXAFS study has determined the solvation structure of chloride as a function of concentration (2.5 m through 16 m) [*JACS **132**, 12597 (2010)*]. A comparison of the 16 m HCl solution to a standard of 2.5 m NaCl reveals dramatic differences in the solvation of chloride (**see Figure 2**). The emergence and experimental assignment of a contracted contact ion pair between chorine and H_3O^+ moiety suggests a picture of acids where the chloride anion is not a mere spectator but an active participant in the determination of the activity of the excess proton. Moreover, these contracted contact ions persist even at moderate concentrations (2.5 m). In our recent study, we have overcome the issues with sampling using DFT for studying high concentration electrolytes and have confirmed the picture put forth by the EXAFS studies and have identified the contracted ion pair to be that of chloride and an *eigen*-like H_3O^+. We have also confirmed that the picture put forth by our DFT and EXAFS studies is consistent with X-ray and neutron diffraction data. Thus, establishing universal consistency of the structure of concentrated HCl between three different experimental probes.

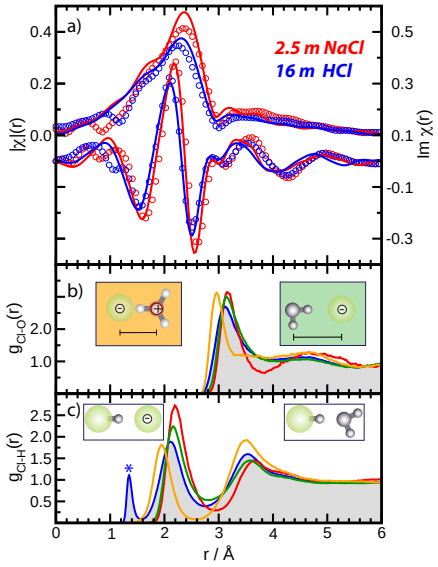

Figure 2: (top) Experimental (circles) and theoretical (solid) EXAFS spectra for NaCl and HCl. The presence of the contracted contact ion pair is seen in the experimental signal and is identified through the structural analysis in the bottom two panels.

The role of short-range structure in hydrophobic solvation

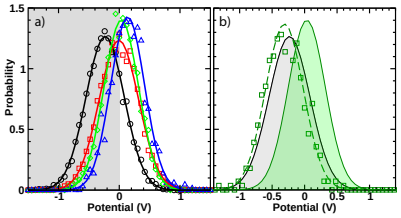

Figure 3: (a) Distributions of the scalar potential at the center of a cavity for DFT (PBE (blue), BLYP (green), SPC/E (black), and TIP5P (red). (b) Distribution of the scalar potential for SPC/E (grey shade), BLYP (green shade), and the value from the SPC/E configurations resampled with BLYP (green dashed line).

Here we study the structural and electrostatic consequences of the various broken symmetries that arise from inserting the simplest model of an uncharged ion core, a hard sphere solute of varying radius into water as described by two classical water models, SPC/E and TIP5P, and by state-of the art quantum density functional calculations. We show, the broken symmetries from hard sphere (HS) solvation generate special configurations that are particularly sensitive to small differences between donor and acceptor hydrogen bonds and to local variations in the induced charge density. This system thus provides a stringent test of classical water models in a physically important application where accurate quantum calculations can be carried out to assess their predictions. These results have implications for nonzero ionic charge and needed improvements to the Born model. In our study we derive explicit expressions for the calculation of the potential at the center of the HS cavity due to the structure of water. These expressions constitute a natural way to decompose long-range dielectric response from the highly correlated short-range electrostatics.

An additional novel aspect of our study is to perform a gedanken experiment to determine the connection between the value of the cavity potential and the model dependent local structure around the HS cavity. In point charge models there is 1-to-1 correspondence between charge density and structure, but there is no simple relationship that can be derived for continuous charge densities. To this end, we resample the configurations generated with SPC/E and TIP5P interaction potentials with DFT. The results are shown in panel b of **Figure 3** for the SPC/E model. The results show that indeed, only the nuclear structure is responsible for cavity potential. This result is an important insight into the sensitivity of thermodynamic quantities, like solvation to the local structure. We have shown in the past, that these fine details of differences in the local structure around broken symmetries have measurable consequences and will influence the underlying thermodynamics of ions in solution[2-5].

Future directions

Future research will be extended to elucidation of the solvation and surface properties of more complex anions such as the oxyanions (with G.K. Schenter and J. Fulton) such as ClO_3^- and BrO_3^- where both exhibit very interesting behavior in the context of the Hofmeister series. We are currently investigating the role of hydrophobic solvation with John D. Weeks. We are using multiple representations of the molecular interaction for water (*e.g.* TIP5P, SPC/E, flavors of DFT) to understand the structural response to charged hard spheres to determine comparisions of short- and long-ranged electrostatic response and the connections to local molecular field (LMF) theory.

Acknowledgements. This work was performed with Yan Levin (Brazil) John D. Weeks (U. Maryland), D.J. Tobias (UC-I), Ilja Siepmann (U. Minn.), and I.-F.W. Kuo (LLNL), Greg Schenter (PNNL), Liem Dang (PNNL), Marcel D. Baer (PNNL), Abe Stern (UC-I), Joost VandeVondele (U. Zurich), Greg Kimmel (PNNL), John Fulton (PNNL), Roger Rousseau (PNNL) and Shawn M. Kathmann (PNNL). We also acknowledge computer resources from NERSC and a 2008-2012 INCITE award. Battelle operates Pacific Northwest National Laboratory for the US Department of Energy.

Publications with BES support (2011-2013):

1. McGrath, MJ; Kuo, I-FW; Ngouana, BF; Ghogomu, JN; **Mundy, CJ**; Marenich, AV; Cramer, CJ; Truhlar, DG; Siepmann, JI, "Calculation of the Gibbs free energy of solvation and dissociation of HCl in water via Monte Carlo simulations and continuum solvation models," *Physical Chemistry Chemical Physics*, in press (2013)

2. Stern, AC; Baer, MD; **Mundy, CJ**; Tobias, DJ, "Thermodynamics of iodide adsorption at the instantaneous air-water interface," *Journal of Chemical Physics* **138**, 114709 (2013)

3. Tobias, DJ; Stern, AC; Baer, MD; Levin, Y; **Mundy CJ,** "Simulation and theory of ions at atmospherically relevant liquid-air interfaces," *Annual Reviews of Physical Chemistry* **64**, 339 (2013)

4. Baer, MD and **Mundy, CJ**, "An *ab initio* approach to understanding the specific ion effect," *Faraday Discussions* **160**, 89-101 (2013)

5. Baer, MD; Stern, AC; Levin, Y; Tobias, DJ; **Mundy, CJ**, "Electrochemical Surface Potential Due to Classical Point Charge Models Drives Anion Adsorption to the Air-Water Interface," *Journal of Physical Chemistry Letters* **3**, 1948-7185 (2012)

6. Kimmel, GA; Baer, M; Petrik, NG; VandeVondele, J; Rousseau, R; **Mundy, CJ**, "Polarization and Azimuth-Resolved Infrared Spectroscopy of Water on TiO_2(110): Anisotropy and the Hydrogen-Bonding Network," *Journal of Physical Chemistry Letters* **3,** 1948-7185 (2012)

7. Lewis, T; Winter, B; Stern, AC; Baer, MD; **Mundy, CJ**; Tobias, DJ; Hemminger, JC, "Does Nitric Acid Dissociate at the Aqueous Solution Surface?" *Journal of Physical Chemistry C* **115,** 21183 (2011)

8. Baer, MD; Pham, VT; Fulton, JL; Schenter, GK; Balasubramanian, M; **Mundy, CJ**, "Is Iodate a Strongly Hydrated Cation?," *Journal of Physical Chemistry Letters* **2**, 2650-2654 (2011)

9. McGrath, MJ; Kuo, IFW; Ghogomu, JN; **Mundy, CJ**; Siepmann, JI, "Vapor-Liquid Coexistence Curves for Methanol and Methane Using Dispersion-Corrected Density Functional Theory," *Journal of Physical Chemistry B* **115**, 11688-11692 (2011)

10. Baer, MD; **Mundy, CJ**; McGrath, MJ; Kuo, IFW; Siepmann, JI; Tobias, DJ, "Re-examining the properties of the aqueous vapor-liquid interface using dispersion corrected density functional theory," *Journal of Chemical Physics* **135,** 124712 (2011)

11. Lewis, T; Winter, B; Stern, AC; Baer, MD; **Mundy, CJ**; Tobias, DJ; Hemminger, JC, "Dissociation of Strong Acid Revisited: X-ray Photoelectron Spectroscopy and Molecular Dynamics Simulations of HNO_3 in Water," *Journal of Physical Chemistry B* **115**, 9445 (2011)

12. Murdachaew, G; **Mundy, CJ**; Schenter, GK; Laino, T; Hutter, J, "Semiempirical Self-Consistent Polarization Description of Bulk Water, the Liquid-Vapor Interface, and Cubic Ice," *Journal of Physical Chemistry A* **115**, 6046-6053 (2011)

13. Baer, MD; **Mundy, CJ**, "Toward an Understanding of the Specific Ion Effect Using Density Functional Theory," *Journal of Physical Chemistry Letters* **2**, 1088-1093 (2011)

14. Kathmann, SM; Kuo, IFW; **Mundy, CJ**; Schenter, GK, "Understanding the Surface Potential of Water," *Journal of Physical Chemistry B* **115**, 4369-4377 (2011)

DYNAMIC STUDIES OF PHOTO- AND ELECTRON-INDUCED REACTIONS ON NANOSTRUCTURED SURFACES - *DE-FG02-90ER14104*

Richard Osgood,
Center for Integrated Science and Engineering, Columbia University, New York, NY 10027, Osgood@columbia.edu

Progress Report

Program Scope or Definition:

Our current research program examines the photon- and electron-initiated reaction mechanisms, half-collision dynamics, and other nonequilibrium-excited dynamics effects, occurring with excitation of adsorbates on well-characterized metal-oxide and nanocrystal surfaces. In order to explore these dynamics, our program we have developed new synthesis methods for uncapped nanocrystals *with specific reconstructions and orientation* in a UHV STM instrument. To identify these nanocrystals and there structure we utilize a recent technique developed in our lab, which does STM nanocrystallography. We will then use the tunneling from the tip of our STM or an *in situ* flood UV lamp to excite adsorbate molecules at specific sites of these nanocrystals. The resulting chemistry and surface dynamics will be investigated via imaging of the reaction fragments in the vicinity of the reaction sites.

Our experiments have been directed toward electronic-tunneling reactions in a series of linear aromatics and on rutile TiO_2(110) surfaces (although we have recently examined other iron-oxide surfaces), as well as exploration of the unexpected "inverse" catalytic activity of uncapped TiO_2 nanocrystals with a known atomic structure on single-crystal Au. Our adsorbate molecules have been chosen to enable studies of physisorbed molecules at room temperature[1]. In addition, we are planning to use chemisorbed carboxylic acids for tip-induced dynamics studies since such acids are already known to show light-induced chemistry on TiO_2. This year we have studied the thermal (and catalytic) chemistry and tip-induced reaction dynamics of these molecules on single-crystal TiO_2 and initiated closer examination of the reactivity and structure of nanocrystal and nanopatterned TiO_2 on Au(111).

Recent Progress:

STM Tip-Induced Dissociation Dynamics on Surfaces.

Studies of STM tip-induced surface reactions have high potential for elucidating the dynamics and mechanism of, generally, any charge-driven surface chemical process; for example in many cases *photoreactions* of adsorbed molecules involve charge transfer between a surface and an adsorbate molecule, followed by its chemical transformation. However, in investigating the reaction mechanism through the use of electron emission from an STM tip, the STM may also very use-

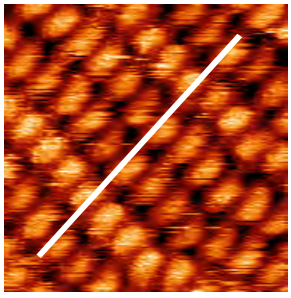

Fig. 1: 10 × 10 nm STM image of 1 ML of 2-chloro-anthracene deposited on rutile(110) surface at room temperature.

fully be employed to image the surface. The advantages of such an approach are that it enables obtaining precise knowledge about (a) the initial adsorption geometry of a specific target molecule, (b) the energy and flux of the exciting electrons, and (c) the reaction products, if they remain bound on the surface.

We have now studied[2] the tip-induced chemical dynamics of 2-chloroanthracene on TiO_2(110). This is an excellent molecule to use for studies of tip-induced reactions since typically such a halogenated species is labile to electron bond cleavage after electron attachment. Our STM images show that at 135 K and low coverage, i.e. ~0.1 ML, these molecules are physisorbed along the five-coordinated titanium rows on the rutile(110) surface as a result of electrostatic interaction; see **Fig. 1**. If we apply electric pulses >2.5 V from the STM tip to individual molecules, either desorption or dissociation of the molecules occurs. Our analysis of the data indicates that we have observed dissociative electron capture of a single 2-chloroanthracene molecule, which leaves behind a surface chlorine atom adsorbed in the on-top configuration on a surface Ti atom. The threshold energy required for the dissociation is found to be ~ 2.7 eV. The other reaction product, an anthracene radical, apparently desorbs into the vacuum or is captured by the STM tip. Many important questions remain: dynamics of surface-bound fragments, effect of nearby molecules, detailed energy-dependent phenomenon.

Catalytic Studies on Structurally Defined TiO_2 Nanocrystals on Au.

We have currently explored TiO_2 grown on Au(111) substrate using a novel approach developed in our laboratory, with the goal of understanding the distinctive chemical properties of our nanocrystalline TiO_2 that may arise both from its <10 nm size and from structural modifications induced by any interactions with the substrate. In particular, we have studied the reactivity of 2-propanol with TiO_2 nanocrystals supported on Au(1 1 1) – the inverse of the usual Au on TiO_2 studies - using temperature-programmed desorption (TPD) and scanning tunneling microscopy (STM)[3]. The nanocrystals are grown through oxidation of a Ti-Au surface alloy and have an average height of 1 nm and width of 15 nm with a dominantly hexagonal morphology. We have observed desorption of propanol and propanol-derived products from the TiO_2 nanocrystal surfaces over a temperature range of 270–570 K, these products could be distinguished from desorption of propanol from the Au(1 1 1) surface below 270 K. With increasing propanol coverage, we also observed that the TiO_2-related TPD peaks were occupied before the appearance of any Au(1 1 1)-related peaks. Our calculations showed that the TiO_2 nanocrystals were saturated at 0.4 ML of propanol concentration, where 1 ML ≡ 5.2×10^{14} cm^{-2} refers to surface density of five-coordinated Ti atoms on rutile(1 1 0). Our TPD measurements also showed that 61% of this adsorbed propanol desorbed molecularly at 310 K, while 23% dehydrated into propene and 6% dehydrogenated to form acetone, both products desorbing in the 370–570 K temperature range. The desorption temperatures of products from supported TiO_2 nanocrystals depended strongly on the morphology of the nanocrystals. Our results provide a clear example of the distinctive reactivity of nanocrystal metals chalcogenides.

Catalytic studies on iron oxide surfaces.

In order to expand our oxide substrate capability, our group has returned to examining surface processes on Fe_3O_4(111) surfaces; this was accomplished via a collabora-

tion with the Flynn Group and the Flytzani-Stephanopoulos Group at Tufts University[3]. In particular, we chose to study the reactivity of $Fe_3O_4(111)$ surface with deuterated methanol, which is of interest for fuel-cell technology applications. The unique combination of STM and TPD capabilities of our experimental chamber allowed us to relate specific reactivity patterns to different surface phases of $Fe_3O_4(111)$ that included $Fe_2O_3(0001)$ and FeO(111). These phases were formed by varying the sample preparation conditions; the phases could be easily distinguished in the STM images. Methanol species were observed to be dissociatively adsorbed only on the Fe-terminated $Fe_3O_4(111)$ surface and physisorbed on the O-terminated FeO(111) and bi-phase surfaces. Methanol is first dissociated into methoxy (CD_3O) attached to the surface terminating Fe sites and D-atom atop the under-coordinated oxygen sites of $Fe_3O_4(111)$. A fraction of these surface species then recombined to desorb as molecular methanol (CD_3OD) from the surface at 365 K. Methoxy (CD_3O) is further dissociated into formaldehyde (CD_2O) and D-atoms at higher temperatures. The gas-phase formaldehyde (CD_2O) and methanol molecules recombinatively desorb from the surface at 635 K. In general, the reaction of methanol on the iron-oxide surface has shown high sensitivity to atomic-level surface reconstructions.

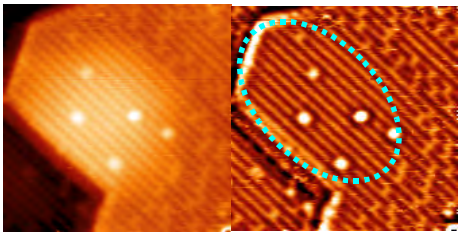

Fig. 2: Two STM images showing an absence of oxygen vacancies in the strained region of a blister; the features due to V_o appear as lighter streaks against the brown background in the right image.

Stress-Induced Nano-Modification of Reactivity on Oxide Surfaces.

We have recently demonstrated the use of nanoscale local strain to control surface reactions on oxide surfaces[4]. This research uses our STM imaging in a UHV environment to show that this strain locally alters reactivity of the surface. In our results, we have used a nanoscale template of extremely small, buried-atom clusters to provide patterned strain in the near surface layers of metal oxides.

The experiments have shown that local (i.e. atomic scale) stress in TiO_2 layers results in a change in the reactivity of that surface and that this change may be used in conjunction with reactions of adsorbate molecules to change the surface composition and thus promote local etching, functionalization, or growth. This effect is shown in an actual image form by **Fig 2**. In particular, a clean, bare surface of reduced $TiO_2(110)$ has atomic rows of five-fold coordinated Ti and bridging O, appearing light and dark in the STM image. Some surface O atoms are missing, creating oxygen vacancies V_O that appear as bright point features between neighboring bright rows. It is possible to use a low-energy (i.e. 1-2 kV) ion beam in combination with high-temperature annealing to implant nm-scale clusters of Ar atoms beneath the sample's surface. In the vicinity of the buried Ar blister, the surface atomic layers are deformed up-

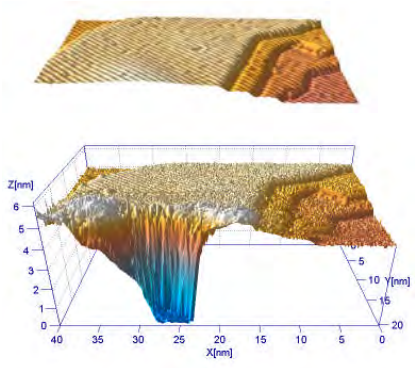

Fig. 3. 3D cross-sectional renderings of STM images taken before and after explosive removal of the TiO_2 lid above the buried cluster.

ward and a local strain field is established. Within this strain field the oxygen vacancies are eliminated, apparently due to higher binding energy of oxygen in the strained region; this effects is shown clearly by comparing the regions within and outside of the blue circle surrounding the implanted cluster in **Fig. 2**. It is possible to control or vary the strain field in such dots via several experimental parameters including temperature and ion flux to study the effects of strain.

In order to explore the nature of the buried Ar clusters we have undertaken an extensive research effort that included STM-probe-tip- controlled nanoetching in the vicinity of the clusters combined with numerical simulation of mechanical deformation of TiO_2 around buried clusters. We have been able to measure the depths, at which the Ar clusters were located under the surface as in an experiment shown in **Fig 3**. For this we used short +8V voltage pulses from the STM tip to cause "rupture" of clusters that left up to 11 nm deep craters on the surface. The conclusion of the study has been that argon forms near-surface horizontal cracks in the volume of TiO_2 filled with highly pressurized solid argon. The values of surface strain induced by these pockets of Ar has been calculated to reach 3% - the values well outside of the limits of the macroscopic sample-deformation experiments. *Due to its potential as method for achieving nano scale pattering we have now initiated a new program, funded by NSF DMR to support this work.*

Recent Grant-Sponsored Publications

1. D. V. Potapenko, N. Choi, and R.M. Osgood, Jr., "Adsorption Geometry of Anthracene and 4-Bromobiphenyl on TiO_2(110) Surfaces." J. Phys. Chem. 114, 19419 (2010)
2. D. V. Potapenko, Z. Li, R. Osgood, "Dissociation of single 2-chloroanthracene molecules by STM-tip electron injection." J. Chem. Phys. 116, 4679 (2012)
3. K. Rim, Z. Li, D.V. Potapenko, R.M. Osgood, M. Flytzani-Stephanopoulos, G.W. Flynn, X.-D. Wen, E.R. Batista, "Stepwise Dissociative Adsorption of Methanol on the Reactive Fe_3O_4 surface" In final preparation.
4. D.V. Potapenko, Z.Li, Y. Lou, R. M. Osgood Jr.," 2-Propanol Reactivity on I*n Situ* Prepared Au(111)-Supported TiO_2 Nanocrystals." J. Catal. 297, 281-288 (2012)
D.V. Potapenko, Z. Li, J.W. Kysar, R. M. Osgood, " Controlled Nanostrained Regions on on the Surface of TiO_2 Crystals" Submitted to Nature Nanotechnology.

Studies of surface adsorbate electronic structure and femtochemistry at the fundamental length and time scales

Hrvoje Petek
Department of Physics and Astronomy and Chemistry
University of Pittsburgh
Pittsburgh, PA 15260

Our research focuses on the electronic structure and dynamics of solids, surfaces, and molecule covered surfaces. We are interested in the surface electronic excitation and the subsequent dynamics leading to charge transfer or photochemistry. The correct description of surface electronic structure, photoexcitation, interfacial charge transfer, energy and momentum relaxation of carriers, and femtochemistry are essential for the intellectual framework for applications of photoinduced phenomena at interfaces, such as the photovoltaic and photocatalytic solar energy conversion. In this report we introduce examples of our femtosecond time-resolved multi-photon photoemission (TR-MPP) and low-temperature STM studies of electronic surfaces and interfaces.

Transient exciton formation in metals. When light interacts with a solid it creates a coherent polarization field, i.e., an exciton-polariton, a quantum mechanical entity with both particle and field properties. An exciton can lose coherence through scattering thereby absorbing a photon, or decay coherently by electron-hole (*e-h*) pair recombination to emit a photon. Excitons have never been reported in metals because the Coulomb interaction between an *e-h* pair is fully screened by charge density fluctuations typically on a few femtosecond time scale, and therefore no bound states exist. An exception is silver, which has a sharp bulk plasmon resonance at ~3.8 eV. Suddenly turning on a charge in Ag creates a plasmon oscillation with ~1 fs period, which dephases on <15 fs time scale. When the screening time scale and the laser pulse duration are comparable, it may be possible to observe a correlated *e-h* pair state, *i.e.* a transient exciton (TE), in an MPP measurement.

We have investigated MPP spectra of Cu(111) and Ag(111) surfaces focusing on the near-resonant and resonant two photon transition from the occupied Shockley surface (SS) state to the unoccupied image potential (IP) penultimate intermediate state before emission of electron into vacuum (Fig. 1). IP states of metals are a consequence of the many-body screening of an external charge. They are the asymptotic states of fully established screening response.

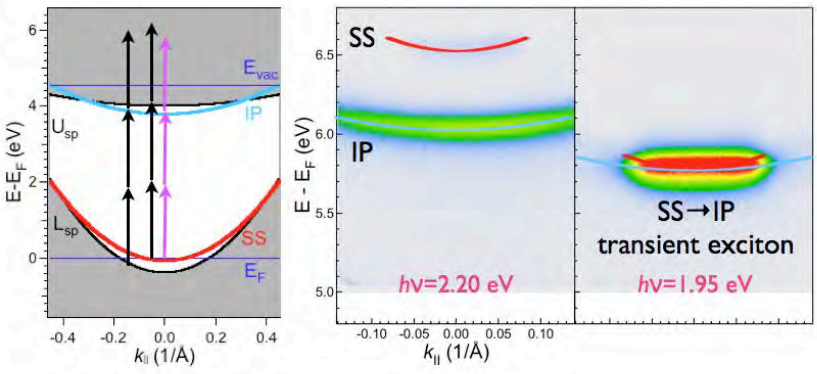

Figure 1 shows the band structure of Ag(111) and 3PP spectra for near-resonant and resonant excitation. For the

Figure 1. *The projected band structure of Ag(111) surface showing the resonant (purple) and nonresonant (black) excitation pathways for the SS and IP states, and 3PP spectra (final state energy vs. parallel momentum) under near-resonant (2.20 eV) and resonant (1.95 eV) conditions.*

near-resonant condition, the energy vs. parallel momentum ($k_{||}$) image of photoemitted electrons shows dispersive SS and IP states indicated by red and blue curves. At the resonant condition, however, the dispersive surface bands collapse into a non-dispersive feature that spans the $k_{||}$ range of SS. Such non-dispersive spectra are expected for photoemission from localized states, such as a correlated *e-h* pair in a TE state. Similar experiments on Cu(111) surface do not show the non-dispersive feature, consistent with faster screening in copper. Because excitonic states are the primary manifestation of interaction between light and-solid state materials, the ability to follow the formation and decay of excitons is fundamental to solar energy conversion processes.

In addition to the MPP spectroscopy, we measured interferometric pump-probe correlations to study the coherent dynamics of the TE dephasing and IP state formation. Figure 2 shows an interferometric measurement for normal emission, from a 3D (*E, k, t*) data set. Fourier transform analysis of the TR-MPP signal obtains 2D electronic spectra of the pathways in the TE and IP state generation and interaction. The analysis of the 2D spectra indicates that polarization leading to the TE state excitation is the local field associated with the IP←SS two-photon resonance at 1.93 eV, which builds up in the sample. By contrast the IP state is excited both directly by the external laser field (2.05 eV) from the bulk and by dephasing of the TE.

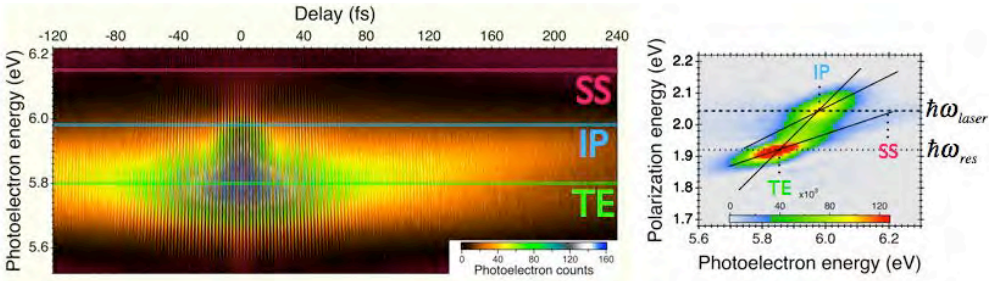

Figure 2. *Interferogram of three-photon photoemission for near resonant two-photon excitation from SS to IP states, and its Fourier transform analysis in the region of the laser driving frequency. The 2D photoelectron spectra provide information in the coherent excitation process of the SS, IP and TE components of the signal. The dashed lines indicate the laser and resonance frequencies. the slanted lines indicate coherent processes of different order.*

Superatom states. In the spatial domain, we have investigated the formation of a molecular quantum-well with single-molecule resolution. 2PP spectroscopy by Zhu (Columbia) and Wolf (Fritz Haber Institute) indicated that the LUMO state with σ* character of C_6F_6 molecules forming a monolayer of flat lying molecules on Cu(111) surface hybridizes into a dispersive conduction band with an effective mass of $2m_e$. How flat lying π-conjugated molecules can hybridize into a delocalized band has been a mystery.

We have performed low temperature STM measurements on C_6F_6 on Cu and Au surfaces from single molecule to multilayer coverages. By dz/dV spectroscopy we could measure the σ* state energy as a function of the number of nearest neighbors, and found that the energy is stabilized consistent with an intermolecular hopping integral β=0.028 eV. This behavior could be reproduced nearly quantitatively by a DFT calculation of the electronic structure of unsupported C_6F_6 monolayer, indicating that the band formation is an intrinsic property of C_6F_6 molecules. We addressed the origin of intermolecular interactions that enable the dispersive band formation.

We investigated the electronic properties of the σ* state by low temperature STM and theory. As required for the strong intermolecular interaction, the σ* state has a diffuse wave function

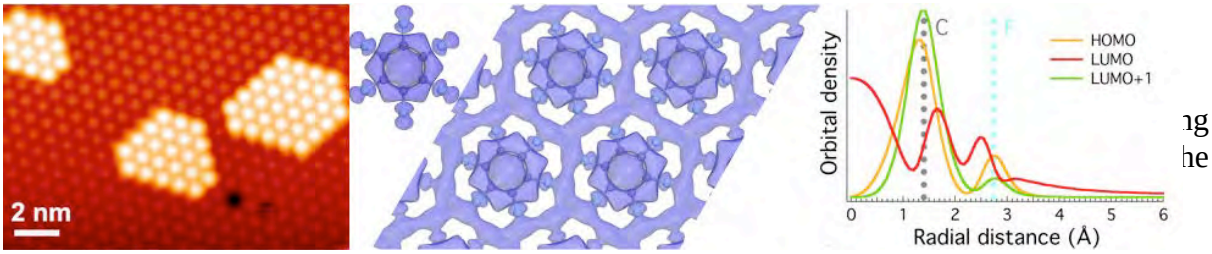

Figure 3. *STM image of C_6F_6 monolayer and partial second monolayer on Cu(111) surface. The calculated probability density of the σ* state for a single molecule and a monolayer quantum well. The wave function cross sections for the π HOMO, σ* LUMO, and π* LUMO+1 orbitals. The nonnuclear density of the σ* state favors wave function hybridization.*

F atom periphery (Fig. 3). This behavior is reminiscent of the superatom molecular orbitals (SAMOs) of hollow molecules, which we discovered in C_{60} and related materials. SAMOs of hollow molecules are bound to the hollow core rather than the ions of the cage. Examining the probability density of the σ* state, we found it distributed in the nonnuclear regions with the density maximum at the center of the benzene ring. This led us to conclude that the σ* state is a 2D superatom state, and suggested a new paradigm for designing molecular semiconducting materials with nearly-free electron band transport. Such electronic orbitals should exist in other flat molecules. We have been exploring by theory the factors that control the energies of SAMOs, in order to discover materials with superior charge transport properties.

In addition, we performed LT-STM measurements on the electronic structure of La@C_{82}. The goal of these experiments was to characterize the stabilization of SAMOs by hybridization with the atomic states of the endohedral atom. Indeed this interaction stabilizes the s-SAMO by ~2 eV, making its nearly free electron properties within reach of experiments.

Molecular chemisorption on 1D substrates. By LT-STM we discovered exceptional behavior of CO molecules on Cu(110)-O (2x1) surface. The substrate consists of 1D Cu-O- chains. To form the Cu-C bond, CO molecules pull Cu atoms out by 1 Å from the Cu-O- chains. Moreover, the entire Cu-CO structure tilts by 45° from the surface normal in two equivalent configurations, to optimize the dipole-image dipole interaction with the surface. Interconversion between the structures causes CO molecules at 77K to appear as two spots separated by 5Å (Fig. 4a). Cooling

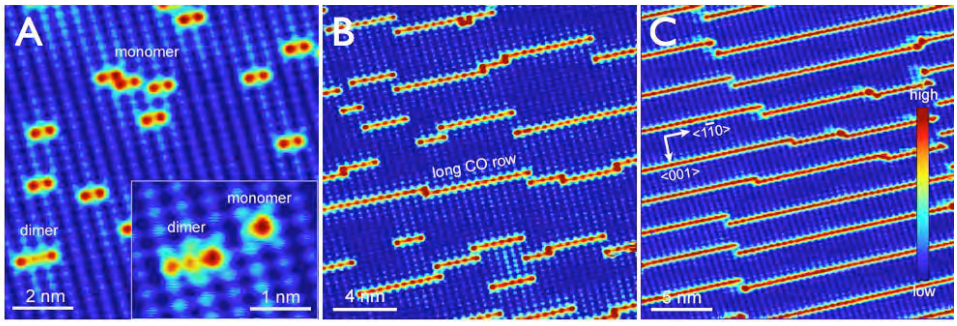

Figure 4. *The structure of CO chemisorption on Cu(110)-(2x1)-O surface. a) Low coverage structure at 77 K; the metronome tilting motion of Cu-CO unit causes CO monomers to appear as pairs of bright spots. The inset shows the frozen tilted structures at 4K. b) At intermediate coverages CO molecules aggregate into linear structures. c) At monolayer coverage CO molecules assemble through repulsion along Cu-O- chains into a grating structure.*

the sample to 4K freezes the molecule in one of the tilted structures.

At higher coverages (Figs. 4b and 4c), the tilted Cu-CO units experience attractive dipole-dipole interaction leading to formation of long, single CO molecule wide rows running perpendicular to the surface Cu-O- chains, with a minimum separation between rows of 8 substrate unit cells. Such strongly anisotropic interactions between molecules are likely to also occur in general at low coordination surface sites and therefore we believe that our measurements and analysis are important to understanding the reactive sites in heterogeneous catalysis.

DOE Basic Energy Sciences Sponsored Publications 2009-2013

1. Achilli, S., Trioni, M.I., Chulkov, E.V., Echenique, P.M., Sametoglu, V., Pontius, N., Winkelmann, A., Kubo, A., Zhao, J., & Petek, H., "Spectral properties of Cs and Ba on Cu(111) at very low coverage: Two-photon photoemission spectroscopy and electronic structure theory." *Phys. Rev. B* **80**, 245419 (2009).
2. Huang, T., Zhao, J., Feng, M., Petek, H., *et al.*, "Superatom orbitals of $Sc_3N@C_{80}$ and their intermolecular hybridization on Cu(110)-(2x1)-O surface." *Phys. Rev. B* **81**, 085434 (2010).
3. Hu, S., Zhao, J., Jin, Y., Yang, J., Petek, H., & Hou, J.G., "Nearly Free Electron Superatom States of Carbon and Boron Nitride Nanotubes." *Nano Lett.* **10**, 4830 (2010).
4. Feng, M., Zhao, J., Huang, T., Zhu, X., & Petek, H., "The Electronic Properties of Superatom States of Hollow Molecules." *Acc. Chem. Res.* **44**, 360 (2011).
5. Wang, L.-M., Sametoglu, V., Winkelmann, A., Zhao, J., & Petek, H., "Two-Photon Photoemission Study of the Coverage-Dependent Electronic Structure of Chemisorbed Alkali Atoms on a Ag(111) Surface." *J. Phys. Chem. A* **115**, 9479 (2011).
6. Feng, M., Cabrera-Sanfelix, P., Lin, C., Arnau, A., Sánchez-Portal, D., Zhao, J., Echenique, P.M., & Petek, H., "Orthogonal Interactions of CO Molecules on a One-Dimensional Substrate." *ACS Nano* **5**, 8877 (2011).
7. Feng, M., Lin, C., Zhao, J., & Petek, H., "Orthogonal Intermolecular Interactions of CO Molecules on a One-Dimensional Substrate." *Annu. Rev. Phys. Chem.* **63**, 201 (2012).
8. Lin, C., Feng, M., Zhao, J., Cabrera-Sanfelix, P., Arnau, A., Sánchez-Portal, D., & Petek, H., "Theory of orthogonal interactions of CO molecules on a one-dimensional substrate." *Phys. Rev. B* 85, 125426 (2012).
9. Dougherty, D. B., Feng, M., Petek, H., *et al.*, "Band formation in a molecular quantum well *via* 2D superatom orbital interactions," *Phys. Rev. Lett.* **109**, 266802 (2012).
10. Feng, M., Zhao, J., Lin, C., Huang, T., Yang, S., and Petek, H., "Energy Stabilization of the s-Symmetry Superatom Molecular Orbital by Endohedral Doping of C_{82} Fullerene with a Lanthanum Atom, *Phys. Rev. B* **88**, 075417 (2013).
11. Petek, H., Feng, M., & Zhao, J., The Electronic Structure of Metal–Molecule Interfaces in *Current-driven phenomena in nanoelectronics*, T. Seideman ed. (World Scientific 2010).
12. Winkelmann, A., Chiang, C.-T., Tusche, C., Ünal, A.A., Kubo, A., Wang, L., & Petek, H., Ultrafast multiphoton photoemission microscopy of solid surfaces in the real and reciprocal space in *Dynamics of interfacial electron and excitation transfer in solar energy conversion: theory and experiment*, P. Piotrowiak ed. (Royal Society of Chemistry, London, 2013).
13. Bovensiepen, U., Petek, H., & Wolf, M. eds., Dynamics at Solid State Surfaces and Interfaces, Vol. 1: Current Developments, 1 ed. (Wiley-VCH Verlag Gmbh & Co., Weinheim, 2010).
14. Bovensiepen, U., Petek, H., & Wolf, M. eds., Dynamics at Solid State Surfaces and Interfaces, Vol. 2: Fundementals, 1 ed. (Wiley-VCH Verlag Gmbh & Co., Weinheim, 2012).

Ultrafast electron transport across nanogaps in nanowire circuits

Eric O. Potma

Department of Chemistry
University of California, Irvine
Irvine, CA 92697
e-mail: epotma@uci.edu

Program Scope

In this Program we aim for a closer look at electron transfer through single molecules. To achieve this, we use ultrafast laser pulses to time stamp an electron tunneling event in a molecule that is connected between two metallic electrodes, while reading out the electron current. A key aspect of this project is the use of metallic substrates with plasmonic activity to efficiently manipulate the tunneling probability. In the first phase of this program we developed highly sensitive tools for the ultrafast optical manipulation of tethered molecules through the evanescent surface field of plasmonic substrates. In the second phase of the program we use these tools for exercising control over the electron tunneling probability.

Recent progress

During Year I and II of this project, we have unambiguously shown that surface plasmon polarition (SPP) excitations can be used to carry out precise nonlinear optical manipulations of molecular systems at designated target sites.[1, 2, 3, 4] The ability to control the density and duration of the electric field at the target site is crucial for performing light-induced tunneling events through molecules. In Year III and IV we have used tailored SPP excitations to induce tunneling currents across open nano-junctions. Below we summarize our most recent results.

Surface plasmon polariton induced tunneling current
We have fabricated nano-junctions in 30-nm thick gold layers on glass coverslips using a combination of lithography, focused ion beam milling and electromigration. Our fabrication method yields reproducible junctions in the sub- 10-nm range. An example of the resulting junction is shown in Figure 1a. Our first goal is to control the tunneling of electrons across the junction with the help of femtosecond light pulses. Our approach is based on the excitation of a traveling SPP mode in the Au layer. To manage and suppress photon-induced heating of the junction, the SPP is excited at a remote location away from the junction. Subsequent propagation of the SPP towards the nano-gap enables manipulation of the surface field at the location of the junction. The changes in the electric field across the gap can induce tunneling of electrons, which can be be measured with a current meter. The basic layout of the experiment is shown in Figure 1b.

Figure 1c shows the dependence of the current across the gap as a function the input polarization of the laser light. A tunneling current is observed when the laser is P-polarized, while no current is flowing when the laser is S-polarized. This experiment proves that the current is controlled exclusively by the surface field of the SPP mode, as the SPP can only be excited with P-polarized light. This experiment proves unambiguously that controlled tunneling of electrons can be achieved

across a nano-junction with femtosecond SPP wavepackets. Moreover, unlike previous work on light-induced tunneling, the tunneling currents here are stable, reproducible and measured under ambient temperatures and pressure.

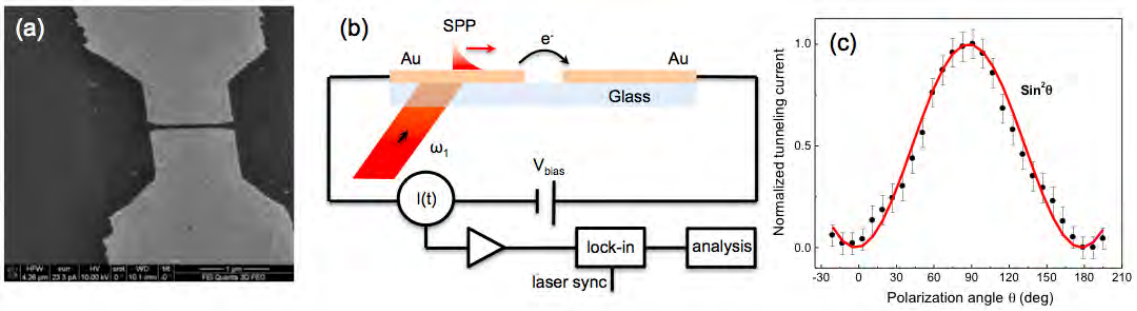

Figure 1: Femtosecond optical rectification in an open circuit. (a) Nanojunction prepared by partial FIB milling and electromigration. The effective gap size at the closest point in the junction is 8 nm. (b) Basic scheme for measuring the SPP induced current. (c) SPP-induced current as a function of laser input polarization. The polarization dependence confirms that the tunneling current is induced by the surface plasmon field.

SPP-induced optical rectification

Figure 2a depicts the I-V curve of the tunneling current for a fixed illumination power. The observed profile is indicative of electron tunneling mediated by the process of optical rectification. In this model, a dc current is generated by the ac surface field due to the second order nonlinearity of the junction. Such nonlinearities are the result of nanometer scale asymmetries in the gap. The red curve is a fit based on the optical rectification model. Further proof for this mechanism is provided by the dependence of the current on the light illumination power, illustrated by Figure 2b. At low excitation fields, the current is strictly linear with the incident power, as expected for the process of optical rectification.

Electron tunneling mediated by optical rectification has been observed before, but never at ambient pressures and temperatures. In addition, these measurements are the first demonstration that dc currents can be generated with femtosecond temporal resolution, as electrons only flow across the junction during the elevated electric fields of the femtosecond SPP wave packet in the gap. One reason why these measurements are possible is that the remote SPP excitation scheme exhibits favorable heat dissipation characteristics which preserves the morphology of the junction and ensures stability of the measurements.

SPP-induced field electron emission

As evidenced by Figure 2b, a different mechanism dominates the electron tunneling for stronger surface fields. The strong exponential power dependence is indicative of field electron emission as described by the Fowler-Nordheim equations. In this limit, the strong gradient of the electric field in the gap narrows the tunneling barrier and thus increases the escape probability of electrons from the metal electrode. This is the first time that a clear transition between low field limit optical rectification and high field limit field electron emission is observed, which underlines the robustness and sensitivity of the SPP-based tunneling scheme developed in this Program.

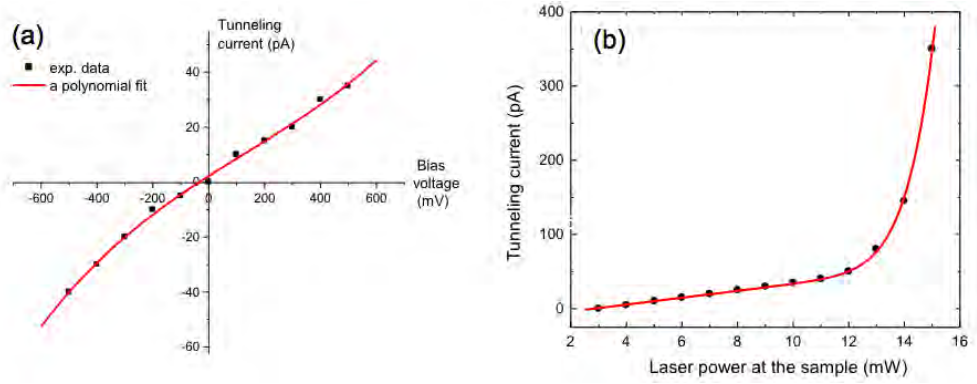

Figure 2: SPP induced current in an open circuit. (a) I-V curve in the limit of optical rectification. The current was measured for at a laser input power of 8 mW. (b) SPP induced current as a function of the laser input power. In the low power limit, optical rectification is the dominating process, while for higher SPP fields Fowler-Nordheim tunneling dominates. The red curve is a fit based on the combined effects of optical rectification and Fowler-Nordheim tunneling.

Future Plans

In Year III and IV, we accomplished our goal of controlling electron tunneling currents across engineered nano-gaps with femtosecond light pulses. We are now in a position to use our scheme for controlling the flow of electrons through a molecule that bridges the gap. In the last phase of the program, we will focus our efforts on incorporating DNA molecules into the nano-circuit. First, we will fabricate nano-junctions with widths of 15 nm or wider, which will effectively suppress the open circuit tunneling current. Second, we will employ the wealth of knowledge on DNA surface chemistry to span the nano-junction with a single molecule. Third, we will perform SPP induced tunneling measurements on the metal-molecule-metal junction, where tunneling occurs solely through the molecule. Once successful, we will carry out double pulse tunneling measurements to determine the electron residence times on the DNA molecule.

Publications with acknowledged DOE support:

[1] Y. Wang, X. Liu, D. Whitmore, W. Xing, and E. O. Potma, "Remote multi-color excitation using femtosecond propagating surface plasmon polaritons in gold films," *Opt. Express* **19**, 13454–13463 (2011).

[2] X. Liu, Y. Wang, and E. O. Potma, "Surface-mediated four-wave mixing of nanostructures with counterpropagating surface plasmon polaritons," *Opt. Lett.* **36**, 2348–2350 (2011).

[3] Y. Wang, X. Liu, A. R. Halpern, K. Cho, R. M. Corn, and E. O. Potma, "Wide field, surface-sensitive four-wave mixing microscopy of nanostructures," *Appl. Opt.*, **51** 3305–3312 (2012).

[4] X. Liu, Y. Wang, and E. O. Potma, "A dual-color plasmonic focus for surface-selective four-wave mixing," *Appl. Phys. Lett.* **101**, 081116 (2012).

[5] J. Brocious and E. O. Potma, "Four-wave mixing imaging for material research," *Materials Today*, in press (2013).

Modification of Semiconductor Surfaces monitored by X-ray Photoelectron Spectroscopy

Sylwia Ptasinska

Radiation Laboratory and Department of Physics, University of Notre Dame, Notre Dame, IN 46556
sptasins@nd.edu

There is a clear trend in contemporary semiconductor-based technology to design and fabricate new combinatorial materials by the production of thin oxide and other compound layers in order to achieve specific well defined properties and functionalities. Some materials, whose surface chemistry as determined by their intrinsic surface composition and properties, can be modified by molecular species to eventually find applications, but first these materials need to be understood, refined and controlled during fabrication. Our aim is to obtain a detailed molecular-level understanding of gas-solid surface interaction by means of an X-ray Photoelectron Spectroscopy (XPS) technique. Using this technique, we have been able to successfully investigate electronic and structural properties of monolayer and submonolayer films of small organic molecules, e.g., amino acids, short peptides and nucleobases, deposited on gold and copper surfaces [1,2]. These studies have now been extended to address semiconductor surfaces modified using two different approaches: (i) by exposing a semiconductor surface to Atmospheric Pressure Plasma Jets (APPJs) or (ii) by treating a sample in a near ambient pressure reactor cell of the XPS system.

(i) In recent years, much effort has been devoted to plasma processing, especially through application of APPJs which possess many favorable features over traditional vacuum plasmas, including low temperature, low cost and a great potential to be utilized in different areas such as coating and material functionalization [3-7]. Moreover, substantial progress has been achieved in understanding the atomic structure and electronic properties of silicon oxynitride ($Si_xO_yN_z$) due to development of quantum chemical calculations and experimental technologies [8-9]. It has been established that modifying the chemical composition of such films allows us to tailor the electrical, optical and physical properties. In this work for the first time we demonstrate a method in which a helium (He) APPJ is used for silicon wafer surface treatment to grow an ultra-thin film of $Si_xO_yN_z$. The main focus of present plasma investigations is on maximizing the catalytic effect of the plasma, particularly leading to an increase of the ratio between nitrogen (N) and oxygen (O) signals in the $Si_xO_yN_z$, by using different N-based compounds in the mixture of an He stream. Surface modifications were monitored by recording core-level photoelectron spectra in XPS studies (Fig. 1).

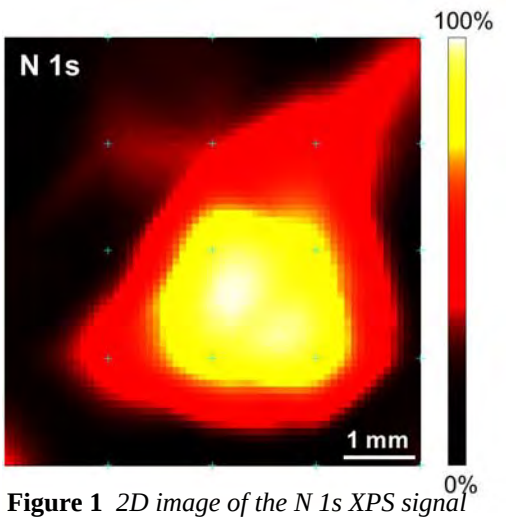

Figure 1 *2D image of the N 1s XPS signal distribution on a silicon wafer substrate treated for 5 minutes by a He/NH_3 APPJ.*

(ii) III-V Semiconductor crystals are widely used throughout the semiconductor industry. Despite this prevalence, a fundamental molecular understanding of the surface interaction between GaAs or GaP and common gaseous molecules such as oxygen, water vapor, and methane is largely unknown. Experimentally, it had proved challenging to probe surface electronic structure of these materials in the pressure range from UHV to atmospheric conditions and the effects of elevated temperatures. Recent advances in surface sensitive techniques, in particular Near Ambient Pressure X-ray Photoelectron Spectroscopy (NAP-XPS) [10], have now allowed the study of Ga-based semiconductors in such environments. Using a chamber-in-chamber design, NAP-XPS was used to track surface chemistry at elevated pressures, up to a few millibar, and at temperatures up to 500 °C.

References:

[1] O. Plekan, V. Feyer, S. Ptasinska, N. Tsud, V. Chab, V. Matolin, K.C. Prince, *Photoemission Study of Thymidine Adsorbed on Au(111) and Cu(110).* J. Phys. Chem. *C 114 (2010) 15036*

[2] V. Feyer, O. Plekan, S. Ptasinska, M. Iakhnenko, N. Tsud, K. Prince, *Adsorption of Histidine and a Histidine Tripeptide on Au(111) and Au(110) from Acidic Solution.* J. Phys. Chem. C 116 (2012) 22960

[3] D. Pappas, *Status and potential of atmospheric plasma processing of materials.* J. Vac. Sci. Technol. A 29 (2011) 020801

[4] J.R. Roth, S. Nourgostar, T.A. Bonds, *The One Atmosphere Uniform Glow Discharge Plasma (OAUGDP) - A Platform Technology for the 21st Century*. IEEE Trans. Plasma Sci 35 (2007) 233

[5] A. Schütze, J.Y. Jeong, S.E. Babayan, J. Park, G.S. Selwyn, R.F. Hicks, *The Atmospheric-Pressure Plasma Jet: A Review and Comparison to Other Plasma Sources.* IEEE Trans. Plasma Sci 26 (1998) 1685-1693

[6] V. Rodriguez-Santiago, L. Vargas-Gonzalez, A.A. Bujanda, J.A. Baeza, M.S. Fleischman, J.H. Yim, D.D. Pappas, *Modification of Silicon Carbide Surfaces by Atmospheric Pressure Plasma for Composite Applications.* ACS Appl. Mater. Interfaces 5 (2013) 4725−4730

[7] D. Mariotti, R.M. Sankaran, *Perspectives on atmospheric-pressure plasmas for nanofabrication.* J. Phys. D: Appl. Phys. 44 (2011) 174023

[8] V. Gritsenko, H. Wong, *Atomic and Electronic Structures of Traps in Silicon Oxynitride.* Critical Review in Solid State and Materials Sciences. 36 (2011) 129-147

[9] S.S. Nekrashevich, V.A. Gritsenko, *Electronic Structure of silicon oxynitride: Ab initio and experimental study, comparison with silicon nitride.* J. App. Phys. 110 (2011) 114103

[10] D. E. Starr, Z. Liu, M. Hävecker, A. Knop-Gericke, H. Bluhm, *Investigation of solid/vapor interfaces using ambient pressure X-ray photoelectron spectroscopy.* Chem. Soc. Rev. 42 (2013) 5833

DOE sponsored publications since 2010:

O. Plekan, V. Feyer, S. Ptasinska, N. Tsud, V. Chab, V. Matolin, K.C. Prince, *Photoemission Study of Thymidine Adsorbed on Au(111) and Cu(110).* J. Phys. Chem. *C 114 (2010) 15036*

E. Alizadeh, D. Gschliesser, P. Bartl, M. Hager, A. Edtbauer, V. Vizcaino, A. Mauracher, M. Probst, T. Maerk, S. Ptasinska, N. Mason, S. Denifl, P. Scheier, *Bond dissociation of the dipeptide dialanine and its derivative alanine anhydride induced by low energy electrons.* J. Chem. Phys. 134 (2011) 054305

F. Ferreira da Silva, S. Ptasińska, S. Denifl, D. Gschliesser, J. Postler, C. Matias, T. D. Märk, P. Limão-Vieira, P. Scheier, *Electron interaction with nitromethane embedded in helium droplets: attachment and ionization measurements.* J. Chem. Phys 135 (2011) 174504

S. Ptasińska, D. Gschliesser, P. Bartl, I. Janik, P. Scheier, S. Denifl, *Dissociative electron attachment to triflates,* J. Chem. Phys. 135 (2011) 214309

S. Jheeta, S. Ptasinska, B. Sivaraman, N. Mason, *The irradiation of 1:1 mixture of ammonia:carbon dioxide ice at 30 K using 1 keV electrons.* Chem. Phys. Lett. 543 (2012) 208

S. Ptasinska, I. Tolbatov, P. Bartl, J. Yurkovich, B. Coffey, D. M. Chipman, C. Leidlmair, H. Schöbel, P. Scheier, N.J. Mason - Electron impact on N2/CH4 mixtures in He droplets, *Probing chemistry in Titan's atmosphere*. RSC Advances, 2 (2012) 10492

V. Feyer, O. Plekan, S. Ptasinska, M. Iakhnenko, N. Tsud, K. Prince, *Adsorption of Histidine and a Histidine Tripeptide on Au(111) and Au(110) from Acidic Solution.* J. Phys. Chem. C 116 (2012) 22960

S. Jheeta, A. Domaracka, S. Ptasinska, B. Sivaraman, N. Mason, *The Irradiation of pure CH_3OH and 1:1 Mixture of NH_3:CH_3OH Ices at 30 K using Low Energy Electrons*. Chem. Phys. Lett. 543 (2013) 208

M. Klas, S. Ptasinska, *Characteristics of N_2 and N_2/O_2 atmospheric pressure glow discharges.* Plasma Sources Sci. Technol. 22 (2013) 025013

X. Han, M. Klas, Y. Liu, S.M. Stack, S. Ptasinska, *DNA damage in oral cancer cells induced by nitrogen atmospheric pressure plasma jets.* Appl. Phys. Lett. 102 (2013) 233703

Richard J. Saykally; Department of Chemistry, University of California *and*
Chemical Sciences Division, Lawrence Berkeley National Laboratory
Berkeley, CA 94720-1460
saykally@berkeley.edu *http://www.cchem.berkeley.edu/rjsgrp/index.html*

Spectroscopy of Liquids and Interfaces

Program Scope or Definition

The goal of this project is to explore, develop, and apply novel methodologies for atom-specific characterization of liquids, solutions, and and their interfaces, employing combinations of liquid microjet technology with synchrotron X-ray and Raman spectroscopies, and to apply nonlinear optical spectroscopy and close connection with state-of-the-art theory for characterization of electrolyte interfaces, seeking to establish the general principles that govern interfacial behavior and of liquid-vapor and solid-liquid interfaces and fundamental processes such as evaporation and surface adsirption.

Recent Progress

Towards a Complete Molecular Mechanism for Ion Adsorption to Aqueous Interfaces [4,5]

As a route to clarifying the mechanism that selectively drives ions to and away from the air/water interface, we have measured the temperature dependence of the adsorption free energy of the thiocyanate ion by UV resonant SHG spectroscopy. Adsorption of aqueous thiocyanate ions from bulk solution to the liquid/vapor interface was measured as a function of temperature . The resulting adsorption enthalpy and entropy changes of this prototypical chaotrope were both determined to be negative. This surprising result is supported by molecular simulations, which clarify the microscopic origins of observed thermodynamic changes. Calculations reveal energetic influences of adsorbed ions on their surroundings to be remarkably local. Negative adsorption enthalpies thus reflect a simple repartitioning of solvent density among surface, bulk, and coordination regions. A different, and much less spatially local, mechanism underlies the concomitant loss of entropy. Simulations indicate that ions at the interface can significantly bias surface height fluctuations even several molecular diameters away, imposing restrictions consistent with the scale of measured and computed adsorption entropies. Based on these results, we expect an ion's position in the Hofmeister lyotropic series to be determined by a combination of driving forces associated with the pinning of capillary waves and with a competition between ion hydration energy and the neat liquid's surface tension.

Characterization of Ion Pairing Between Like-charged Ions in Aqueous Solution[1]

We have recently reported[1] the observation and characterization of "contact pairing" between positively charged ions in aqueous solution, using the combination of synchrotron X-ray spectroscopy of liquid microjets and first principles' theory. The ion(guanidinium-$CN_3H_6^+$) is very important in biology, used routinely as a protein denaturant, and comprising the side chain of one of the 20 natural amino acids(arginine). The cation-cation pairing is driven by the solvent(water) binding energy. The planar guanidinium ions form strong N-H donor hydrogen bonds in the plane of the molecule, but weak acceptor hydrogen bonds with the pi electrons orthogonal to the plane. When fluctuations bring the solvated ions near each other, the strong van der Waals attraction between the pi electron clouds squeezes out the wekly held water molecules, which move into the bulk solution and form much stronger hydrogen bonds with other waters. This mechanism is similar to that recently identified as responsible for weakly hydrated molecules residing at the surface of aqueous solutions .

Contact pairing between guanidinium ions in water had been predicted theoretically by a number of methodologies, but never definitively observed before. The observation by X-ray spectroscopy et al may set a general precedent for such unexpected behavior. For example, mobility studies have evidenced an affinity of guanidinium ions for polymers of arginine, and it is known that arginine interacts strongly with nucleotides. So perhaps "Like charges attract!" may become an accepted paradigm for aqueous solutions.

Towards a Predictive Theory of Water Evaporation [2,17]

Liquid microjet technology affords the opportunity to study the details of water evaporation, free from the obfuscating effects of condensation that have plagued previous studies. Studying small (diameter < 5 μm) jets with Raman thermometry, we find compelling evidence for the existence of a small but significant energetic barrier to evaporation, in contrast to most current models. Studies of heavy water indicate a similar evaporation coefficient, and thus an energetic barrier similar to that of normal water[. A transition state model developed for this process provides a plausible mechanism for evaporation in which variations in libration and translational frequencies account for the small observed isotope effects. The most important practical result of this work is the quantification of the water evaporation coefficient (0.6), which has been highly controversial, and is a critical parameter in models of climate and cloud dynamics. A molecular-level description of the mechanism for water evaporation has been developed by the Chandler group using their TPS methodology for simulating such rare events, and a paper has recently been published by them.

We have measured the effects of ionic solutes on water evaporation rates. Ammonium sulfate, the most common ionic solute in atmospheric aerosols, was shown to have no statistically significant effect on the rate, whereas sodium perchlorate effected a 25% reduction. Most recently, the presence of acetic acid-a surface active component of natural aerosols- was likewise shown not to effect significant changes in the evpaoration rate.

Towards a Complete Understanding of CO_2 – Carbonate Equilibria [6]

The dissolution of carbon dioxide in water and the ensuing hydrolysis reactions are of profound importance for understanding the behavior and control of carbon in the terrestrial environment. Using liquid microjet technology, the first X-ray absorption spectra of aqueous carbonate have been measured as a function of pH to characterize the evolution of electronic structure of carbonate, bicarbonate, carbonic acid and dissolved CO2. The corresponding carbon K-edge core-level spectra were calculated using a first-principles electronic structure approach which samples molecular dynamics trajectories. Measured and calculated spectra are in excellent agreement. Each species exhibits similar, but distinct, spectral features which are interpreted in terms of the relative C–O bond strengths, molecular configuration, and hydration strength. This work provides benchmarks for future studies of this system.

Electronic Structure of Aqueous Borohydride: A Potential Hydrogen Storage Medium [7,8]

With large weight percent hydrogen capacity, stable reactants, and benign reaction products, borohydride salts have been considered as good prospects for transportable hydrogen storage materials, with molecular hydrogen released via hydrolysis. We examine details of the hydration of sodium borohydride by the combination of X-ray absorption spectroscopy of liquid microjets and first principles' theory. Compared to solid sodium borohydride, the aqueous sample exhibits an uncharacteristically narrow absorption feature that is shifted to lower energy, and ascribed to the formation of dihydrogen bonds between borohydride and water that weaken the boron–hydrogen covalent bonds. Water also acts to localize the highly excited molecular orbitals of borohydride, causing transitions to excited states with p character to become more

intense and a sharp feature, uncharacteristic of tetrahedral molecules, to emerge. The simulations indicate that water preferentially associates with borohydride on the tetrahedral corners and edges.

Towards a Predictive Theory of Core-Level Molecular Spectra {9-12,14-16]

The development of near edge X-ray absorption fine structure spectroscopy (NEXAFS) of liquid microjets has provided a useful new tool for characterizing the details of solvation for increasingly complex systems. NEXAFS probes the unoccupied molecular orbitals, which are highly sensitive to intermolecular interactions. This new approach to the study of liquids is yielding important insights into the behavior of aqueous systems, but the chemical information that can be extracted from the measurements is currently limited by the reliability of available theoretical methods for computing core-level spectra. The accurate description of an absorption event of several hundreds of eV of energy is an ongoing challenge in theoretical chemistry. In collaboration with LBL scientist David Prendergast, we are using the excited core hole (XCH) method recently developed by Prendergast and Galli to compute the NEXAFS spectra of prototype systems and compare the results with experimental spectra measured at the ALS.

Using liquid microjets to avoid the often incapacitating problem of radiation damage to fragile solutes has enabled the measurement of pH-dependent NEXAFS spectra of amino acids, including glycine, proline, lysine, and the tripeptide triglycine, as well as ATP and peptoid molecules. This, in turn, has permitted the study of the effets of selected salts on polypeptide conformations, with the aim of elucidating the origins of Hofmeister effects in biology.

Future Plans

1. Develop a microfluidics-based mixing system for generating short lived species, e.g. carbonic acid, in liquid microjets for study by X-ray spectroscopy. Apply this technology to the study of hydration and hydrolysis of carbon dioxide, nitrogen oxides, and sulfur oxides.
2. Complete the XAS study of ionic perturbation of local water structure, such that the entire Hofmeister series is ultimately addressed. We seek a comprehensive picture of the effects of both cations and anions on the local structure of water. Raman spectroscopy measurements will also be performed on these systems, the data from which provide complementary insights and aid in the theoretical modeling.
3. Extend our studies of amino acid hydration vs. pH to include all natural amino acids. Use the same approach to continue the study of hydration of the peptide bonds in small polypeptides, nucleotide bases, nucleosides, and nucleotides, as well as the novel “peptoid” molecules.
4. Explore the generality of like-charge ion pairing in aqueous solution by examining other candidate systems, such as arginine-guanadinium and arginine-arginine.
5. Temperature dependences for surface adsorption of some other prototype salts will be measured, as we work with the Geissler group to develop a general understanding and predictive theory of the forces that drive some ions to the surface and repel others.
6. Extension of these measurements to solid/liquid interfaces will be explored, seeking to develop ways to study electrode interfaces.

References (DOE supported papers: 2010-present) – 17 total

[available at http://www.cchem.berkeley.edu/rjsgrp/opening/pubs.htm]

1. Shih, O., England, A.H., Dallinger, G.C., Smith, J.W., Duffey, K.C., Cohen, R.C., Prendergast, D., and Saykally, R. J. "*Cation-Cation Contact Pairing in Water: Guanidinium" J. Chem. Phys* ***139,*** Article Number: 035104 DOI: 10.1063/1.4813281 Published: JUL 21 2013.

2. *Duffey, K.C., Shih, O., Wong, N.L., Drisdell, W.S., Saykally, R.J., and Cohen, R.C. "Evaporation kinetics of aqueous acetic acid droplets: effects of soluble organic aerosol components on the mechanism of water evaporation"*Phys. Chem. Chem. Phys.* ***2013*****,** 15 (28), 11634 - 11639. *Cover Article.1]
3. Saykally, R.J. "Air/Water Interface: Two Sides of the Acid Base Story" *Nature Chem.* **5,**82-84*,* 2013.
4. D.E. Otten, R. Onorato, R. Michaels, J. Goodknight, R. J. Saykally "Strong Surface Adsorption of Aqueous Sodium Nitrite as an Ion Pair," *Chem. Phys. Lett.* **519-520**, 45-48 (2012).
5. *D.E. Otten, P. Shaffer, P. Geissler, R.J. Saykally "Elucidating the Mechanism of Selective Ion Adsorption to the Liguid Water Surface," PNAS **109** (3), 701-705 (2012). *featured in Editor's Choice *Science* **335,** 505(2012), "Sacrifices at the Surface".
6. *A. H. England, A. M. Duffin, C. P. Schwartz, J. S. Uejio, D. Prendergast, and R. J. Saykally "On the Hydration and Hydrolysis of Carbon Dioxide," *Chem. Phys. Letters* **514,** 187(2011)*Cover Article.
7. *A. M. Duffin, A. H. England, C. P. Schwartz, J. S. Uejio, G. C. Dallinger, O. Shih, D. Prendergast, and R. J. Saykally "Electronic Structure of Aqueous Borohydride: A Potential Hydrogen Storage Medium" *Phys. Chem. Chem. Phys.*, **13**, 17077 (2011) *Cover Article.
8. A. Duffin, C. Schwartz, A. England, J. Uejio, D. Prendergast, and R.J. Saykally, "pH-Dependent X-ray Absorption Spectra of Aqueous Boron Hydrides," *J. Chem. Phys.* **134**, 154503 (2011).
9. C.P. Schwartz, S. Fatehi, R.J. Saykally, and D. Prendergast, "The importance of electronic relaxation for intercoulombic decay in aqueous systems," *Phys. Rev. Lett.* **105,** 198102 (2010).
10. C.P. Schwartz, R.J. Saykally, and D. Prendergast, "An analysis of the NEXAFS spectra of molecular crystal: α-glycine," *J. Chem. Phys.* **133,** 044507 (2010).
11. D. Kelly, C.P. Schwartz, J.S. Uejio, A.M. Duffin, A.H. England, and R.J. Saykally, "Near edge x-ray absorption fine structure spectroscopy of aqueous adenosine triphosphate at the carbon and nitrogen K-edges," *J. Chem. Phys.* **133,** 101103-101106 (2010).
12. C.P. Schwartz, J.S. Uejio, A.M. Duffin, A.H. England, D. Kelly, D. Prendergast, and R.J. Saykally, "Investigation of Protein Conformation and Interactions with Salts via X-ray Absorption Sectroscopy," *PNAS* **107,** 14008-14013 (2010).
13. G.N.I. Clark, C.D. Cappa, J.D. Smith, R.J. Saykally, and T. Head-Gordon "The Structure of Ambient Water," *Mol. Phys.* **108,** 1415-1433 (2010).
14. C.P. Schwartz, J.S. Uejio, A.M. Duffin, W.S. Drisdell, J.D. Smith, and R.J. Saykally, "Soft X-ray Absorption spectra of aqueous salt solutions with highly charged cations in liquid microjets," *Chem. Phys. Lett.* **493,** 94-96 (2010). LBNL-3897E
15. J.S. Uejio, C.P. Schwartz, A.M. Duffin, A.H. England, D. Prendergast, And R.J. Saykally, "Monopeptide versus Monopeptoid: Insights on Structure and Hydration of Aqueous Alanine and Sarcosine via X-ray Absorption Spectroscopy," *J. Phys. Chem. B* **114,** 4702(2010). LBNL-3896E
16. S. Fatehi, C.P. Schwartz, R.J. Saykally, and D. Prendergast, "Nuclear quantum effects in the structure and lineshapes of the N_2 NEXAFS spectrum," *J. Chem. Phys.* **132,** 094302-094309 (2010). LBNL-3895E
17. W.S. Drisdell, R.J. Saykally, and R.C. Cohen, "Effect of Surface Active Ions on the Rate of Water Evaporation," *J. Phys. Chem.C* **114,** 11880-11885 (2010).

Molecular Theory & Modeling

Development of Statistical Mechanical Techniques for Complex Condensed-Phase Systems

Gregory K. Schenter
Physical Sciences Division
Pacific Northwest National Laboratory
902 Battelle Blvd.
Mail Stop K1-83
Richland, WA 99352
greg.schenter@pnnl.gov

The long-term objective of this project is to advance the development of molecular simulation techniques to better understand the relation between the details of molecular interaction and the prediction and characterization of macroscopic collective properties. This involves the investigation of representations of molecular interaction as well as statistical mechanical sampling techniques. Molecular simulation has the promise to provide insight and predictive capability of complex physical and chemical processes in condensed phases and interfaces. It is also serves as the foundation for understanding complexity in systems with broken symmetry, hierarchical structures, and multiple length and time scales. Our focus has been the transport and reactivity of species in aqueous solutions, at designed surfaces, in clusters and in nanostructured materials that play significant roles in problems important to the Department of Energy. This includes the design, control and characterization of catalytic systems for energy storage and conversion.

In our development of molecular simulation methods we seek the balance between efficiency and accuracy in the description of molecular interaction. We search for the appropriate amount of explicit treatment of electronic structure that allows for efficient sampling of a statistical mechanical ensemble of a system of interest. Recently, we have explored the fact that this balance is different for the description of local versus long range collective interaction. Furthermore, the requirements for bulk, homogeneous systems are less stringent than systems with broken symmetries, such as vacuum/liquid, liquid/solid, and liquid/liquid interfaces or highly concentrated electrolytes.

Including this detail provides a more accurate and robust description of the multipole structure of the charge density of molecules and their polarization and charge transfer response. We have been exploring the extent that empirical potentials can be modified to take these effects into account, through point polarizability or flexibility. We have also been exploring empirical corrections to semi-empirical (NDDO) theory [a,4] and DFT [b] that make these approaches both accurate and tractable. Recently, we have discovered that a Density Functional Theory (DFT) description of molecular interaction provides a quantitative representation of the short-range interaction and structure when compared to Extended X-ray Absorption Fine Structure (EXAFS) measurements. In these studies we generated a statistical ensemble of configurations using the electronic structure based description of molecular interaction. From this ensemble, a series of electron multiple scattering calculations are performed using the FEFF9 code [c] to generate a configuration average EXAFS spectra to compare to experimental measurement. This MD-EXAFS approach is used in References 1,2,5,6, and 7.

Many of our past studies involved characterizing the solvation structure about anions. In contrast, recently we have investigated metal cation solvation using MD-EXAFS. In this case the

subtle balance between charge transfer, bonding, solvation structure and thermodynamics must be recovered in descriptions of molecular interaction. In our studies we take advantage of symmetry-dependent, multiple edge analysis (K- and L- edge) of the EXAFS spectra. This provides unique insights into the symmetry of the first hydration shell. Certain multiple scattering paths are only weakly allowed at the K- or L1-edge (s-electrons) but fully allowed for the L2- or L3-edges (2p-electrons). We explored a series of first-row transition metals [6]. In this work we collaborate with Eric Bylaska at PNNL and John Weare at University of California, San Diego. We invoke MD sampling of a Perdew-Burke-Ernzerhof (PBE) DFT functional. The DFT-MD-EXAFS results quantitatively reproduce the EXAFS measurements. The simulation reproduces the peak shapes in the 1-2 Å region, reproducing the first peak in the metal-O radial distribution function. Furthermore, the agreement in the multiple scattering region at 2 to 4 Å is exceptional. (See Figure 1.) In addition, we explored the role of including exact exchange in a QM/MM DFT-MD-EXAFS analysis using a PBE0 functional. These same MD-EXAFS techniques have been used to elucidate the solvation structure of actinides, Cm [1] and U [5].

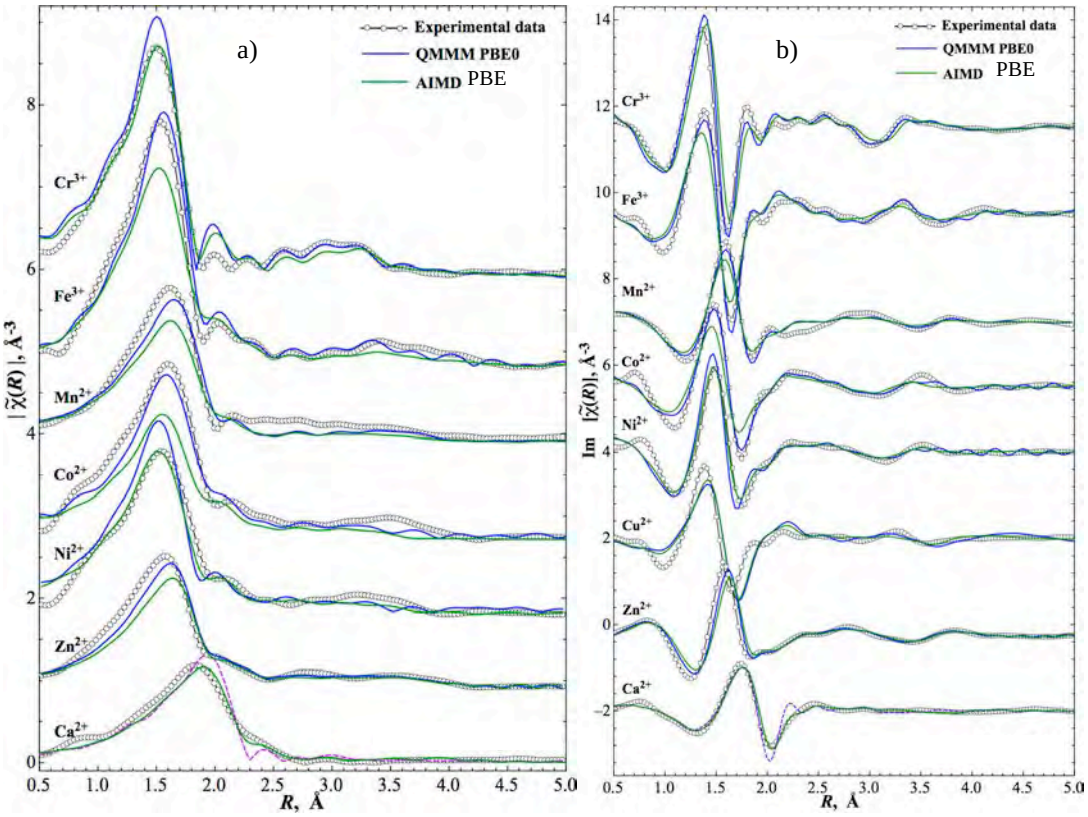

Figure 1. k^2-weighted MD-EXAFS-generated a) $\left|\tilde{\chi}(R)\right|$ and b) $\mathrm{Im}\,\tilde{\chi}(R)$ plots for various metal ions are compared to experimental data. The sets of spectra have been offset for clarity. The MD-XAFS result for a well-parametrized classical potential (dashed purple line) is included in the plot for Ca^{2+}.

As MD-EXAFS provides an effective benchmark of the local structure, and x-ray and diffraction provide an effective benchmark of long-range collective structure, future efforts will concentrate on systems that can be studied using both techniques. We will seek consistency

between both measurements and molecular statistical mechanical simulation. In our studies we will look for collective variables that effectively characterize and distinguish both local and long-range structure. As an example of our approach, in Figure 2 we display some preliminary X-ray diffraction as well as MD-EXAFS results for bulk water, comparing DFT and recent empirical potentials, including HBB2-pol, TTM3F and the Dang-Chang models. We are currently examining the agreement between DFT and various empirical potentials and HBB2-pol for a variety of different simulation conditions. Interestingly, the HBB2-pol agrees better (as compared to DFT) for the main features of the HEXS spectra and DFT agrees better than HBB2-pol in the main features of the measured EXAFS data. These preliminary findings bring into full relief the non-trivial nature of comparing both state-of-the-art simulations and experiments.

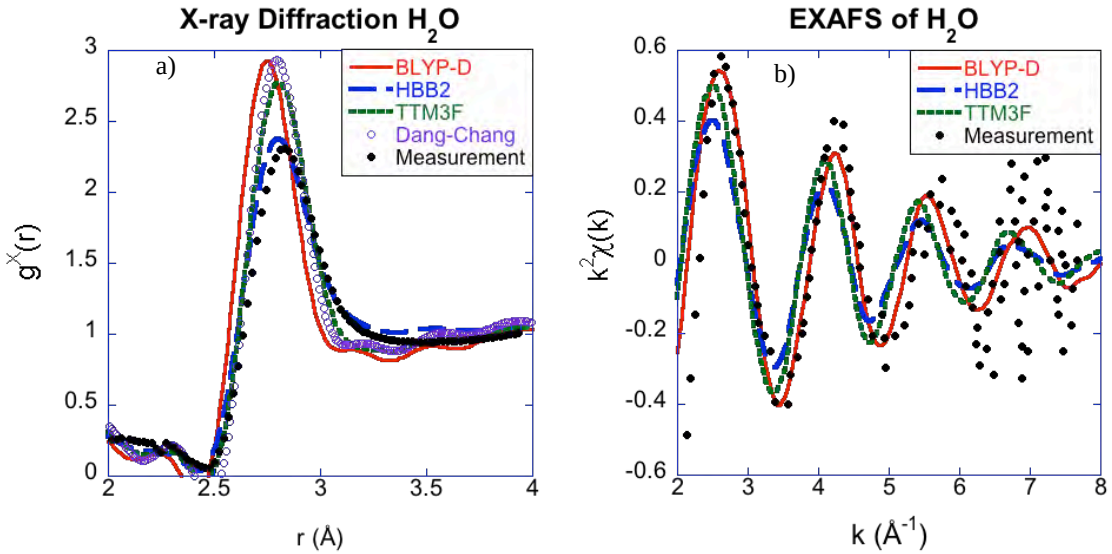

Figure 2 a) X-ray diffraction of water, comparing DFT generated ensemble (BLYP-D), HBB2-pol [d], TTM3F [e], Dang-Chang [f] and Measurement [g] b) EXAFS of water, comparing simulation to Measurement [h].

In the future we will extend these studies to concentrated electrolytes and more complex ions such as the oxyanion series: IO_3^-, BrO_3^-, ClO_3^-, and ClO^-. We will continue to explore the relation of EXAFS analysis to neutron and X-ray diffraction measurements.

Acknowledgements: Direct collaborators on this project include C. J. Mundy, M. Baer and J. Fulton. Interactions with S. S. Xantheas, L. X. Dang and S. M. Kathmann have significantly influenced the course of this work.

This research was performed in part using the computational resources in the National Energy Research Supercomputing Center (NERSC) at Lawrence Livermore National Laboratory. Battelle operates Pacific Northwest National Laboratory for the US Department of Energy.

References

a. D. T. Chang, G. K. Schenter, and B. C. Garrett "Self-consistent polarization neglect of diatomic differential overlap: Application to water clusters," J. Chem. Phys. **128** (16), 164111 (2008).

b. K. A. Maerzke, G. Murdachaew, C. J. Mundy, G. K. Schenter, and J. I. Siepmann, "Self-Consistent Polarization Density Functional Theory: Application to Argon," J. Phys. Chem. A **113** (10), 2075-2085 (2009).
c. J. J. Rehr, R. C. Albers, S. I. Zabinsky, Phys. Rev. Lett. **69**, 3397 (1992); M. Newville, B. Ravel, D. Haskel, J. J. Rehr, E. A. Stern, and Y. Yacoby, Physica B, **208-209**, 154 (1995); A. L. Ankudinov, C. Bouldin, J. J. Rehr, H. Sims, and H. Hung, Phys Rev. B **65**, 104107 (2002).
d. V. Babin, G.R. Medders, and F. Paesani, J. Phys. Chem. Lett **3**, 3765 (2012).
e. G.S. Fanourgakis, S.S. Xantheas, J. Chem. Phys. **128**, 074506 (2008).
f. L.X. Dang and T.M. Chang, J. Chem. Phys. **106**, 8149 (1997).
g. Skinner LB, CJ Benmore, and JB Parise, J. of Phys. Cond. **24**, 338002 (2012).
h. Bergmann U, A Di Cicco, P Wernet, E Principi, P Glatzel, and A Nilsson JCP **127**, 174504 (2007); Wikfeldt KT, M Leetmaa, A Mace, A Nilsson, and LGM Pettersson JCP **132**, 104513 (2010).

References to publications of DOE sponsored research (2011-present)

1. R. Atta-Fynn, E. J. Bylaska, G. K. Schenter, and W. A. de Jong, "Hydration Shell Structure and Dynamics of Curium(III) in Aqueous Solution: First Principles and Empirical Studies," J. Phys. Chem. A **115** (18), 4665-4677 (2011).
2. M. D. Baer, V. T. Pham, J. L. Fulton, G. K. Schenter, M. Balasubramanian, and C. J. Mundy, "Is Iodate a Strongly Hydrated Cation?," J. Phys. Chem. Lett. **2** (20), 2650-2654 (2011).
3. S. M. Kathmann, I. F. W. Kuo, C. J. Mundy, and G. K. Schenter, "Understanding the Surface Potential of Water," J. Phys. Chem. B **115** (15), 4369-4377 (2011).
4. G. Murdachaew, C. J. Mundy, G. K. Schenter, T. Laino, and J. Hutter, "Semiempirical Self-Consistent Polarization Description of Bulk Water, the Liquid-Vapor Interface, and Cubic Ice," J. Phys. Chem. A **115** (23), 6046-6053 (2011).
5. R. Atta-Fynn, D. F. Johnson, E. J. Bylaska, E. S. Ilton, G. K. Schenter, and W. A. de Jong, "Structure and Hydrolysis of the U(IV), U(V), and U(VI) Aqua Ions from Ab Initio Molecular Simulations," Inorg. Chem. **51** (5), 3016-3024 (2012).
6. J. L. Fulton, E. J. Bylaska, S. Bogatko, M. Balasubramanian, E. Cauet, G. K. Schenter, and J. H. Weare, "Near-Quantitative Agreement of Model-Free DFT-MD Predictions with XAFS Observations of the Hydration Structure of Highly Charged Transition-Metal Ions," J. Phys. Chem. Lett. **3** (18), 2588-2593 (2012).
7. S. Bogatko, E. Cauet, E. Bylaska, G. Schenter, J. Fulton, and J. Weare, "The Aqueous Ca^{2+} System, in Comparison with Zn^{2+}, Fe^{3+}, and Al^{3+}: An Ab Initio Molecular Dynamics Study," Chem.-Eur. J. 19 (9), 3047-3060 (2013).

SOFT X-RAY SPECTROSCOPY AND MICROSCOPY OF INTERFACES UNDER *IN SITU* CONDITIONS

David K. Shuh, Hendrik Bluhm, Mary K. Gilles
Chemical Sciences Division, Lawrence Berkeley National Laboratory, Berkeley, CA 94720
DKShuh@lbl.gov; HBluhm@lbl.gov; MKGilles@lbl.gov

I. Program Scope

A fundamental, molecular level understanding of interfaces is essential for energy research since their physical and chemical properties influence system performance. The scientific program at the Molecular Environmental Sciences (MES) Beamline focuses on interfacial processes under realistic conditions of gas pressure and composition, temperature, and electrical bias. The scanning transmission X-ray microscope (STXM) is ideal for obtaining spatially resolved molecular information on materials important for energy sciences. The ongoing development of *in situ* reaction cells will enable measurements under reactive gas flow and liquid samples. The ambient pressure X-ray photoelectron spectroscopy (APXPS) instruments complement the STXM through their capability to investigate the interfaces of liquid and solid samples under reaction conditions, at pressures of up to 20 Torr. The high surface sensitivity of APXPS (~ 1 nm), combined with the range of tailored *in situ* cells, allows the correlation of the surface chemistry of a solid or liquid with other reaction parameters, such as yield and conversion. These unique capabilities at the MES beamline enable cutting-edge research on *in operando* interfacial chemistry, which is described in detail below.

II. Recent Progress

A. Surface Chemistry of Metal and Metal Oxides

The interaction of surfaces with trace gases (e.g., NO_x, SO_x, CO, CO_2, CH_4, O_3, and OH*) in the presence of ambient relative humidity (RH) governs processes in heterogeneous catalysis, the environment, and electrochemistry. To understand the physical chemistry at the surface of minerals, aerosols, and oxide supports for modern multiphase catalysts, fundamental information on basic properties such as the onset RH for surface hydroxylation and the thickness of water layers as a function of RH are crucial. The presence of hydroxyl and/or water molecules at the interface may alter its reactivity with trace gas species, and influence electronic and ionic conductivity, friction, and adhesion. Ultrathin oxide films are model systems for oxide supports in heterogeneous catalysis. In particular thermally grown Al_2O_3/NiAl(110) is utilized as a support for metal nanoparticles in model catalysis studies. We have investigated the reaction of water vapor, an important product in oxidation reactions, with Al_2O_3/NiAl(110) ultrathin films. APXPS measurements were done over the pressure range from ultra-high vacuum up to a RH of 10%. A sharp onset in the oxide/hydroxide film thickness at a RH of about 0.01% to 0.1 % is observed (see Fig. 1). This

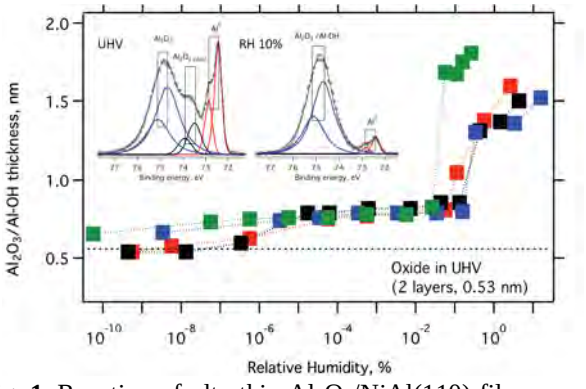

Fig. 1. Reaction of ultrathin Al_2O_3/NiAl(110) films as a function of RH. The insets show Al 2p APXPS spectra under ultra-high vacuum and in 10% RH.

most likely results from dissociation of water molecules that subsequently react with Al from the metal substrate. The onset of water dissociation at about 0.01% RH agrees with our previous studies on other oxide surfaces (Fe_2O_3, Fe_3O_4, MgO) and points to a common mechanism for the hydroxylation of metal oxides. The coverage of the oxide surfaces at low RH by a hydroxyl layer needs to be considered when modeling the reactivity of metal oxides in heterogeneous reactions.

B. In operando spectromicroscopy of heterogeneous interfaces

While the research described above focuses on the investigation of water adsorption on well defined, homogeneous single crystal surfaces, most realistic interfaces are chemically and morphologically heterogeneous. To address the need for high spatial spectroscopic measurements on heterogeneous interfaces, we designed, fabricated, and tested a compact gas-phase reactor for *in situ* STXM measurements. It was designed specifically for measurements under water vapor at realistic relative humidities but can accommodate other gases. To minimize uncertainties, an on-board sensor measures the RH and temperature inside the reactor. The reactor reduces X-ray absorption from the process gas by over 85% compared to experiments that fill the STXM chamber with process gas. This allows data collection at full instrumental resolution, minimizes radiation dose to the sample, and results in much more stable imaging conditions, all of which are essential for further in situ studies.

C. Metal Ion Solution Chemistry

The metal ion liquid phase research draws on insights from recent soft X-ray STXM studies on model solid-state metal oxyanions. The effects of coordination and charge donation, factors that will be encountered in solution to an even larger degree, have been successfully measured. A vital component of the metal ion solution effort was theory and computational developments, which is in particularly important for data obtained in the presence of solvents where the interpretation of the experimental results is more complex. Progress in this area was made to understand the detailed aspects of electron donation and withdrawal to metal ion centers by ligands, both simple and complex, in relevant solid state materials that will in part form the pre-requisite knowledge base from which to interpret soft X-ray spectra obtained from the liquid phase.

III. Future Plans

A. Competition between water vapor and reactive gases on surfaces

The role of defect sites in reactions with CO_2 and other trace gases as a function of RH with oxide and metal surfaces will be examined. In the case of cubic metal oxides (such as MgO) the surface chemistry of (100) surfaces (mostly terrace sites) will be compared to (310) surfaces, which exhibit a high concentration of step sites. A compelling line of inquiry is how the presence of water vapor might promote or prevent the direct interaction of trace gases with substrate surfaces. Molecular dynamics simulations suggest that in such cases small molecules (such as HCl and CO_2) will diffuse only to a position between the first and second adsorbed water layer, but not reach the liquid/solid interface. These findings, if experimentally verified, are critical for the understanding of chemical reactions of, e.g., pollutants with airborne particles in a humid environment, and for carbon capture and sequestration by minerals and rocks. By using higher kinetic energy photoelectrons to penetrate several nanometers into liquid films we can explore directly the adsorption of solution ions at the liquid/solid interface. Strategies

for performing these technically challenging experiments will be developed and proof-of-principle measurements performed.

B. Relative humidity (RH) effects on chemical reactions and phase separation

In the atmosphere, aerosols encounter a wide range of RH, which can control the surface chemical composition, and ultimately govern aerosol reactivity. The role of RH in liquid-liquid phase separation will be examined using the *in situ* STXM reactor. Mixtures of salts and organics (surrogates for atmospheric aerosols) will be exposed to increasing RH to monitor mixing and deliquescence. The extent of mixing and any potential chemical composition gradients across the particles can be probed and the effect of phase-transitions on chemistry explored. Recent studies showed that volatile liquid phase reaction products (e.g., HCl) could be released during dehydration. With hydration-dehydration cycling, relatively weak acid reactions can be driven by the loss of products during the liquid-solid phase transition.

C. Metal Ion Solution Chemistry

New ground in the application of soft x-ray synchrotron radiation near-edge X-ray absorption fine structure can be made by probing metal ion solution chemistry employing *in situ* cells. This bridge into solution chemistry will yield new information on the nature of chemical bonding in metal ion solution species and solvent effects, while establishing a foundation for longer term objectives of probing the electronic structure and chemistry of specifically-selected molecular species originating from solution. The initial metal ion species systems include solution phase measurements of selected symmetric metal (Ti, Cr, Al, Si, Hf) alkoxide species $[M(OR)_x(R')_y]$ for which the multiple bond nature of the metal oxygen bond is not yet understood. Solid-state analogs of the metal alkoxides with different countercations replacing the R groups should prove worthwhile for comparison.

Synergistic activities: The PIs are organizing a workshop on "Soft X-ray Spectroscopy of Heterogeneous Interfaces" at the 2013 ALS User Meeting to engage CPIMS scientists at the MES Beamline. Related to this effort is an AGU Meeting session on “Chemical Imaging Analysis of Atmospheric Particles”, organized by M. K. Gilles (December 9-13, San Francisco, CA), and a Physical Chemistry session at the 2013 Western Regional ACS Meeting in Santa Clara, October 3-6, 2013, organized by H. Bluhm (with M. Ahmed and O. Gessner).

The ALS is supported by the Director, Office of Science, Office of Basic Energy Sciences, and the MES Beamline 11.0.2 is supported by the Director, Office of Science, Office of Basic Energy Sciences, Division of Chemical Sciences, Geosciences, and Biosciences (CSGB) Condensed Phase and Interfacial Molecular Sciences (CPIMS) program, both of the U.S. Department of Energy at LBNL under Contract No. DE-AC02-05CH11231.

Selected Recent Beamline Publications 2012-2013 (supported by or in part by the Director, Office of Science, Office of Basic Energy Sciences, Division of CSGB and/or the CPIMS program of the CSGB [1-17]

1. Balmes, O.; Resta, A.; Wermeille, D., *et. al.*: Reversible Formation of a PdCx phase in Pd Nanoparticles. *Phys .Chem. Chem. Phys.* **2012**, *14*, 4796.

2. Bartels-Rausch, T.; Jacobi, H.-W.; Kahan, T. F., *et. al.*: Snow Microstructure and Physical and Chemical Processes. *Atmos. Chem. Phys. Discuss.* **2012**, *12*, 30409.
3. Cheng, M. H.; Callahan, K. M.; Margarella, A. M., *et. al.*: Ambient Pressure XPS and Molecular Dynamics Simulation Studies of Liquid/Vapor Interfaces of Aqueous NaCl, RbCl, and RbBr Solutions. *J. Phys. Chem. C* **2012**, *116*, 4545.
4. Chueh, W. C.; McDaniel, A. H.; Grass, M. E., *et. al.*: Highly Enhanced Concentration and Stability of Reactive Ce_3^+ on Doped CeO_2 Surface Revealed In Operando. *Chem. Mater.* **2012**, *24*, 1876.
5. Crumlin, E. J.; Mutoro, E.; Liu, Z., *et. al.*: Surface Strontium Enrichment on Highly Active Perovskites for Oxygen Electrocatalysis in Solid Oxide Fuel Cells. *Energ. Environ. Sci.* **2012**, *5*, 6081.
6. El Gabaly, F.; McDaniel, A. H.; Grass, M., *et. al.*: Intermediate Species in H_2 Oxidation on Solid Electrolytes. *Chem. Commun.* **2012**, *48*, 8338.
7. Jiang, P.; Prendergast, D.; Borondics, F., *et. al.*: Investigation of the Electronic Structure of Cu_2O and CuO Thin Films on Cu(110) Using XPS and Absorption Spectroscopy. *J. Chem. Phys.* **2013**, *138*, 024706.
8. Kaya, S.; Schlesinger, D.; Yamamoto, S., *et. al.*: Highly Compressed Two-Dimensional Form of Water at Ambient Conditions. *Sci. Rep.* **2013**, *3*, 1074.
9. Kelly, S. T.; Nigge, P.; Prakash, S., *et. al.*: An Environmental Sample Chamber for Reliable Scanning Transmission X-ray Microscopy Measurements Under Water Vapor. *Rev. Sci. Inst.* **2013**, *84*, 073708.
10. Kendelewicz, T.; Kaya, S.; Newberg, J. T., *et. al.*: X-ray Photoemission and Density Functional Theory Study of Water Vapor with the Fe_3O_4(001) Surface at Near-Ambient Conditions. *J. Phys. Chem. C* **2013**, *117*, 2719.
11. Krepelova, A.; Bartels-Rausch, T.; Brown, M. A., *et. al.*: Adsorption of Acetic Acid on Ice Studied by Ambient-Pressure XPS and Partial-Electron-Yield NEXAFS Spectroscopy at 230-240 K. *J. Phys .Chem. A* **2013**, *117*, 401.
12. Laskin, A.; Moffet, R. C.; Gilles, M. K., *et. al.*: Tropospheric Chemistry of Internally Mixed Sea Salt and Organic Particles: Surprising Reactivity of NaCl with Weak Organic Acids. *J. Geophys. Res.-Atmos.* **2012**, *117*, 15302.
13. Minasian, S. G.; Keith, J. M.; Batista, E. R., *et. al.*: Covalency in Metal-Oxygen Multiple Bonds Evaluated Using Oxygen K-edge Spectroscopy and Electronic Structure Theory. *J. Am. Chem. Soc.* **2013**, *135*, 1864.
14. Rosseler, O.; Sleiman, M.; Montesinos, V. N., *et. al.*: Chemistry of NO_x on TiO_2 Surfaces Studied by Ambient Pressure XPS: Products, Effect of UV Irradiation, Water, and Coadsorbed K+. *J. Phys. Chem. Lett.* **2013**, *4*, 536.
15. Shavorskiy, A.; Eralp, T.; Schulte, K., *et. al.*: Surface Chemistry of Glycine on Pt{111} in Different Aqueous Environments. *Surf. Sci.* **2013**, *607*, 10.
16. Starr, D. E.; Bluhm, H.: CO Adsorption and Dissociation on Ru(0001) at Elevated Pressures. *Surf. Sci.* **2013**, *608*, 241.
17. Zhang, C. J.; Grass, M. E.; Yu, Y., *et. al.*: Multielement Activity Mapping and Potential Mapping in Solid Oxide Electrochemical Cells Through the Use of Operando XPS. *ACS Catal.* **2012**, *2*, 2297.

Generation, Detection and Characterization of Gas-Phase Transition Metal Containing Molecules (DE-FG02-04ER15603)

Timothy C. Steimle
Department of Chemistry and Biochemistry
Arizona State University
Tempe, Arizona 85287-1604
E-mail: tsteimle@asu.edu

I. Program Scope

The objective of this project is to generate, detect, and characterize small, gas-phase, metal containing molecules. In addition to being relevant to high temperature chemical environments (e.g. plasmas and combustion), gas-phase experiments on metal containing molecules serve as the most direct link to a molecular-level theoretical model for catalysis. In principle, simple gas-phase reactions, such as Pt + CH_4, can be modeled to the same level of accuracy that is now being achieved for lighter systems such as F + CH_4 (Bowman, J. M. et al. *PCCP* **2011**, *13*, 8094) and the same molecular level insight into chemical reactions garnered. The theoretical formulism for predicting reaction cross sections for these simple reactions involves using quasi-classical trajectory methods in conjunction with an accurately calculated, multi-dimensional, potential energy surface (PES). The major limitation for extending the formalism used for the lighter systems to metal containing systems is the current inability to generate high quality PES. Careful evaluation of the performance of the various electronic structure methodologies being developed for PES predictions can be achieved via a comparison of predicted and experimentally measured properties. The small molecules that we study are the species associated with the bound portions of the multi-dimensional PES. Metals atoms or clusters are, in general, more reactive than their condensed phase counterparts. Thus, gas-phase studies in themselves will not reveal all aspects of hetero- or homogeneous catalysis. Fortunately, the conceptual framework developed by the experiential/theoretical synergism established for the simple gas-phase systems will be applicable to modeling the chemistry of the more extended systems.

The ground and excited electronic state properties we determine are: a) electronic state distributions and lifetimes, b) vibrational frequencies, c) bond lengths and angles, d) hyperfine interactions, e) permanent electric dipole moments, $\vec{\mu}_{el}$, and f) magnetic dipoles, $\vec{\mu}_{m}$. In general terms, $\vec{\mu}_{el}$ gives insight into the charge distribution and $\vec{\mu}_{m}$ into the number and nature of the unpaired electrons. Analysis of the hyperfine interactions (i.e. Fermi-contact, nuclear electric quadrupole, etc.) is particularly insightful because it results from the interaction of nuclei with non-zero spin and the chemically important valence electrons. The bulk of the spectroscopic techniques used in these studies exploit the sensitivity of laser induced fluorescence (LIF) detection. The spectroscopic schemes employed include: a) cw and pulsed laser field-free(FF) excitation and dispersed LIF (DLIF); b) optical Stark; c) optical Zeeman; d) pump/probe microwave double resonance (PPMODR); e) fluorescence lifetimes, and f) resonant and non-resonant two-photon ionization TOF mass spectrometry. Vibrational spacing, force constants and electronic states distributions are derived from the analysis of pulsed dye laser excitation and DLIF spectra. Geometric structure (bond lengths and angles) and hyperfine parameters are derived from the analysis of cw-laser LIF and PPMODR spectra. Permanent electric dipole moments, $\vec{\mu}_{el}$, and magnetic dipole moments, $\vec{\mu}_{m}$, are derived from the analysis of optical Stark and Zeeman spectra, respectively. Transition moments are derived from the analysis of radiative lifetimes. A supersonic molecular beam sample of these ephemeral molecules is generated by skimming the products of either a laser ablation/reaction source or a d.c. discharge source.

II. Recent Progress

1. Iridium Containing Molecules: IrF, IrSi, IrH and IrO

Iridium is one of the rarest transition metal elements in the earth's crust and yet is of great technological importance. For example, iridium organometallic complexes are particularly important as catalysts for a wide range of organic syntheses and as a media for light emitting electrochemical cells. The utility of iridium organometallic complexes is due, in part, to their thermal and chemical stability, and high efficiency for triplet to singlet state conversion due to the large spin-orbit coupling (SOC) of the Ir(III) centers. Increasingly, the design of new iridium organometallic complexes is assisted by high-level electronic structure predictions that must account for large SOC and other relativistic effects.

We have undertaken a systematic study of bonding in IrX (X=H,F,C,O and Si) molecules. In the case of IrF (Publ. #1), we recorded and analyzed the ^{191}Ir (I_1 =3/2), ^{193}Ir (I_1 =3/2) and ^{19}F (I_2 =1/2) hyperfine interactions and used the hyperfine parameters to develop a molecular orbital correlation description for ground state bonding. More recently, we reported (Publ. # 8) on the analysis of the (6,0)[16.0]1.5 - $X^2\Delta_{5/2}$ and (7,0)[16.0]3.5- $X^2\Delta_{5/2}$ bands of IrSi. This project was a collaboration with Prof. Stanton's group (Chemistry, U. Texas- Austin) who is developing new, fully relativistic, computational methodologies. Fine, magnetic hyperfine, and nuclear quadrupole hyperfine parameters for the $X^2\Delta_{5/2}(v=0)$, [16.0]1.5(v=6) and [16.0]3.5 (v=7) states of the ^{191}IrSi and ^{193}IrSi isotopologues were determined and predicted. The observed optical Stark shifts were also analyzed to produce $\vec{\mu}_{el}$ values of -0.414(6)D and 0.782(6)D for the $X^2\Delta_{5/2}$ and [16.0]1.5 (v=6) states, respectively. The determined reduced dipole moment ($\equiv \vec{\mu}_{el}/r_e$) for IrSi, along with those we previously determined for IrC, IrN, and IrF, are plotted as a function of the difference of the electronegativity of Ir (2.20) and the electronegativities (Pauling scale) of Si (=1.90), C (=2.55), N (=3.04), and F (=3.98) in Figure 1. The near linear dependence predicts, as observed, that the charge distribution for IrSi is $Ir^{\delta-}Si^{\delta+}$.

We are currently analyzing the field-free, optical Stark and optical Zeeman spectra of IrO, IrH and IrD and collaborating with Prof. Stanton's group, who is attempting to predict the ground state properties for these highly relativistic molecules.

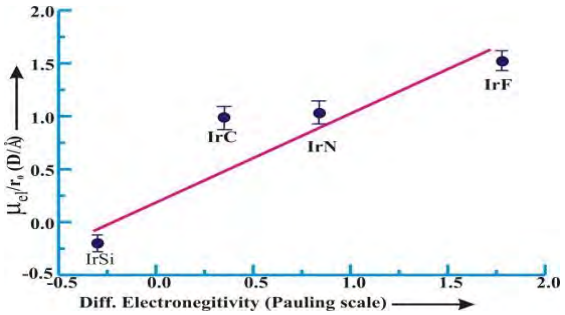

Fig. 1. Our measured reduced dipole moments ($\equiv \vec{\mu}_{el}/r_e$) for the series of Ir-containing molecules plotted as a function of the difference in electronegativities. Note that the charge distribution of IrSi is $Ir^{\delta-}Si^{\delta+}$ (i.e. Si is more electrophilic than Ir).

2. U-Containing Molecules :UF

A description of bonding in the actinides is very complicated because of simultaneous *d*- and *f*-orbital contribution and the massive relativistic effects. Previously, in collaboration with Prof. Heaven's group (Emory University), we experimentally determined the $\vec{\mu}_{el}$ values and magnetic *g*-factors for the ground and two excited electronic states of uranium monoxide, UO (*J. Chem. Phys.* **2006,** *125*, 204314/1). Recently, Heaven's group reported on the analysis of the visible, medium resolution, LIF, DLIF and REMPI spectra, and a supporting theoretical prediction, of UF (*J. Phys. Chem. A*, (accepted)). Using this as a basis we have: a) recorded the high resolution field free spectra;

b) recorded the optical Stark spectra (Figure 2), and c) the optical Zeeman spectra (Figure 3). The small splitting of the field-free spectra is due to the ^{19}F hyperfine interaction. The analyses are in progress.

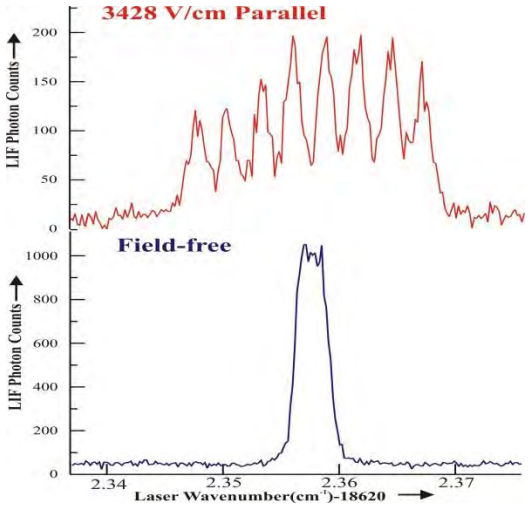

Fig. 2. The field-free (lower) and Stark (upper) spectra of the P(4.5) line of the [18.6]3.5-X(1)4.5 transition of UF.

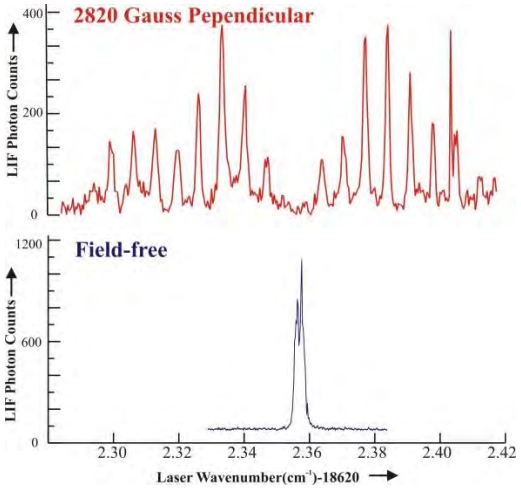

Fig.3. The field-free (lower) and Zeeman (upper) spectra of the P(4.5) line of the [18.6]3.5-X(1)4.5 transition of UF.

3. Microwave Spectroscopy of Metal Containing Molecules: RuC

Compared to that 5*d*-metal containing molecules, the 4*d* analogues should pose less of a challenge for computational methodologies. Here we tested this hypothesis via an experimental and theoretical study of RuC. Some time ago we recorded and analyzed the field-free and optical Stark spectra of the (0.0)[18.1]$^1\Pi \leftarrow X\ ^1\Sigma^+$ band system of RuC (*J. Chem. Phys.* **2003,** *118,* 2620). The 30 MHz spectral resolution was insufficient to fully resolve the hyperfine interaction. Here the PPMODR technique, which has a 30 kHz resolution, was implemented to precisely determine the rotational, B_0, and hyperfine parameters. Prof. Stanton's group will predict these parameters using the X2C relativistic approach. The pure rotational spectrum for the $J=2 \leftarrow J=1$, $F=9/2 \leftarrow F=7/2$ transition of the ^{101}RuC isotopologue is presented in Figure 4.

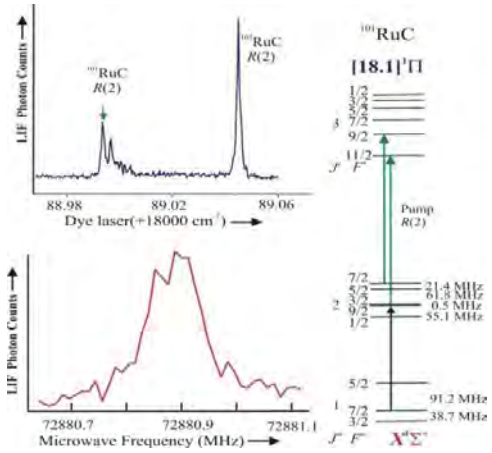

Fig. 4. The $J=2 \leftarrow J=1$, $F=9/2 \leftarrow F=7/2$ pure rotational transition of ^{101}RuC in its $X\ ^1\Sigma^+$ (v=0) state. The transition was detected as an increase in the LIF signal as a function of swept microwave frequency. The blended $F=9/2 \leftarrow F=7/2$ and $F=11/2 \leftarrow F=11/2$ components of the R(2) line of the [18.1]$^1\Pi \leftarrow X\ ^1\Sigma^+$ band, which is marked with "←", was used for the optical pumping and probing in the PPMODR method.

III. Future Plans

A. Buffer Gas Cooled Source for the Study of Metal Dioxides and Dicarbides

As demonstrated in our high-resolution studies of ZrO_2 (Publ. 1) and TiO_2 (*PCCP* **2010,** *12*, 12018) the spectra of even simple polyatomic free radicals produced using the current supersonic molecular beam source (SSMB) source are extremely complex and in some cases uninterruptable. The current SSMB source will be replaced by a slow, cold, mono-energetic, molecular beam source based upon cryogenic buffer gas cooling (BGMB), which is schematically represented in Figure 5. Great simplification of the spectra of polyatomic molecule is expected due to the lowering of the internal temperature, T_I, from the current value of 20K to the 2K of a BGMB source. The narrower spread in kinetic energy, $\langle \Delta v \rangle$, and will also be beneficial. This source will be used to study late metal containing dioxides and dicarbides (e.g.IrX_2, PtX_2 AuX_2, ThX_2 and UX_2; X=C and O)

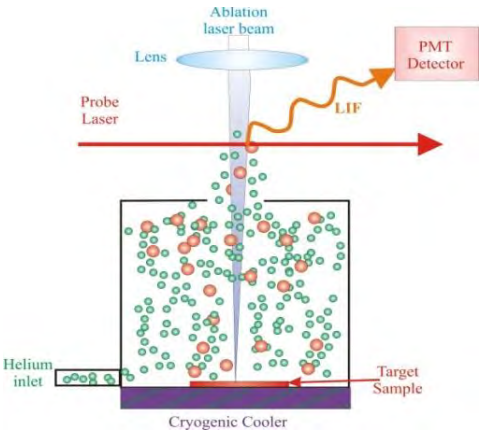

Figure 5. The proposed BGMB source to be used for the generation of an intense, ultra-cold, slow moving, molecular beam. The molecules and clusters are generated using laser ablation of a solid target (e.g. zirconia for the production of ZrO_2). The helium buffer gas is cooled by collisions with the wall of the container which are held at 4K by a closed cycle refrigerator. Further cooling to 2K is achieved during the expansion out of the container.

Publications of DOE sponsored research - 2011-present:

1. "Hyperfine interaction in the $A^3\Phi_4$ and $X\,^3\Phi_4$ states of iridium monofluoride, IrF" C. Linton, X. Zhuang T. C. Steimle, and Allen Adam, J. Chem. Phys. (2011) **135** 034305.
2. " The visible spectrum of zirconium dioxide, ZrO_2", Anh Le, Timothy C. Steimle, Varun Gupta, Corey A. Rice, John P. Maier, Sheng H. Lin, and Chih-Kai Lin, J. Chem. Phys. (2011)) **135** 104303.
3. "The Pure Rotational Spectrum of Platinum Monocarbide, PtC" Chengbing Qin, Ruohan Zhang, Fang Wang and Timothy C. Steimle, Chem. Phys. Lett. 535,40 (2012).
4. "Optical Stark Spectroscopy of the 2_0^6 $\widetilde{A}^1A'' - \widetilde{X}^1A'$ Band of Chloro-Methylene, HCCl", T.C. Steimle, F. Wang, X. Zhuang and Z. Wang J. Chem. Phys. **136**, 114309 (2012) .
5. "The Zeeman effect in holmium monoxide" C. Linton, T.C. Steimle and H. Wang, J. Mol. Spectrosc. **275**, 15-20 (2012).
6. "The permanent electric dipole moment and hyperfine interactions in platinum monofluoride" C. Qin, R. Zhang, F. Wang and T.C. Steimle, J. Chem. Phys. **137(5)**, 054309/1-054309/9 (2012).
7. "A Molecular-Beam Optical Stark and Zeeman Study of the [17.8])+-$X^1\Sigma^+$ (0,0) band of AuF" Timothy C. Steimle, Ruohan Zhang, Chengbing Qin and Thomas D. Varberg ; Journal of Physical Chemistry A, (accepted and available online)
8. "Hyperfine Interactions and Electric Dipole Moments in the [16.0]1.5(v=6), [16.0]3.5(v=7) and $X^2\Delta_{5/2}$ States of Iridium Monosilicide, IrSi" Anh Le, Timothy C. Steimle, Michael Morse, Maria A. Garcia, Lan Cheng and John F. Stanton ; Journal of Physical Chemistry A, (accepted and available online)

A Single-Molecule Approach for Understanding and Utilizing Surface and Subsurface Adsorption to Control Chemical Reactivity and Selectivity

E. Charles H. Sykes
(charles.sykes@tufts.edu)
Department of Chemistry
Tufts University
62 Talbot Ave
Medford, MA 02155

Program Scope:

Hydrogen activation, uptake and reaction are important phenomena in heterogeneous catalysis, fuel cells, hydrogen storage devices, materials processing, and sensing. The third year of the research program has been focused on understanding the adsorption, diffusion and spillover of hydrogen in a number of systems. Much attention has been devoted to materials that exhibit facile activation and weak binding of hydrogen, as these properties lead to the best energy landscape for storage or chemical reactivity. We designed well-defined Pd, Co, Au and Cu surfaces and nanoparticles to be amenable to high resolution scanning probe studies, X-ray photoelectron spectroscopy, and chemical analysis of adsorbate binding, diffusion and reaction [1-17]. We discovered a new phenomena that we term the "molecular cork effect," which allows the hydrogen spillover pathway from atomic Pd dissociation sites to Cu reaction sites to be controlled via molecular adsorption [1,9,14]. This effect enables us to create a non-equilibrium form of hydrogen, weakly bound to Cu but prevented from desorbing from the surface. In related work, by studying Co nanoparticles we discovered a previously unreported but catalytically relevant high coverage phase of hydrogen that could only be formed by virtue of the Co/Cu interface sites [2,3]. These types of alloy systems allow us to address previously unobtainable structures, densities and phases of hydrogen due to the limitations of single crystal work in ultra-high vacuum. By understanding the energy landscape for hydrogen activation, adsorption and spillover we have been able to generate catalytically relevant high coverage hydrogen phases and to trap hydrogen on surfaces beyond its normal desorption point yielding novel catalytic intermediates.

Recent Progress and Future Plans:

A New Method for Controlling Spillover; the Molecular Cork Effect

Spillover is a common method by which a reagent can be activated at one location and then reacted at another, and it is commonly invoked to explain the synergistic relationship between metals in an alloy or metal/metal oxide mixtures. The traditional view of these processes involves molecules adsorbing somewhat uniformly over a surface, migrating to preferred/active sites, then either reacting or desorbing. For example, in heterogeneous catalysis hydrogen spillover from metal particles to reducible oxide supports is implicated as an important step in a variety of reactions including hydrogenations, hydroisomerizations, and methanol synthesis. Hydrogen spillover has also been shown to significantly enhance the performance of hydrogen storage materials such as metal organic frameworks, zeolites and many carbon-based nanostructures. Despite these advances, the mechanism of spillover in most systems remains poorly understood, and with the exception of hydrogen bridges in storage systems, methods for mediating the spillover pathway do not exist. We discovered a system in which the uptake and release of hydrogen from a copper surface occurs solely through 1% of the surface sites which are individual,

isolated, catalytically active palladium atoms [1,9,14]. **Figure 1** illustrates that the surface can either be kept free of hydrogen by pre-adsorption of carbon monoxide or that hydrogen can be trapped on the surface by post-adsorption [1]. In this way the coverage of the surface as a whole can be controlled by the addition of a single molecule to a minority atomic-scale site which we term a *molecular cork* effect. This non-equilibrium effect can be used to produce superheated hydrogen atoms, a more reactive form than regular surface bound hydrogen. We also demonstrate in a model system that the molecular cork effect could offer a new method for mediating the kinetics of hydrogen uptake and release from storage materials that rely on spillover from small metal particles. By using the superheated hydrogen created by the molecular cork effect, our future work will focus on tuning the selectivity of hydrogenation reactions, taking advantage of the controllable residence time of hydrogen on the Cu(111) surface.

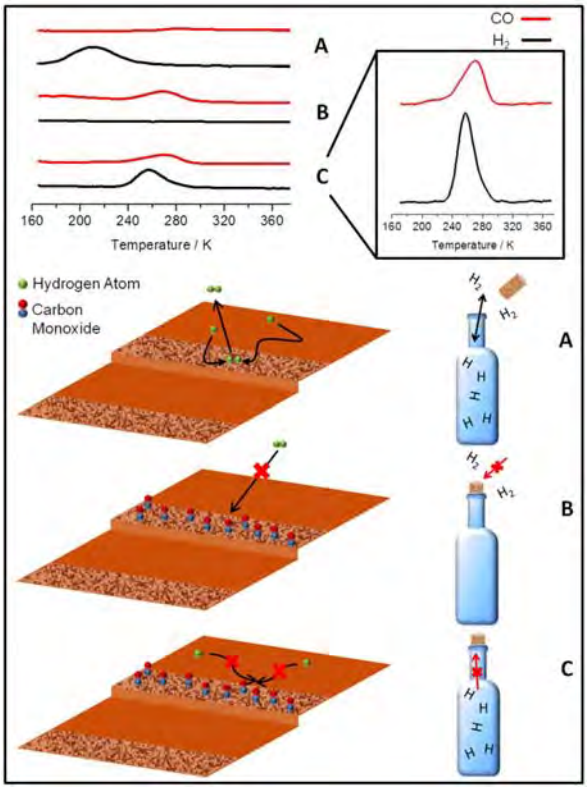

Figure 1. *The molecular cork effect. Temperature programmed desorption spectra a: In the absence of CO, hydrogen desorption occurs from the 1% Pd/Cu surface at 210 K. Spectra b: Pre-dosing CO inhibits the uptake of hydrogen. Spectra c: Deposition of CO after hydrogen uptake leads to higher temperature (260 K) hydrogen desorption.*

New Hydrogen Phases on Cobalt Nanoparticle Surfaces

The dissociative adsorption of hydrogen on cobalt is central to a number of catalytic reactions, yet to date, there are relatively few studies examining this important process. We have utilized Co nanoparticles grown on Cu(111), instead of the traditional planar Co single crystals, to study a more catalytically-relevant form of Co (**Figure 2**) [2,3,8]. Using scanning tunneling microscopy we discovered different phases of H on the close-packed Co nanoparticle surfaces with a range of densities [3]. Our data reveal a so-far unreported high coverage phase of H with a (1x1) structure, which is only amenable to surface science techniques via a nanoparticle model system with a high step to terrace ratio. We also found that, in contrast to the low density phases, the H-(1x1) structure can only be formed at an intermediate temperature, indicating that compression to this higher-density phase is activated [3,8]. This work is the first to report on higher coverage (> 0.75 ML) phases of H on Co, which are undoubtedly important in catalytic systems at elevated pressure, and spillover from step edges to the terrace sites should play a critical role in populating reaction sites on the Co close-packed nanoparticle surfaces. Thus, we demonstrate that the coverage of H on Co nanoparticles may, in fact, be much higher than previously expected from single crystal work, especially considering the elevated pressures that are employed during catalysis. We have further investigated the interaction of these H phases with CO [8], and we hope to use this system elucidate the atomic-scale details of CO hydrogenation. Additionally, our preliminary results indicate that the Co/Cu interface sites may facilitate H spillover from Co to Cu, which could provide another novel molecular cork system with which to study hydrogenations.

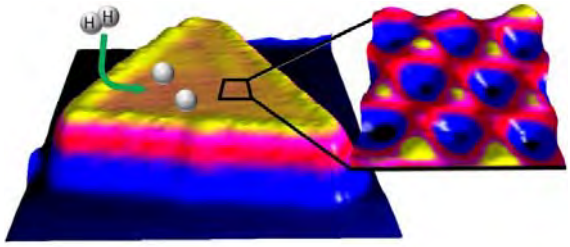

Figure 2. *STM images of the the 2H-(2x2) overlayer structure on a triangular Co nanoparticle. Hydrogen atoms appear in STM images with alternating contrast, as can be seen in the high resolution inset, depending on which three-fold hollow site they occupy.*

Quantum Tunneling Enabled Motion, Interaction and Assembly of Hydrogen on Cu(111):

The weak binding of hydrogen to Cu enables a variety of selective hydrogenation reaction chemistry. We have demonstrated that diffusion of both H and D on Cu(111) at low temperature is enabled primarily by quantum tunneling (**Figure 3**) [4]. We also showed the tunneling-enabled self-assembly of H(D) atoms, which can be explained in terms of local attractive pairwise interactions between atoms and leads to cluster formation. This stabilization also results in a slower rate of diffusion of clusters, as explicitly shown in the case of D. In the case of H, which diffuses fast due to its higher tunneling probability, pairs are formed which then aggregate into large islands that remain intact but constantly change in shape. D clusters, in contrast, have a much slower tunneling rate; hence, large scale self-assembly of D clusters was not observed over the timescale of our experiments. Given the difference in tunneling rates, we would presumably have to watch a D atom sample at 5 K for a period of >10,000 hours in order to directly observe the same large scale self-assembly of islands of D clusters as was seen for H. What is perhaps most remarkable about our experiment is that unlike a thermally assisted self-assembly process in which higher order structures are “frozen out” as the temperature drops, quantum tunneling occurs down to 0 Kelvin. All the H atoms in the structures we observe are subject to constant quantum tunneling driven motion but the self assembled islands persist in a dynamic state and actually grow over time. To our knowledge, this study represents the first evidence for quantum-mechanical-tunneling enabled self-assembly of any species. Furthermore, the complex ordering behavior of H(D) atoms on a Cu(111) surface give new physical insight into this important species on a catalytically-relevant surface, revealing a very different picture of the geometry of H as compared to all other metal surfaces studied to date.

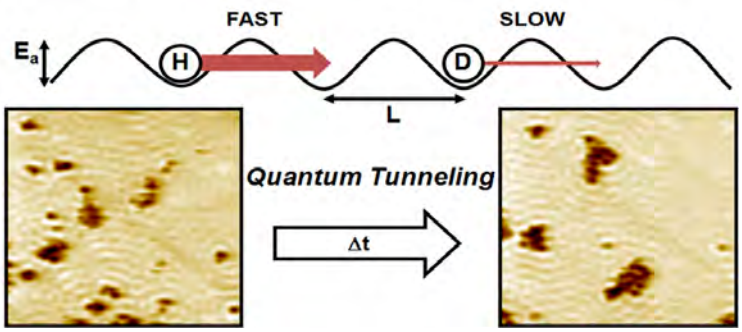

Figure 3. *Time-lapse STM imaging reveals the quantum tunneling mediated aggregation of H atoms into large clusters on a copper surface.*

DOE-Sponsored Research Publications (2010–2013):

1) "Controlling the Spillover Pathway with the Molecular Cork Effect" M. D. Marcinkowski, A. D. Jewell, M. Stamatakis, M. B. Boucher, E. A. Lewis, C. J. Murphy, G. Kyriakou and E. C. H. Sykes - ***Nature Materials***, 2013, *12*, 523-528
2) "Visualization of Compression and Spillover in a Coadsorbed System: Syngas on Cobalt Nanoparticles" E. A. Lewis, D. Le, A. D. Jewell, C. J. Murphy, T. S. Rahman and E. C. H. Sykes - ***ACS Nano***, 2013, *7*, 4384-4392
3) "Dissociative Hydrogen Adsorption on Close-Packed Cobalt Nanoparticle Surfaces" E. A. Lewis, D. Le, C. J. Murphy, A. D. Jewell, M. F. G. Mattera, M. L. Liriano, T. S. Rahman and E. C. H. Sykes - ***Journal of Physical Chemistry C***, 2012, *116*, 25868-25873 [Cover Story]
4) "Quantum Tunneling Enabled Self-Assembly of Hydrogen Atoms on Cu(111)" A. D. Jewell, G. Peng, M. F. G. Mattera, E. A. Lewis, C. J. Murphy, G. Kyriakou, M. Mavrikakis and E. C. H. Sykes - ***ACS Nano***, 2012, *6*, 10115-10121
5) "Viewing and Inducing Symmetry Breaking at the Single-Molecule Limit" H. L. Tierney, A. D. Jewell, A. E. Baber, E. V. Iski and E. C. H. Sykes - ***Chirality***, 2012, *24*, 1051-1054
6) "Hydrogen Bonding and Chirality in Functionalized Thioether Self-Assembly" - A. F. McGuire, A. D. Jewell, T. J. Lawton, C. J. Murphy, E. A. Lewis and E. C. H. Sykes - ***Journal of Physical Chemistry C***, 2012, *116*, 14992-14997
7) "Molecular-Scale Surface Chemistry of a Common Metal Nanoparticle Capping Agent: Triphenylphosphine on Au(111)" - A. D. Jewell, E. C.H. Sykes and G. Kyriakou - ***ACS Nano***, 2012, *6*, 3545-3552
8) "Rediscovering Cobalt's Surface Chemistry" E. A. Lewis, A. D. Jewell, G. Kyriakou, E. C. H. Sykes - ***Physical Chemistry Chemical Physics***, 2012, *14*, 7215-7224 [Cover Story]
9) "Isolated Metal Atom Geometries as a Strategy for Selective Heterogeneous Hydrogenations" - G. Kyriakou, M. B. Boucher, A. D. Jewell, E. A. Lewis, T. J. Lawton, A. E. Baber, H. L. Tierney, M. Flytzani-Stephanopoulos and E. C. H. Sykes - ***Science***, 2012, *335*, 1209-1212
10) "Controllable Restructuring of a Metal Substrate: Tuning the Surface Morphology of Gold" E. V. Iski, A. D. Jewell, H. L. Tierney, G. Kyriakou and E. C. H. Sykes - ***Surface Science***, 2012, *606*, 536-541
11) "Visualization of Hydrogen Bonding and Associated Chirality in Methanol Hexamers" T. J. Lawton, J. Carrasco, A. E. Baber, A. Michaelides and E. C. H. Sykes - ***Physical Review Letters***, 2011, *107*, 2561011-2561015
12) "Asymmetric Thioethers as Building Blocks for Chiral Monolayers" A. D. Jewell, H. L. Tierney, O. Zenasni, T. R. Lee and E. C. H. Sykes - ***Topics in Catalysis***, 2011, *54*, 1357-1367
13) "Hydrogen-bonded Networks in Surface-bound Methanol" A. E. Baber, T. J. Lawton and E. C. H. Sykes - ***Journal of Physical Chemistry C***, 2011, *115*, 9157-9163
14) "An Atomic-scale View of Palladium Alloys and their Ability to Dissociate Molecular Hydrogen" A. E. Baber, H. L. Tierney, T. J. Lawton and E. C. H. Sykes – ***ChemCatChem***, 2011, *3*, 607-614
15) "Gently Lifting Gold's Herringbone Reconstruction: Trimethylphosphine on Au(111)" A. D. Jewell, H. L. Tierney, and E. C. H. Sykes – ***Physical Review B***, 2010, *82*, 205401
16) "Dynamics of Molecular Adsorption at Non-Equilibrium Sites" H. L. Tierney, A. D. Jewell, A. E. Baber, E. V. Iski, and E. C. H. Sykes – ***Langmuir***, 2010, *26*, 15350-15355
17) "Adsorption, Assembly, and Dynamics of Dibutyl Sulfide on Au{111}" D. O. Bellisario, A. D. Jewell, H. L. Tierney, A. E. Baber, and E. C. H. Sykes – ***Journal of Physical Chemistry C***, 2010, *114*, 14583-14589

Solvation Dynamics in Nanoconfined and Interfacial Liquids

Ward H. Thompson
Department of Chemistry, University of Kansas, Lawrence, KS 66045
wthompson@ku.edu

Program Scope

There is currently significant interest in nanostructured materials that can confine liquids in nanoscale pores, due to both the appearance of new fundamental phenomena in these systems and their wide range of potential applications, including catalysis, sensing, separations, electrochemistry, and optical materials. However, the design principles are still lacking for the development of such mesoporous (2 nm $\leq$ *diameter* $\leq$ 50 nm) materials for practical applications that take advantage of their large surface area-to-volume ratio and their high degree of tunability through pore size, shape, roughness, and chemical functionality. At the same time, this gap points to the need to improve our fundamental understanding of how complex liquid dynamics can arise from nanoscale confinement and vary strongly with the confining environment properties.

We are addressing some of the outstanding questions regarding these nanoconfined liquid dynamics and the implications for chemical reactions – *i.e.*, *How does a chemical reaction occur differently in a nanoconfined solvent than in a bulk solvent?* – by using solvation dynamics as a basis. Solvation dynamics is closely related to the reaction coordinate for charge transfer reactions such as electron or proton transfer reactions and is often dramatically affected by nanoconfinement.

Recent Progress & Future Plans

Reorientational Dynamics of Nanoconfined and Bulk Hydrogen-bonded Liquids.

Reorientational motion of the solvent molecules is a key component in a wide variety of chemical processes, including solvation dynamics and proton transfer reactions. Thus, it is important to understand how liquid molecules rotate when confined within nanoscale frameworks. We have examined this question by examining the reorientational dynamics of water, methanol, and ethanol in $\sim$ 2.4 nm diameter hydrophilic (OH-terminated) silica pores. The results are generally expressed in terms of a reorientational correlation function, $C_2(t) = \langle P_2[\mathbf{e}(0) \cdot \mathbf{e}(t)] \rangle$ with $\mathbf{e}$ the OH unit vector, which provides a measure of the rotational times of the OH bonds in the liquid. We have previously found[7] that the long-time decay of $C_2(t)$ for water confined in hydrophilic pores, Fig. 1, appears to follow a power law, *i.e.*, $C_2(t) \sim (t/\tau)^{\alpha}$ with exponent $\alpha = -1.1$. In methanol

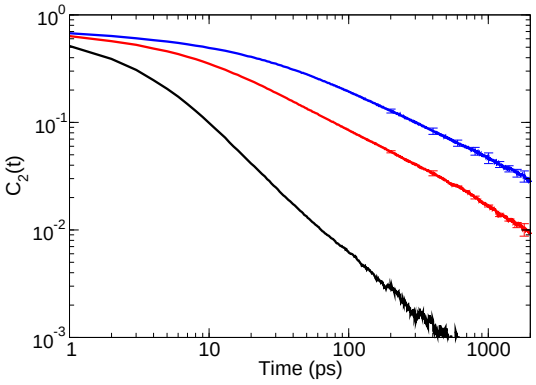

Figure 1: Reorientational correlation function, $C_2(t)$, for water (black), methanol (red), and ethanol (blue) confined in a $\sim$ 2.4 nm hydrophilic silica pore.

and ethanol, the long-time decay appears to also exhibit a power-law decay, but the methanol dynamics are considerably slower than for water and the ethanol dynamics even slower (Fig. 1). These results point to the important role of steric effects that we are continuing to examine.

The origin of this power-law decay is also of considerable interest. We were able to understand some of the origins of the heterogeneity by examining the hydrogen-bond exchange times associated with particularly oxygen atoms on the silica pore surface.[7] We found that the hydrogen-bond exchange for a particular acceptor at the surface can be characterized by a single timescale, the "jump" time, but that those timescales are widely distributed. We can describe the jump time for a particular acceptor based on entropic and enthalpic contributions. In principle both can be estimated with a molecular dynamics simulation, the former by calculating the excluded volume around the acceptor and the latter by determining the hydrogen-bond strength. We are making these estimates to see if the dramatic reorientational heterogeneity can be predicted in this way – without a dynamics simulation – based only on the pore surface interactions and topology. We are further exploring whether the same decomposition of the heterogeneity applies in the case of the simple alcohols, methanol and ethanol, or if the behavior is qualitatively modified due to the presence of steric effects.

The reorientation of nanoconfined alcohols induced us to examine the reorientation of bulk alcohols. Generally for linear alcohols, NMR measurements have found that reorientation is slower the longer the alkyl chain, a result reproduced in molecular dynamics simulations. We have found that the extended jump mechanism developed for water, which predicts that the OH reorientation is governed by the switching of hydrogen-bonding partners and the reorientation of intact hydrogen bonds, also describes reorientation in the lower alcohols (methanol and ethanol).[5] We have extended this analysis to the higher linear alcohols up to 1-hexanol. Generally, in alcohols the hydrocarbon moiety blocks the approach of potential new hydrogen-bond acceptors, significantly slowing down hydrogen-bond exchanges (or jumps). This excluded volume effect naturally increases with the size of the alkyl group; simulations suggest this increase is linear in chain length as shown in Fig. 2. However, the dynamics also become more complex as more than one timescale is necessary to describe the hydrogen-bond exchange dynamics; this is related to the increased structure in the hydrogen-bond patterns of the alcohols as the hydrophobic bulk grows. While for water the hydrogen-bond exchange time is the dominant contribution to OH reorientation, the slower jump dynamics for alcohols means the intact hydrogen bond reorientation becomes the dominant component for methanol and ethanol.[5] However, the intact bond reorientation also slows with alkyl chain length, but quadratically, so that the two contributions are roughly the same for propanol and the hydrogen-bond exchanges again dominate for longer chain alcohols. Thus, the OH reorientation of the different alcohols can all be described

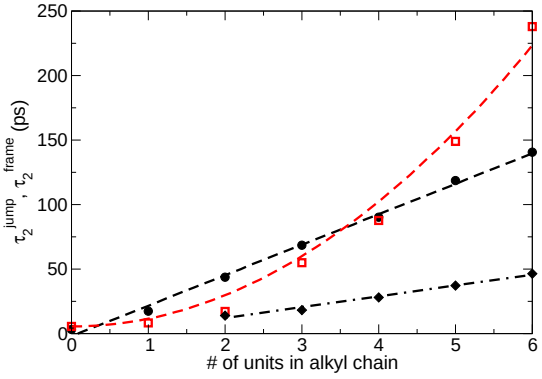

Figure 2: Contributions to the reorientation time from hydrogen-bond exchange (black symbols and lines) and intact hydrogen-bond reorientation (red symbols and line) for water and the linear alcohols.

by two components (exchanges and intact reorientation) but the dominant component changes more than once along the series leading to interesting, non-monotonic trends. We are currently examining branched alcohols to investigate the impact of the specific arrangement of the steric bulk.

Solvation Dynamics in Nanoconfined Solvents.

Solvation dynamics in nanoconfined solvents are generally marked by dramatic changes relative to the corresponding bulk solvent. In particular, long time scales not seen in the bulk solvent – often as long as hundreds of picoseconds or several nanoseconds – are observed in the time-dependent fluorescence signal. A number of models have been proposed to explain the origin of this multi-exponential, long-time decay. However, clear comparisons of theoretical predictions with experimental measurements is lacking as is, by extension, a rigorous test of the models.[3] To address this, we have developed a number of models for both the dye molecule and the confining framework to allow for more general exploration of the phenomena and driving forces involved in TDF experiments, and chemistry in general, in nanoconfined solvents.

We have calculated the free energy for a Stockmayer-type solute as a function of position in atomistic silica pores, using different solute dipole moments.[8] We found that the solute *and* solvent interactions with the pore interface lead to a dependence of the solute position distribution on the solute dipole. This is a general effect – we have observed it not only for this Stockmayer solute in a silica pore, but every system we have examined. It arises fundamentally from the fact that the system Hamiltonian must depend on solute position differently for different solute charge distributions. It can thus be observed even in cases where there are weak solute and solvent interactions with the pore, as illustrated in Fig. 3. The generality of these results indicate that solute position may be a component of the mechanism for a number of chemical processes in nanoconfined solvents. The fact that this effect originates with the solute-pore and solvent-pore interactions further suggests that the confining framework can be tuned to affect the chemistry of the confined liquid. It is less clear whether time-dependent fluorescence measurements are sensitive to this kind of solute dynamics or whether different experimental probes will be needed to fully understand solvation in nanoconfined solvents.

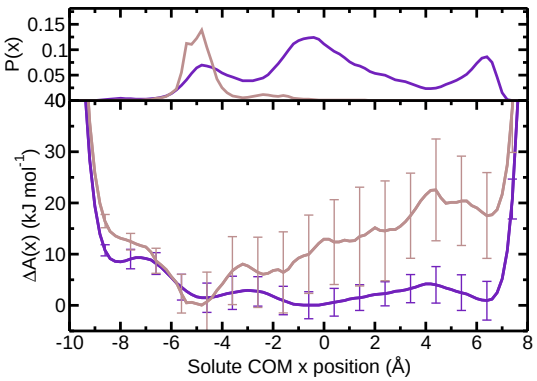

Figure 3: Free energy, $\Delta A(x)$, and probability distribution, $P(s)$, as a function of solute position along a slice across an ethanol-filled hydrophobic silica pore for a 5 D (purple) and 15 D (brown) Stockmayer-type solute.

DOE-Supported Publications (2010 – present)

[1] X. Feng and W.H. Thompson, *J. Phys. Chem. C* **114**, 4279-4290 (2010). "Time-dependent Fluorescence in Nanoconfined Solvents. A Smoluchowski Equation Model Study"

[2] B.J. Ka and W.H. Thompson, *J. Phys. Chem. B* **114**, 7535-7542 (2010). "Nonadiabatic Effects on Proton Transfer Rate Constants in a Nanoconfined Solvent"

[3] W.H. Thompson, *Annu. Rev. Phys. Chem.* **62**, 599-619 (2011). "Solvation Dynamics and Proton Transfer in Nanoconfined Liquids"

[4] B.B. Laird and W.H. Thompson, *J. Chem. Phys.* **135** 084511 (2011). "Time-Dependent Fluorescence in Nanoconfined Solvents: Linear Response Approximations and Gaussian Statistics"

[5] A.A. Vartia, K.R. Mitchell-Koch, G. Stirnemann, D. Laage, and W.H. Thompson, *J. Phys. Chem. B* **115**, 12173-12178 (2011). "On the Reorientation and Hydrogen-Bond Dynamics of Alcohols"

[6] B.J. Ka and W.H. Thompson, *J. Phys. Chem. A* **116**, 832-838 (2012). "Sampling the Transition State of a Proton Transfer Reaction in Mixed Quantum-Classical Molecular Dynamics Simulations"

[7] D. Laage and W.H. Thompson *J. Chem. Phys.* **136**, 044513 (2012). "Reorientation Dynamics of Nanoconfined Water: Power-law Decay, Hydrogen-bond Jumps, and Test of a Two-State Model"

[8] A.A. Vartia and W.H. Thompson, *J. Phys. Chem. B* **116**, 5414-5424 (2012). "Solvation and Spectra of a Charge Transfer Solute in Nanoconfined Ethanol"

Imaging Interfacial Electric Fields on Ultrafast Timescales

William A. Tisdale
Assistant Professor, Department of Chemical Engineering
Massachusetts Institute of Technology, Cambridge, MA 02139
tisdale@mit.edu

Program Scope

The objective of this project is to explore a novel methodology for visualization of ultrafast electronic processes at interfaces. The method, which is based on optical stimulation, builds upon previous success using spontaneous second-order nonlinear optical probes to track the temporal evolution of interfacial electric fields resulting from charge separation across an interface. A goal is to speed signal acquisition by more than six orders of magnitude so that laser scanning ultrafast microscopy becomes feasible. The ultimate aim is to generate movies of interfacial electronic phenomena occurring on femtosecond timescales and submicron length scales, thereby informing our understanding of disorder, heterogeneity, and morphology, and how these factors affect ensemble behavior in photovoltaic, electrochemical, and optoelectronic systems.

Recent Progress

Since receiving our initial funds transfer in July, we have begun work on two parallel fronts: 1) proof-of-principle demonstration of stimulated second harmonic generation, including quantification of the signal enhancement factor and scaling of the signal with fundamental and stimulating field intensities, and 2) synthesis and characterization of materials for future studies of interfacial electron transfer. While work is progressing satisfactorily on both fronts, we have enjoyed the greatest success thus far in synthesizing extremely high-quality colloidal quantum dot materials. Recent examples are shown in Figure 1.

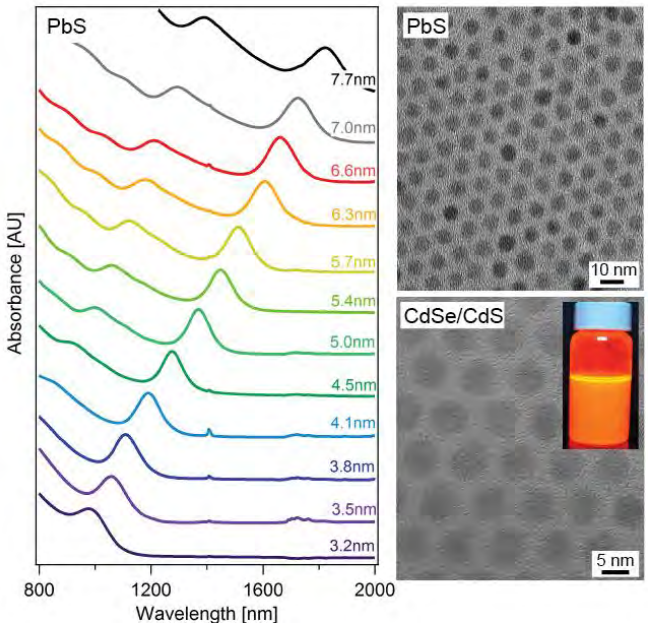

Figure 1 *Characterization of colloidal QDs synthesized in the PI's lab.* (Left) Absorption spectra for a series of highly monodisperse PbS QDs, showing first absorption feature FWHM <60 meV for dots larger than 4.0 nm. (Right, Top) Transmission electron micrograph of PbS QDs. (Right, Bottom) High-resolution transmission electron micrograph of CdSe/CdS core/shell QDs. (Inset) Bright photoluminescence from the CdSe/CdS core/shell QD dispersion.

Future Plans

Construction of the ultrafast laser scanning optical microscope will begin after the arrival of a newly-hired postdoctoral associate funded by the Early Career Award, who is scheduled to begin work at MIT on October 1. Our immediate goal is successful demonstration of the stimulated second harmonic generation technique in a model system.

Structural Dynamics in Complex Liquids Studied with Multidimensional Vibrational Spectroscopy

Andrei Tokmakoff

Department of Chemistry, James Franck Institute, and Institute for Biophysical Dynamics
The University of Chicago, Chicago, IL 60637
E-mail: tokmakoff@uchicago.edu

The ability for water molecules to participate in up to four hydrogen bonds in the condensed phase is what gives liquid water its unique physical and chemical properties. In particular, rapid hydrogen-bond fluctuations and ultrafast energy dissipation make water an unusual solvent, which can facilitate the transport of protons and stabilize the products of a chemical reaction. The importance of these phenomena is evident in biological systems where water aids in biological charge transport and redox chemistry. The goal of our research is to further understand what underlie these processes. We design and develop nonlinear ultrafast infrared spectroscopies to probe the chemical dynamics of water and aqueous solutions. Our work also continues to elucidate the vibrational dynamics and spectroscopy of water that enables the observation of changing hydrogen bonding structures. Over the course of the past year, our work can be divided into three areas: (1) the generation of short pulses of broadband infrared light (BBIR) and use in two-dimensional (2DIR) spectroscopy; (2) the investigation of intra- and intermolecular coupling in the vibrational relaxation process both in neat and isotopically dilute water; and (3) the study of aqueous hydroxide and strong acids to assign particular molecular vibrations to absorptions in the IR and to explore the dynamics of proton transfer in water.

In our effort to experimentally study water dynamics through ultrafast vibrational spectroscopy, the fundamental bandwidth ceiling of optical parametric amplifiers (OPAs) has limited our ability to study different vibrational features in water. Acute issues are foregrounded by the ~1750 cm^{-1} energy gap between the OH stretch and the HOH bend vibrations as well as the broad continuum absorption which span the entire mid-IR in aqueous acids and bases. When one considers these factors, it is obvious that the 350-400 cm^{-1} of bandwidth offered by OPA sources is insufficient for studying vibrational energy relaxation or proton transfer dynamics in water. Using our new Ti:sapphire regenerative amplifier laser system that generates 20 femtosecond 6 mJ pulses centered at 800 nm, we have been able to implement our recent design of a laser plasma source to generate pulses of BBIR for ultrafast pump-probe and 2DIR spectroscopy. The pulses are <70 fs long and have a spectrum spanning the entire mid-IR, from 3800 cm^{-1} to <1000 cm^{-1}.

With this novel light source, we have modified our 2DIR experiment. In this scheme, a pulse pair of two 45 fs pulses from a homebuilt OPA source, centered at 3400 cm^{-1}, vibrationally excites the system and the subsequent response is studied using the BBIR as a probe. The pulse pair consists. Now we are able to correlate vibrations of the OH stretch in water to other molecular vibrations across the mid-IR, allowing us to accurately study vibrational coupling between various modes of drastically different character. We also use a single pump pulse, followed by the BBIR, to measure the transient absorption of the sample after an experimentally controlled time delay. This provides the opportunity to directly observe the redistribution and cascade of energy throughout the various states of the system. Furthermore, since we are always monitoring the entire mid-IR, we have been able to observe excited-state transitions at frequencies at which the linear spectrum shows no absorption.

The natural starting point for this new spectrometer was the study of isotopically dilute HOD in D_2O. We have already extensively characterized this system using narrowband spectroscopy in the context of the hydrogen bond switching mechanism, but questions regarding vibrational relaxation mechanisms remain. In the broadband 2DIR spectrum of HOD, we observed a cross-peak between the

OH stretching mode and the HOD bending mode immediately upon excitation of the OH stretch. In a 2DIR spectrum, the presence of a cross-peak between two vibrations upon excitation of one suggests that the vibrations are strongly coupled; that is, excitation of the OH stretch changes the frequency of the HOD bend. This is somewhat surprising given that the two vibrations are over 1900 cm^{-1} off resonance. From lineshape analysis and the presence of a bend overtone in the linear IR spectrum, we were able to conclude that the vibrations were coupled by Fermi resonance. This is a third-order anharmonic interaction that occurs when the overtone of a vibration is in resonance with the fundamental mode of another. Similarly, we identified another strong Fermi resonance interaction among excited bend and stretch states occurring at a frequency at which the linear spectrum shows no absorption. Fermi resonance interactions play an important role in the relaxation dynamics of the OH stretch. Using broadband transient absorption, we showed that the OH stretch primarily relaxes to the bend on a 320 fs timescale. The population of the bend then decays on a 1 ps timescale, consistent with the relaxation timescale of the D_2O solvent. The disparity between the relaxation timescale of the OH stretch (610 fs) and the time for population transfer to the bend shows that there are in fact multiple paths for relaxation, with the second most likely path being direct relaxation to the solvent. This is evidenced by the immediate response of the solvent upon OH stretch excitation. Finally, using pump-probe anisotropy, we measured a 70° angle between the transition dipole of the OH stretch and HOD bend.

The large bandwidth of the probe frequency has afforded us the opportunity to study the broad absorption features in neat H_2O. In the broadband 2DIR and transient absorption spectra of H_2O, we observed several unique features which differ qualitatively from the observations of other researchers. The most striking feature is the broad excited state absorption between the $\nu = 1$ and $\nu = 2$ states of the OH stretch which is over 1000 cm^{-1} broad and relaxes with a 275 fs time constant. Additionally, the long-time transient absorption spectrum characteristic of a temperature rise grows in on a 722 fs timescale resulting in an appreciable amount of low-frequency mode excitation on timescales faster than the period of oscillation. The extreme broadening and ultrafast energy dissipation indicate that the OH stretching vibrations are not localized to a single bond, but rather, the vibrational wavefunctions are delocalized over many molecules. Theoreticians have explored this idea via simulations, but few experiments have been able to address this delocalization. On the other hand, the rapid growth of the long-time spectrum suggests that it is inappropriate to treat relaxation in the weak coupling limit. We instead attribute the extreme relaxation rate to vibrational non-adiabatic effects and suspect a vibrational conical intersection exists between the OH stretching modes and the low frequency intramolecular motions. The 2DIR spectrum shows, as in HOD, that the OH stretch and bend are strongly coupled. We performed pump-probe anisotropy on the cross-peak to further explore the nature of this coupling. These experiments showed that there was no correlation between the transition dipole orientation of the OH stretch and the HOH bend – consistent with our conclusions regarding the localized nature of the OH stretch.

We are also making use of the broadband probe to continue our study of the role of water in the stabilization and transport of hydroxide ions, focusing on the various solvation structures of the ion in neat H_2O. Whether the hydroxide ion is coordinated by three or four water molecules or whether the proton is equally shared between two oxygen atoms ($H_3O_2^-$) continues to be debated. In addition to the growth of a broad continuum absorption with increasing hydroxide concentration, the linear IR spectrum shows a distinct shoulder on the main OH stretch absorption band at 2850 cm^{-1}. We measured broadband 2DIR spectra to clarify the nature of this shoulder and found that the shoulder had a cross-peak to the main OH stretching band. It also had an extremely broad excited state absorption ranging from 2000 cm^{-1} to well below our detection limit. In order to help assign the vibrations responsible for the spectral features, we performed a normal mode analysis of solvated hydroxide clusters taken from an empirical valence bond molecular dynamics trajectory obtained from Todd Martinez (Stanford University). From the density of vibrational states (DOS) calculated from ~1000 clusters, we concluded that 3 and 4 coordinate species are indistinguishable based on the vibrational frequency of their normal modes. Normal mode calculations also revealed that the OH stretch vibrations of the waters solvating the ion are

delocalized over 5-8 water molecules and can be classified based on their symmetry of vibration. Symmetric vibrations occur when the OH bonds in the first solvation shell of the ion oscillate in phase with each other. All other vibrations are termed asymmetric. From the DOS of normal modes, we observed that asymmetric vibrations absorb at lower frequencies and are more intense when compared to symmetric vibrations. The 2850 cm^{-1} feature was therefore assigned to the asymmetric stretch vibrations. The symmetric stretch vibrations absorb at higher frequencies, overlapping with the bulk water OH stretch, but these vibrations can be observed through cross peak features in 2D IR spectra.

Focusing on our long-term objective to characterize the structure and transport of excess protons in water, we have begun to study the BBIR spectroscopy of aqueous strong acids. Similar to hydroxide solutions, excess protons in water give rise to a continuum absorption in the mid-infrared that is largely featureless and spans over 2000 cm^{-1}. This continuum arises from the absorption of protons with potentials that vary from weakly anharmonic to double well and can be related to configurations ranging from hydronium or Eigen complex to Zundel complex. Rapid interchange between proton configurations is also thought to lead to the observed line-broadening. Using the BBIR source, we investigated the spectroscopy of the acid continuum to gain insight into aqueous proton complexes in water and their interconversion dynamics. 2D IR spectroscopy reveals that the entire continuum responds immediately upon exciting OH stretching vibrations and the relaxation of this continuum occurs on sub-100 fs timescales. This indicates that the proton is highly polarizable and is excited in unstable configurations that relax on the time scale of the fastest motions of water. Such configurations indicate the importance of collective electric field in determining the position of the proton. Our ongoing work is aimed at making vibrational assignments to various features within the continuum and using excitation and probing throughout the IR to follow the ultrafast exchange of proton structures.

DOE Supported Publications (2010-2013)

1. Nicodemus, R. A.; Ramasesha, K.; Roberts, S. T.; Tokmakoff, A., Hydrogen Bond Rearrangements in Water Probed with Temperature-Dependent 2D IR. *J. Phys. Chem. Letters* **2010**, *1*, 1068-1072.
2. "Orientational Dynamics of Water Probed with 2D-IR Anisotropy Measurements," by Krupa Ramasesha, Rebecca A. Nicodemus, Aritra Mandal and Andrei Tokmakoff, in *International Conference on Ultrafast Phenomena*, OSA Technical Digest (CD) (Optical Society of America, 2010), paper MF2. http://www.opticsinfobase.org/abstract.cfm?uri=UP-2010-MF2
3. "A Source for Ultrafast Continuum Infrared and Terahertz Radiation," Poul B. Petersen and Andrei Tokmakoff, *Optics Letters*, **35** (2010) 1962–1964.
4. "Feature Article: Melting of a β-hairpin peptide using isotope-edited 2D IR spectroscopy and simulations," Adam W. Smith, Joshua Lessing, Ziad Ganim, Chunte Sam Peng, Andrei Tokmakoff, Santanu Roy, Thomas L. C. Jansen, and Jasper Knoester, *Journal of Physical Chemistry B*, **114** (2010) 10913–10924.
5. "A Fast-Scanning Fourier Transform 2D IR Interferometer," Sean T. Roberts, Joseph J. Loparo, Krupa Ramasesha, and Andrei Tokmakoff, *Optics Communications*, **284** (2011) 1062–106.
6. "Proton Transfer in Concentrated Aqueous Hydroxide Visualized using Ultrafast Infrared Spectroscopy," Sean T. Roberts, Krupa Ramasesha, Poul B. Petersen, Aritra Mandal, and Andrei Tokmakoff, *Journal of Physical Chemistry A*, **115** (2011) 3957-3972.
7. "Collective Hydrogen Bond Reorganization in Water Studied with Temperature-Dependent Ultrafast Infrared Spectroscopy," Rebecca A. Nicodemus, S. A. Corcelli, J. L. Skinner, and Andrei Tokmakoff, *Journal of Physical Chemistry B*, **115** (2011) 5604-5616.
8. "Ultrafast 2D IR Anisotropy of Water Reveals Reorientation during Hydrogen-Bond Switching," Krupa Ramasesha, Sean T. Roberts, Rebecca A. Nicodemus, Aritra Mandal and Andrei Tokmakoff, *Journal of Chemical Physics*, **135** (2011) 054509.
9. "A Phenomenological Approach to Modeling Chemical Dynamics in Nonlinear and Two-Dimensional Spectroscopy," Krupa Ramasesha, Luigi De Marco, Andrew D. Horning, Aritra Mandal, and Andrei Tokmakoff, *The Journal of Chemical Physics*, **135** (2012) 134507.
10. "Experimental Evidence of Fermi Resonances in Isotopically Dilute Water from Ultrafast Broadband IR Spectroscopy," Luigi De Marco, Krupa Ramasesha, and Andrei Tokmakoff, *The Journal of Physical B*, (2013) doi: 10.1021/jp4034613.
11. "Water Vibrations have Strongly Mixed Intra- and Inter-Molecular Character," Krupa Ramasesha, Luigi De Marco, Aritra Mandal, and Andrei Tokmakoff, *Nature Chemistry*, (2013) in press.

The Role of Electronic Excitations on Chemical Reaction Dynamics at Metal, Semiconductor and Nanoparticle Surfaces

John C. Tully
Department of Chemistry, Yale University, 225 Prospect Street, P. O. Box 208107, New Haven, CT, 06520-8107 USA
john.tully@yale.edu

Program Scope

Achieving enhanced control of the rates and molecular pathways of chemical reactions at the surfaces of metals, semiconductors and nanoparticles will have impact in many fields of science and engineering, including heterogeneous catalysis, photocatalysis, materials processing, corrosion, solar energy conversion and nanoscience. However, our current atomic-level understanding of chemical reactions at surfaces is incomplete and flawed. Conventional theories of chemical dynamics are based on the Born-Oppenheimer separation of electronic and nuclear motion. Even when describing dynamics at metal surfaces where it has long been recognized that the Born-Oppenheimer approximation is not valid, the conventional approach is still used, perhaps patched up by introducing friction to account for electron-hole pair excitations or curve crossings to account for electron transfer. There is growing experimental evidence that this is not adequate. We are examining the influence of electronic transitions on chemical reaction dynamics at metal and semiconductor surfaces. Our program includes the development of new theoretical and computational methods for nonadiabatic dynamics at surfaces, as well as the application of these methods to specific chemical systems of experimental attention. Our objective is not only to advance our ability to simulate experiments quantitatively, but also to construct the theoretical framework for understanding the underlying factors that govern molecular motion at surfaces and to aid in the conception of new experiments that most directly probe the critical issues.

Recent Progress

NO scattering from Au(111)

Our Independent Electron Surface Hopping (IESH) simulations of vibrationally and rotationally inelastic scattering of NO molecules from a gold (111) surface have proved very successful, in most cases producing quantitative agreement with experimental results of Alec Wodtke and coworkers (Gottingen) for both vibrational de-excitation and excitation. However, there are some discrepancies, the most significant of which are trapping (multiple bounce) probabilities, translational energy loss and widths of the angular scattering distributions. All of these are computed to be too large compared to experiment. It is important to identify the source(s) of these discrepancies. Inaccuracies may arise either from input to the IESH theory - the potential energy surfaces and nonadiabatic couplings – or from the limitations of the IESH theory itself. We carried out a systematic study of NO-Au scattering under three different approximations.

1. Adiabatic simulations, i.e., motion on the ground state potential energy surface only.
2. Electronic Friction, i.e., motion on the ground state but with n nonadiabatic electronic transitions incorporated through frictions and fluctuating forces.

3. IESH; i.e., with nonadiabatic transitions accounted for by surface hopping among the huge manifold of electron-hole pair and negative ion excited states. Analysis of the results has demonstrated convincingly that by far the major source of error is the density functional theory ground state potential energy surface employed. The assumed gas-surface interaction is too soft and too highly corrugated. This is an important result, supporting our belief that the IESH algorithm itself is indeed capable of highly accurate simulation of nonadiabatic chemical dynamics at metal surfaces, if based on accurate interactions.

Quantum Mechanical Treatment of Vibration.

One concern about our IESH simulations of NO scattering from Au(111) is classical mechanical treatment of nuclear motion. Low frequency phonons of the gold surface should be adequately described by classical mechanics, but classical treatment of the high frequency NO stretching vibration is suspect. In the IESH simulations we needed to bin trajectories according to their vibrational energy in order to make comparison with measured probabilities of quantum states. This binning procedure is somewhat arbitrary and zero point energy is not treated correctly. In order to assess the magnitude of error introduced by the classical treatment of NO stretching motion, we carried out extended IESH simulations in which the NO vibrational mode was treated quantum mechanically. This is straightforward in principle, although it increases the computational costs. Surface hopping is a procedure for accounting for transitions between quantum mechanical levels of any kind, electronic or vibrational. Including N quantum vibrational modes for each electronic state increases the number of quantum levels by a factor of N, a relatively modest cost. In addition, at each position of the classical particles, the N lowest vibrational wave functions must be computed numerically, as well as derivative couplings among them, again a relatively modest cost compared to computing the energies and couplings among myriads of electronic states. The results for simulations of vibrational excitation of NO molecules scattered from gold, using IESH with quantized NO vibration, are in surprisingly good agreement with both fully classical IESH results and experiment. This demonstrates the feasibility of quantizing selective vibrational degrees of freedom as well as shedding light on the severity of treating high frequency vibrations classically and using somewhat arbitrary binning procedures.

Constrained Density Functional Theory

IESH requires the calculation of multidimensional potential energy surfaces for ground and excited states of molecules near metal or semiconductor surfaces. Moreover it is desirable, although not necessarily mandatory, to construct a diabatic Hamiltonian. For example, for the NO/Au scattering simulations a Newns-Anderson Hamiltonian was used, based on NO neutral and NO^- configurations, dressed by a continuum of conduction electron levels. The neutral and ionic potential energy surfaces were computed by density functional theory, with application of external electric fields to extract neutral and ionic components. This procedure was physically motivated, but it lacks rigor and perhaps underlies some of the inaccuracies uncovered in the simulations. A more rigorous and more general procedure is required, especially in cases where more than two configurations are required (e.g., $O(^3P)$, $O(^1D)$, $O^-(^2P)$, $O^{2-}(^1S)$, etc.). We have developed such a procedure, employing an appropriately designed form of constrained density

functional theory. We have applied the method initially to a simple system, a hydrogen atom interacting with a metal surface (gold). The method is quite practical and produces neutral and negative ion potential energy surfaces that appear reasonable. One complication that we need to address is that the neutral and ionic states are not orthogonal, requiring care in the calculation of nonadiabatic couplings. While there are no high accuracy calculations against which to test our results, we anticipate that experiments on scattering of H atoms from Au(111), initiated by the Wodtke group, will provide a test of the method, albeit not a perfect test.

Future Plans

Applications of IESH

We plan to extend the NO/Au IESH calculations to semiconductor surfaces and to metal surfaces with varying work functions. Calculating the required ground and excited potential energy surfaces and nonadiabatic couplings for each new chemical system is a daunting task. In order to obtain qualitative insights about general trends, we plan to use the NO/Au interactions we derived previously, with simple alterations. We can change the effective work function of the metal simply by altering the asymptotic energy of the negative ion state relative to the neutral state. This will not properly incorporate the chemical differences between the surfaces of copper, silver, platinum, etc., but it may give us a preliminary view of the sensitivity of energy transfer rates to the work function and, perhaps more importantly, suggest fruitful experiments. Similarly, we can introduce a band gap in the substrate electron density of states, again using the NO/Au interactions, in order to obtain an initial glimpse of vibrational energy transfer at semiconductor surfaces. This may reveal, for example, insight into the competition between electronic and phonon mechanisms of energy transfer.

Inelastic Scattering of H atoms from metal surfaces

The hydrogen atom is the simplest example of an open shell species. While the interaction of an H atom with a metal surface does not exhibit all of the complexities of more complicated systems, because of its simplicity it affords an excellent opportunity to develop and test our constrained density functional approach for computing ground and excited states of adsorbates near metal surfaces. Equally importantly, the experimental group of Alec Wodtke (Göttingen) is planning an extensive molecular-beam study of this system, with the objective of producing detailed and quantitative data about angular distributions, inelasticity, temperature dependence, etc. We will carry out extensive calculations of the potential energy surfaces and nonadiabatic couplings for these systems, using constrained DFT. We will pay particular attention to electron spin. Note that since DFT is in practice based on a density arising from a single-determinant Kohn-Sham wavefunction, it may not correctly portray the open-shell nature of the hydrogen atom which requires the intermixing of at least two electronic configurations (spin up and spin down), and perhaps three if the hydrogen negative ion plays a significant role. We will simulate scattering dynamics with electronic friction, Ehrenfest and IESH methods, and compare each to the Wodtke experiments. This will be the most complete study to date of the role of nonadiabaticity in atom-metal interactions and the accuracy of current theories of nonadiabatic dynamics.

Constrained Density Functional Theory for Diabatic Molecule-Surface Interactions
We plan to further develop constrained density functional theory (CDFT) for computing "diabatic" potential energy surfaces and their off-diagonal couplings for molecules interacting with surfaces. The IESH method appears capable of accurately simulating nonadiabatic dynamics at metal and semiconductor surfaces, provided the required input is available and reliable. The necessary input is a diabatic Hamiltonian matrix that accurately represents the charge and excited states of the molecule embedded in the continuum of conduction band levels, and does so for all relevant molecule and surface atom positions. For NO interacting with the gold surface, we were able to construct a satisfactory diabatic Hamiltonian using density functional theory with the application of fictitious electric fields to modulate the energies of ionic states. This procedure is not applicable to most systems of experimental interest, however. The most critical challenge to further progress is to develop more generally applicable ab initio procedures for computing the necessary diabatic Hamiltonians. We propose to further develop and apply CDFT for this purpose. CDFT is conceptually simple; a DFT calculation is carried out with an imposed constraint, such as constraining the net local charge on a molecule to be minus one. This will produce the lowest energy potential energy surface consistent with this charge constraint. This can be repeated with different constraints to produce diagonal elements of the desired diabatic Hamiltonian. However, there are unsolved issues with computing the off-diagonal elements, including the absence of a proper wave function in DFT and non-orthogonality of Kohn-Sham determinants corresponding to different constraints. We will address these issues. In particular, we are exploring the possibility of enforcing orthogonality via an additional constraint. As we overcome these obstacles, we will apply this approach to hydrogen atom scattering from metals, as described above. We will also apply CDFT with spin constraints to oxygen atoms and oxygen molecules interacting with metals surfaces. For both of these cases, transitions between the ground state triplet and low-lying singlet states may occur without spin-orbit interactions via a two-electron exchange with the conduction band, possibly with major implications to chemical reactivity.

References to Publications of DOE-Sponsored Research since October 1, 2010

1. R. Cooper, C. Bartels, A. Kandratsenka, I. Rahinov, N. Shenvi, K. Golibrzuch, Z. S. Li, D. J. Auerbach, J. C. Tully and A. M. Wodtke, "Multiquantum Vibrational Excitation of NO Scattered from Au(111): Quantitative Comparison of Benchmark Data to Ab Initio Theories of Nonadiabatic Molecule-Surface Interactions", *Angewandte Chemie-Int. Ed*. **51**, 4954-4958 (2012).

2. S. T. Edwards, M. A. Johnson and J. C. Tully, "Vibrational Fano resonances in dipole-bound anions", *J. Chem. Phys*. **136**, 154305 (2012).

3. N. Shenvi and J. C. Tully, "Nonadiabatic dynamics at metal surfaces: independent electron surface hopping with phonon and electron thermostats", *Faraday Discussions* **157**, 325-335 (2012).

Reactive Processes in Aqueous Environment

Marat Valiev
[1]Environmental Molecular Sciences Laboratory and
Pacific Northwest National Laboratory
902 Battelle Blvd.
Mail Stop K9-90
Richland, WA 99352
marat.valiev@pnl.gov

The major objective of our research is to gain fundamental understanding of reactive processes in aqueous systems ranging from clusters to bulk solvation environments. We are interested in the impact of solvation environment on the specific observable properties of the solute molecules, as well as the effect of the solute specific properties on the solvent structure. Our investigation is focused mainly on polyatomic solutes, which can adopt different structural forms, electronic states, and tautomeric configurations.

One of the important directions in our research is to provide molecular-level understanding of selectivity and specificity effects of ion solvation in aqueous environments. It is now accepted that the spherically symmetric representation of the solute species gives inadequate description even in the case of monoatomic ions. In the latter case the first non-vanishing symmetry-breaking contribution comes from the induced dipole moment proving to be critical for understanding the surface propensity of these species on the basis of their size and polarizability (soft vs. hard). The effects of solute anisotropy are expected to be even more important for the solvation of complex polyatomic species. Unlike monatomic ions, the presence of internal molecular structure leads to permanent inhomogeneities in the charge density distribution, which can have a bigger impact on the solute-solvent interactions than induced (polarization) effects. Similar to polarization, these charge density distribution effects are specific (they depend on the particular molecule) and have an inherent capacity to differentiate or select between bulk (isotropic) and surface (anisotropic) solvent environments. Our research is aimed to provide first-

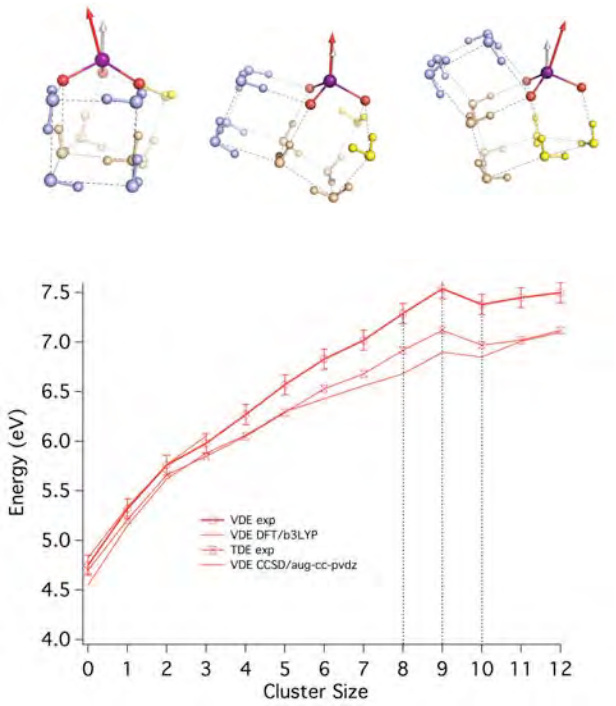

Figure 1: (top) global minimum structures of n= 9, 10, 11 iodate water cluster; (bottom) comparison between experimental and calculated EBE binding energy as a function of water cluster size.

principles description of these effects based on combined molecular modeling in conjunction with experimental photoelectron spectroscopy (PES) measurements performed by Dr. Xuebin Wang (PNNL). The relevant quantity of interest is the electron binding energy (EBE) – the vertical energy difference between the anion and neutral complex at the stable structure of the anion. Sensitive to the solvent environment, the EBE provides a precise measure of the incremental solvation process. The absence of "bulk" solvent in the cluster environment exposes the fine details of the solute-solvent interactions and provides an ideal setting to assess the potential impact of charge anisotropy effects. The latter can have a significant impact on the PES spectrum, as was the case with iodate $(IO_3^-)(H_2O)_n$ water clusters that showed an unusual drop in EBE value at n=10 (see Fig.1). Our investigation showed that this anomalous behavior is a result of strong anisotropic effects resulting from highly ordered solvent structure. These results indicate the observed PES anomaly that may be a general feature in the cluster solvation of polyatomic solutes, and we currently working on other polyatomic solutes.

Another direction of our research is focused on fundamental chemistry of radical and anion molecular species in aqueous solution. This work is done in close collaboration with Sergei Lymar at BNL and aimed at understanding thermodynamics, electronic structure, and reactivity of nitrogen-oxide base compounds. The two systems that are of particular interest to us are NONOate (XN(O)NO-) and nitrate/nitrite systems. NONOate compounds can be viewed as adducts of NO dimer with general electron donating group X^-. The latter provides the necessary "electron" glue that holds together otherwise weakly bound NO dimers. Depending on nature of the electron-donating group the strength of this bond can be varied, which can be employed in the engineered delivery of NO species. In our earlier work, we have investigated the case of X = e- resulting in hyponitrite radical N(O)NO- species. Presently we are looking at other members of NONOate family – amino NONOates $(X=Et_2N^-)$ and Angeli salt $(X=O_2^-)$. In addition to equilibrium properties, our investigation is also focused on the kinetics of the pH-induced NO release(see Fig. 2). The challenging feature of these systems is that high levels of ab-initio theory (e.g. CCSD(T)) are require for proper description of electron correlation effects.

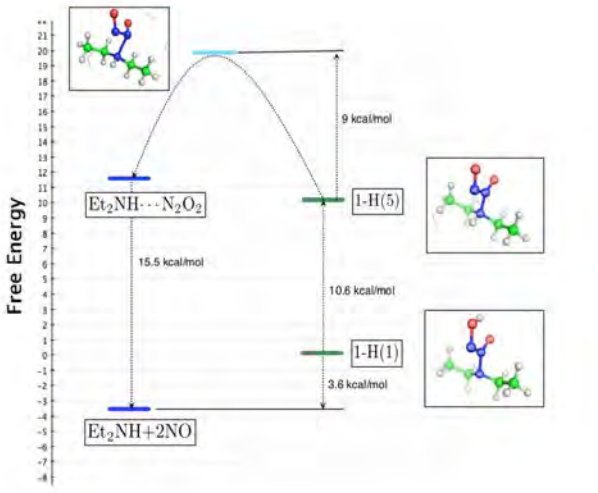

Figure 2: Thermodynamic cycle of pH-driven NO release in amino NONOate.

Both of the application areas discussed above require high levels of ab-initio treatment to properly capture the changes in the electronic structure as well as the sufficient amount of statistical sampling to account for the aqueous environment. While QM/MM approach remains our main method for these types of simulations, we are investigating other methodologies including combination of quantum mechanical and classical density functional approach (QM/cDFT).

1. Valiev M, EJ Bylaska, N Govind, K Kowalski, TP Straatsma, HJJ Van Dam, D Wang, J Nieplocha, E Apra, TL Windus, and WA de Jong. 2010. “NWChem: A Comprehensive and Scalable Open-source Solution for Large Scale Molecular Simulations.” Computer Physics Communications 181(9):1477-1489.
2. Cauet E, M Valiev, and JH Weare. 2010. “Vertical Ionization Potentials of Nucleobases in a Fully Solvated DNA Environment.” Journal of Physical Chemistry B 114(17):5886-5894.
3. Wang DY, M Valiev, and BC Garrett. 2011. “CH(2)Cl(2)+OH(-) Reaction in Aqueous Solution: A Combined Quantum Mechanical and Molecular Mechanics Study.” Journal of Physical Chemistry A 115(8):1380-1384.
4. H. Y. Yin, D. Y. Wang, and M. Valiev, (2011). “Hybrid Quantum Mechanical/Molecular Mechanics Study of the S(N)2 Reaction of Ch3cl+Oh- in Water”, Journal of Physical Chemistry A, 115 12047-52.
5. M. Valiev, and S. V. Lymar, (2011). “Structural and Mechanistic Analysis through Electronic Spectra: Aqueous Hyponitrite Radical (N2o2-) and Nitrosyl Hyponitrite Anion (N3o3-)”, Journal of Physical Chemistry A, 115, 12004-10.
6. G. N. Chuev, M. Valiev, and Mq. V. Fedotova, (2012). “Integral Equation Theory of Molecular Solvation Coupled with Quantum Mechanical/Molecular Mechanics Method in NWChem Package”, Journal of Chemical Theory and Computation, 8, 1246-54.
7. G. Murdachaew, M. Valiev, S. M. Kathmann, and X. B. Wang, (2012). “Study of Ion Specific Interactions of Alkali Cations with Dicarboxylate Dianions”, Journal of Physical Chemistry A, 116, 2055-61.
8. T. T. Wang, H. Y. Yin, D. Y. Wang, and M. Valiev, (2012). “Hybrid Quantum Mechanical and Molecular Mechanics Study of the S(N)2 Reaction of Ccl4 + Oh- in Aqueous Solution: The Potential of Mean Force, Reaction Energetics, and Rate Constants”, 116 , 2371-76.
9. Wen, H.; Hou, G.-L.; Kathmann, S. M.; Valiev, M.; Wang, X.-B.: Communication: Solute anisotropy effects in hydrated anion and neutral clusters. *The Journal of Chemical Physics* 2013, *138*, 031101.
10. Sellner, B.; Valiev, M.; Kathmann, S. M.: Charge and Electric Field Fluctuations in Aqueous NaCl Electrolytes. *The Journal of Physical Chemistry B* 2013.

Probing the Actinide-Ligand Binding and the Electronic Structure of Gaseous Actinide Molecules and Clusters Using Anion Photoelectron Spectroscopy

PI: Lai-Sheng Wang

Department of Chemistry
Brown University
324 Brook Street
Providence, RI 02912
Email: lai-sheng_wang@brown.edu

Program Scope

The broad scope of this program is to better understand actinide chemistry using new spectroscopic techniques and to provide accurate spectroscopic data for the validation of new theoretical methods aimed at actinide chemistry. This program contains three thrust areas:

- probing ligand-uranyl (UO_2^{2+}) interactions in gaseous anionic complexes in the form of $[UO_2L_x]^{n-}$ produced by electrospray ionization
- probing the electronic structure and bonding of inorganic and organometallic compounds of actinides in the gas phase
- probing the metal-metal bonding and size-dependent electronic structures in U_x^- and $U_xO_y^-$ clusters as a function of size and composition.

Understanding the chemistry of the actinide elements is of critical importance to the mission of DOE. My group has developed a number of experimental apparatuses, including a magnetic-bottle photoelectron spectroscopy instrument equipped with a laser vaporization supersonic cluster source and a combined photoelectron imaging and magnetic-bottle instrument equipped with an electrospray ionization source. This suite of state-of-the-art instruments are uniquely suitable to investigate the three classes of actinide compounds. Photodetachment involves removal of electrons from occupied molecular orbitals and probes directly the chemical bonding properties of the underlying molecular species. Photoelectron spectroscopy of anions yields electron affinities and low-lying electronic state information for the corresponding neutral species. The application of *anion* photoelectron spectroscopy to actinide molecules opens up new research opportunities and yields accurate and systematic electronic structure and spectroscopic information that can be used to verify computational methods and advance our understanding of the reactivity, structure, and bonding of actinide molecules.

Recent Progress (August 2012 to August 2013)

In this funding period, we have made significant progresses in both uranyl complexes and novel uranium clusters, resulting in four publications. We completed the construction of a temperature-controlled ion trap, which has allowed us to produce cold anions and significantly enhanced our ability to obtain better spectroscopic data. For example, the cold anions allowed us to measure very accurately the electron affinity of UF_5. Preliminary data have been obtained on a number of interesting and novel U-oxide (UO_x^- and $U_2O_x^-$, x = 1–6) and U-fluoride (UF_x^-, x = 2–4 and $U_2F_x^-$, x = 1–6) clusters, which are being analyzed and prepared for publication.

Photoelectron spectroscopy and the electronic structure of the uranyl tetrachloride dianion: $UO_2Cl_4^{2-}$. The uranyl tetrachloride dianion ($UO_2Cl_4^{2-}$) was observed in the gas phase using electrospray ionization and investigated by photoelectron spectroscopy and

relativistic quantum chemical calculations. The free $UO_2Cl_4^{2-}$ dianion was found to be highly stable electronically with an adiabatic electron binding energy of 2.40 eV. *Ab initio* calculations were carried out and used to interpret the photoelectron spectra and elucidate the electronic structure of $UO_2Cl_4^{2-}$. The calculations showed that the frontier molecular orbitals in $UO_2Cl_4^{2-}$ are dominated by the ligand Cl 3p orbitals, while the U-O bonding orbitals are much more stable. The electronic structure of $UO_2Cl_4^{2-}$ was compared with that of the previously reported $UO_2F_4^{2-}$. The electron binding energy of $UO_2Cl_4^{2-}$ was found to be greater than that of $UO_2F_4^{2-}$ by 1.3 eV. The differences in the electronic stability and electronic structure between $UO_2Cl_4^{2-}$ and $UO_2F_4^{2-}$ were elucidated.

Probing the electronic structure and chemical bonding in tricoordinate uranyl complexes $UO_2X_3^-$ (X = F, Cl, Br, I): Competition between Coulomb repulsion and U–X bonding. While the uranyl halide complexes $[UO_2(\text{halogen})_n]^{2-n}$ (n = 1, 2, 4) are ubiquitous, the tricoordinate species have been relatively unknown until very recently. We used photoelectron spectroscopy and relativistic quantum chemistry to investigate the bonding and stability of a series of gaseous tricoordinate uranyl complexes, $UO_2X_3^-$ (X = F, Cl, Br, I). The isolated $UO_2X_3^-$ ions were produced by electrospray ionization and observed to be highly stable with very large adiabatic electron detachment energies. Theoretical calculations revealed that the frontier molecular orbitals are mainly of uranyl U–O bonding characters in $UO_2F_3^-$, but they are from the ligand valence *n*p lone pairs in the heavier halogen complexes. Extensive bonding analyses were carried out for $UO_2X_3^-$, as well as for the doubly-charged tetracoordinate complexes ($UO_2X_4^{2-}$), showing that the U–X bonds are dominated by ionic interactions with weak covalency. The U–X bond strength decreases down the periodic table from F to I. The Coulomb barriers and dissociation energies of $UO_2X_4^{2-} \rightarrow UO_2X_3^- + X^-$ were calculated, revealing that all the gaseous dianions are in fact metastable. The dielectric constant of the environment is shown to be the key in controlling the thermodynamic and kinetic stabilities of the tetracoordinate uranyl complexes via modulation of the ligand-ligand Coulomb repulsions.

A joint photoelectron spectroscopy and theoretical study on the electronic structure of UCl_5^- and UCl_5. The UCl_5^- complex was thought to be formed under excess Cl^- in molten salts, but there have been few studies about its physical and chemical properties. We were able to produce the UCl_5^- anion using electrospray ionization and investigated its electronic structure and bonding using photoelectron spectroscopy and theoretical calculations. A large electron affinity of 4.76 eV was measured for the first time for the neutral UCl_5 molecule. Theoretical investigations revealed that the ground state of UCl_5^- has an open shell with two unpaired electrons occupying two primarily U $5f_z3$ and $5f_{xyz}$ based molecular orbitals. The structures of both UCl_5^- and UCl_5 were confirmed to have C_{4v} symmetry. The computational results further provided insights into the electronic structure and valence molecular orbitals of UCl_5^- and UCl_5. A systematic theoretical examination was done on all the uranium pentahalide complexes UX_5^- (X = F, Cl, Br, I). Chemical bonding analyses indicated that the U–X interactions in UX_5^- are dominated by ionic bonding, with increasing covalent contributions for the heavier halogen complexes. This work has been recently accepted by Chem. Asian J. and is designated as a VIP (very important Paper) article and will be highlighted by the journal.

Future Plans

In the next funding period, we will continue to investigate UO_2^{2+} coordinated by different ligands. We have found that we can also produce UCl_6^- and UCl_6^{2-} complexes using our electrospray ionization source. We will study the chemical bonding and electronic structures of these species and compare them with the corresponding fluoride complexes. We have obtained preliminary data of U_x^- clusters and novel U-oxide and fluoride clusters, which will be the focus of the next funding period.

Publications from DOE Supported Research (FY12-FY13)

1. "Observation and Investigation of the Uranyl Tetrafluoride Dianion ($UO_2F_4^{2-}$) and Its Solvation Complexes with Water and Acetonitrile" (P. D. Dau, J. Su, H. T. Liu, J. B. Liu, D. L. Huang, J. Li, and L. S. Wang), *Chem. Sci*. **3**, 1137-1146 (2012). (DOI: 10.1039/c2sc01052f)

2. "Photoelectron Spectroscopy and Theoretical Studies of UF_5^- and UF_6^-" (P. D. Dau, J. Su, H. T. Liu, D. L. Huang, F. Wei, J. Li, and L. S. Wang), *J. Chem. Phys.* **136**, 194304 (2012). (DOI: 10.1063/1.4716182)

3. "Photoelectron Spectroscopy and the Electronic Structure of the Uranyl Tetrachloride Dianion: $UO_2Cl_4^{2-}$" (P. D. Dau, J. Su, H. T. Liu, D. L. Huang, J. Li, and L. S. Wang), *J. Chem. Phys.* **137**, 064315 (8) (2012). (DOI: 10.1063/1.4742062)

4. "Photoelectron Spectroscopy of Cold UF_5^-" (P. D. Dau, H. T. Liu, D. L. Huang, and L. S. Wang) *J. Chem. Phys*. **137**, 116101 (2) (2012). (DOI: 10.1063/1.4753421)

5. "Probing the Electronic Structure and Chemical Bonding in Tricoordinate Uranyl Complexes $UO_2X_3^-$ (X = F, Cl, Br, I): Competition between Coulomb Repulsion and U–X Bonding" (J. Su, P. D. Dau, Y. H. Qiu, H. T. Liu, C. F. Xu, D. L. Huang, L. S. Wang, and J. Li), *Inorg. Chem*. **52**, 6617-6626 (2013). (DOI: 10.1021/ic4006482)

6. "A Joint Photoelectron Spectroscopy and Theoretical Study on the Electronic Structure of UCl_5^- and UCl_5" (J. Su, P. D. Dau, C. F. Xu, D. L. Huang, H. T. Liu, F. Wei, L. S. Wang, and J. Li, *Chem. Asian J.*, Jul 12, 2013. (DOI: 10.1002/asia.201300627)

Chemical Kinetics and Dynamics at Interfaces

Cluster Model Investigation of Condensed Phase Phenomena

Xue-Bin Wang

Physical Sciences Division, Pacific Northwest National Laboratory, P.O. Box 999, MS K8-88, Richland, WA 99352. E-mail: xuebin.wang@pnnl.gov

Program Scope

We aim at obtaining a microscopic understanding of solution chemistry and condensed phase phenomena using gas phase clusters as model systems. Clusters occupy an intermediate region between gas phase molecules and the condensed states of matter and play an important role in heterogeneous catalysis, aerosol chemistry, and biological processes. We use electrospray ionization (ESI) to generate a wide variety of molecular and ionic clusters to simulate key species involved in the condensed phase reactions and transformations, and characterize them using low temperature, and temperature-controlled negative ion photoelectron spectroscopy (NIPES). Inter- and intra-molecular interactions and their variation as function of size and composition, important to understand complex chemical reactions and nucleation processes in condensed and interfacial phases can be directly obtained. Experiments and *ab initio* calculations are synergistically combined to

- Probe solute anisotropic effects in hydrated anion and neutral clusters
- Obtain a molecular-level understanding of the solvation and stabilization of complex singly- and multiply-charged anions important in condensed phases
- Quantify thermodynamic driving forces resulted from hydrogen-bonded networks formed in aerosol nucleation processes and enzymatic catalytic reactions.
- Study temperature-dependent conformation changes and isomer populations of complex solvated clusters
- Investigate intrinsic electronic structures of environmentally and catalytically important species and reactive diradicals.
- Understand the molecular processes and initial steps of dissolution of salt molecules in polar solvents

The central theme of this research program lies at obtaining a fundamental understanding of environmental materials and solution chemistry important to many primary DOE missions (waste storage, subsurface and atmospheric contaminant transport, catalysis, etc.), and enhances scientific synergies between experimental and theoretical studies towards achieving such goals.

Recent Progress

Solute Anisotropy Effects in Hydrated Anion and Neutral Clusters. Specific ion effects in solvation processes are often rationalized in terms of spherically symmetric models involving an ion's size, charge, and polarizability. The effects of permanent charge anisotropy, related to the polyatomic nature of complex solutes, are expected to play a role in solvation but the extent of their importance remains unexplored. We have provided compelling experimental and theoretical evidence that the anisotropic nature of complex polyoxyanion solutes can have a critical influence on the solvation process. Combined photoelectron spectroscopy and theoretical modeling results show that the electron binding energy (EBE) of $IO_3^-(H_2O)_n$ (n = 0 – 12) clusters is characterized by an anomalous drop at n = 10. Such behavior is

unprecedented for rigid solute molecules, and is related to the anisotropy of the neutral iodate radical that displays a strong selectivity to solvent configurations generated by the charged anion complex. These results highlight significant differences for hydrated neutral clusters from their ionic counterparts where the dominant charge (monopole) field is absent. Our study suggests that charge anisotropy (permanent dipole) of polar solute molecules play an important role in selecting favorable solvent network configurations, and consequently influencing their chemical reactivity and physical properties. The rationale of preferred specific solvation structures based on a simple geometrical argument between the solute permanent dipole axis and the solvent-network electric field is conceptually simple, and provides a new way of understanding structures and properties of complex molecules in aqueous environments, including ubiquitous zwitterions of biological molecules.

Negative Ion Photoelectron Spectroscopy Reveals Thermodynamic Advantage of Organic Acids in Facilitating Formation of Bisulfate Ion Clusters: Atmospheric Implications. Recent lab and field measurements have indicated critical roles of organic acids in enhancing new atmospheric aerosol formation. Such findings have stimulated theoretical studies with the aim of understanding interaction of organic acids with common aerosol nucleation precursors like bisulfate (HSO_4^-). We carried out a combined negative ion photoelectron spectroscopic and theoretical investigation of molecular clusters formed by HSO_4^- with succinic acid (SUA, $HO_2C(CH_2)_2CO_2H$), $HSO_4^-(SUA)_n$ (n = 0-2), along with $HSO_4^-(H_2O)_n$ and $HSO_4^-(H_2SO_4)_n$. It is found that one SUA molecule can stabilize HSO_4^- by ca. 39 kcal/mol, triple the corresponding value that one water molecule is capable of (ca. 13 kcal/mol). Molecular dynamics simulations and quantum chemical calculations reveal the most plausible structures of these clusters and attribute the stability of these clusters due to formation of strong hydrogen bonds. This work provides direct experimental evidence showing significant thermodynamic advantage by involving organic acid molecules to promote formation and growth in bisulfate clusters and aerosols.

***Metal-Centered 17-Electron Radicals $CpM(CO)_3^\bullet$ (M = Cr, Mo, W): A Combined Negative Ion Photoelectron Spectroscopic and Theoretical Study*.** Despite the importance of group 6 metal-centered 17-electron radicals $CpM(CO)_3^\bullet$ (M = Cr, Mo, W) in establishing many of the fundamental reactions now known for metal-centered radicals, spectroscopic characterization of their electronic properties and structures has been very challenging due to their high reactivity. We conducted a gas-phase study of these species by photodetachment photoelectron spectroscopy (PES) of their corresponding 18-electron anions and theoretical electronic structure calculations. Three well-separated spectral features are observed by PES for each anionic species. Electron affinities (EAs) of $CpM(CO)_3^\bullet$ were experimentally measured from the threshold of each spectrum and were found to correlate well with the reported redox potentials measured in solution. Theoretical calculations for all anionic and neutral (radical) species gave calculated EAs and band gaps that are in good agreement with the experimental data. Molecular orbital (MO) analyses for each anion indicate that the *top three* occupied MOs are mainly metal-based and contribute to the first spectral feature, whereas the *next two* MOs are associated with Cp-M π bonding and contribute to the second spectral feature. The calculations further exhibit appreciable anion-to-neutral structural changes for all three species, with the change for the W species being the smallest. The intrinsic energetic and structural information obtained in this study, including excited states, can help explain and understand fundamental reactivity patterns for this class of organometallic complexes.

Probing Intrinsic Electronic Structure Properties of Fullerene Derivatives for Better Electron Acceptors. Carbon and fluorine are at the heart of a family of chemical compounds that can be used for nonstick coatings, blood substitutes, and seemingly everything in between. Differences in the structures of these compounds dictate their suitability for different applications. In collaboration with Drs. Boltalina and Strauss from Colorado State University, a series of seven structurally-similar compounds with different pairs of perfluoroalkyl (R_F) groups, 1,7-$C_{60}(R_F)_2$ (R_F = CF_3, C_2F_5, i-C_3F_7, n-C_3F_7, s-C_4F_9, n-C_4F_9

and n-C_8F_{21}) were prepared, and characterized by low-temperature anion photoelectron spectroscopy, DFT calculations, and electrochemical methods. It is found that the gas phase electron affinities, solution phase reduction potentials, and computational energies of LUMOs of these molecules are not correlated, an unprecedented finding that challenges widely accepted assumptions. The new knowledge afforded by this study will help chemists better choose the right organofluorine groups to design new materials with optimized morphological, electronic, optical, and/or magnetic properties.

Future Directions

The main thrust of our BES program will continue to be on cluster model studies of condensed phase phenomena in the gas phase. The experimental capabilities that we have developed give us the opportunity to attack a broad range of fundamental chemical physics problems pertinent to ionic solvation, solution chemistry, homogeneous / heterogeneous catalysis, aerosol chemistry, biological processes, and material synthesis. The ability to cool and control ion temperature affords us to study different isomer populations and conformation changes of environmentally important hydrated clusters. We will also be able to study physisorption of various gas molecules onto negatively-charged ions and plan to select various molecules and clusters that strongly interact with H_2 or CO_2 molecules for searching and identifying more efficient materials in H_2 storage and CO_2 conversion. Another major direction is to use gaseous clusters to model ion-specific interactions in solutions, ion transport and ion-receptor interactions in biological systems, and initial nucleation processes relevant to atmospheric aerosol formation. We also plan to initiate new research directions in the coming years to study excited state properties of solvated clusters to model possible aerosol photochemistry and high-energy processes at interfaces.

References to Publications of DOE CPIMS Sponsored Research (10/1/2010 - present)

1. Q Fu, J Yang, and XB Wang, "On the Electronic Structures and Electron Affinities of the m-Benzoquinone (BQ) Diradical and the o-, p-BQ Molecules: A Synergetic Photoelectron Spectroscopic and Theoretical Study" *Journal of Physical Chemistry A* 115, 3201-3207 (2011).

2. XB Wang and SS Xantheas, "Photodetachment of Isolated Bicarbonate Anion: Electron Binding Energy of HCO_3^-", *Journal of Physical Chemistry Letters* 2, 1204-1210 (2011).

3. H Wen, GL Hou, W Huang, N Govind, and XB Wang, "Photoelectron Spectroscopy of Higher Bromine and Iodine Oxide Anions: Electron Affinities and Electronic Structures of $BrO_{2,3}$ and IO_{2-4} Radicals", *Journal of Chemical Physics* 135, 184309-1-11 (2011).

4. A Shokri, JC Schmidt, XB Wang, and SR Kass, "Hydrogen Bonded Arrays: The Power of Multiple Hydrogen Bonds", *Journal of the American Chemical Society* 134, 2094-2099 (2012).

5. JC Guo, G Hou, SD Li, and XB Wang, "Probing the Low-lying Electronic States of Cyclobutanetetraone (C_4O_4) and its Radical Anion: A Low-Temperature Anion Photoelectron Spectroscopic Approach", *Journal of Physical Chemistry Letters* 3, 304-308 (2012).

6. G Murdachaew, M Valiev, SM Kathmann, and XB Wang, "Study of Ion Specific Interactions of Alkali Cations with Dicarboxylate Dianions", *Journal of Physical Chemistry A* 116, 2055-2061 (2012).

7. IV Kuvychko, JB Whitaker, BW Larson, TC Folsom, NB Shustova, SM Avdoshenko, YS Chen, H Wen, XB Wang, L Dunsch, AA Popov, SH Strauss, and OV Boltalina, "Substituent Effects in a Series of 1,7-$C_{60}(R_F)_2$ Compounds (R_F = CF_3, C_2F_5, *n*-C_3F_7, *i*-C_3F_7, *n*-C_4F_9, *s*-C_4F_9, *n*-C_8F_{17}): Electron Affinities, Reduction Potentials and *E*(LUMO) Values Are Not Always Correlated", *Chemical Science* 3, 1399-1407 (2012).

8. GH Hou, H Wen, KA Lopata, W Zheng, K Kowalski, N Govind, XB Wang, and SS Xantheas, "A Combined Gas-Phase Photoelectron Spectroscopic and Theoretical Study of Zeise's Anion and Its Br- and I-Analogs", *Angewandte Chemie International Edition* 51, 6356-6360 (2012).

9. A Shokri, JC Schmidt, XB Wang, and SR Kass, "Characterization of a Saturated and Flexible Aliphatic Polyol Anion Receptor", *Journal of the American Chemical Society* 134, 16944-16947 (2012).

10. EV Beletskiy, JC Schmidt, XB Wang, and SR Kass, "Three Hydrogen Bond Donor Catalysts: Oxyanion Hole Mimics and Transition State Analogues", *Journal of the American Chemical Society* 134, 18534-18537 (2012).

11. H Wen, GL Hou, SM Kathmann, M Valiev, and XB Wang, "Solute Anisotropy Effects in Hydrated Anion and Neutral Clusters", *Journal of Chemical Physics* 138, 031101-1-4 (2013).

12. X Bao, DA Hrovat, WT Borden, and XB Wang, "Negative Ion Photoelectron Spectroscopy Confirms the Prediction that $(CO)_5$ and $(CO)_6$ Each Has a Singlet Ground State", *Journal of the American Chemical Society* 135, 4291-4298 (2013).

13. GL Hou, W Lin, SH Deng, J Zhang, W Zheng, F Paesani, and XB Wang, "Negative Ion Photoelectron Spectroscopy Reveals Thermodynamic Advantage of Organic Acids in Facilitating Formation of Bisulfate Ion Clusters: Atmospheric Implications", *The Journal of Physical Chemistry Letters* 4, 779-785 (2013).

14. IV Kuvychko, KP Castro, SH Deng, XB Wang, SH Strauss, and OV Boltalina, "Taming Hot CF_3 Radicals: Incrementally Tuned Families of Polyarene Electron Acceptors for Air-Stable Molecular Optoelectronics", *Angewandte Chemie International Edition* 52, 4871-4874 (2013).

15. EF van der Eide, GL Hou, SH Deng, H Wen, P Yang, RM Bullock, and XB Wang, "Metal-Centered 17-Electron Radicals $CpM(CO)_3^{\bullet}$ (M = Cr, Mo, W): A Combined Negative Ion Photoelectron Spectroscopic and Theoretical Study", *Organometallics* 32, 2084-2091 (2013).

16. IV Kuvychko, C Dubceac, SH Deng, XB Wang, AA Granovsky, AA Popov, MA Petrukhina, SH Strauss, and OV Boltalina, "$C_{20}H_4(C_4F_8)_3$: A Fluorine-Containing Annulated Corannulene that Is a Better Electron Acceptor Than C_{60}", *Angewandte Chemie International Edition* 52, 7505-7508 (2013).

17. A Shokri, XB Wang, and SR Kass, "Electron-Withdrawing Trifluoromethyl Groups in Combination with Hydrogen Bonds in Polyols: Brønsted Acids, Hydrogen-Bond Catalysts, and Anion Receptors", *Journal of the American Chemical Society* 135, 9525-9530 (2013).

18. BW Larson, JB Whitaker, XB Wang, AA Popov, G Rumbles, N Kopidakis, SH Strauss, and OV Boltalina, "Electron Affinity of Phenyl−C_{61}−Butyric Acid Methyl Ester (PCBM)", *Journal of Physical Chemistry C* 117, 14958-14964 (2013).

19. GL Hou, MM Wu, H Wen, Q Sun, XB Wang, WJ Zheng, "Photoelectron spectroscopy and theoretical study of $M(IO_3)_2^-$ (M=H, Li, Na, K): Structural evolution, optical isomers, and hyperhalogen behavior", *Journal of Chemical Physics* 139, 044312-1-7 (2013).

20. J Zhang, DA Hrovat, ZR Sun, X Bao, WT Borden, and XB Wang, "The Ground State of $(CS)_4$ Is Different from that of $(CO)_4$: An Experimental Test of a Computational Prediction by Negative Ion Photoelectron Spectroscopy", *Journal of Physical Chemistry A* (in press) http://dx.doi.org/10.1021/jp406160d.

Free Radical Reactions of Hydrocarbons at Aqueous Interfaces

Principal Investigator: Kevin R. Wilson
Lawrence Berkeley National Laboratory, 1 Cyclotron Road, MS 6R2100, Berkeley, CA 94720
Email: krwilson@lbl.gov

Program Scope

This project will probe the surface chemistry of hydrocarbons molecules residing on nanometer and micron-sized aqueous droplets exposed to gas phase hydroxyl radicals using ambient pressure surface sensitive mass spectrometry and photoelectron spectroscopy. This program aims to:

(1) Quantify the link between molecular structure and surface reactivity of hydrocarbon free radicals at the gas liquid (solid) interface.

(2) Determine how the presence and distribution of interfacial ions control the surface reactivity of a hydrocarbon at an aqueous interface.

This work broadly supports the Department of Energy's Basic Energy Sciences program to better assess, mitigate and control the efficiency, utilization, and environmental impacts of energy use. This work seeks a rigorous molecular understanding of how heterogeneous reaction pathways lead to either bulk solvation of a surface active organic molecule or its removal from the interface through decomposition into gas phase products. These fundamental processes are critical for understanding the chemical fate of hydrocarbon byproducts of energy use and consumption.

Recent Progress (published work)

Surface Sensitive Mass Spectrometry of Nanoparticles and Micron Sized Droplets

One of the key technological advances necessary for probing the proposed surface chemistry on droplet surfaces is the development of surface sensitive mass spectrometry, based upon Direct Analysis in Real Time (DART) ionization. As a result much of the first year of this project was dedicated to a fundamental study of the interfacial probing depth of this technique. The production of ions in DART proceeds via a two step process. First thermal helium gas desorbs molecules from the particle or droplet surface after which ionization in the gas phase occurs directly by metastable helium atom bombardment or indirectly through secondary ion-molecule reactions. The ion signal observed by DART was observed to scale with particle surface area rather than droplet volume as shown in Fig. 1. These measurements were conducted for model nanometer-sized particles comprised of oleic acid. Further efforts were devoted to quantifying the actual probing depth of DART. This was accomplished by precisely measuring the change in particle size, produced

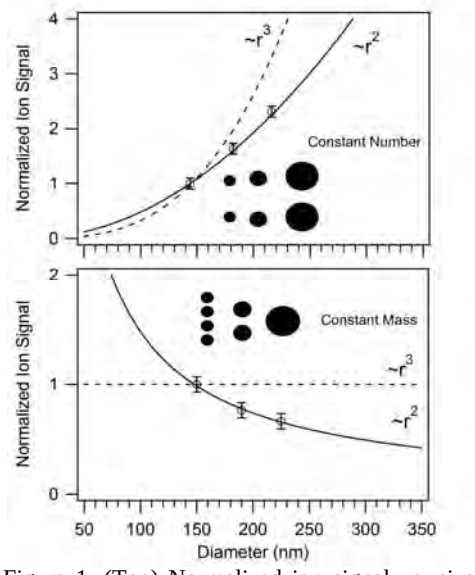

Figure 1. (Top) Normalized ion signal vs. size recorded for a constant number of particles in each size bin. (Bottom) normalized ion signal vs. size for size bins containing equal numbers of oleic acid molecules. Solid lines show the predicted instrument response if the instrument were sensitive to particle surface area. Dashed lines show the predicted instrument response to the total number of oleic acid molecules (i.e. particle volume).

by thermal desorption, as the nanoparticle transits through the ionization region of the DART mass spectrometer. As shown in Fig. 2, the change in particle diameter is observed to be a sensitive function of starting aerosol size and desorption temperature. Increasing the DART desorption temperature produces a change in particle size, due to thermal desorption of material from the aerosol surface. From the measured change in particle size these results reveal that the radial probing depth is on the order of 1 to 10 nm and depends upon initial particle or droplet size and DART desorption temperature. Shown as solid lines in Fig. 2 are predictions from a particle evaporation model using the Hertz Knudsen equation and the thermodynamic properties of oleic acid (i.e. enthalpy of vaporization). Shown in Fig. 3 are companion measurements of the DART ion signal as a function of desorption temperature for the same set of particle diameters as are shown in Fig. 2. The solid lines are results from the same model shown in Fig. 2. Overall, the agreement between model and measurement, in both Figs. 2 and 3, is good, revealing a robust correlation between the observed ion signal and the change in particle size. These results provide a quantitative picture of the thermal desorption behavior of nanoparticles and droplets in the DART source as well as a good estimate of how probing depth scales with desorption temperature.

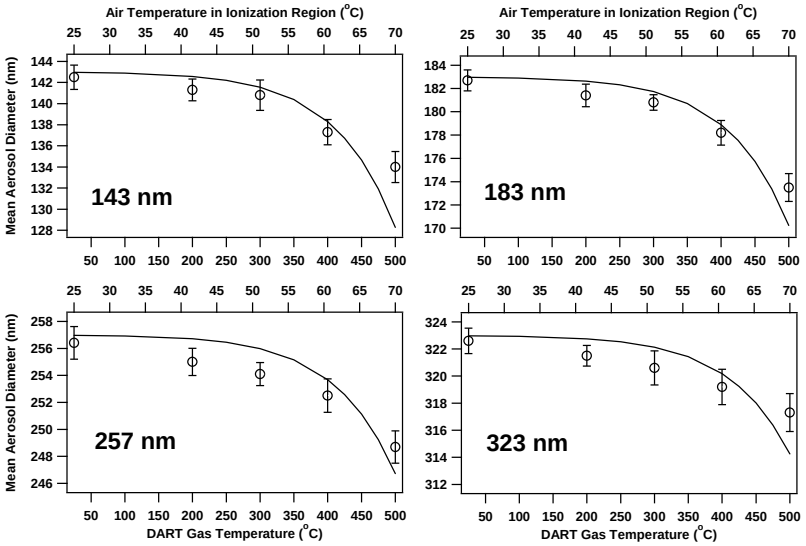

Figure 2: The mean aerosol diameter of oleic acid aerosols as a function of DART gas temperature. The solid line shows the aerosol diameter predicted by an aerosol evaporation model. The DART gas temperature is shown on the bottom x-axis with the corresponding measured air temperature near the middle of the ionization region shown on the top x-axis.

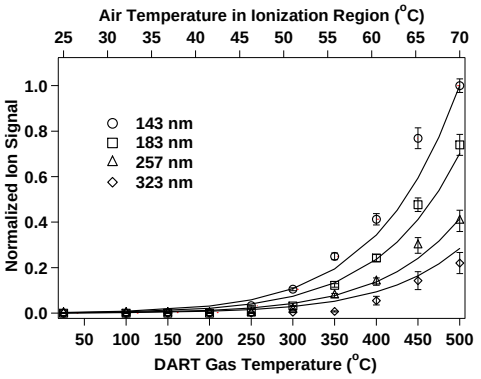

Figure 3: The normalized ion signal produced by oleic acid aerosols as a function of aerosol size and DART gas temperature. The solid lines are model predictions of ion signal using an aerosol evaporation model.

During the last 6 months, significant effort has been devoted to developing two other key aspects of the proposed research program. First, a quartz photochemical droplet reactor was designed and fabricated. Characterization of the performance of this flow tube system for quantifying heterogeneous reactions has been completed. A key design parameter is the ability to control the relative humidity (a key parameter to form and stabilize liquid water droplets) over the 8 foot long reactor tube. Initial results show that high relative humidity (RH > 95%) can indeed be generated and sustained over the length of the reactor. Various other experimental components necessary to quantify (e.g. gas chromatograph) and produce OH radicals in the photochemical reactor have been built, interfaced and tested.

Ongoing and Future Work

Heterogeneous Chemistry of Glassy Particles

As a first study in this new reactor we have begun experiments examining the heterogeneous chemistry of OH radicals with nanoparticles of sucrose (diameter ~200 nm). Sucrose was selected for study since it has relatively high glass transition temperature (~70 °C). As such both aqueous particles (with diffusion times that are fast relative to collision frequency of OH) and particles in a glassy (extremely high viscosity) state can be easily generated in our reactor at room temperature. A key question this work will address is how surface reaction pathways are altered by the underlying slow or fast transport of reactants and products to and from the particle surface.

A very sharp transition in the heterogeneous reaction of OH with sucrose is observed at RH=54 +/- 1%, which at 15 °C is consistent with the glass transition point predicted from macroscopic water activity measurements. At lower RH, sucrose remained in its initial glassy state. The reaction kinetics are bi-exponential, consistent with rapid oxidation of the surface layer at low OH exposures, followed by a much smaller reaction rate that is consistent with slow diffusion of sucrose through the glassy interior of the particle to the surface. At RH > 60%, where the droplets are aqueous, the reactive decay of sucrose follows a single exponential function (i.e. a single rate).

In addition to the change in sucrose decay kinetics, distinct heterogeneous oxidation products for glassy and aqueous sucrose particles were detected by DART. As OH exposure increased, the mass spectrometric (MS) signal revealed ~10 prominent reaction products for the glassy particles. In contrast relatively few reaction products (1 dominate product) were observed for sucrose in aqueous droplets. These preliminary data suggests a greater degree of complexity in the reaction mechanism at glassy surfaces. Future work on this system will focus on a complete description how surface reaction rates and product distributions depend upon the transport properties of the sucrose particles, whose viscosity, in our flow tube, can be changed over 6-7 orders of magnitude (via temperature and relative humidity).

Surface partitioning of Organic Molecules in Nanometer and Micron Sized Droplets

Developing a fundamental description of how the surface concentration of an organic molecule depends upon bulk composition in submicron droplets is an important first step in understanding the surface reactions of OH at the liquid-gas interfaces. There is emerging evidence that traditional parameterizations of surface tension and surface partitioning of organic molecules in aqueous solutions derived from macroscopic measurements is in fact inadequate for describing analogous behavior in small droplets in which the surface layer comprises a significant fraction of the total number of molecules in the droplet. For example, a 1 mm aqueous droplet of an ideal solution with a water activity of 0.999, corresponds to a solute concentration of 0.06 M. For an organic solute that has a surface excess concentration of 5×10^{-6} mol/m^2, only about 0.05% of the solute will partition to the surface, causing a negligible decrease in the bulk droplet concentration. This is in contrast to a 1 μm droplet wherein 50% of the total solute (with the same surface activity) will partition to the surface, causing an appreciable depletion of the bulk concentration. Therefore, to the extent that empirical relationships between bulk concentration and surface tension based on measurements of macroscopic sized aqueous solutions rely on this lack of sensitivity of bulk concentration to surface partitioning,

they will result in serious errors in describing both surface concentration and surface tension depression in the 1 μm or smaller droplets used to study the heterogeneous reaction described here.

A technique for quantifying the surface activity of organic molecules in microscopic particles has been developed to measure the size of aqueous droplets (ammonium sulfate + soluble hydrocarbons) that form at high (~100%) relative humidity. These measurements allow us to independently distinguish the Raoult's Law and Kelvin effects in droplet formation.

Using this technique, we have observed that many organic compounds are surface active in submicron droplets, sometimes to a greater extent than would be predicted based on macroscopic solution data. At high RH, particles containing such compounds tend to grow to the point where the organic molecules form a surface film. For example, lauric (n-C_{12}) acid and myrstic (n-C_{14}) acid form droplet surface films that are ~ 2.4 ± 0.6 and 2.8 ± 0.5 nm thick, respectively. Dicarboxlic acids form films less than half as thick as their mono-acid analogs. These results suggests that in submicron aqueous droplets with much higher surface-to-volume fractions, organic molecules, even soluble ones, reside almost entirely at the droplet-air interface. In other words, these results suggests that water soluble organic molecules behave much more like insoluble or "film-forming" surfactants when confined in small aqueous water droplets.

Future work will focus on developing a comprehensive description of the surface partitioning of organic molecules at the droplet air interface, which will later be combined with mass spectrometry measurements of free radical reactions at droplet interfaces in an effort to construct a better understanding of how reaction mechanisms depend upon interfacial phase as well as the diffusive transport of reactants and products from the droplet interior to the solid-vapor interface.

Publications Acknowledging CPIMS-DOE (Early Career Award) support (2012-present).

C. W. Harmon, C. R. Ruehl, C. D. Cappa, and K. R. Wilson, "A Statistical Description of the Evolution of Cloud Condensation Nuclei Activity during the Heterogeneous Oxidation of Squalane and Bis (2-ethylhexyl) Sebacate Aerosol by Hydroxyl Radicals," *Phys. Chem. Chem. Phys.*, **15**, 9679 (2013)

C. R. Ruehl, T. Nah, G. Isaacman, D. R. Worton, A. W. H. Chan, K. R. Kolesar, C. D. Cappa, A. H. Goldstein, and K. R. Wilson, "The influence of molecular structure and aerosol phase on the heterogeneous oxidation of normal and branched alkanes by OH," *J. Phys. Chem. A.*, **117**, 3990 (2013)

M.N. Chan, T. Nah, and K. R. Wilson, "In-Situ Chemical Detection of Sub-micron Organic Aerosols using Direct Analysis in Real Time Mass Spectrometry (DART-MS): The Effect of Aerosol Size and Volatility," *Analyst*, **138**, 3749 (2013)

T. Nah, M.N. Chan, S. R. Leone, and K. R. Wilson, "Real Time in Situ Chemical Characterization of Submicrometer Organic Particles Using Direct Analysis in Real Time-Mass Spectrometry," *Anal. Chem.*, **85**, 2087 (2013)

Catalytic Reactions and Highly Accurate Electronic Structure Methods

Theresa L. Windus
Ames Laboratory, 125 Spedding Hall,
Iowa State University, Ames, IA 50011
twindus@iastate.edu

PROGRAM SCOPE:

This component of the Chemical Physics Program at Ames Laboratory focuses on modeling of homogeneous catalytic reactions, the development of highly accurate electronic structure methods and their use in non-adiabatic chemical reactions. The modeling of homogeneous catalysis is in collaboration with the experimental group of Aaron Sadow in the Catalysis program at Ames Laboratory. The highly accurate electronic structure methods have been developed in collaboration with Klaus Ruedenberg and are focused on extending the correlation energy extrapolation by intrinsic scaling (CEEIS) method to larger molecular systems. In addition, the development of R12 technology with a local multi-reference configuration interaction (MRCI) is in progress. The development of non-adiabatic chemical methods is in collaboration with Mark Gordon's group.

RECENT PROGRESS:

HOMOGENEOUS CATALYSTS:

(i) In a collaboration with the Catalysis program at Ames Laboratory, the infrared assignments for ytterbium, calcium, and potassium tris(dimethylsilyl)methyl containing catalysts were confirmed. [1] These catalysts are unusually stable for β-hydrogen containing Si-H moieties, and are able to undergo facile β-hydrogen abstraction reactions when the auxiliary ligands are THF. β-hydrogen abstraction reactions are important for chemical transformations such as carbonyl reductions, alcohol oxidations and ester synthesis. When the auxiliary ligand is TMEDA, the metal-carbon bond is activated instead. The density functional calculations for these complexes agreed well with the X-ray crystal structures and helped to identify the locations of the hydrogens. In addition, the calculations showed that the SiH groups with short metal-SiH distances for the THF compounds were the lower frequency bands in the experiments suggesting β-agostic SiH.

(ii) The reaction mechanism for stereospecific cycloamination reactions with cyclopentadienyl-bis(oxazolinyl)borato zirconium complexes is being examined in collaboration with the Sadow group. While experimental and computational models agree on the structures and IR spectrum of the complexes [2], the reaction mechanism is proving to be elusive. Multiple possible mechanisms agree with the experimental kinetics and there is debate in the experimental community on the mechanisms of cylcoamination in general (especially with d^0 metals). The major proposed mechanisms involve (A) insertion, (B) $2\pi+2\pi$ cycloaddition, or (C) concerted CN/CH bond formation (Scheme 1).

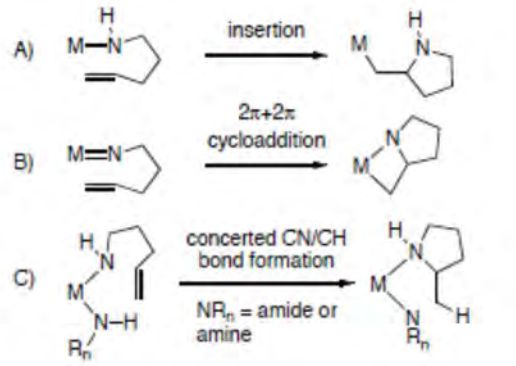

Scheme 1. Proposed pathways for C-N bond formation in metal catalyzed aminopentene cyclization.

Each of these mechanisms (and several others) are being examined using density functional methods (B3LYP, PBE0 and M06-2L) for structures and energetics with additional MP2 single point energies to improve the energetics in collaboration with Mark Gordon's group. The structures change minimally between the different functionals, which implies (unsurprisingly) that the structures can be represented without too much difficulty. Interestingly, though, the newer M06-2L functionals give energetics similar to the MP2, while the others give reaction barriers that are much higher in energy. Ligand effects on the reaction barriers for the different mechanisms are also being examined since these are seen in the experimental results.

HIGHLY ACCURATE ELECTRONIC STRUCTURE CALCULATIONS:

(i) Highly accurate CEEIS calculations have been examined by Windus and Ruedenberg for the dissociation curves of the ground and first three singlet excited states of C_2. [3] The results obtained so far have demonstrated that the CEEIS approach, in addition to being more accurate than the conventional state-averaged (SA) approach, is also independent of the weighting of the reference states. Typical SA-MCSCF calculations usually assume either an equal weighting of all states involved or a dynamical weighting based on a smoothly varying state energy difference functional. Werner et al have shown that the differences in these two approaches can significantly change the wavefunction, the energetics of the states involved, and the energetics of correlated methods based on these wavefunction. By contrast, using the two weighting methods in constructing the SA-MCSCF references did not affect the CEEIS procedure: the same high accuracy dissociation curves were obtained once the triple excitation contributions were included.

(ii) Windus and Ruedenberg have extended the CEEIS method to take advantage of many-body effects in a new correlation energy extrapolation by many body expansion method (CEEMBE). The CEEMBE method combines several ideas to obtain a reliable estimate for the configuration interaction (CI) energy of the chemical system. First, the valence orbitals in the reference MCSCF calculation are separated into groups (or "bodies"), each with a preset number of valence electrons using occupationally restricted multiple active space (ORMAS). Next, a series of computations are performed for each of the smaller ORMAS references where a certain level of excitations (doubles, triples, quadruples, etc.) are made into a limited number of virtual orbitals, n, where n increases toward the full virtual space. Many body expansion techniques are then used to approximate the value of the total CI energy from the energies of the smaller CI

calculations. Additional accuracy can then be obtained by linearly extrapolating the changes that occur in the approximate energy against the changes that occur in the exact energy as the number of virtual orbitals is varied.

(iii) Windus and Ruedenberg have also initiated a careful examination of important portions of the ozone potential energy surface using SA-MCSCF. The stationary points include the "traditional" open ring structure, the equilateral ring structure (yet, to be found experimentally), and the transition state between the two. In addition, the minimum on the excited state surface and the conical intersection between the ground and lowest excited state have been located. Interestingly, the ground state transition state, excited state minimum and the conical intersection all lie quite close to one another. Further study with the CEEMBE method is underway to fully understand the energetics and spectroscopy of this complicated potential energy surface.

FUTURE PLANS:

HOMOGENEOUS CATALYSTS:

Stronger ties to the catalysis groups at Ames will be made by examining catalytic and photocatalytic mechanisms of the native molecular systems and with those on mesoporous silica nanoparticles (MSNs) or $CdS_{1-x}Se_x$ nanocrystals. Of initial interest is completing the study of the Zr catalyzed hydromination reaction mechanism. Interestingly, the Y substituted catalysis provides the opposite stereochemical products than the Zr catalyst does. So, the Y substituted catalysis reaction will also be examined to understand the energetic and mechanistic differences between the two metals. Rhodium catalyzed decarbonylation reactions for alcohols will also be examined since they react both thermally and photochemically and provide a rich chemistry to explore. Understanding the different reaction pathways and the modifications of these paths when interacting with a nanocrystal and the MSN is a long term goal of the research.

HIGHLY ACCURATE ELECTRONIC STRUCTURE CALCULATIONS:

(i) Development of the CEEMBE method will continue and be expanded to allow for much larger molecular systems than previously explored using the CEEIS method. In particular, different virtual space specifications to allow for a more localized virtual space will be used to decrease the number of determinants in the calculations. Early explorations into this approach appear promising, but many more computations will be required to verify the approach.

(ii) In a recent collaboration with Professor Emily Carter, a local MRCI program has been implemented into GAMESS, which allows much larger systems and their excited states to be examined. In an effort to improve the convergence of the excited and ground state calculations with respect to basis set, the explicitly correlated R12 method as formulated by Valeev is being integrated with the localized MRCI code. The R12 approach has shown that quadruple zeta quality results can be obtained using a double zeta basis set for small ground state molecules – decreasing the overall cost by using a smaller basis set. To date, the second-order density matrix (SODM) - required by the R12 perturbative approach - has been implemented within the local MRCI code symmetric group approach (SGA). The SODM is then passed to the R12 code within MPQC to calculate the correction. While the proof of concept has been completed for very small molecules,

general improvements in the formalism and in the implementation must be pursued to make the software viable for larger chemical systems. In particular, the sparsity of the memory needs to be taken into account.

NON-ADIABATIC DYNAMICS:

While it is anticipated that investigation of the electronic structure surfaces will provide significant information, it is likely that reaction rates will need to be computed to understand the final product distributions of the reactions. Depending on the electronic coupling of the ground and excited state calculations, Marcus and variational transition state theory will be used to determine the rates of the reactions. If there is the potential for strong non-adiabatic coupling, the Tully fewest switches surface hopping method as implemented in NEWTON-X will be used with the least expensive, most appropriate electronic structure method. This will likely require the time-dependent DFT (TDDFT) and spin-flip TDDFT capabilities of GAMESS to be interfaced with NEWTON-X in collaboration with Mark Gordon's group. Since the systems to be examined are large and the relaxation times are relatively long, the simulations will start with a distribution of many trajectories near the important surface crossings. While the distribution of the initial states for non-adiabatic dynamics is still an area of research, in this work, initial simulations will use the appropriately scaled Wigner distributions to probe the region.

PUBLICATIONS:

[1] "Intermolecular β-hydrogen abstraction in ytterbium, calcium and potassium tris(dimethylsilyl)methyl compounds.", K. Yan, G. Schoendorff, B.M. Upton, A. Ellern, T.L. Windus, and A.D. Sadow, *Organometallics*, **2013**, *32*, 1300–1316.

[2] "Highly Enantioselective Zirconium-Catalyzed Cyclization of Aminoalkenes", K. Manna, W.C. Everrett, G. Schoendorff, A. Ellern, T.L. Windus, and A.D. Sadow, *J. Am. Chem. Soc.*, **2013**, *13*, 7235–7250.

[3] "Accurate ab initio potential energy curves and electronic and vibrational spectra for C_2", J. Boschen, L. Bytautas, K. Ruedenberg, T.L. Windus, *Theor. Chem. Acc.*, invited, submitted

Ionic Liquids: Radiation Chemistry, Solvation Dynamics and Reactivity Patterns

James F. Wishart
Chemistry Department, Brookhaven National Laboratory, Upton, NY 11973-5000
wishart@bnl.gov

Program Definition

Ionic liquids (ILs) are a rapidly expanding family of condensed-phase media with important applications in energy production, storage and consumption, including advanced devices and processes and nuclear fuel and waste processing. ILs generally have low volatilities and are combustion-resistant, highly conductive, recyclable and capable of dissolving a wide variety of materials. They are finding new uses in dye-sensitized solar cells, chemical synthesis, catalysis, separations chemistry, batteries, supercapacitors and other areas. Ionic liquids have dramatically different properties compared to conventional molecular solvents, and they provide a new and unusual environment to test our theoretical understanding of primary radiation chemistry, charge transfer and other reactions. We are interested in how IL properties influence physical and dynamical processes that determine the stability and lifetimes of reactive intermediates and thereby affect the courses of reactions and product distributions. We study these issues by characterization of primary radiolysis products and measurements of their yields and reactivity, quantification of electron solvation dynamics and scavenging of electrons in different states of solvation. From this knowledge we wish to learn how to predict radiolytic mechanisms and control them or mitigate their effects on the properties of materials used in nuclear fuel processing, for example, and to apply IL radiation chemistry to answer questions about general chemical reactivity in ionic liquids that will aid in the development of applications listed above.

Soon after our radiolysis studies began it became evident that the slow solvation dynamics of the excess electron in ILs (which vary over a wide viscosity range) increase the importance of pre-solvated electron reactivity and consequently alter product distributions and subsequent chemistry. This difference from conventional solvents has profound effects on predicting and controlling radiolytic yields, which need to be quantified for the successful use under radiolytic conditions. Electron solvation dynamics in ILs are measured directly when possible and estimated using proxies (e.g. coumarin-153 dynamic emission Stokes shifts or benzophenone anion solvation) in other cases. Electron reactivity is measured using ultrafast kinetics techniques for comparison with the solvation process.

A second important aspect of our interest in ionic liquids is how their unusual sets of properties affect charge transfer and charge transport processes. This is important because of the many applications of ionic liquids in devices that operate on the basis of charge transport. While interest in understanding these processes in ionic liquids is growing, the field is still in an early stage of development. We are using donor-bridge-acceptor systems to study electron transfer reactions across variable distances in a series of ionic liquids with a range of structural motifs and whose dynamical time scales vary from moderately fast to extremely slow, and to compare them with conventional solvents.

Methods. Picosecond pulse radiolysis studies at BNL's Laser-Electron Accelerator Facility (LEAF) are used to identify reactive species in ionic liquids and measure their solvation and reaction rates. This work is aided greatly by the development of Optical Fiber Single-Shot (OFSS) detection at LEAF by A. Cook (DOI: 10.1063/1.3156048) and its present extension into the NIR regime. IL solvation and rotational dynamics, and electron transfer reactions are measured by TCSPC in the laboratory of E. W. Castner at Rutgers Univ. Picosecond transient absorption measurements of excited state dynamics and electron transfer reactions are done in the laboratory of R. Crowell (BNL). Diffusion rates of anions, cations and solutes are obtained by PGSE NMR in S. Greenbaum's lab at Hunter College, CUNY and by Castner's group at Rutgers. We have extensive collaborations with other major groups in ionic liquid synthesis, physical chemistry, simulations and radiation chemistry.

Ionic liquid synthesis and characterization. Our work often involves novel ILs that we design to the requirements of our radiolysis and solvation dynamics studies and are not commercially available. We have developed in-house capabilities and a network of collaborations (particularly with S. Lall-Ramnarine of Queensborough CC and R. Engel of Queens College) to design, prepare and characterize ILs in support of our research objectives. Cation synthesis is done with a CEM microwave reactor, resulting in higher yields of purer products in much shorter time than traditional methods. We have assembled an instrumentation cluster including DSC, TGA, viscometry, AC conductivity, Karl Fischer moisture determination, ion chromatography and ESI-mass spec (for purity analysis and radiolytic product identification). The cluster serves as a resource for our collaborators in the New York Regional Alliance for Ionic Liquid Studies and other institutions (Penn State, ANL, ORNL). Our efforts are substantially augmented by student internships from the BNL Office of Educational Programs, particularly the VFP (formerly FaST) program, which brings collaborative faculty members and their students into the lab for ten weeks each summer. Since 2003, a total of 37 undergrads, two graduate students, one pre-service teacher, one high school student and four junior faculty have worked on IL projects in our lab, many of them for more than one summer.

Recent Progress

Phosphorus for nitrogen substitution in cyclic IL cations. Efforts are continually underway to improve IL properties (such as viscosity, conductivity, thermal stability, *etc.*) to help expand their energy-related applications. The most widely investigated ILs are composed primarily of nitrogen-centered cations, however phosphonium ILs have been observed to have more favorable characteristics, including lower costs, lower viscosity (by ~50%), greater thermal stability (by ~100 ˚C), and wider electrochemical windows compared to their ammonium congeners. ILs with cyclic cations (e.g., pyrrolidinium and piperidinium) have better transport and physical properties than most acyclic ammonium ILs, but their phosphorus analogs have not been studied. We prepared four new cyclic phosphonium ILs that are representatives of a much wider class of potentially useful ILs. However, these exemplars are slightly less conductive and have slightly smaller self-diffusion coefficients than their cyclic ammonium congeners, and their viscosities are not significantly lower either. Although the points of comparison are few so far, these results defied expectations based on the behaviors of linear phosphonium and ammonium ILs. Such "surprises" often lead to deeper insights into the dynamical workings of ILs that have had important impacts on the field. For this reason we will continue to explore cyclic phosphonium ILs through synthesis of a wider variety of structural types and substituents, variation of anions, and more extensive characterization of their physical, structural, and dynamical properties. In particular, this family of ILs, by comparison with the more familiar cyclic ammonium ILs, should reveal the dynamical effects of cyclic *vs.* linear alkyl chains on the physical properties of ionic liquids. A manuscript has been submitted. (with S. Lall-Ramnarine and R. Engel, CUNY)

Mid-infrared observation and kinetics of radicals in ionic liquids. LEAF has recently added a third beam line dedicated to mid-infrared (1050-2330 cm^{-1}) transient absorption pulse radiolysis on the nanosecond time scale, based on quantum cascade laser IR sources. Preliminary work has begun to use vibrational spectroscopy to identify and characterize radiation-induced transient species in ILs, starting with tetracyanoborate and thiocyanate ILs. Knowing the dose of radiation delivered to the sample is an important aspect of radiation chemistry and it facilitates quantitation of transient species, so some form of chemical dosimeter is needed. We demonstrated that 1-ethyl-3-methyl-imidazolium thiocyanate, dissolved in other ILs, could serve as a reliable dosimeter by observing the second-order recovery of the SCN^- nitrile stretch at 2054 cm^{-1} due to the well-known disproportionation of $(SCN)_2^{-\bullet}$ radical. The observed recovery rate is a function of the absorbed dose, and the IR data can be calibrated by visible TA pulse radiolysis of the same sample at 470 nm where the yield and second-order rate constant are easily determined.

Future Plans

Effects of ionic liquids on intramolecular ET processes. Over the years, we have used oligoproline-bridged electron donor-bridge-acceptor (D-B-A) systems to probe various aspects of the energetics and distance dependence of ET processes in conventional solvents. We are now using these D-B-A systems to study how ionic liquids affect ET processes. Our first study[2] looked at a single D-B-A system in four solvents, including two ILs with short alkyl chains (butyl), and showed how slow IL dynamics leads to distributed ET kinetics as predicted by theory. We are extending our studies to include ILs with longer decyl chains that form discreet nonpolar domains within the IL. The question of local environment effects (dynamical and energetic) is very important in ILs because of their molecular-scale polar/non-polar heterogeneity. To probe deeper into these aspects, we have prepared D-B-A systems of different charge types, which we expect to occupy different regions within the IL. The neutral DMPD-pro$_n$-C343 system (n = 0-2) undergoes photoinduced charge separation to form a zwitterion, followed by charge recombination during the back electron transfer. Building on the previous emission work on the n = 1 complex,[2] we are using picosecond transient absorption techniques to observe the back ET process and any forward ET processes too fast for TCSPC, and we are changing the bridge length to look for effects of IL structural heterogeneity on both processes using TA and TCSPC. For comparison, we will study the charged $[(bpy)_2Ru^{II}MCbpy\text{-}(pro)_n\text{-}ampyRu^{III}(NH_3)_5]^{5+}$ (n = 1,2) system that we have investigated extensively in water, which should preferably be located in the polar region of the IL. The $(bpy)_2Ru^{II}MCbpy$ center is an excited-state electron donor, so the forward and back ET reactions are charge-shift (2+,3+/3+,2+) instead of separation and recombination. (with R. Crowell (BNL, psec TA), E. W. Castner (Rutgers, TCSPC) and R. Rachid (Fordham, synthesis))

Scavenging and solvation processes of pre-solvated electrons in ionic liquids. Our early work in the reactivity of excess electrons in ionic liquids demonstrated the importance of pre-solvated electron scavenging in trying to understand and predict the distributions of early radiolysis products and radiolytic damage accumulation. It was also clear that the slower relaxation dynamics of ILs made them excellent media for the general study of fundamental radiolysis processes without the need to use cryogenic techniques, in combination with the advanced instrumentation of the LEAF Facility. We recently connected our observed electron solvation dynamics to the kinetics of electron scavenging.[1] In other preliminary work we have observed that selected scavengers (e.g., nitrate, benzophenone) in ILs show different reaction profiles towards the various precursor states to the solvated electron. Different scavenger reactivities towards pre-solvated and solvated electrons have been known empirically for many years and cryogenic kinetic work by Jonah and Lewis showed specific mechanistic differences between scavengers similar to what we have seen in ILs. However, the combination of extended IL dynamical time scales and the time resolution of the LEAF OFSS detection system, coupled with the fact that it uses only small amounts of samples that do not have to be flowed, as well as the ability of ILs to dissolve polar and nonpolar scavengers, provides a unique opportunity to characterize the fundamental reactivity of pre-solvated electron species and understand how the properties of scavengers control their reaction profiles. The extension of the LEAF OFSS detection capability to the NIR (900-1700 nm) will greatly facilitate the study of dynamical and electron solvation processes in our ILs. This knowledge will permit the design of better systems to control radiation-induced reactivity, for example in the processing of radioactive materials (whether in ionic liquids or not), in systems for radiation processing and sterilization, and during long-term exposure to space, for example. (with A. Cook, BNL)

Cage escape and recombination in ILs. The early steps of photoinduced reactions often involve a competition between recombination and escape of the photoproducts, whether they are radicals or charge-separated states, which largely determines the quantum efficiency of energy capture and in some cases, photodegradation yields in catalytic systems. Recent quantum MD simulations by our collaborators imply that

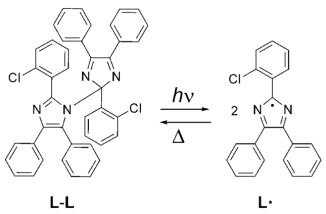

cage escape/recombination of radiation-induced radical species is important to explain yields of early radiolysis products as well. Compared to molecular solvents, ionic liquids may show unusual dynamical effects in cage relaxation, in addition to slower cage escape due to higher viscosity. In previous work, we observed such effects in the photolysis of *ortho*-chloro-hexaarylbisimidazole (*o*-Cl-HABI, L-L in the adjacent scheme) where quantum yields of the lophyl radical (L•) were much lower in three ILs than in DMSO. Work by others showed that even the recombination of lophyl radical pairs that are covalently constrained in a near-optimal configuration is quite slow ($t_{1/2}$ = 33 ms, $\Delta G^{\neq}$ = 65.5 kJ/mol) due to the large structural rearrangement required. We would like to know if ILs promote recombination through slower cage structural relaxation, holding the radical pair close to the transition state configuration for a longer time, and whether the viscosity-lengthened cage escape time promotes recombination of the relaxed pair through interactions with the IL environment. The OFSS system is critical to this effort because the diffusive recombination of lophyl radicals takes many seconds in ILs and in ordinary solvents, making typical repetitive pump-probe experiments completely impractical. In contrast, OFSS provides picosecond-resolution, 5-nanosecond-range transient absorption data using relatively small numbers of shots that can be collected at arbitrarily long delays in-between. With this advantage, we will examine the kinetics of cage escape and recombination in ILs of different viscosities, and the effects of slow IL relaxation dynamics on the planarization of the lophyl radical, which provides the very large reorganization barrier for radical dimerization. (Collaboration with Prof. V. Strehmel (U. of Applied Sci., Krefeld, Germany) and A. Cook and D. Polyanskiy (BNL))

Publications

1. *Electron solvation dynamics and reactivity in ionic liquids observed by picosecond radiolysis techniques* J. F. Wishart, A. M. Funston, T. Szreder, A. R. Cook and M. Gohdo, *Faraday Discuss.* **154**, 353-363 (2012).
2. *A Comparison of Electron-Transfer Dynamics in Ionic Liquids and Neutral Solvents* H. Y. Lee, J. B. Issa, S. S. Isied, E. W. Castner, Jr., Y. Pan, C. L. Hussey, K. S. Lee and J. F. Wishart, *J. Phys. Chem. C,* **116**, 5197-5208 (2012).

Molecular level understanding of hydrogen bonded environments

Sotiris S. Xantheas
Physical Sciences Division, Pacific Northwest National Laboratory
902 Battelle Blvd., Mail Stop K1-83, Richland, WA 99352
sotiris.xantheas@pnnl.gov

The objective of this research effort aims toward developing a comprehensive, molecular-level understanding of the collective phenomena associated with intermolecular interactions occurring in guest/host molecular systems and aqueous environments. The motivation of the present work stems from the desire to establish the key elements that describe the structural and associated spectral features of simple ions in a variety of hydrogen bonded environments such as bulk water, aqueous interfaces and aqueous hydrates. Simple model systems including small molecules of complex electronic structure as well as aqueous clusters offer a starting point in this process by providing the test bed for validating new approaches for analyzing the electronic structure as well as the nature of interactions and the magnitude of collective phenomena at the molecular level. For instance, high level first-principles electronic structure calculations of the structures, energetics, and vibrational spectra of aqueous neutral and ionic clusters provide useful information needed to assess the accuracy of reduced representations of intermolecular interactions, such as classical potentials used to model the macroscopic structural and thermodynamic properties of those systems. The database of accurate cluster structures, binding energies, and vibrational spectra can, furthermore, aid in the development of new density functionals, which are appropriate for studying the underlying interactions. Representative applications include the modeling of liquid water and ice, aqueous ion solvation and applications, including the structure of clathrate hydrates and the interaction of host molecules with those guest networks. The detailed molecular-scale account of aqueous systems provided by these studies are relevant to Department of Energy programs in contaminant fate and transport and waste processing as well as hydrogen storage.

We have investigated the molecular origin of the difference in the HOH bend of the IR spectra between liquid water and ice (S. Imoto *et al.*, *J. Chem. Phys.* **138**, 054506 (2013)). The intensity of the HOH bend in the IR spectrum of ice is significantly smaller than the corresponding one in liquid water. This difference in the IR intensities of the HOH bend in the two systems was investigated using MD simulations with the flexible, polarizable, *ab-initio* based TTM3-F model for water, a potential that correctly reproduces the experimentally observed increase of the HOH angle in liquid water and ice from the water monomer value. We have identified two factors that are responsible for the difference in the intensity of the HOH bend in liquid water and ice: (*i*) the decrease of the intensity of the HOH bend in ice caused by the strong anti-correlation between the permanent dipole moment of a molecule and the induced dipole moment of a neighboring hydrogen bond acceptor molecule and (*ii*) the weakening of this anti-correlation by the disordered hydrogen bond network in liquid water. The presence of the anti-correlation in ice is further confirmed by *ab initio* electronic structure calculations of water pentamer clusters extracted from the trajectories of the MD simulations for ice and liquid water.

In contrast to the HOH bend, the OH stretch shows a positive correlation between the permanent dipole moment of a molecule and the induced dipole moment of its HB acceptor.

Since the ordered HB structure increases the positive correlation, the IR intensity of the OH stretch in ice is larger than that in liquid water. The sensitivity of the OH stretch on the underlying HB environment is well established. In our study we demonstrated that the IR intensity of the HOH bend is also sensitive to the HB structure. Since the HOH bend is more delocalized than the OH stretch, the properties of the HOH bend would be more strongly dependent on the HB network than for the OH stretch.

We also investigated the frequency fluctuations of the OH stretch and the HOH bend in liquid water from MD simulations with the TTM3-F *ab inito*-based potential (S. Imoto *et al. J. Chem. Phys.* **139**, 044503 (2013)). The 2D IR spectra and peak shifts of the OH stretch and HOH bend were calculated directly from the third-order response function, for which only the high T approximation is used. The 2D IR spectrum of the OH stretch at the delay time T = 0 fs is diagonally elongated because of the strong correlation between ω_1 and ω_3. The calculated decrease in the diagonal width and corresponding increase in the anti-diagonal width with increasing delay time are due to the loss of the initial inhomogeneity. The slope of 2D IR spectra of the OH stretch in liquid water suggests three processes, i.e. an initial decay with a time constant of 40 fs, a plateau from 60 to 100 fs, and a slow decay with a time constant of 180 fs, similar to those of the OH stretch in liquid D_2O, though these processes in liquid H_2O are faster than those in liquid D_2O. Normal mode analysis suggests that the frequency fluctuation of the OH stretch mainly arises from the intermolecular HB stretch and the librational motion.

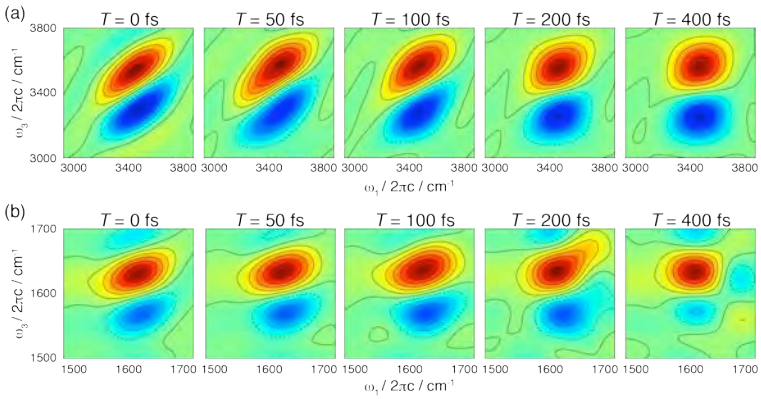

Figure 1. 2D IR spectra as a function of delay time for (a) the OH stretch and (b) the HOH bend in liquid water.

Our calculation revealed that the ultrafast decay of the frequency correlation of the HOH bend, i.e. the 2D IR spectrum at T = 0 fs already leans to the ω_1 axis. The frequency fluctuation of the HOH bend consists of three processes: an initial spectral diffusion with a time constant of 60 fs, a plateau from 100 to 150 fs, and a slow decay with a time constant of 120 fs. The time evolution of the normal mode frequency of the HOH bend along equilibrium MD trajectories reveals the strong couplings between the frequency of the HOH bend and the OH stretch as well as the intermolecular HB bend. Although the direct coupling between the HOH bend and the intermolecular HB stretch is not large, the effect of the intermolecular HB stretch, i.e., the fluctuation of the HB environment, via the OH stretch is seen as the plateau region from 100 to 150 fs in the time evolution of the slope of the 2D IR spectra and the peak shift. The present results demonstrate that the coupling between the HOH bend and the OH stretch is essential to reproduce the correct properties of the HOH bend though the coupling can have minimal effect on the

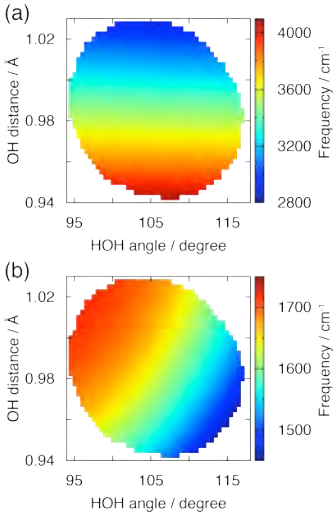

Figure 2. Relationship between the intramolecular structure and the normal mode frequencies of (a) the OH stretch and (b) the HOH bend in liquid water.

frequency fluctuation of the OH stretch. The frequency fluctuation of the OH stretch is caused by the intermolecular HB stretch and the libration, while that of the HOH bend by the OH stretch as well as the intermolecular HB bend. The reason why the frequency of the HOH bend is modulated by the OH stretch, but that of the OH stretch is not by the HOH bend, is because the frequency of the OH stretch depends almost only on the OH distance, whereas that of the HOH bend indeed depends on both the HOH angle and the OH distance. As a result, the frequency fluctuation of the HOH bend is caused by the coupling the OH stretch, but that of the OH stretch is not significantly affected by the HOH bend.

We have finally revisited the previous hypothesis regarding the existence of two kinds of hydrogen bonds in ice Ih, as an explanation of the existence of two peaks in the Inelastic Neutron Scattering (INS) spectra. By using a linear-scaling, embedded-fragment MP2-based method for an infinitely extended, three-dimensional crystal of ice Ih, we were able to predict ice's structural parameters, IR, Raman, and INS spectra, as well as the heat capacity from the first principles, i.e., without resorting to the use of density functionals or empirical potentials (X. He *et al. J. Chem. Phys.* **137**, 204505 (2012)). Our calculations predicted a narrow distribution of O–H bond lengths centered at the experimental values for proton-ordered ice II and IX and the two peaks in the hydrogen-bond-stretching region of INS spectra. They do not support and indeed disprove the previous hypothesis of Li and Ross that there exist two types of hydrogen bonds with vastly different bond strengths. While the two peaks are reasonably described as hydrogen-bond stretches, they do not originate from the difference in the force constants associated with different nearest-neighbor local arrangements, but rather from the different directionalities of motion, manifested in the distinct polarizations of absorbed photons. Our calculations also shed light on the assignments of individual IR, Raman, and INS peaks and their variation with deuterium concentration. They also elucidate the cause of anomaly in the low temperature heat capacity of ice.

References to publications of DOE sponsored research (10/01/2010 - present)

1. S. Yoo, E. Aprà, X.-C. Zeng and S. S. Xantheas, "Lowest-Energy Structures of Water Clusters $(H_2O)_{16}$ and $(H_2O)_{17}$ from high-level ab initio calculations", *Journal of Physical Chemistry Letters* **1**, 3122 (2010)
2. J. C. Werhahn, S. Pandelov, S. Yoo, S. S. Xantheas, H. Iglev, "Dynamics of Confined Water Molecules in Aqueous Salt Hydrates", in *Ultrafast Phenomena XVII*, M. Cherqui, D. M. Jonas, E. Riedle, R. W. Schoenlein, A. J. Taylor (Eds.), Oxford University Press, pp. 463-465 (2011)
3. S. Yoo and S. S. Xantheas, "The Effect of Dispersion Corrections on the Melting Temperature of Liquid Water", Communication to the Editor, *Journal of Chemical Physics* **134**, 121105 (2011). Featured in the *Virtual Journal of Biological Physics Research*. 5th most downloaded paper in April 2011
4. X.-B. Wang and S. S. Xantheas, "Photodetachment of Isolated Bicarbonate Anion: Electron Binding Energy of HCO_3^-", *Journal of Physical Chemistry Letters* **2**, 1204 (2011)
5. S. Yoo and S. S. Xantheas**,** "The Role of Hydrophobic Surfaces in Altering Water-Mediated Peptide-Peptide Interactions in an Aqueous Environment" Victoria Buch Memorial Issue (invited), *Journal of Physical Chemistry A* **115**, 6088 (2011)
6. J. C. Werhahn, S. Pandelov, S. S. Xantheas, H. Iglev, "Dynamics of Weak, Bifurcated and Strong Hydrogen Bonds in Lithium Nitrate Trihydrate", *Journal of Physical Chemistry Letters* **2**, 1633 (2011)
7. S. Kaneko, Y. Inokuchi, T. Ebata, E. Aprà and S. S. Xantheas, "Laser Spectroscopic and Theoretical Studies of Encapsulation Complexes of Calix[4]arene", *Journal of Physical Chemistry A*, **115**, 10846 (2011)

8. A. Whiteside, S. S. Xantheas, M. Gutowski, "Is Electronegativity a Useful Descriptor for the "Pseudo-Alkali-Metal" NH_4?", *Chemistry A European Journal* **17**, 13197 (2011). Journal cover. Included as a Feature Article in *DOE Pulse*, #356, Feb. 13, 2012: http://www.ornl.gov/info/news/pulse/no356/feature.shtml. Highlighted in Royal Society of Chemistry's "*Chemistry World*", 23 September 2011: http://www.rsc.org/chemistryworld/News/2011/September/23091104.asp

9. J. Liu, W. H. Miller, G. S. Fanourgakis, S. S. Xantheas, S. Imoto and S. Saito, "Insights in Quantum Dynamical Effects in the Infrared Spectroscopy of Liquid Water from a Semiclassical Study with an Ab Initio-Based Force Field", *Journal of Chemical Physics* **135**, 244503 (2011)

10. S. Yoo and S. S. Xantheas, "Structures, Energetics and Spectroscopic Fingerprints of Water Clusters *n*=2-24" in *Handbook of Computational Chemistry*, J. Leszczynski (ed.), Springer Science+Business Media B. V., ISBN 978-94-007-0710-8, Chapter 21, pp. 761-792 (2012)

11. S. Yoo and S. S. Xantheas, "Enhancement of Hydrogen Storage Capacity in Hydrate Lattices", *Chemical Physics Letters*, **525-526**, 13-18 (2012). Editor's Choice article. Featured in DOE's *In Focus* online publication: http://science.energy.gov/news/in-focus/2012/02-06-12/, Science Daily, EV Driven, Deixis magazine (Computational Science at the National Laboratories) http://www.deixismagazine.org/2012/07/twice-stuffed-permafrost/?utm_source=rss&utm_medium=rss&utm_campaign=twice-stuffed-permafrost

12. R. L. Sams, S. S. Xantheas, and T. A. Blake, "Vapor Phase Infrared Spectroscopy and *ab initio* Fundamental Anharmonic Frequencies of Ammonia Borane", *Journal of Physical Chemistry A* **116**, 3124 (2012)

13. G.-L. Hou, H. Wen, K. Lopata, W.-J. Zheng, K. Kowalski, N. Govind, X.-B. Wang, and S. S. Xantheas, "Zeise's Anion and Its Br- and I-Analogs: A Combined Gas-Phase Photoelectron Spectroscopic and Theoretical Study", Communication to the Editor, *Angewandte Chemie International Edition* **51**, 6356 (2012). Journal Cover

14. S. S. Xantheas, "Low-lying energy isomers and global minima of aqueous nanoclusters: Structures and corresponding spectroscopic features of the pentagonal dodecahedron $(H_2O)_{20}$ and $(H_3O)^+(H2O)_{20}$", Special issue on "Nano-Thailand: Nanotechnology for A Sustainable World" (invited), *Canadian Journal of Chemical Engineering* **90**, 843 (2012)

15. D. S. Lambrecht, L. McCaslin, S. S. Xantheas, E. Epifanovsky, and M. Head-Gordon, "Refined energetic ordering for sulfate-water (n=3-6) clusters using high-level electronic structure calculations", Peter Taylor Special Issue (invited), *Molecular Physics* **110**, 2513 (2012)

16. X. He, O. Sode, S. S. Xantheas, and S. Hirata, "Second-order many-body perturbation study of Ice Ih", *Journal of Chemical Physics* **137**, 204505 (2012)

17. S. Imoto, S. S. Xantheas, S. Saito, "Molecular origin of the difference in the HOH bend of the IR spectra between liquid water and ice", *Journal of Chemical Physics* **138**, 054506 (2013)

18. N. Mardirossian, D. S. Lambrecht, L. McCaslin, S. S. Xantheas, and M. Head-Gordon, "The Performance of Density Functionals for Sulfate-Water Clusters", *Journal of Chemical Theory and Computation* **9**, 1368 (2013)

19. K. Doi, E. Togano, S. S. Xantheas, R. Nakanishi, T. Nagata, T. Ebata and Y. Inokuchi, "Microhydration Effects on the Intermediates of the (I^- + CH_3I) S_N2 Reaction", Communication to the Editor, *Angewandte Chemie International Edition* **52**, 4380 (2013). Highlighted in the "Science Concentrates" section, Chemical & Engineering News, vol. **91** (8), p. 34-35 (2013)

20. E. Miliordos, K. Ruedenberg and S. S. Xantheas, "Unusual inorganic biradicals: A Theoretical Analysis", Communication to the Editor, *Angewandte Chemie International Edition* **52**, 5736 (2013)

21. S. Imoto, S. S. Xantheas, S. Saito, "Ultrafast Dynamics of Liquid Water: Frequency Fluctuations of the OH stretch and the HOH Bend", *Journal of Chemical Physics* **139**, 044503 (2013)

22. S. Iwata, P. Bandyopadhyay, and S. S. Xantheas, "Cooperative roles of charge-transfer and dispersion terms in hydrogen-bonded networks of $(H_2O)_n$, n = 6, 11 and 16", *Journal of Physical Chemistry A* **117**, 6641 (2013)

23. E. Miliordos and S. S. Xantheas, "Efficient procedure for the numerical calculation of harmonic vibrational frequencies based on internal coordinates" Joel M. Bowman Special Issue (invited), *Journal of Physical Chemistry A* **117**, 7019 (2013)

Room temperature Single-Molecule Detection and Imaging by Stimulated Raman Scattering Microscopy

Principle Investigator: X. Sunney Xie

Department of Chemistry and Chemical Biology, Harvard University
12 Oxford Street, Cambridge, MA 0213, Cambridge, MA 02138
xie@chemistry.harvard.edu

Program Scope

The scope of this program is to push the sensitivity limit of stimulated Raman microscopy to the single molecule limit, in order to probe chemical and biochemical reactions. Single molecule Raman detection without surface enhancement has long been a major technical challenge. Unlike fluorescence, which has a large cross-section, the Raman excitation efficiency is many orders of magnitude lower. However, Raman provides specific vibrational signatures of chemical bonds, which enables new modes of chemical imaging without labels. We attempt to tackle this challenge with our newly developed stimulated Raman scattering (SRS) imaging technique. SRS can sensitively detect molecular vibrations by implementing high-frequency (megahertz) phase-sensitive detection. Towards single molecule Raman detection, we study SRS of long-chain π-bond conjugated molecules and use near-resonance enhancement to further increase Raman cross-section.

Recent Progress

Towards the goal of single molecule Raman scattering detection, we attempted both further technological development of lasers sources and imaging approaches as well as synthesis of new molecules with large Raman cross-section and high photostability for SRS imaging.

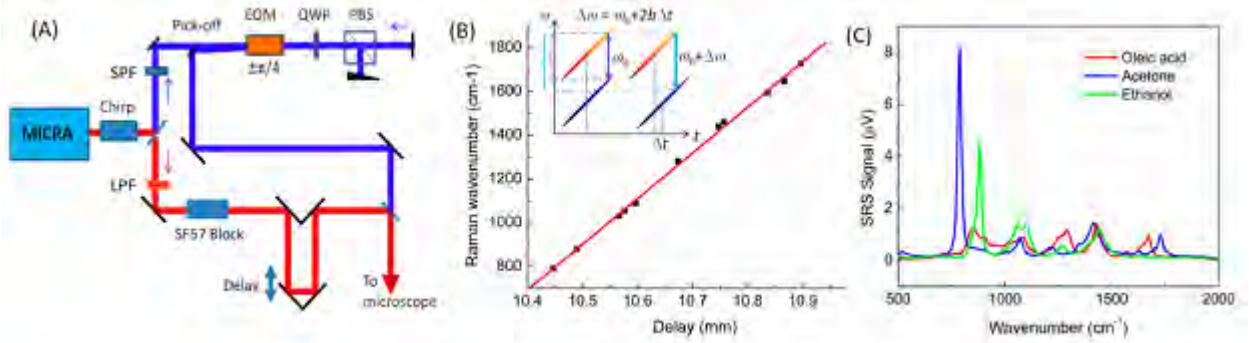

Figure 1: (A) Schematic diagram of the SRS spectroscopy setup based on a single ultra-broadband Ti:sapphire laser. SPF, short-passfilter; LPF, long-passfilter; EOM, electro-optical modulator; QWP, quarter waveplate; PBS, polarizing beamsplitter. (B) Calibration of Raman shift with respect to pump-Stokes pulse delay using a set of Raman peaks of acetone and ethanol; insets showing the schematic diagram illustrating the relationship between Raman shift and interpulse delay. (C) SRS spectroscopy measured by swept-delay chirped femtosecond pulses.

Hyperspectral SRS imaging by spectral focusing: We developed spectral focusing SRS imaging, which allows highly sensitive SRS imaging with chirped femtosecond lasers. The spectral focusing approach uses pulse chirp and time delay to control the Raman band being excited. The advantage of this approach is that by scanning the time delay, a hyperspectral SRS dataset can be acquired without changing the laser wavelength (Figure 1). Hyperspectral SRS imaging is particularly useful in identification and quantification of a chemical species among many other species with different Raman background. It is also going to be very important in single molecule SRS detection because the non-Raman background

signal will become comparable or even larger than Raman signal from a single molecule of interest. To remove that large background and reveal the SRS signal, we can take the hyperspectral SRS data and separate the SRS peak from the broad background. It is also possible to take a simpler approach by using frequency modulation SRS. Because SRS peaks are typically very narrow, by implementing a modulation of pump-laser wavelength instead of amplitude modulation, the obtained SRS signal is a subtraction of off-resonance signal from on-resonance signal, which effectively removes the non-Raman background signal. This can be easily achieved with the spectral focusing approach by using both laser beams after the polarizing beamsplitter and setting them at two different delays.

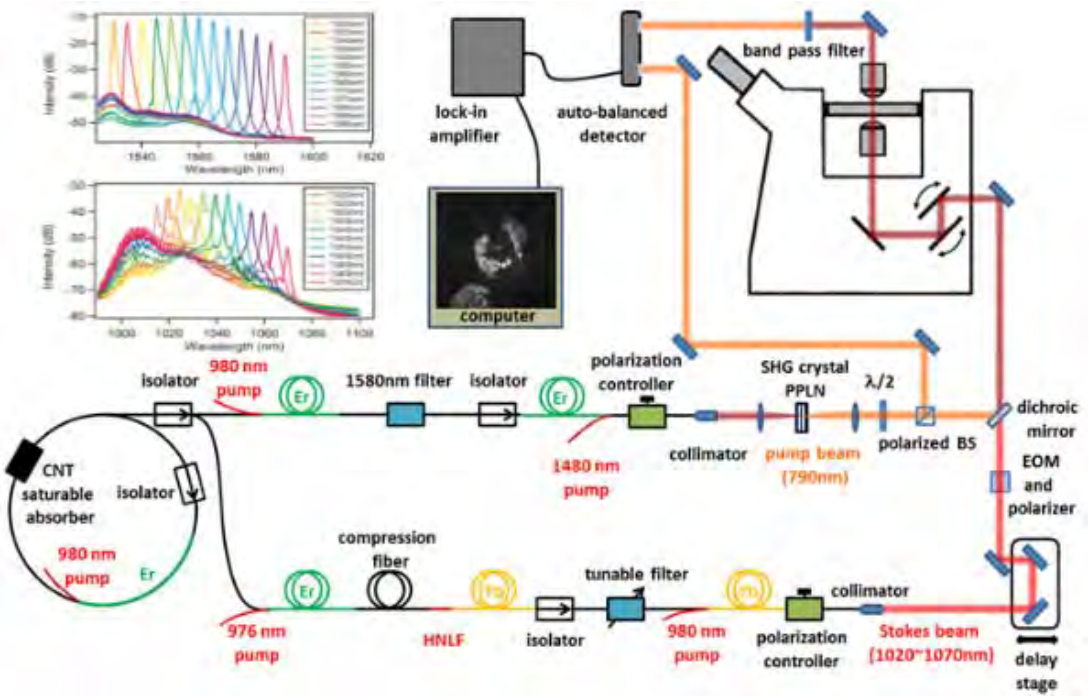

Figure 2: Fiber laser SRS schematic. The lower part demonstrates the fiber laser source. It is composed of a carbon nanotube (CNT) saturable absorber based oscillator, power amplifier arm and a frequency shift arm. Stokes beam is modulated at 10MHz and temporally and spatially combined with pump beam. The combined beam is sent to scanning unit and focused on a sample. The Stokes beam is filtered out and the pump beam is detected by a home-made auto-balanced detector balanced with a separated beam from original pump beam. The two lasers can be independently tuned, allowing for C-H stretching coverage.

Fiber laser source for SRS imaging

Another major development is our construction of an all-fiber laser source for SRS imaging. The laser is built upon standard Erbium and Ytterbium fiber-optics technology and offers significant advantage in terms of compactness and robustness over solid-state laser system. By deriving a supercontinuum from an Erbium femtosecond oscillator and amplify the 1030-1070nm portion with a Yb fiber amplifier, we demonstrated the first all-fiber laser for SRS imaging. The issue with fiber laser is its excessive laser noise compared to solid-state lasers which are typically shot-noise limited at high modulation frequency. The laser noise prevents direct SRS imaging. To circumvent this issue, we built a double-balanced detector that effectively removed the excess laser noise and performed SRS imaging of tissue with a signal to noise comparable to solid-state lasers. Further amplification of the fiber laser power to watt level and reducing laser repetition rate could increase the detection sensitivity of the fiber laser system.

SRS detection of photo-stabilized β-carotene molecule

We have tested detection limit of β-carotene for SRS imaging at visible excitation wavelength. β-carotene molecule has strong absorption near 470 nm. Based on spontaneous Raman measurement, we showed that visible excitation at 532 nm presents an increase in cross-section of more than 400 fold compared to excitation at 785 nm, provided that excitation power remains the same. We used visible picosecond lasers as both pump and Stokes beam to excite the SRS of β-carotene molecule. In a flow cell experiment, we were able to detection β-carotene down to 1μM level. A major limitation in further increase in sensitivity is the photobleaching of β-carotene. To overcome this problem, we adapted a strategy that has been successfully used to improve the stability of fluorophores. When a stabilizer group (e.g. cyclooctatetraene) is covalently linked to a fluorophore, the photostability of the fluorophore can be greatly improved. We synthesized a molecule that conjugates trans-β-Apo-8′-carotenal to cyclooctatetraene through a butane-1,4-diamine linker (Figure 3A). The measured Raman spectrum is similar to that of β-carotene (Figure 3B). SRS spectrum in the NIR range is markedly different. We are still investigating the origin of those spectral changes.

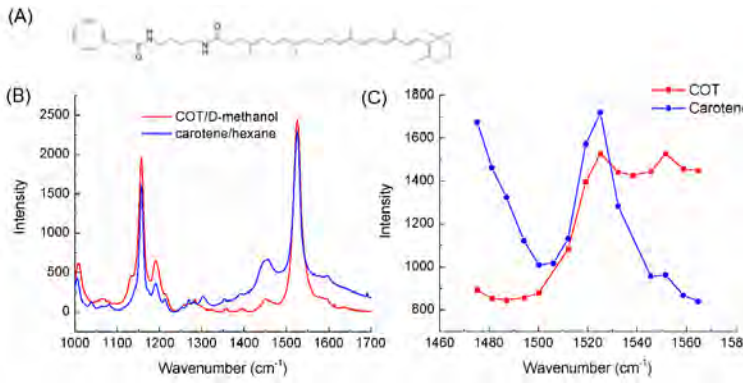

Figure 3: (A) synthesized polyene (n = 10) molecule conjugated to cyclooctatetraene. (B) Spontaneous Raman spectrum of carotene-COT compared to that of β-carotene. (C) SRS spectra of carotene-COT and carotene under NIR excitation

Future Plans

We will evaluate performance of β-carotene – COT conjugated molecule in visible excitation SRS. Other commonly used stabilizer groups such as nitrobenzyl alcohol, and trolox can also be tested. If the photo-stabilization strategy works, we anticipate a 10-fold increase in detection sensitivity. Polyene molecules with longer conjugated double bond chain that are covalently linked to stabilizers can also be synthesized to further increase the Raman cross-section. Another class of molecule we will investigate is long-chain conjugated polyyne molecule. Molecules with more than ten conjugated triple bonds have been synthesized. Similar to polyene molecules, Raman cross-section of polyyne increases exponentially with the length of the molecule. Implementation of frequency modulation of SRS will be useful in removing two-photon absorption background, which is a big obstacle in extracting SRS signal.

DOE Publications/Manuscripts 2012-present

1. Lu, Fa-Ke; Ji, Minbiao; Fu, Dan; Ni, Xiaohui; Freudiger, Christian W.; Holtom, Gary; Xie, X. Sunney. "Multicolor stimulated Raman scattering microscopy," *Mol. Phys.* 110, 1927-1932 (2012).
2. Fu, Dan; Holtom, Gary; Freudiger, Christian; Zhang, Xu; Xie, X. Sunney. "Hyperspectral Imaging with Stimulated Raman Scattering by Chirped Femtosecond Lasers," *J Phys Chem B* 117, 4634-4640

List of Participants

LIST OF PARTICIPANTS

Dr. Musahid Ahmed
Lawrence Berkeley National Laboratory
http://www.lbl.gov/csd/directory/bio_ahmed_m.html

Professor Scott Anderson
University of Utah
http://www.chem.utah.edu/faculty/anderson/anderson.html

Dr. David Bartels
Notre Dame Radiation Laboratory
http://www.rad.nd.edu/faculty/bartels.htm

Dr. Ali Belkacem
Lawrence Berkeley National Laboratory
http://www.lbl.gov/csd/directory/bio_belkacem_a.html

Dr. Hendrik Bluhm
Lawrence Berkeley National Laboratory
http://www.lbl.gov/csd/directory/bio_bluhm_h.html

Dr. Nicholas Camillone
Brookhaven National Laboratory
http://www.bnl.gov/chemistry/bio/Camillone%20IIINicholas.asp

Professor Ian Carmichael
Notre Dame Radiaton Laboratory
http://www.rad.nd.edu/faculty/carmichael.htm

Dr. Michael Casassa
US DOE/Basic Energy Sciences
http://science.energy.gov/bes/csgb/about/staff/dr-michael-p-casassa/

Professor David Chandler
Lawrence Berkeley National Laboratory
http://gold.cchem.berkeley.edu/The_Chandler_Group/Home.html

Dr. Daniel Chipman
Notre Dame Radiation Laboratory
http://www.rad.nd.edu/faculty/chipman.htm

Dr. Andrew Cook
Brookhaven National Laboratory
http://www.chemistry.bnl.gov/sciandtech/PRC/acook/cook.html

Professor Tanja Cuk
Lawrence Berkeley National Laboratory
http://www.cchem.berkeley.edu/tkgrp/

Dr. Liem Dang
Pacific Northwest National Laboratory
http://www.pnl.gov/science/staff/staff_info.asp?staff_num=5604

Professor Michael Duncan
University of Georgia
http://maduncan.myweb.uga.edu/

Dr. Michel Dupuis
Pacific Northwest National Laboratory
http://www.pnl.gov/cmsd/staff/staff_info.asp?staff_num=5599

Professor Mostafa El-Sayed
Georgia Institute of Technology
http://ldl.gatech.edu/

Professor James Evans
Ames Laboratory
http://www.ameslab.gov/cbs/evans

Professor Michael Fayer
Stanford University
http://www.stanford.edu/group/fayer/

Dr. Gregory Fiechtner
DOE/Basic Energy Sciences
http://science.energy.gov/bes/csgb/about/staff/dr-gregory-j-fiechtner/

Mr. John L. Fulton
Pacific Northwest National Laboratory
http://www.pnl.gov/cmsd/staff/staff_info.asp?staff_num=5587

Professor Etienne Garand
University of Wisconsin
http://garand.chem.wisc.edu/

Dr. Bruce Garrett
Pacific Northwest National Laboratory
http://www.pnl.gov/science/staff/staff_info.asp?staff_num=5496

Professor Phillip Geissler
Lawrence Berkeley National Laboratory
http://www.cchem.berkeley.edu/plggrp/index.html

Dr. Mary K. Gilles
Lawrence Berkeley National Laboratory
http://www.lbl.gov/csd/directory/bio_gilles_mk.html

Professor Mark Gordon
Ames Laboratory
http://www.msg.ameslab.gov/

Dr. Jeffrey Guest
Argonne National Laboratory
http://nano.anl.gov/docs/people/guest.pdf

Dr. Alexander Harris
Brookhaven National Laboratory
http://www.bnl.gov/chemistry/bio/HarrisAlex.asp

Professor Mark Hersam
Northwestern University
http://www.hersam-group.northwestern.edu/

Dr. Wayne Hess
Pacific Northwest National Laboratory
http://www.pnl.gov/science/staff/staff_info.asp?staff_num=5505

Professor Wilson Ho
University of California, Irvine
http://www.physics.uci.edu/~wilsonho/whoghp.htm

Dr. Libai Huang
Notre Dame Radiation Laboratory
http://www.rad.nd.edu/faculty/huang.htm

Professor Bret Jackson
University of Massachusetts Amherst
http://www.chem.umass.edu/faculty/jackson.html

Dr. Ireneusz Janik
Notre Dame Radiation Laboratory
http://www.rad.nd.edu/faculty/Janik.htm

Professor Caroline Chick Jarrold
Indiana University
http://mypage.iu.edu/~cjarrold/index.htm

Dr. Cynthia J. Jenks
Ames Laboratory
http://www.ameslab.gov/cbs/cjenks

Professor Mark Johnson
Yale University
http://jlab.chem.yale.edu/

Professor Kenneth Jordan
University of Pittsburgh
http://www.pitt.edu/~jordan/

Dr. Shawn Kathmann
Pacific Northwest National Laboratory
http://www.pnl.gov/science/staff/staff_info.asp?staff_num=5601

Dr. Bruce Kay
Pacific Northwest National Laboratory
http://www.pnl.gov/science/staff/staff_info.asp?staff_num=5530

Dr. Greg Kimmel
Pacific Northwest National Laboratory
http://www.pnl.gov/science/staff/staff_info.asp?staff_num=5527

Dr. Jay LaVerne
Notre Dame Radiation Laboratory
http://www.rad.nd.edu/faculty/laverne.htm

Professor H. Peter Lu
Bowling Green State University
http://www.bgsu.edu/departments/chem/faculty/hplu/peterlu.htm

Dr. Sergei Lymar
Brookhaven National Laboratory
http://www.bnl.gov/chemistry/bio/LymarSergei.asp

Diane Marceau
DOE/Basic Energy Sciences
http://science.energy.gov/bes/csgb/about/staff/

Dr. John Miller
Brookhaven National Laboratory
http://www.chemistry.bnl.gov/SciandTech/PRC/miller/miller.html

Professor Michael D. Morse
University of Utah
http://www.chem.utah.edu/directory/faculty/morse.html

Dr. Christopher Mundy
Pacific Northwest National Laboratory
http://www.pnl.gov/science/staff/staff_info.asp?staff_num=5981

Professor Richard Osgood
Columbia University
http://cumsl.msl.columbia.edu/

Dr. Mark Pederson
DOE/Basic Energy Sciences
http://science.energy.gov/bes/csgb/about/staff/dr-mark-r-pederson/

Professor Hrvoje Petek
University of Pittsburgh
http://www.ultrafast.phyast.pitt.edu/Home.html

Professor Eric Potma
University of California, Irvine
http://www.chem.uci.edu/~potma/webpage_test.htm

Professor Sylwia Ptasinska
University of Notre Dame
http://www3.nd.edu/~sptasins/

Professor Krishnan Raghavachari
Indiana University
http://php.indiana.edu/~krgroup/

Professor Richard Saykally
Lawrence Berkeley National Laboratory
http://www.cchem.berkeley.edu/rjsgrp/

Dr. Gregory Schenter
Pacific Northwest National Laboratory
http://www.pnl.gov/science/staff/staff_info.asp?staff_num=5615

Dr. David K. Shuh
Lawrence Berkeley National Laboratory
http://www.lbl.gov/csd/directory/cv_shuh.html

Dr. Wade Sisk
US DOE/Basic Energy Sciences
http://science.energy.gov/bes/csgb/about/staff/dr-wade-sisk/

Professor Timothy Steimle
Arizona State University
http://www.public.asu.edu/~steimle/

Professor Charles Sykes
Tufts University
http://ase.tufts.edu/chemistry/sykes/Sykes%20Lab%20Research%20Group.html

Professor Ward Thompson
University of Kansas
http://thompsongroup.ku.edu/

Professor William A. Tisdale
Massachusetts Institute of Technology
http://web.mit.edu/tisdalelab

Professor Andrei Tokmakoff
University of Chicago
http://tokmakofflab.uchicago.edu/

Professor John Tully
Yale University
http://www.chem.yale.edu/~tully/

Dr. Marat Valiev
Pacific Northwest National Laboratory
http://emslbios.pnl.gov/bios/biosketch.nsf/bynameinit/valiev_m

Dr. Xue-Bin Wang
Pacific Northwest National Laboratory
http://emslbios.pnl.gov/bios/biosketch.nsf/bynameinit/wang_x

Professor Michael White
Brookhaven National Laboratory
http://www.bnl.gov/chemistry/bio/WhiteMichael.asp

Dr. Kevin R. Wilson
Lawrence Berkeley National Laboratory
http://wilsonresearchgroup.lbl.gov/home

Professor Theresa L. Windus
Ames Laboratory
https://www.ameslab.gov/cbs/theresa

Dr. James Wishart
Brookhaven National Laboratory
http://www.chemistry.bnl.gov/SciandTech/PRC/wishart/wishart.html

Dr. Sotiris Xantheas
Pacific Northwest National Laboratory
http://www.pnl.gov/science/staff/staff_info.asp?staff_num=5610

Professor X. Sunney Xie
Harvard University
http://bernstein.harvard.edu/